amU
Aix Marseille Université

NNT : 2024AIXM0465

THÈSE DE DOCTORAT

Soutenue à Aix-Marseille Université
le 6 décembre 2024 par

Gabriela POLIACIKOVA

La régulation transcriptionnelle du développement des muscles de vol adultes chez la drosophile

The transcriptional regulation of Drosophila adult flight muscle development

Discipline
Biologie santé

Spécialité
Biologie du développement

École doctorale
ED 62 – Sciences de la vie et de la santé

Laboratoire/Partenaires de recherche
Institut de Biologie du Développement de Marseille (IBDM)

Composition du jury

Krzysztof JAGLA Rapporteur
DR, iGReD, CNRS UMR6293, INSERM U1103, Université Clermont Auvergne, France

Hadi BOUKHATMI Rapporteur
CR, IGDR, CNRS UMR6290, Université de Rennes 1, France

Karen OCORR Examinatrice
Assistant Professor, Stanford Burnham Prebys Medical Discovery Institute, La Jolla, CA, 92037, United States

Sophie CHAUVET Présidente du jury
PU, IBDM, CNRS UMR7288, Université Aix-Marseille, France

Andrew SAURIN Directeur de thèse
DR, IBDM, CNRS UMR7288, Université Aix-Marseille, France

Corinne MAUREL-ZAFFRAN Co-directrice de thèse
MCU, IBDM, CNRS UMR7288, Université Aix-Marseille, France

IBDM cnrs Fondation pour la Recherche Médicale

Affidavit

I, undersigned, Gabriela Poliacikova, hereby declare that the work presented in this manuscript is my own work, carried out under the scientific supervision of Andrew Saurin and Corinne Maurel-Zaffran, in accordance with the principles of honesty, integrity and responsibility inherent to the research mission. The research work and the writing of this manuscript have been carried out in compliance with both the French national charter for Research Integrity and the Aix-Marseille University charter on the fight against plagiarism.

This work has not been submitted previously either in this country or in another country in the same or in a similar version to any other examination body.

Marseille, le 8 octobre 2024



Cette œuvre est mise à disposition selon les termes de la Licence Creative Commons Attribution - Pas d'Utilisation Commerciale - Pas de Modification 4.0 International.

Liste de publications et/ou brevets et participation aux conférences

1) Liste des publications et/ou brevet [1] réalisées dans le cadre du projet de thèse :

1. Poliacikova G, Maurel-Zaffran C, Graba Y, Saurin AJ. Hox Proteins in the Regulation of Muscle Development. Front Cell Dev Biol. 2021 Oct 18;9:731996. doi: 10.3389/fcell.2021.731996. PMID: 34733846; PMCID: PMC8558437.
2. Poliacikova G, Barthez M, Rival T, Aouane A, Luis NM, Richard F, Daian F, Brouilly N, Schnorrer F, Maurel-Zaffran C, Graba Y, Saurin AJ. M1BP is an essential transcriptional activator of oxidative metabolism during Drosophila development. Nat Commun. 2023 Jun 2;14(1):3187. doi: 10.1038/s41467-023-38986-5. PMID: 37268614; PMCID: PMC10238438.
3. Poliacikova G, Aouane A, Caruso N, Brouilly N, Maurel-Zaffran C, Graba Y, Saurin AJ. The Hox protein Antennapedia orchestrates Drosophila adult flight muscle development. Under revision in Science Advances.

2) Participation aux conférences[2] et écoles d'été au cours de la période de thèse :

1. Cell symposium Multifaceted mitochondria (6 – 8 Novembre 2022), Seville, Espagne, présentation d'un poster
2. European Developmental Biology Congress (25 – 28 Septembre 2023), Oxford, United Kingdom, présentation d'un poster
3. European Drosophila Research Conference (20 – 23 Octobre 2023), Lyon, France, présentation d'un poster
4. Nordic Developmental Biology Societies & Michael Sars Symposium Joint Meeting (28 – 31 Mai 2024), Bergen, Norvège, présentation d'un short talk de 11 minutes sélectionné sur l'abstract

Résumé

Le développement musculaire implique des réseaux complexes de régulateurs transcriptionnels qui assurent la spécification et la diversification des différents types de muscles. L'identification de ces facteurs est essentielle pour la mise en place de thérapies régénératives musculaires qui seraient efficaces pour guérir les myopathies. Au cours de ma thèse, j'ai abordé deux aspects du développement musculaire, d'une part la régulation transcriptionnelle du métabolisme mitochondrial au cours de la myogenèse adulte, et d'autre part la régulation de la différenciation des précurseurs musculaires adultes.

En ce qui concerne le premier aspect, j'ai identifié un nouveau régulateur transcriptionnel du métabolisme oxydatif pendant le développement du muscle de vol, M1BP. J'ai montré que M1BP est un activateur transcriptionnel de gènes codant pour des protéines qui constituent et sont essentielles à la formation des complexes de la chaîne respiratoire mitochondriale pendant le développement du muscle de vol.

Dans un deuxième temps, pour mieux comprendre la régulation transcriptionnelle de la différenciation musculaire, j'ai cherché à comprendre les réseaux de régulation médiés par M1BP. Sachant que M1BP a été identifié comme un cofacteur des gènes Hox, j'ai cherché un gène Hox qui régulerait le métabolisme mitochondrial avec M1BP. Corrigeant une croyance de longue date selon laquelle le développement des muscles de vol se produit sans l'apport des facteurs de transcription Hox, je montre que le gène Hox Antennapedia (Antp) est exprimé dans les précurseurs des muscles de vol et qu'il est nécessaire à leur développement. Antp intervient dans l'établissement du pool de progéniteurs dans l'embryon jusqu'à la différenciation des myoblastes au début de la pupe et également dans l'acquisition du destin fibrillaire, unique du muscle de vol.

Mots clés : Hox, muscle, transcription

Abstract

Muscle development involves complex networks of transcriptional regulators that ensure the specification and diversification of different muscle types. The identification of these factors is essential for the establishment of muscle regenerative therapies that would be effective in curing myopathies. During my thesis, I addressed two aspects of muscle development, firstly the transcriptional regulation of mitochondrial metabolism during adult myogenesis, and secondly the regulation of adult muscle precursor differentiation.

Regarding the first aspect, I identified a novel transcriptional regulator of oxidative metabolism during flight muscle development, M1BP. I have shown that M1BP is a transcriptional activator of genes encoding proteins that constitute and are essential for the formation of mitochondrial respiratory chain complexes during flight muscle development.

In a second step, to better understand the transcriptional regulation of muscle differentiation, I sought to understand the regulatory networks mediated by M1BP. Knowing that M1BP was identified as a Hox gene cofactor, I looked for a Hox gene that would regulate mitochondrial metabolism with M1BP. Correcting a long-standing belief that flight muscle development occurs without the input of Hox transcription factors, I show that the Hox gene Antennapedia (Antp) is expressed in flight muscle precursors and is required for their development. Antp intervenes at several stages of flight muscle development, from the establishment of the progenitor pool in the embryo to myoblast differentiation in the early pupa and is also required to allow for the unique, fibrillar, flight muscle fate acquisition.

Keywords : Hox, muscle, transcription

Remerciements

En premier lieu je remercie mon jury de thèse, Karen Ocorr, Sophie Chauvet, Krzysztof Jagla et Hadi Boukhatmi d'avoir accepté d'évaluer mon travail.

Je remercie mon équipe d'accueil, l'équipe Graba/Saurin. Andy, merci pour ces quatre années sous tes ailes. Nous avons des approches très différentes pour la science, mais je pense c'est ce qui a fait notre force et je suis très fière du travail qu'on a pu faire ensemble. A chaque fois que je venais te voir dans ton bureau tu m'as souri et as toujours pris le temps de m'écouter, merci pour ça. Si c'était à refaire je le referai sans hésiter. Je remercie ma co-directrice de thèse, Corinne, la meilleure chef. Merci Corinne pour ta gentillesse avec moi, pour tout ton aide avec les mouches, tous nos repas de midi, tous les moments où je me plaignais de la vie de thèse et où tu étais là pour m'écouter. Merci à Yacine pour ta bonne humeur, pour tes points de vue toujours intéressants, donnant des discussions enrichissantes pour moi.

Grand merci à Nathalie, ma collègue du bureau, mais bien plus que ça, ma chère amie. Merci pour tous les jours avec toi, tu es une personne en or et je suis très reconnaissante d'avoir pu partager ce bout du chemin avec toi. Merci à Axelle, Marine et Marwa, les thésardes de l'équipe qui sont parties peu après mon arrivée, merci pour vos conseils et votre gentillesse. Axelle, merci d'être ma maman thésarde qui m'a tout montré dans le labo et d'être une bonne amie. Je remercie Lucie, l'ingénieure de l'équipe, qui m'a beaucoup aidé à la fin de la thèse avec les expériences et les planifications. Merci à Laurianne, la thésarde qui reprend le flambeau, je te souhaite de t'épanouir et de te trouver pendant ta thèse, comme j'ai pu un peu le faire moi.

Je remercie mes super stagiaires Georges, Océane, Caroline et pour une courte durée Romain et Erwin. Océane et Georges, merci d'avoir pu être votre encadrante, vous m'avez beaucoup appris sur moi. Le sujet que je vous ai donné est vraiment très loin d'être simple, bravo à vous pour votre travail. De même merci à Caroline, qui a créé une lignée transgénique pendant son L2, bravo.

Je remercie chaleureusement mon comité de thèse, Frank, René, Vani et mention spéciale pour mon parrain de thèse Bernard Charroux, merci pour tes encouragements sans faille.

Je voudrais remercier toute l'équipe de Frank Schnorrer pour leur aide inestimable, tous les stocks de mouches qu'ils ont bien voulu partager avec moi, tous leurs conseils de Nuno, Jérôme et Vincent dans les deux publications. Je remercie surtout Clément, qui m'a initié dans l'art complexe de stadation et dissection de muscles de pupe. C'étaient les 40 min d'explication de dissection dans son bureau et plusieurs semaines de galère qui ont sauvé l'article de M1BP, merci Clément !

Je voudrais remercier chaleureusement la plateforme de microscopie électronique, qui a joué un rôle primordial pendant ma thèse, surtout à Aïcha, qui a été une maman de thèse pour moi, qui s'est toujours occupé de mon bien-être et du bien-être de mes échantillons.

Je remercie Thomas Rival et Olena Varuk, nos deux membres de l'équipe adoptifs. Thomas, merci pour toutes nos discussions, pour tout le travail que j'ai pu réaliser avec toi avant ma thèse, qui m'a très bien préparé à la vie de jeune thésarde. Grâce à toi le démarrage de ma thèse était presque facile ! Olena, merci pour ta compagnie, pour partager les valeurs du travail qu'on

nous a transmis chez nous, quand on était petites, et de trouver des solutions comment les appliquer sans nous épuiser, bref, merci pour ton amitié.

Je remercie Claudio Collinet pour m'avoir accueilli pour mon stage de Master 1 et pour son encadrement si encourageant avec moi. Je remercie aussi à Jean-Marc Philippe de la même équipe, avec qui j'ai pu réaliser mon premier stage à l'IBDM, qui m'a initié au plus beau modèle de Drosophile, et m'a fait tellement confiance de m'avoir laissé toutes ses manips en partant en vacances. Merci, tu m'as donné plein de confiance en moi, et merci pour tous les conseils de biologie moléculaire dans les années suivantes.

Je voudrais remercier Elsa, Brice et Daniel de la plateforme de microscopie, pour m'avoir formé au confocal et avoir toujours résolus tous les problèmes possibles et impossibles qui ont survenus pendant des longues heures d'acquisition.

Je remercie toutes les autres personnes d'IBDM que j'ai pu côtoyer pendant ces années, qui rendent l'IBDM un endroit chaleureux pour travailler, Pierre Mangeol, Marvin, Thomas Légier, Laurianne, Elise, Chris, Jordan, Stephen, Fanny, Jules, Anaïs et j'en oublie certainement. Je remercie à Olivier et Elise, qui ont passé la Licence et le Master avec moi, pour leur amitié.

Je remercie toutes les personnes en dehors de l'institut qui m'ont soutenu pendant ma thèse, commençant par mon partenaire Saran, le meilleur partenaire dont j'aurai pu rêver, avec son soutien sans faute. Merci pour tous les moments, où la thèse était dure, où je perdais perspective, et tu m'aidais à avancer. Merci à toute ma famille, maman, papa, Palko, mon frère super beau et Simonka. Merci d'avoir toujours cru en moi, de vous priver pour me donner les moyens de partir et de réussir. Je sais que chaque enfant dit que ses parents sont les meilleurs, mais c'est une vérité. Je remercie à mon oncle, qui se languissait de venir à ma soutenance, mais qui n'est malheureusement plus parmi nous. Sache que sans ton soutien moral et financier je n'aurai jamais pu venir en France il y a 9 ans, cette thèse n'existerai pas, il n'y aurait rien de tout ça. Merci à toi.

Merci à ma famille française adoptive, Célia, Patrick et Sophie, de m'avoir accueilli pendant le confinement, de m'avoir toujours aidé quand j'en avais besoin. Célia, tu es une amie infiniment précieuse pour moi, qui a vécu toute l'aventure d'études et thèse avec moi, comme amie et aussi colloque. C'était un honneur pour moi d'avoir vécu nos thèses ensemble, j'ai adoré vivre avec toi dans notre super grand appart. Merci pour tout.

Je remercie à mon amie qui amène toujours le soleil, Victoria, pour son soutien, pour sa capacité incroyable à alléger chaque situation.

Je remercie à Béatriz, Jimena, Andrée-Laure, Daniel et Nathalie pour leur amitié et soutien.

Last but not least, je remercie (et m'excuse) à mes petites Drosophiles, pour leur contribution plus qu'essentielle et leur force malgré toutes mes tentatives de perturber leurs petits muscles.

“God in his wisdom made the fly
And then forgot to tell us why.”
Ogden Nash

List of figures

Figure 1. Mesodermal subdivision in *Drosophila* embryo

Figure 2. Overview of larval muscle development

Figure 3. Promuscular cluster formation and muscle progenitor specification

Figure 4. The process of myoblast fusion

Figure 5. Ultrastructural features of myoblast fusion

Figure 6. Ultrastructural analysis of the fusion contact

Figure 7. Schematics of the larval muscle pattern

Figure 8. Adult *Drosophila* muscle pattern

Figure 9. AMPs division along the D-V axis

Figure 10. AMPs closely associate with larval muscles and nerves

Figure 11. Thoracic AMP localisation with respect to disc primordia

Figure 12. The development of *Drosophila* indirect flight muscles

Figure 13. Schematic view of larval FC diversification

Figure 14. Genomic organisation and expression of *Drosophila* and vertebrate Hox genes

Figure 15. Schematic representation of factors modulating Hox-cofactor specificity

Figure 16. Antp gene displays a complex structure

Figure 17. Structure of Antp gene products

Figure 18. Complex distribution of *Antp* transcripts from its two promoters

Figure 19. Hox genes specify the embryonic AMP pattern

Figure 20. First high-resolution TEM micrographs of the mitochondrial membrane.

Figure 21. Complexes of the mitochondrial respiratory chain.

Figure 22. Schematic representation of the Q-cycle occurring in the CIII.

Figure 23. Antp does not regulate oxidative metabolism in flight muscles with M1BP

Figure 24. Presence of mitochondrial inclusions in various pathological conditions.

Figure 25. Inverse correlation between the number of larval and adult muscle progenitors along the A-P axis

Figure 26. Myoblasts can re-appear in the *Antp* P2 mutant condition

Figure 27. Antp overexpression leads to muscle fibres adopting a jump-like fate

Figure 28. *Hox* gene expression in adult musculature at the single-cell level

Figure 29. Model of Antp role during flight myogenesis

Table of contents

Affidavit 1
Liste de publications et/ou brevets et participation aux conférences 2
Résumé 3
Abstract 4
Remerciements 5
List of figures 7
Table of contents 9
Introduction 11
Chapter I. How to fly? – Drosophila muscle development 11

Part 1. Mesodermal development and patterning 11
1.1 The development of mesoderm 11
1.2 Mesodermal subdivision 12
1.3 Promuscular cluster formation 13
1.4 Muscle progenitor specification 15

Part 2. Larval muscle development 17
2.1 Founder cell specification 17
2.2 Larval muscle differentiation 18
2.2.1 Larval myoblast fusion 18
2.2.2 Larval myofibrillogenesis 23
2.2.3 Final larval muscle pattern 24

Part 3. Adult muscle development 26
3.1 Adult muscle pattern 26
3.2 Specification of adult muscle progenitors 27
3.3 Adult muscle differentiation 29
3.3.1 Exit from quiescence and proliferation 29
3.3.2 Adult founder cell selection 30
3.3.3 Adult myoblast fusion 32
3.3.4 Adult myofibrillogenesis 33

Chapter II. How to create muscle diversity? – Hox genes and mesodermal patterning 35

Part 1. Muscle diversification 35
1.1 Larval muscle diversification 35
1.2 Adult muscle diversification 38

Part 2. Hox genes 40
2.1 Hox gene discovery and function 40
2.2 Hox gene cofactors 43
2.2.1 M1BP, a novel Hox cofactor 43
2.3 Hox gene Antennapedia 44
2.3.1 Antennapedia, a "giant" gene 44
2.3.2 Antennapedia expression 46
2.3.3 Antennapedia function 48

Part 3. The role of Hox genes in mesodermal patterning 49

3.1 The role of Hox genes in larval muscle patterning 50
3.2 The role of Hox genes in adult muscle patterning 50

Chapter III. How do flies have the energy to fly? – Muscle mitochondria ***52***

Part 1. Mitochondrial development **52**
1.1 The biology of mitochondria 52
1.2 Mitochondrial respiratory chain 53
1.2.1 Roles of assembly factors 55
1.2.2 Drosophila respiratory chain 56
1.3 Mitochondrial quality control 57
1.3.1 Ubiquitin-proteasome 57
1.3.2 Mitochondrial proteases 58
1.3.3 Mitochondrial unfolded protein response 59
1.3.4 Mitophagy 59

Part 2. Transcriptional control of mitochondrial respiration **60**
Part 3. Mitochondrial changes during muscle development **61**

Thesis objectives ***63***
Results ***65***

Article 1. M1BP is an essential transcriptional activator of oxidative metabolism during *Drosophila* development **65**
Article 2. Antp orchestrates *Drosophila* adult flight muscle development **86**

Discussion and perspectives ***109***

Part 1. M1BP is an essential transcriptional activator of oxidative metabolism during *Drosophila* development **109**
Part 2. Antp orchestrates *Drosophila* adult flight muscle development **113**

Supplementary data ***122***

Supplementary data article *M1BP* is an essential transcriptional activator of oxidative metabolism during Drosophila development **122**
Supplementary data article *Antp* orchestrates Drosophila adult flight muscle development **140**

Annexe ***161***

Article 3. Hox proteins in the Regulation of Muscle development (Review) **161**

Bibliography ***176***

Introduction

Chapter I. How to fly? – *Drosophila* muscle development

Part 1. Mesodermal development and patterning

1.1 The development of mesoderm

Drosophila mesoderm develops during gastrulation, starting approximately 3 hours (h) after fertilisation (stage 6-7), from the ventral-most cells that express high nuclear levels of the maternal gene *dorsal* (*dl*) (Roth et al., 1989; Rushlow et al., 1989; Simpson, 1983; Steward, 1989). Heterozygous *dl* mutant females at high temperature display the so-called dorsal-dominant phenotype, where the cells situated ventrally do not invaginate, no ventral furrow is thus formed and no mesodermal derivates are made (Nüsslein-Volhard, 1979). Similar phenotypes were observed in embryos mutant for zygotic genes *twist* (*twi*) and *snail* (*sna*) (Leptin and Grunewald, 1990; Nüsslein-Volhard et al., 1984; Simpson, 1983). It was later shown that *twi* is a direct *Dl* target (Jiang et al., 1991) and that both Twi and Dl are required for *sna* activation, contributing to the precise mesoderm-neuroectoderm boundary establishment by the middle of nuclear cycle 14 (Ip et al., 1992; Kosman et al., 1991). Twi is a basic helix-loop-helix (bHLH) transcription factor (TF) (Murre et al., 1989; Thisse et al., 1988) and acts mainly as a transcriptional activator, while Sna is a zinc-finger TF (Boulay et al., 1987) and acts mainly as a transcriptional repressor.

During gastrulation, cells expressing Twi and Sna undergo morphological changes, flatten and constrict their apical membranes, adopting a wedge shape, and forming a ventral furrow. The invagination of the ventral furrow forms a tube inside the embryo. When the invagination is complete the cells forming the tube undergo epithelial-to-mesenchymal transition, enter the cell cycle and spread out dorsolaterally to form a mesodermal layer underneath the ectoderm, between stages 7 to 9 (Leptin and Grunewald, 1990). The ordered movement of mesodermal cells depends on the Fibroblast Growth Factor (FGF) signalling, mediated by one of its receptors Heartless (Htl) (Beiman et al., 1996; Stathopoulos et al., 2004). In *htl* mutant embryos, mesodermal cells fail to attain the dorsal margin of the ectoderm, leading to a loss of heart, visceral and dorsal somatic muscles (Beiman et al., 1996; Gisselbrecht et al., 1996). The entry into mitosis is regulated by String (Stg, a homologue of Cdc25), whose expression is regulated by Twi. The precise timing of its activity is achieved through the counteracting activity of a kinase-like protein Tribbles (Trb) (Grosshans and Wieschaus, 2000) and a RNA-binding protein Held out wings (How) (Nabel-Rosen et al., 2005).

With the avenue of whole genome analyses a great effort was put into characterising gene regulatory networks (GRN) responsible for the mesoderm formation. Distinct embryonic regions along the dorso-ventral (D-V) axis would have a distinct threshold, where depending on the concentration of the Dl protein different target genes would be activated: I. mesodermal targets, containing enhancers with low binding affinities, such as *twi*, *sna* and *folded gastrulation* (*fog*) II. neuroectodermal targets, containing enhancers with intermediate binding affinities, such as *rhomboid* (*rho*) and III. dorsal ectodermal targets, containing enhancers with high binding activities and responding thus to low Dl concentration, such as *decapentaplegic* (*dpp*) (Stathopoulos et al., 2002; Zeitlinger et al., 2007). Downstream of Dl, Twi was proposed

to bind to almost 500 direct targets, covering 25% of all *Drosophila* TFs, placing Twi on the top of an intricate GRN governing early mesodermal development (Sandmann et al., 2007). Interestingly, Sna was later shown besides its main role as a transcriptional repressor to also bind and activate more than 50 enhancers loci co-bound by Twi (Rembold et al., 2014).

1.2 Mesodermal subdivision

Once the mesodermal layer is formed, it is patterned into distinct domains, segregating the progenitors of different mesodermal derivatives, namely the somatic, visceral and cardiac mesoderm (Poulson, 1950). Along the D-V axis, the gradient of Dpp secreted from the dorsal ectoderm restricts the expression of a homeobox-containing gene *tinman* (*tin,* homologue of msh-2) in dorsal mesodermal cells, providing competence to become midgut visceral mesoderm, dorsal muscles and heart (Bodmer, 1993; Frasch, 1995; Staehling-Hampton et al., 1994). Under the control of Tin and other regulators, another homeotic gene *bagpipe* (*bap*) is expressed in dorsal segmental clusters of cells, the majority of which defines the primordium of midgut visceral muscles (Azpiazu and Frasch, 1993). High Dpp levels at the same time as activating *tin* expression repress the lateral and ventral somatic muscle regulators, *Drosophila Six-4* (*D-Six4*) (Clark et al., 2006) and *Pox meso* (*Poxm*) (Duan et al., 2007; Staehling-Hampton et al., 1994). The fat body (FB) primordium lies below the visceral primordium and is marked by a TF *serpent* (*srp*) (Abel et al., 1993; Azpiazu et al., 1996).

Concomitantly, another major mesodermal subdivision occurs along the anterior-posterior (A-P) axis. The first pattern to be described was that of Twi, showing a regular fluctuation along the AP axis. This graduation develops from stage 9 and by stage 10, Twi shows a low expression in the A portion of each segment and a high expression in the P portion of each segment (Borkowski et al., 1995). This modulation of Twi expression requires Notch signalling (Tapanes-Castillo and Baylies, 2004).

Following this work, it was proposed that up to embryonic stage 11, the subdivision of mesoderm along the A-P axis should not be thought in segmental, but rather parasegmental domains, because the parasegmental borders of mesoderm coincide with the ectodermal ones (a parasegment being constituted of a P portion of one segment and the A portion of an adjacent segment). Following this subdivision, the visceral mesoderm and future fat body fall into the P domain (corresponding to the P part of the parasegment) and the cardiac and somatic muscles into the A domain (A part of the parasegment) (Azpiazu et al., 1996). The nomenclature that has been adopted uses pair-rule gene names that are essential for the development of these regions: the homeobox gene *even-skipped* (*eve*) marks the P domain, with low Twi expression and the fork-head TF *sloppy-paired* (*slp*) the A domain, presenting high Twi expression (Azpiazu et al., 1996; Baylies and Bate, 1996; Riechmann et al., 1997). In the *eve* mutant, Bap and Srp patches are lost, resulting in the absence of visceral muscles and fat body (Azpiazu et al., 1996) and in the *slp* mutant, the whole mesoderm presents low Twi expression and cardiac and somatic muscles do not develop. Interestingly, in the *slp* mutant, the whole mesoderm adopts a visceral fate, marked by Bap expression (Riechmann et al., 1997). As for the D-V patterning, A-P mesodermal patterning depends crucially on the integration of ectodermal signalling cues. In the *eve* domain, Engrailed (En) and Hedgehog (Hh) signalling from the ectoderm contribute to pattern the A domain into visceral mesoderm and FB, which involves

bap regulation (Azpiazu et al., 1996), while ectodermal Wingless (Wg) signalling induces Slp mesodermal expression and further patterns the P domain into cardiac and somatic muscles, presenting high Twi expression (Lee and Frasch, 2000). High Twi expression is thought to act as a myogenic switch, providing the cells with the competence to become somatic muscles, because uniform high Twi overexpression in the mesoderm inhibits visceral muscle development and promotes somatic muscle development instead (Baylies and Bate, 1996). Consequently, at the end of mesodermal subdivision, the mesoderm separates into I; an inner cell layer containing visceral muscle progenitors, II; dorsal cells that remain on either side of the embryo, giving rise to the cardiac muscle and the most dorsal somatic muscles and III; an outer cell layer, in contact with the ectoderm, producing somatic muscles (**Fig. 1**).

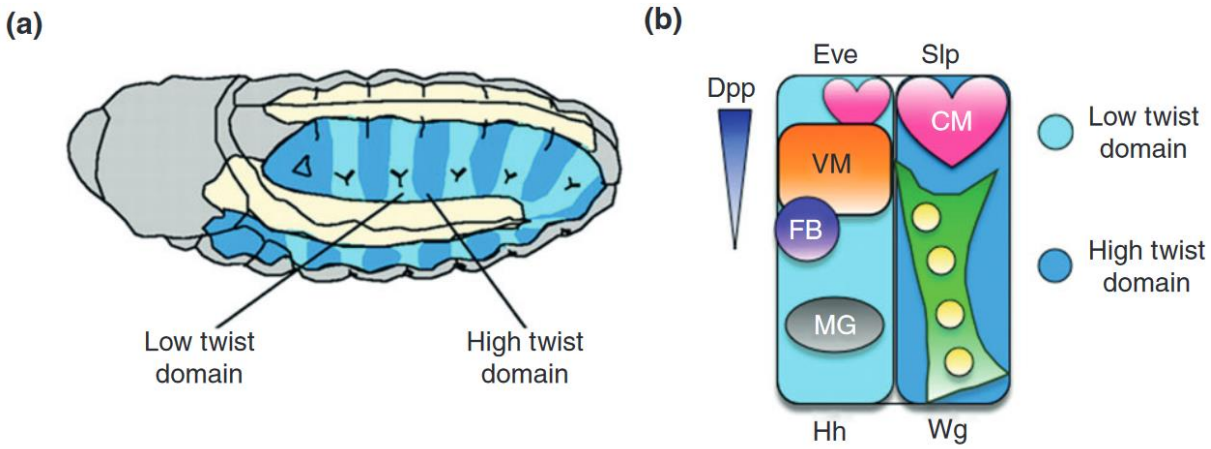

Figure 1. Mesodermal subdivision in *Drosophila* embryo. (a) Stage 10 embryo showing the fluctuating Twi expression along the A-P axis. **(b)** Fate map of a single hemisegment, in which, the high Twi, anterior Slp domain gives rise in the dorsalmost part to the cardiac mesoderm and all somatic muscles and the low Twi, posterior, Eve domain that gives rise to the visceral mesoderm, fat body and mesodermal glial cells (Figure adapted from (Dobi et al., 2015)).

1.3 Promuscular cluster formation

After the initial mesodermal subdivision, muscle progenitors of the somatic musculature arise within the high-Twi A domain between late stage 10 and 12 (Baylies and Bate, 1996) **(Fig. 2)**. The mechanisms of somatic muscle progenitor segregation were described based on studies conducted in the embryonic ventral ectoderm. In the ventral ectoderm, a neurogenic population is segregated from the epidermal progenitors under the influence of neurogenic genes, such as *Notch* (*N*), *Delta* (*D*) and *Enhancer of split* (*E(spl)*). In the neurogenic population, the groups of equivalently competent cells, called proneural clusters, from which neuroblasts (NB) arise are marked by the expression of proneural genes, including members from the *achaete-scute* complex (AS-C) (reviewed in Campos-Ortega, 1993). Interestingly, several neurogenic genes were shown to be expressed at high levels in the mesoderm and their mutations affect mesodermal differentiation (Corbin et al., 1991). Several observations in the mesoderm suggested that an equivalent mechanism operates during both ectodermal and mesodermal patterning. First, screening for novel homeobox genes led to the description of the *S59* gene

(later named *slouch (slou)*), restricted to a specific subset of somatic muscles, neurons and a small region of the midgut (Dohrmann et al., 1990).

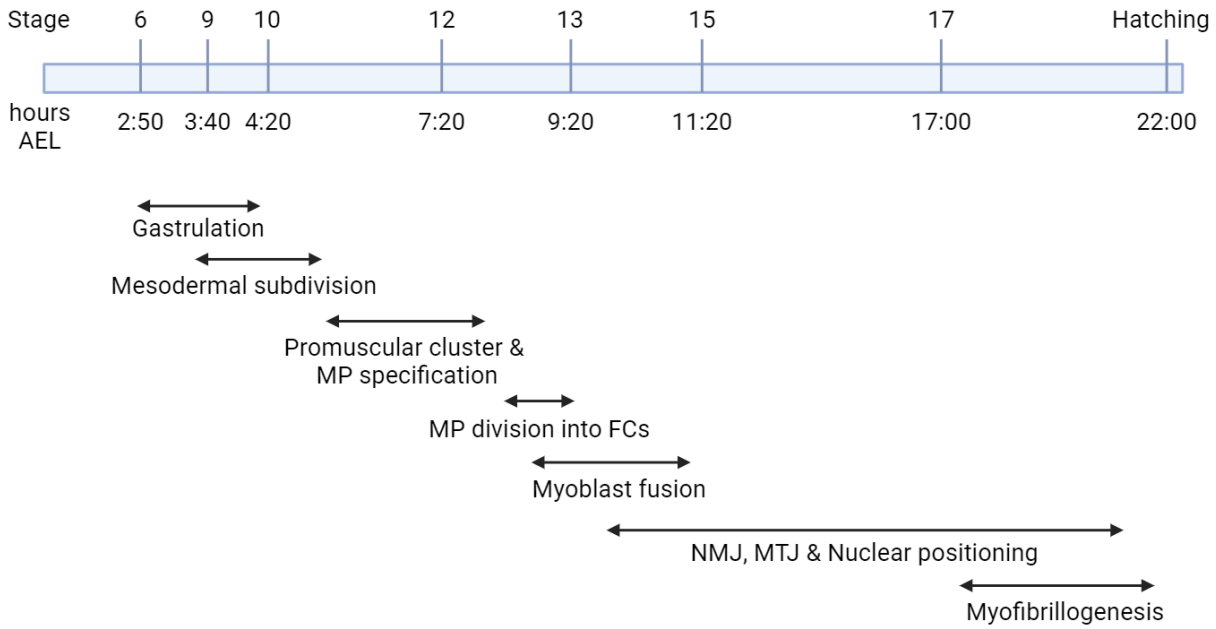

Figure 2. Overview of larval muscle development. Main events occurring during larval somatic muscle specification and development are shown, with embryonic stages and corresponding hours of development at 25°C, adapted from (Poovathumkadavil and Jagla, 2020). AEL- after egg laying, MP - muscle progenitor, FC- founder cell, NMJ- neuromuscular junction, MTJ- myotendinous junction

Using *S59/slou* as a marker, the existence of mesodermal single cells with the capacity to form a particular muscle was revealed in embryos mutant for *myoblast city* (*mbc*) gene, where the fusion between muscle progenitors and their neighbours is abolished. In this case, mononucleate muscle fibres are formed from these single cells, with appropriate attachments and innervation, while neighbouring cells remain round and undifferentiated (Rushton et al., 1995).

Based on these observations, within the high Twi domain, analogous to proneural clusters, the existence of promuscular clusters, also called equivalence groups, marked by a member of the AS-C, a pro-neurogenic bHLH TF *lethal of scute* (*l'sc*) was described. Promuscular clusters arise within the high Twi domain from late stage 10 and continue appearing until stage 12 with the final pattern of 19 clusters present in thoracic and 18 in abdominal segments, numbered according to the timing of their appearance. They contain between 2 to 7 cells (Carmena et al., 1995). Even though the main role in promuscular cluster formation has been given to *l'sc*, other pro-neurogenic genes *mastermind* (*mam*) and *e(spl)* were shown to be involved in the segregation of the *ladybird* (*lb*)-expressing progenitor from its promuscular cluster, which is independent on *l'sc* (*lb* is a collective name for *ladybirdearly* (*lbe*) and *ladybirdlate* (*lbl*) genes) (Jagla et al., 1998).

The competence of mesodermal cells in the high Twi domain to become somatic muscle is first determined by the intersection of Wg and Dpp signals coming from the ectoderm that induces L'sc expression in several cells, called a precluster. This whole domain is responsive to Ras1

signalling, and under the influence of distinct Receptor Tyrosin Kinases (RTK) signalling pathways (such as Htl and Drosophila Epidermal growth factor Receptor (DER)), the MAPK-RAS activity is restricted to distinct promuscular clusters (Carmena, Gisselbrecht, et al., 1998). A synergistic input of several TFs, induced by all the above-mentioned signalling pathways induces the expression of a specific marker in all cells of the cluster (Halfon et al., 2000). All these cells have a capacity to become a progenitor, they are thus developmentally equivalent, hence their name equivalence groups (Carmena, Gisselbrecht, et al., 1998).

1.4 Muscle progenitor specification

In most clusters, one cell of the cluster accumulates higher levels of *l'sc* than its neighbours in the group and over time, *l'sc* expression is eventually lost from this cell as well. The *S59/slou* gene, proposed to be expressed in some muscle-forming cells (Dohrmann et al., 1990) was found to be co-expressed with some of the single L'sc-positive cells in promuscular clusters. These cells were named muscle progenitors (MP), defined as a distinctive cell that segregates from L'sc-expressing clusters. In favour of the statement that *l'sc*-positive single cells are muscle progenitors is the fact that the mutation of *l'sc* leads to the occasional disappearance of some *S59/slou*-dependent muscles, while its overexpression leads to muscle duplication (Carmena et al., 1995).

The specification of MP depends on intricate cross-talks of several signalling pathways (**Fig. 3**). In addition to depending on the high Twi expression the MP specification depends also on extrinsic signalling molecules coming from the ectoderm, such as Wg (Baylies et al., 1995; Lawrence et al., 1995; Ranganayakulu et al., 1996) and the RAS-MAPK signalling activated by RTKs (Buff et al., 1998b; Michelson et al., 1998). In the *wg* mutant embryos the expression of *S59/slou* is missing from the entire mesoderm (Baylies et al., 1995), the expression of *eve* is lost in the most dorsal cells, which include the future DA1 muscle and the heart (Lawrence et al., 1995) and most *nautilus (nau)*-positive progenitors are missing as well (Michelson et al., 1990; Ranganayakulu et al., 1996). The specification of the DA1 *eve* and *Kruppel* (*Kr*)-positive progenitor, as well as other more ventrolateral progenitors, is also under the control of FGF signalling mediated by the FGF receptor Htl (Michelson et al., 1998). In mutant embryos for the *spitz* (*spi*) gene, encoding the ligand of the DER (Rutledge et al., 1992), approximately half of larval muscle fibres are missing. The progenitor of the DA1 muscle does not form, phenocopying the *wg* and *htl* mutant conditions, and other Kr-positive ventral MP are missing as well (Buff et al., 1998a).

The DA1 muscle is thus patterned through inputs coming from Wg, FGF and EGF signalling and constitutes an excellent example of the intricate integration of these different signalling pathways that pattern the mesoderm. In every embryonic hemisegment, two Eve-expressing progenitors, P2 and P15 arise within the dorsal mesoderm at the embryonic stage 11 (Buff et al., 1998a; Carmena, Gisselbrecht, et al., 1998). By their combinatorial expression, ectodermal Wg and Dpp precede and induce the precise L'sc expression in the precluster region within the dorsal mesoderm, which encompasses some or all cells later belonging to clusters 2 and 14-17 (Carmena, Gisselbrecht, et al., 1998). The P2 gives rise to an *eve*-positive FC that divides again and produces two heart accessory persistently *eve*-positive pericardial cells (PC), while P15 gives the *eve*-expressing DA1 muscle. This pattern is determined by RTK/Ras1 signalling,

where FGF signalling via the Htl receptor is required for both cluster 2 and 15 formation, while DER is required for cluster 15 formation only. While the whole *l'sc*-expressing precluster is competent to respond to Ras1, it is the localised activation of Htl and DER, which involves Wg and Dpp, that refines its domain of activity. For Eve activation in P2 and P15, synergistical inputs from tissue-specific TFs Tin and Twi and signal-responsive TFs dTCF/Pangolin (Pan ; downstream of Wg), Mothers against dpp (Mad ; downstream of Dpp) and Pointed (Pnt ; downstream of Ras) are all required (Halfon et al., 2000). Wg and Dpp thus induce the initial L'sc expression within the dorsal mesoderm, which is further refined under the influence of RTK signalling into clusters giving cardiac (requiring only Htl signalling) or somatic DA1 progenitor fate (requiring both Htl and DER signalling) (Carmena, Gisselbrecht, et al., 1998).

For the single cell of the cluster to become a muscle progenitor, the inductive Ras-mediated signals are opposed by lateral inhibitory N-mediated signals (Baker and Schubiger, 1996; Fuerstenberg and Giniger, 1998). In *N* or *Dl* mutant embryos, the singling out of the individual *l'sc*-expressing cell does not occur. Taking again the example of the *S59/slou* gene, in the promuscular cluster 3, the singled-out L'sc-positive cell normally co-expresses S59/slou. In the neurogenic genes mutant embryos, such as *N* or *Dl*, the whole cluster 3 continues to express L'sc as well as S59/slou, with all cells retaining the capacity to become the progenitor (Bate et al., 1993; Carmena et al., 1995).

The selection of the progenitor involves several reciprocal regulatory interactions between Ras and N signalling (**Fig. 3**). On the one hand, Ras activates the expression of Htl signalling components which leads to the reinforcement of Ras signalling in the future progenitor cell (positive feedback loop) and also activates the expression of *Dl*, which in non-autonomous fashion increases inhibitory N signalling in adjacent cells. On the other hand, N downregulates *Dl* expression, reinforces its own expression and blocks the Ras-mediated positive feedback loop in adjacent, thus non-progenitor cells.

Furthermore, the N-mediated lateral inhibition involves the diffusible DER inhibitor Argos (Aos) that synergises with Dl, activated by the Ras signalling (negative feedback loop) (Carmena et al., 2002). The non-progenitor cell will become a so-called fusion-competent myoblast (FCM), marked by the expression of a zinc-finger TF *lame duck (lmd)* (Duan et al., 2001) and a transcriptional repressor *tramtrack69 (ttk69)* (Ciglar et al., 2014), both required for the FCM fate. A slightly diverging explanation was offered, where at the beginning of progenitor selection N signalling would maintain the whole mesoderm in an uncommitted state, and then under the influence of Wg signalling, this inhibition would be alleviated to form equivalence groups. For example, the expression of S59/Slou in cluster 3 would not be induced *per se*, but permitted (K. Brennan et al., 1999; Rusconi and Corbin, 1998).

In conclusion, the selection of progenitor vs non-progenitor fate lies on reciprocal, opposing interactions of the N pathway and Ras signalling pathways. To create distinct muscle progenitors for all different muscle types, mesodermal cells integrate positive and negative inputs from several signalling pathways, decoding the threshold and duration of the signal into a specific muscle fate by the activation of signal-responsive and tissue-specific TFs.

Therefore, even though a relatively small number of signalling pathways and downstream TFs operate in mesodermal patterning, it is their combinatorial activation and the different affinities of their binding sites that allow for progenitor diversity.

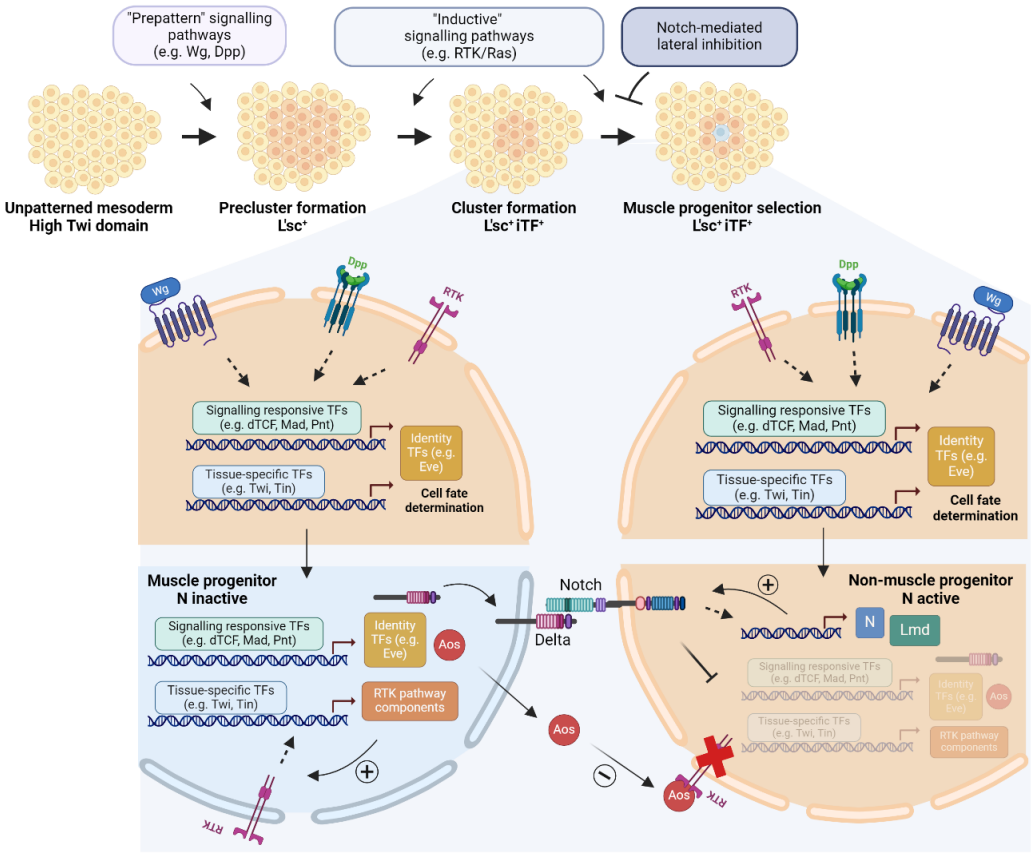

Figure 3. Promuscular cluster formation and muscle progenitor specification. During embryonic stages 9-11, within the A, high-Twi domain, at the intersection of Wg and Dpp signalling pathways a part of the mesoderm becomes competent to form a L'sc-expressing precluster. Under the influence of RTK/Ras pathways (such as Htl and DER) distinct promuscular clusters are formed, in which all cells of the cluster start to express a specific marker (such as Eve, Nau or S59/Slou). The expression of the marker is activated by several TFs, in response to the combinatorial action of all the above-mentioned signalling pathways. The RTK signalling reinforces its own activity and activates the expression of Dl and a diffusible DER inhibitor Aos in the future muscle progenitor cell. Through lateral inhibition Dl activates the N pathway which inhibits the RTK positive feedback loop and Aos further shuts down the RTK signalling in the neighbouring cell, which will not become a muscle progenitor, but a Lmd-positive, fusion-competent myoblast instead.

Even though we gained a solid understanding of the segregation of MP from the mesoderm, the picture is still incomplete. For example, in *l'sc* mutant embryos, only a few MP are missing, even though all promuscular clusters and selected MP express L'sc (Carmena et al., 1995), suggesting that other factors with redundant function, such as Poxm (Duan et al., 2007), are at play during this process. Additionally, this process was described in dorsal abdominal MPs, whether the same pathways operate in more lateral and ventral groups was not studied.

Part 2. Larval muscle development

2.1 Founder cell specification

Following the formation of promuscular clusters in the somatic mesoderm and singling out of MP within each cluster, the MP moves closer to the ectoderm and divides by the mid-

stage 12, giving rise to their progeny, two muscle founder cells (FCs), or one FC and one PC (Carmena, Gisselbrecht, et al., 1998) or one FC and one adult muscle progenitor (AMP) (Carmena et al., 1995). The term *founder cell* was coined by *Dohrmann et al.* to designate a muscle cell that can seed the formation of an individual muscle and it was postulated that *S59/slou* labels a subset of them (Dohrmann et al., 1990). In fact, two MPs express *S59/slou* and produce four FCs, whereas only one sibling maintains *S59/slou* expression (Carmena et al., 1995). This was also demonstrated in the case of *Kr* and *Eve*-expressing progenitors, postulating that when an MP divides, only one FC keeps the marker expression, giving rise to two muscles with different characteristics (Ruiz-Gómez et al., 1997). It is believed that it is the combinatorial expression of such markers, called identity TFs (iTFs), that determines the individual FC fate.

After the initial MP segregation from promuscular clusters, the mesoderm is thus further patterned through progenitor asymmetric division. Distinct fates of daughter cells produced by the division of MP depend once again as in the case of the nervous system development (Spana and Doe, 1996) on the asymmetric expression of the membrane-associated protein Numb (Carmena, Murugasu-Oei, et al., 1998; Ruiz Gómez and Bate, 1997). As mentioned earlier, even though both daughter cells that are born after MP division initially express identical markers, only one of them ultimately keeps the marker expression. This allows the two daughter cells to acquire distinct fates and generate distinct muscles. To achieve this segregation, Numb is asymmetrically distributed between the two FCs, which requires an adaptor protein Inscuteable (Insc), and Numb is inherited only by one of the two siblings. In the absence of Numb, there is a failure to distinguish between the two sibling cells, often leading to the duplication of one muscle at the expense of its neighbour. In MPs expressing *Kr*, *S59/Slou* and *eve* that are mutant for *numb*, the expression of these factors is initiated normally, but lost from both FC after they are born (Ruiz Gómez and Bate, 1997). As in the case of the central nervous system (CNS) development, Numb action is through the interference with the N pathway (Spana and Doe, 1996), where Numb prevents the translocation of the Notch intracellular domain (NICD) to the nucleus (Frise et al., 1996). In *numb* mutant, N signalling is thus active in both daughter cells, leading to the loss of specific markers and an acquisition of identical fate in both sister FCs (Ruiz Gómez and Bate, 1997). N pathway has thus a multistep role during muscle development, first mediating the lateral inhibition required for MP segregation, and second in determining alternative cell fates in their daughter cells. Alternative cell fates are thus a result of the interaction between extrinsic signals (operating through N signalling activation/inhibition between cells) and an intrinsic factor Numb, further regulating the N signalling.

2.2 Larval muscle differentiation

2.2.1 Larval myoblast fusion

After FCs are specified, they seed the formation of individual muscle fibres by fusing with FCMs, generating first syncytial muscle precursors (one FC fused with one or two FCMs), and by additional fusions forming a myotube. It is a directional and heterotypic process, as it always happens between FCs and FCMs, and not between two FCs or two FCMs (Bate, 1990; Dohrmann et al., 1990; Rushton et al., 1995). The myoblast fusion happens during stages 12 to 15, with the first fusions occurring at the most ventral edge of the mesoderm, between cells in

close contact with the nervous system. Muscle precursors appear exclusively in the most outer mesodermal layer, but they are not at first attached to the epidermis and show extensive processes. All precursors appear by the completion of germ band shortening at late stage 12/13. The pool of FCMs lies immediately internal to the precursors and becomes depleted as muscle precursors grow. Fusion continues as the attachment sites are being created. Depending on the specific muscle, there are between 2 to 25 fusions. The muscle size is also determined by the length of time for which fusion continues, thus, for example, the muscle 29 (VA3) is one of the smallest muscles. The mature larval muscle pattern can be seen at stage 16 (Bate, 1990).

In the *mbc* mutant, in which the fusion process is abolished, the expression of iTFs is correctly initiated in FCs, but the induction of these factors in FCMs does not occur (Rushton et al., 1995). It is thus FCs that hold all the necessary information about the future muscle, and after their fusion, FCMs adopt this distinctive program imposed by the FC (Crozatier and Vincent, 1999; Knirr et al., 1999). Furthermore, the FCM viability seems to depend on the fusion, since in several fusion mutants FCMs lose myosin expression and are eliminated (Doberstein et al., 1997; Rushton et al., 1995).

Based on phenotypes of mutants for genes involved at different stages of the fusion process, myoblast fusion can be described as follows: A. Migration, recognition and adhesion, B. Cytoskeletal rearrangements and plaque formation, C. Pore formation, D. Mixing of cytoplasms and nuclear reprogramming, E. Resetting of the fusion machinery.

A. Migration, recognition and adhesion

Unfused myoblasts display a teardrop shape, with a single pseudopod, resembling closely vertebrate myoblasts (Doberstein et al., 1997). Their shape and orientation suggest that they are attracted to the FCs, a process involving cell adhesion molecules (CAMs) of the Immunoglobulin (Ig) superfamily. Mechanisms of FCM attraction/migration towards FCs are still elusive. The FC expresses Dumbfounded (Duf), also known as Kin-of Irre (Kirre) (Ruiz-Gómez et al., 2000) and its paralogue Roughest (Rst), also known as Irregular chiasm C (Irre C), expressed by both FCs and FCMs (Strünkelnberg et al., 2001). Both genes arise from gene duplication (Strünkelnberg et al., 2003), encoding for single-pass transmembrane proteins, with five extracellular Ig domains and are functionally redundant (Strünkelnberg et al., 2001). While individual mutations in *duf* or *rst* have very little consequence on muscle development, in double, *duf/rst* deficient embryos the fusion is blocked, with FCMs extending their filopodia in random orientations and failing to migrate towards FCs located closer to the ectoderm. Furthermore, *duf* or *rst* overexpression using *Wg-Gal4*, causes FCMs to redirect their migration towards sites of ectopic Duf/Rst expression in ectodermal bands, demonstrating that both of these proteins act as myoblast attractors at a distance (Ruiz-Gómez et al., 2000; Strünkelnberg et al., 2001).

On the other side, the FCMs specifically express Sticks and stones (Sns) (Bour et al., 2000) and its paralogue Hibris (Hbs) (Artero et al., 2001), in a N-dependent manner. Both are single-pass transmembrane proteins, with 8 (Sns) and 9 (Hbs) predicted extracellular Ig domains, followed by a Fibronectin type III domain. Similarly to *duf/rst* mutation, *sns* mutant embryos display a complete inability of FCs and FCMs to fuse. Sns and Hbs have overlapping functions, but Sns seems to have a dominant fusion function (Shelton et al., 2009).

B. Cytoskeletal rearrangements and plaque formation

Following cell recognition and adhesion, intracellular signalling mediated by the above-mentioned receptors is relayed to several adaptor proteins. Even though cell-adhesion molecules are necessary for myoblast fusion, it is believed that they do not bring cell membranes in close enough contact for the fusion to occur. Adaptor proteins are thought to be necessary for relaying the information to the actin cytoskeleton and actomyosin contractile networks **(Fig. 4)**.

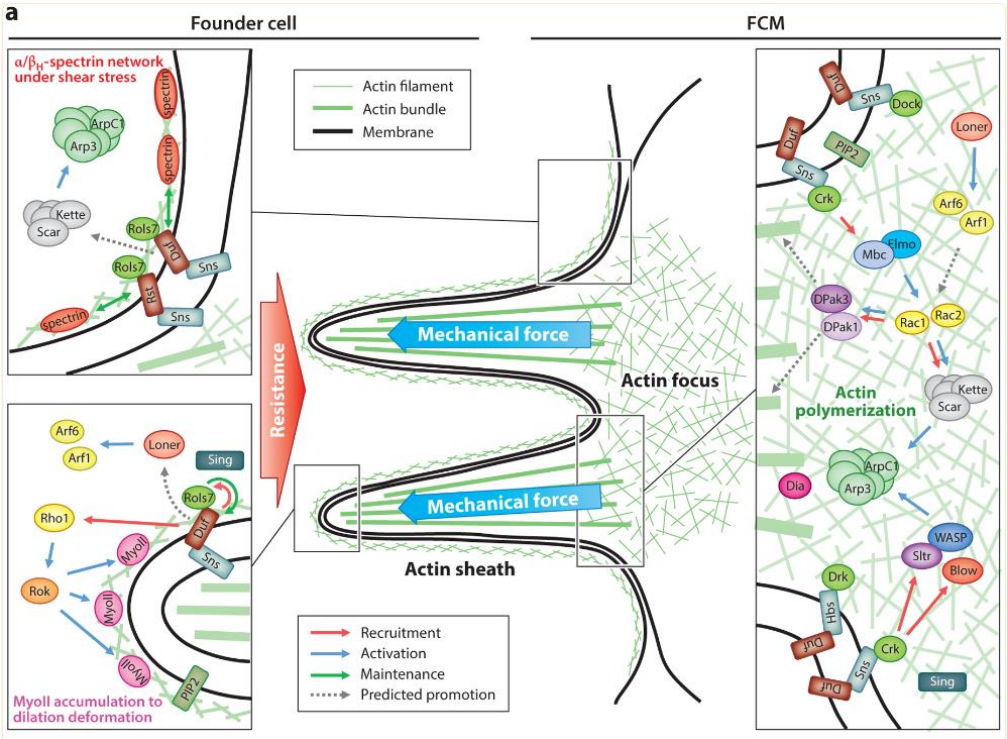

Figure 4. The process of myoblast fusion. Schematic representation of main players involved during *Drosophila* embryonic myoblast fusion. Illustration from (Lee and Chen, 2019).

Some adaptor proteins are present in both FCs and FCMs, such as Dreadlocks (Dock) (Kaipa et al., 2013), Loner, also known as Schizo (Siz) (Chen et al., 2003; Richardson et al., 2007) and Kette, now known as Hem (Richardson et al., 2007; Schröter et al., 2004), and some are specific to either of these two cell populations. Among them, Rolling pebbles (Isoform7, Rols7), also known as Antisocial (Ants) (Chen and Olson, 2001; Menon and Chia, 2001; Rau et al., 2001) is FC-specific, while previously mentioned Mbc (Rushton et al., 1995), Solitary (Sltr), also known as WASp-interacting protein (dWIP) or Verprolin 1 (Vrp1) (Kim et al., 2007) and Blown fuse (Blow) are required in FCMs (Haralalka et al., 2011; Jin et al., 2011).

Downstream of adaptor proteins is the actin cytoskeleton Actin-related protein complex Arp2/3 (Massarwa et al., 2007; Schäfer et al., 2007), which becomes activated during the fusion process by nucleation-promoting factors Scar (Berger et al., 2008; Richardson et al., 2007; Sens et al., 2010) and Wiskott-Aldrich Syndrome protein (WASp) (Massarwa et al., 2007; Schäfer et al., 2007).

Morphological analyses of the fusion processes described underlying actin-based processes occurring during this process. The first transmission electron microscopy (TEM) description of the myoblast fusion stated that early contact sites between fusing myoblasts are enriched in about 40 nm-sized vesicles, located near the plasma membrane in both FCs and FCMs. These pairs of vesicles, one in each cell, line up with each other across the apposed plasma membranes, with electron-dense material present around and between them, and were termed as prefusion complex (**Fig. 5B**). The prefusion complex was then proposed to resolve into short-lived electron-dense membrane plaques along the cytoplasmic face of the apposed membranes (**Fig. 5D**) (Doberstein et al., 1997).

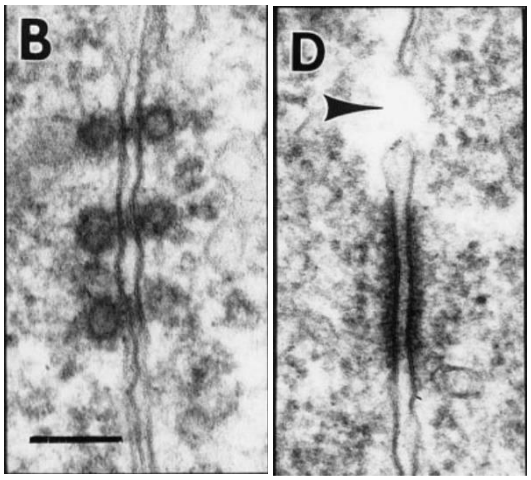

Figure 5. Ultrastructural features of myoblast fusion. (B) Paired vesicles between fusing myoblasts. **(D)** An electron-dense plaque, with a presumptive fusion pore indicated by an arrow. Panels from (Doberstein et al., 1997).

Subsequent studies, using confocal imaging, showed that during early fusion, F-actin in FCMs forms filopodia projections directly towards a FC/myotube. At the contact points, a ring-shaped accumulation of Sns in FCM filopodia and on the opposite side, in the FC, of Duf and Rols7 was described and named FuRMAS (fusion-restricted myogenic-adhesive structure). The centre of the ring is enriched in F-actin in both cells. FuRMAS was thus proposed to function as a link between adhesion molecules and other proteins leading to the rearrangement of actin cytoskeleton (Kesper et al., 2007). Spherical F-actin foci were also detected using live imaging, showing that they measure around 2 μm^2 in size, are highly dynamic with a lifetime of around 12 min and importantly, that their dissolution directly precedes and is necessary for the fusion event (Richardson et al., 2007). Actin-foci were shown to contain several actin regulators, such as WASp (Schäfer et al., 2007), Sltr/dWIP/Vrp1 (Kim et al., 2007), Mbc and Kette/Hem (Richardson et al., 2007). Reconciling these two descriptions, it was proposed that FuRMAS appear prior to the prefusion complex (Kesper et al., 2007), followed by the exocytosis of electron-dense vesicles of the prefusion complex, in an presumably actin polymerisation-dependent manner (Kim et al., 2007).

Subsequent higher-magnification studies showed that actin foci are not symmetrical as previously thought, but that the F-actin focus resides predominantly in the FCM, with only a thin actin sheath on the opposing FC membrane. Interestingly, the actin focus in the FCM acts as a podosome-like structure (PLS), distinct from filopodia, that invades the juxtaposed FC membrane, creating an inward curvature. This actin focus forms finger-like protrusions, a process that involves both SCAR and WASp that invade the FC and evolve into a fusion pore, a process that is dependent solely on WASp **(Fig. 6)**. The asymmetric cell adhesive junction and the exocytosis of prefusion vesicles led to the proposition that myoblast fusion involves an

asymmetric *fusogenic synapse*, analogous to neural and immunological synapses (Sens et al., 2010).

The PLS apply mechanical pressure on the thin FC actin sheath, which mounts a nonmuscle Myosin II (Myo-II) mechanosensory response, creating tension for resisting the PLS invasion, which promotes cell membranes to get into close enough contact and juxtapose before fusion (Kim et al., 2015).

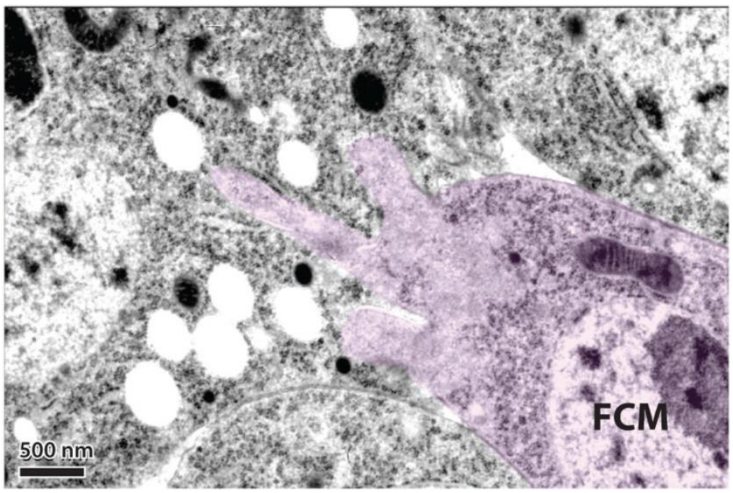

Figure 6. Ultrastructural analysis of the fusion contact. During fusion, the FCM projects several finger-like protrusions towards FC. Image adapted from (Sens et al., 2010).

Interestingly, Spectrin, known as a membrane skeleton scaffold protein for maintaining the cell shape is required in FC to restrict the boundaries of the fusogenic synapse (Duan et al., 2018). Both F-actin foci and Spectrin dissolve prior to the pore formation.

C. Pore formation

Initial ultrastructural observations of the fusion process revealed the presence of several membrane discontinuities, leading to the proposition that several fusion pores are established between fusing cells (Doberstein et al., 1997). These observations proved to be the artefacts of the fixation methods used for TEM, and using the high-pressure freezing and freeze substitution (HPF/FS) EM method instead, it was proposed that fusion pore is, in fact, a single-channel opening, ranging from 300 nm to 1.5 μm in size (Sens et al., 2010). No electron-dense vesicles or plaques were observed using this method, suggesting they may correspond to early events in the fusion process or are also artefacts of the room-temperature fixation methods. Whether these two models of one single pore involving the invasive podosome and of several smaller pores before membrane merging exclude each other or could coexist remains unclear (Schulman et al., 2015). Furthermore, the molecular players involved in pore formation remain also elusive (Lee and Chen, 2019).

D. Mixing of cytoplasms and nuclear reprogramming

As mentioned previously, after fusion the nucleus of the FCM adopts the transcriptional fate of the FC (Dohrmann et al., 1990; Rushton et al., 1995). This has been demonstrated in vivo, using a fusion construct between *ap* and the DsRed fluorescent protein, expressed specifically in the FC. Upon fusion of the FCM with the myotube, the initially DsRed-negative nucleus of the

FCM starts to express *ap* within 5 min post-fusion (Richardson et al., 2007). How this nuclear reprogramming occurs, and what proportion of FC-specific genes start to be expressed by FCMs is well not understood. Since FCs and FCMs both derive from MPs, FCMs have expressed iTFs transiently during their development (Buff et al., 1998a; Carmena, Murugasu-Oei, et al., 1998). This transient iTF expression does not however seem to bias them to fuse with a specific fibre, but FCMs are thought to be naïve and follow local cues. It was proposed that after fusion, the FCM reprogramming involves the loss of FCM-specific genes, such as *sns*, and subsequent activation of FC-specific genes, namely *duf* (Bataillé et al., 2017). The high energetic requirements of FCs to fuse and accommodate all the new nuclei are met by stimulation of glycolysis and of the TOR pathway in these cells (Tixier et al., 2013). After FC and FCM fuse, the nuclei of FCMs are positioned along the periphery of the myotube in a microtubule-dependent manner. The positioning of nuclei is far from being random because when incorrect, the muscle function is perturbed (reviewed in Azevedo & Baylies, 2020).

E. Resetting of the fusion machinery

It is believed that myoblast fusion is an iterative process (Beckett and Baylies, 2007), where the myotube resets the fusion machinery after each round of fusion with the FCM. Rols7/Ants is involved in this process, by returning and stabilising Duf to the membrane (Menon et al., 2005). Interestingly, 1 to 2 fusion events can occur in Rols7/Ants absence, suggesting that other players are involved in this process (Chen and Olson, 2001).

Depending on the muscle, FC incorporate a predetermined number of nuclei, which led to the notion of fusion counting. It was proposed that the fusion counting could be controlled by iTFs and it was indeed demonstrated to be the case at least for *eve*, *lb* and *S59/slou*. They achieve this by regulating the expression of genes involved in actin cytoskeleton and adhesion, *Muscle protein 20* (*Mp20)*, *Paxillin* (*Pax*) and *M-spondin* (*mspo*) in a fibre-specific manner (Bataillé et al., 2010).

2.2.2 Larval myofibrillogenesis

Alongside and after myoblast fusion is complete, each muscle elongates towards the epidermis to create stable junctions with the exoskeleton, called myotendinous junctions (MTJ) (reviewed in Moucaud et al., 2023; Schweitzer et al., 2010) and becomes innervated by motoneurons, creating neuromuscular junctions (NMJ) (reviewed in Menon, Carrillo, et Zinn 2013). Concurrent with the establishment of MTJs and NMJs, myotubes build their contractile apparatus that supports muscle contraction.

The contractile apparatus is composed of an array of sarcomeres, defined by two bordering Z-discs. Z-discs cross-link the plus-ends of thin actin filaments while the minus-ends of actin filaments face towards the centrally located thick myosin filaments that anchor at the M-line. Each myosin consists of a myosin tail and two myosin heads that attach to actin filaments, where the myosin motor moves its heads and pulls on actin filaments that slide towards the M-line, leading to sarcomere shortening (Huxley and Hanson, 1954; Huxley and Niedergerke, 1954). Even though the sarcomere structure was resolved many years ago, the orderly events

leading to its development are still unknown, and are a topic of intensive research, currently favouring a model of sarcomere components self-assembly (Kolley et al., 2024).

For muscle differentiation to occur, it is thought that iTFs not only determine the fate of FCs but also activate so-called downstream realisator genes. Even though only a few of them were identified, realisator genes are thought to control muscle properties such as the specific attachment and number of fusion events (Bataillé et al., 2010). In concert with iTFs acts Myocyte enhancer factor 2 (Mef2), a conserved master muscle differentiation factor. Its loss of function (LOF) does not prevent initial muscle specification, but completely blocks muscle differentiation leading to muscle apoptosis at later stages, without any syncytial fibre formation (Bour et al., 1995; Lilly et al., 1995; Ranganayakulu et al., 1995).

Extensive efforts were put into identifying GRNs downstream of Mef2, which seems to control all major muscle differentiation steps (Junion et al., 2005; Sandmann et al., 2006). Indeed, genes involved in myoblast fusion, NMJ and MTJ establishment and energy production, but also genes involved in the early specification, such as genes of the N pathway and several iTFs were found to be Mef2 targets. Among these are also *Hox* genes, such as *Abdominal-A* (*Abd-A*) (Junion et al., 2005) and *Ultrabithorax* (*Ubx*) (Sandmann et al., 2006). Since *Mef2* mutations allow for early muscle specification steps to occur, it is believed that Mef2 acts as an additional regulatory layer to help buffer stochastic fluctuations in iTFs expression levels (Sandmann et al., 2006). Knowing that Mef2 expression increases during development, its target genes were shown to respond to distinct levels of Mef2, e.g. genes requiring higher levels are activated later, partially explaining how Mef2 can control such a vast array of genes at different time points of muscle development (Elgar et al., 2008). Mef2 is regulated by many distinct inputs including autoregulation (Cripps et al., 2004), other TFs such as Twi (Cripps et al., 1998) and Lmd (Cunha et al., 2010), by microRNAs (Chen et al., 2012) and most recently described in *Drosophila* muscles, by phosphorylation (Vishal et al., 2023).

During late differentiation, the guidance of myotubes towards tendon cells and their targeting occurs during stages 14-15 and is completed at stage 16. When muscle contraction starts, mechanical forces stabilise MTJs by reducing integrin turnover (Pines et al., 2012). In parallel to FC specification, NBs differentiate into motoneurons (MNs) (Landgraf et al., 1997) and extend filopodia towards muscles to find their target at stage 14 (reviewed in Nose, 2012). Finally, the sarcomere assembly is initiated at stage 17, where first coordinated muscle contractions can be observed (Crisp et al., 2008). Embryonic muscles allow larvae to hatch, to crawl and feed. By continuous feeding, larvae increase their mass 200-fold (Church and Robertson, 1966), and their muscle fibres grow almost 100-times by endoreplication (S. Wang et al., 2018), without any increase in sarcomere length, suggesting that new sarcomeres need to be added during larval life by an unknown mechanism (Demontis and Perrimon, 2009).

2.2.3 Final larval muscle pattern

At stage 16, every abdominal segment between A2-A7 displays a stereotypical pattern of 30 muscles and segments A1, A8 and thoracic segments display muscle patterns which is a variation of the A2-A7 pattern. Using an enhancer trap insertion rP298-lacZ (Nose et al., 1998), recapitulating the expression of *duf/kirre* (Ruiz-Gómez et al., 2000), MPs can be seen from stage 11 and their division into FCs from mid stage 12. Using this marker, the 30 abdominal

muscles in A2-A7 segments were divided into four domains according to the position of their progenitors along the D-V axis (Nose et al., 1998) (colour-coded in **Fig. 7**) :

I. Dorsal domain comprising muscles: 1 (DA1), 2 (DA2), 9 (DO1) and 10 (DO2)

II. Dorsolateral domain comprising muscles: 3 (DA3), 4 (LL1), 11 (DO3), 18 (DT1), 19 (DO4) and 20 (D05)

III. Lateral domain comprising muscles: 21-24 (LT1-LT4) and 26 (VA1), 27 (VA2), 29 (VA3), for VA1-VA3 the progenitors lie in the lateral domain even though the final muscle position is in the ventral domain

IV. Ventral domain comprising the highest number of muscles: 5 (LO1), 6 (VL3), 7 (VL4), 8 (SBM), 12 (VL1), 13 (VL2), 14 (VO2), 15 (VO4), 16 (VO5), 17 (VO6), 25 (VT1), 28 (VO3) and 30 (VO1).

Muscle names are indicated as follows: muscle position (D, dorsal; V, ventral; L, lateral) followed by orientation (A, acute; L, longitudinal; O, oblique; T, transverse); SBM, segment border muscle. With the marked exception of VA1-3 muscles, muscles differentiate close the position of their MP.

The division that is more commonly used considers the muscle position with respect to the ectoderm (**Fig. 7**):

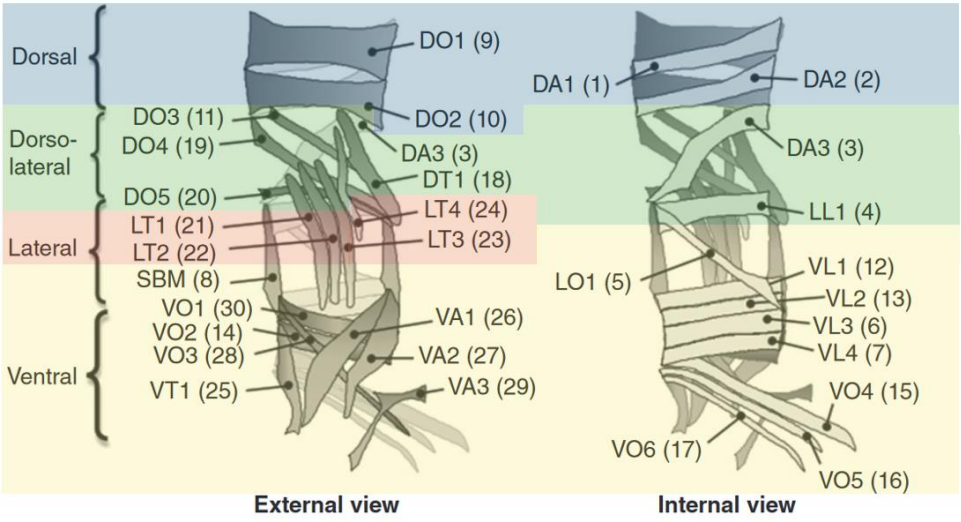

Figure 7. Schematics of larval muscle pattern. Muscles are color-coded according to their position along the DV axis and two views, external and internal with respect to the epidermis are shown. Adapted from (Dobi et al., 2015).

I. External muscle layer which is just below the epidermis: DO1, DO2, DT1, LT1-LT4, VA1-VA3 and VT1

II. Intermediate muscle layer: DO3-DO5, SBM, VO1-VO6

III. Internal muscle layer which is the furthest away from the epidermis: DA1-DA3, LL1, LO1, VL1-VL4

There are several variations on this canonical muscle pattern along the A-P axis. The A1 segment lacks muscle VT1 and VO6 muscles and has one additional muscle compared to other abdominal segments (Bate, 1990). As a general rule, thoracic segments present gradually fewer larval muscles than abdominal segments, e.g. the T3 lacks VO4 and VO5 muscles, T2 lacks muscles VO3-5 and T1 has no VO muscles (Hessinger et al., 2017).

Part 3. Adult muscle development

3.1 Adult muscle pattern

The adult fly muscles consist of flight muscles, leg muscles, abdominal muscles and a jump muscle, also known as the tergal depressor of the trochanter (TDT) **(Fig. 8)**. Flight muscles are further composed of indirect flight muscles (IFMs) that power the wing stroke and direct flight muscles (DFMs) that regulate the wing angle. IFMs are composed of six fibres of dorsal longitudinal muscles (DLMs) that span the thorax dorsolaterally and depress the wing and seven fibres of dorsoventral muscles (DVMs) that span the thorax dorsoventrally and elevate the wing (Fernandes et al., 1991). DFMs are comprised of several smaller muscles, referred to as 49 to 58 (Müller et al., 2010). In adult legs, there are 14 multifibre muscles composed of about 140 muscle fibres that are located in the coxa, femur, trochanter and tibia leg parts, while the tarsus is devoid of muscles. These 14 multifibre muscles are divided into two major types, depressor and dorsal levator muscles, that at the ultrastructural level differ by their sarcomere size and mitochondrial content (Soler et al., 2004). In the abdomen, there are three major adult muscle groups, ventral (5-8 fibres), lateral (20 fibres) and dorsal (17-22 fibres) and a small muscle associated with the lateral spiracle (Currie and Bate, 1991).

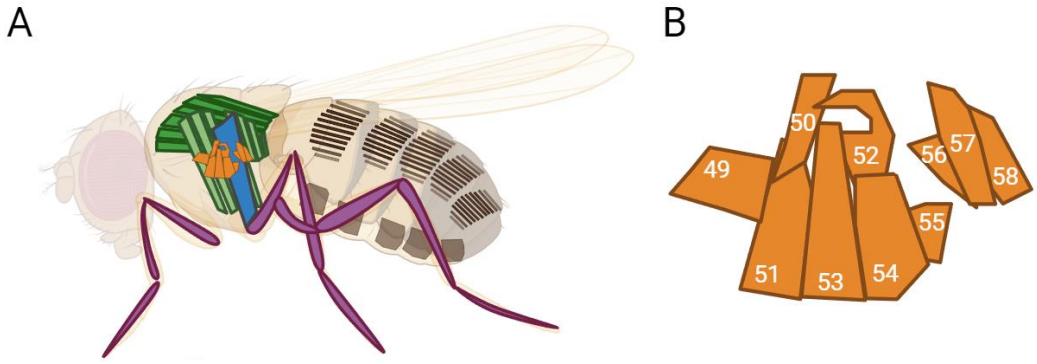

Figure 8. Adult *Drosophila* muscle pattern. (A) The biggest muscle in the adult fly is the flight muscle, composed of indirect flight muscles, which are composed of DLMs (dark green) and DVMs (light green), and direct flight muscles (orange). Between DVMs and direct flight muscles locates the jump muscle (blue), there are leg muscles in each pair of legs (magenta) and abdominal muscles in the abdomen (brown). **(B)** Zoom and nomenclature of direct flight muscles. Adapted from (Everetts et al., 2021; Müller et al., 2010). DLM - dorsal longitudinal muscles, DVM - dorsoventral muscles

3.2 Specification of adult muscle progenitors

Drosophila adult muscles arise from adult muscle progenitors (AMPs) that develop at embryonic stage 12 from the division of MPs, as sister cells of larval FCs. There are between 15-18 AMPs per thoracic segment and 6 per abdominal segment, in the abdomen divided into one ventral (vAMP), two lateral (lAMPs), two dorsolateral (dlAMPs) and one dorsal AMP (dAMP) (Bate et al., 1991) **(Fig. 9)**.

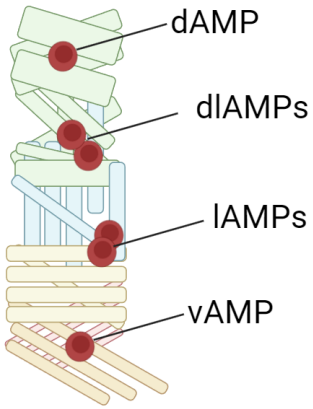

Figure 9. AMPs division along the DV axis. Scheme of AMP positioning with respect to larval muscle fibres along the D-V axis in an embryonic abdominal segment.

AMPs do not fuse and do not divide during embryogenesis, and associate with imaginal discs in the thorax and with the peripheral nervous system (PNS) in the abdomen (Bate et al., 1991; Broadie and Bate, 1991; Currie and Bate, 1991). They are closely associated with larval muscles and nerves in both the abdominal (Figeac et al., 2010) and thoracic segments (**Fig. 10**). In the abdomen, lAMPs not only associate with nerves but actively contribute to the larval muscle innervation (Lavergne et al., 2020).

That AMPs arise as sister cells of larval founders was identified while studying the promuscular cluster 10, where two MPs are singled out one after the other, the second progenitor giving rise to one FC, later differentiating into larval muscle 29 (VA3) and its sister cell into a ventral AMP (vAMP) (Carmena et al., 1995). A similar principle was demonstrated for a progenitor that gives rise to muscle 8 (SBM) and 2 lateral AMPs (lAMPs), which is under the control of *lb* (Jagla et al., 1998). As described above for larval founders, the MP division that produces AMPs also requires Numb asymmetric expression, where Numb is inherited by only the FC and not by the AMP. Consequently, in the *numb* mutant, the vAMP is duplicated, while the VA3 muscle is missing. All six AMPs present in abdominal segments 2 to 7 (A2-7) are also duplicated in this condition. Conversely, in the *N* mutant embryos, AMPs do not generate, together with *numb* mutant data demonstrating that N activity is required for allocating the AMP fate. In all these cases, the formation of AMPs is associated with the repression of iTF expression (Ruiz Gómez and Bate, 1997) and the maintenance of Twi expression (Bate et al., 1991; Thisse et al., 1988). AMP specification is also dependent on the EGF-Ras pathway that protects them from apoptosis, but not on the FGF pathway (Figeac et al., 2010).

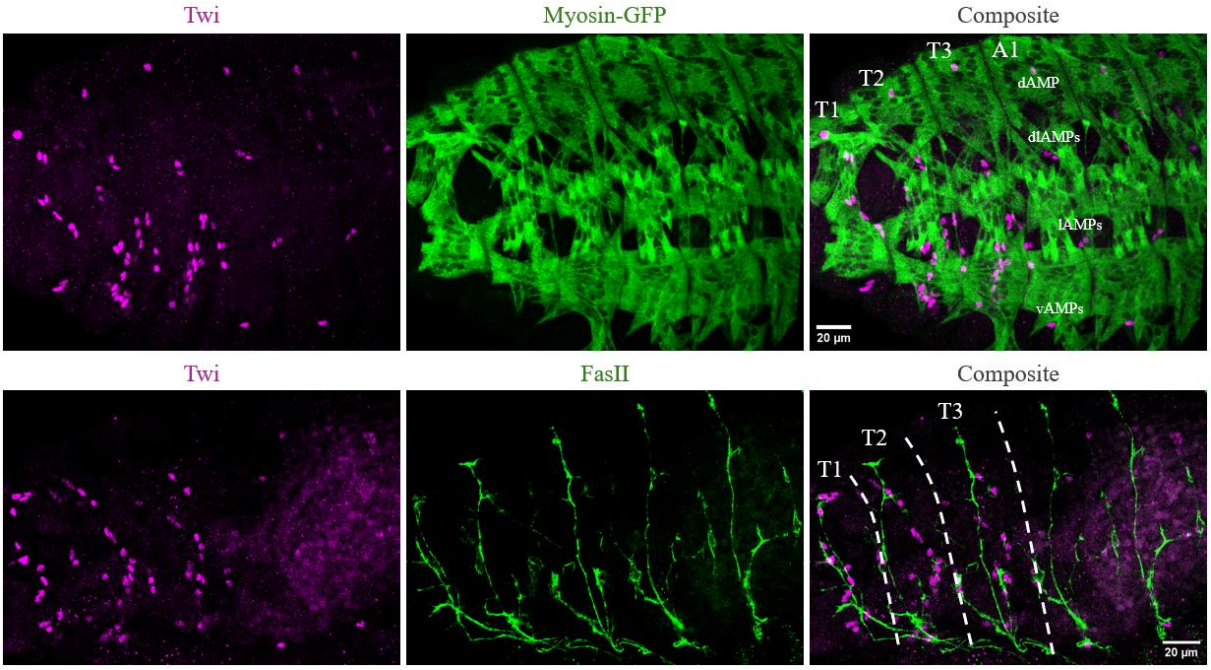

Figure 10. AMPs closely associate with larval muscles and nerves. (Top) Confocal projection of stage 15/16 embryo labelled with GFP to visualise Myosin (green) and anti-Twi to visualise AMPs (magenta). Embryos carry the transgene *weep26*, where GFP is inserted in the *Mhc* gene (Orfanos and Sparrow, 2013). (Bottom) Confocal projection of Wild-type stage 15 embryo labelled with anti-FasII antibody to visualise motor axons (green) and anti-Twi to visualise AMPs (magenta). T1, T2 and T3 depicts the three thoracic segments and A1 is the first abdominal segment. My unpublished data.

Besides expressing *Twi*, AMPs in the abdomen express *N* pathway target genes *Enhancer of split m6* (*E(spl)m6)* and *Holes in muscles* (*Him*) as well as TFs *Zn finger homeodomain 1* (*Zfh1)* and *Cut (Ct)*. Other markers can be found in subsets of AMPs, such as *S59/slou* and *Poxm* in vAMPs, *lb* and *Kr* in lAMPs, demonstrating that AMPs are a heterogeneous population. The expression of *lb* in lAMPs was shown to be dependent on the EGF pathway. Interestingly, the enhancer sequence driving *lb* expression in lAMPs alone, or both in lAMP and its sister cell, differentiating into SBM larval muscle were identified. While both enhancers showed sequences responsive to Lb and EGF effectors, the common enhancer for lAMP and SBM showed an additional Mef2-binding site, providing important molecular cues about distinct regulation between FCs and their AMP sister cells (Figeac et al., 2010).

Using a membrane-tagged GFP reporter it has been shown that in late embryos abdominal AMPs form an interconnected network by sending long cellular processes along PNS nerves. When disconnected by laser ablation, AMPs become highly mobile, fail to re-establish contacts and in some cases undergo cell division, suggesting that these connections are involved in quiescence maintenance (Figeac et al., 2010).

In the thorax, three segments can be distinguished. While the precise lineage of thoracic AMPs is not known, we know that AMPs giving rise to flight muscles associate with the wing disc in the second thoracic segment (T2), while AMPs giving rise to leg and jump muscles are associated with leg discs (Bate et al., 1991; Fernandes et al., 1991; Lawrence, 1982). It is not straightforward to distinguish the flight and leg AMPs and their precise numbers at the embryonic stage, due to their localisation in between disc primordia (**Fig. 11**). Some myoblasts

associate with the haltere disc in the third thoracic segment (T3) (Roy et al., 1997), probably contributing to one indirect power muscle and seven direct steering muscles (Dickerson et al., 2019). Whether AMP specification in the thorax involves Notch/Numb and EGF pathway was not studied.

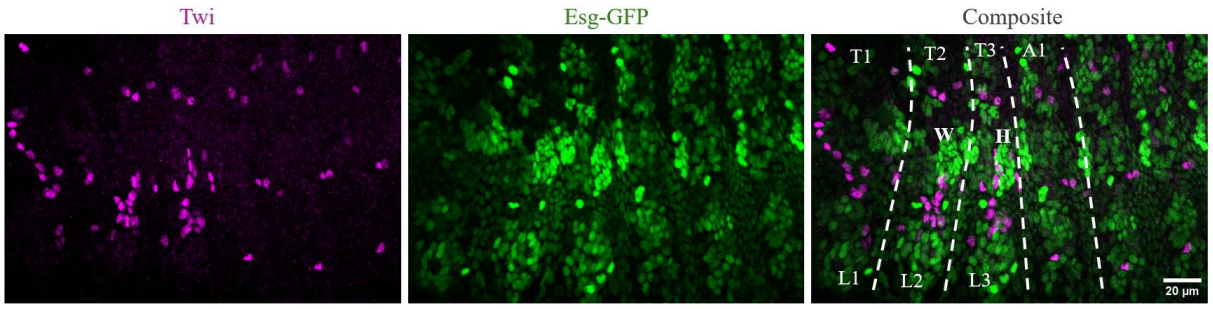

Figure 11. Thoracic AMP localisation with respect to disc primordia. Confocal projection of stage 15 embryo labelled with GFP to visualise Escargot (Esg), labelling wing and leg disc primordia (green) and anti-Twi to visualise AMPs (magenta). Embryos carry the transgene *esg::GFP* (gift from C. Estella). T1, T2 and T3 depict the three thoracic segments and A1 is the first abdominal segment. My unpublished data. W- wing, H-haltere, L1-L3 - legs

3.3 Adult muscle differentiation

3.3.1 Exit from quiescence and proliferation

During the mid-second larval stage, AMPs are reactivated, exit quiescence and start to proliferate (Bate et al., 1991). How this is achieved was discovered relatively recently and similarly to neural stem cells (P.-K. Nguyen and Cheng, 2022), involves a nutritional checkpoint. At least in abdominal AMPs, neighbouring muscles were shown to provide Insulin-like peptide 6 (dilp6), activating the Insulin/TOR pathway in AMPs, leading to ligand-independent Notch activation, activating dMyc, driving AMP proliferation. It has been proposed that neighbouring muscles thus act as a niche for AMPs, contacted by both AMP cell bodies and also by thin filopodia extended from them, referred to as homing behaviour (Aradhya et al., 2015). These studies shift our perspective about the shape and dynamics of AMPs, which are connected not only to each other sending long processes (Figeac et al., 2010), but also to specific neighbouring muscles sending shorter thin projections, which seems crucial for their positioning but also survival (Aradhya et al., 2015). When abdominal AMPs start to proliferate during the second larval stage, they change their shape from elongated to rounder and reach the number of 8-15 cells per abdominal group, with a total of six AMP groups in the L3 larvae (Aradhya et al., 2015; Currie and Bate, 1991).

In the thorax, whether the exit from quiescence and subsequent proliferation of AMPs involves the Insulin-Notch-dMyc axis is not known. Nevertheless, many studies focused on the proliferation of easily accessible wing disc-associated flight AMPs during larval stages (referred for simplicity as myoblasts at this stage), demonstrating, that the wing disc epithelium acts as a stem cell niche, providing many signalling molecules for myoblast maintenance and proliferation (Gunage et al., 2014). Myoblasts adhere to the disc epithelium via niche-adhering cytonemes, which create an FGF-signalling loop that reinforces the adhesion (Patel et al., 2022).

The number of flight AMPs in the larva was shown to increase from 10 to 250 during the second larval stage (L2) (Gunage et al., 2014) and to at least 1500 at the end of the third larval stage (L3) (Poliacikova et al., 2023).

This intensive proliferation of wing disc-associated myoblasts was shown to be dependent on several signalling pathways. It is dependent on the Wg signalling coming from underlying wing disc epithelium, which maintains Vg myoblast expression (Sudarsan et al., 2001) and also on Moleskin (Msk)/Importin-7 (Dim7), through the regulation of Armadillo (Arm), Wg pathway effector (Vishal et al., 2017).

Unlike in the abdomen where AMP proliferation does not involve asymmetric cell division (Aradhya et al., 2015), it was proposed that the thoracic flight AMP division involves an initial symmetrical division happening until L2 and subsequent asymmetric cell divisions during L3, dependent on the Notch/Numb pathway. The mitotically active cells were found to localise immediately adjacent to wing disc epithelium, first aligning their mitotic spindle parallel to epithelial cells, resulting in symmetrical divisions and later aligning their mitotic spindle perpendicular to epithelial cells, resulting in asymmetric divisions, where one cell loses contact with the niche and becomes postmitotic. Unlike in the abdomen, this division was shown to be dependent on Notch ligand-dependent signalling, where wing disc epithelium would provide the Serrate (Ser) Notch ligand to adjacent AMPs. The switch to the asymmetric division mode during L3 was shown, like during embryonic AMP specification, to depend on Numb. Numb in AMPs is activated by Wg, secreted from disc epithelium during the L3 stage, demonstrating how Notch and Wg pathways integrate to regulate myoblast proliferation (Gunage et al., 2014).

Wing disc-associated myoblast proliferation depends also on the FGF pathway, by acting on Wg signalling (Everetts et al., 2021; Vishal et al., 2020). Interestingly, the FGF pathway was also shown to regulate the number of leg disc-associated myoblasts (Maqbool et al., 2006) and non-autonomously the number of adult abdominal muscles (Sarkissian et al., 2016).

3.3.2 Adult founder cell selection

Like in the case of larval muscles, the fusion to create adult muscles happens between FCs and FCMs. One important difference between larval and adult muscles is that while larval muscles are composed of a single fibre, seeded by a single FC, adult muscles are composed of multiple fibres, seeded by several FCs. The important question that arises from this observation is how several founders are selected for each multi-fibre adult muscle. Another difference is that while embryonic FCs are born from the division of MPs, shortly after their specification, adult FCs are selected from the AMP pool much later, at the beginning of the pupal stage (Dutta, 2004; Rivlin et al., 2000).

The first adult FCs were described for the TDT and DVMs, composed of three muscle groups (I, II, and III), where group I is composed of three fibres, and groups II and III are composed of two fibres, giving together seven DVM fibres (Rivlin et al., 2000). The FCs for each of these seven fibres can be detected at 7 h APF (hours after puparium formation) at the precise location where DVM fibres will develop, and like in the case of embryonic FCs, these cells are Duf-positive. They were presumed to originate from the wing disc (Dutta, 2004). Interestingly, it was proposed that DVM FCs and TDT FCs could originate from leg discs instead (Atreya and

Fernandes, 2008; Rivlin et al., 2000). In the same way, each abdominal fibre is preceded by a Duf-expressing FC that can be visible at 24 h APF (Dutta, 2004) and Duf-positive AMPs were detected invaginating inside the leg disc at the early pupa stage (Soler et al., 2004).

DLMs display a different way of development, in which the role of founders is assured by so-called persisting larval muscles DO1-DO3 (Fernandes et al., 1991). In the absence of these larval muscles, DLM development proceeds at the correct localisation *de novo*, like in the case of DVM muscles, but is markedly delayed and an aberrant number of adult DLM fibres develop (Farrell et al., 1996). It is thus thought that the use of larval muscles as founders is a superimposition on the existing mode of *de novo* adult fly muscle development (Fernandes and Keshishian, 1996). These larval muscles are called persisting because by an unknown mechanism, they escape histolysis that operates in early pupa until 12 h APF and is used to eliminate most larval muscles (Fernandes et al., 1991). Like other adult FCs, larval scaffolds express Duf starting from 7 h APF (Dutta, 2004).

For all the above-mentioned muscles, it was found that at the L3 stage, all AMPs express low levels of Duf (which is not the case in the embryo (Ruiz-Gómez et al., 2000)) and then by 12 h APF in flight AMPs and by 24 h APF in abdominal AMPs, this uniform expression is replaced by a specific, strong expression in few cells. The selection of adult FCs does not depend on the Notch/Numb pathway like in the embryo but depends at least in the abdomen on the FGF/Htl signalling, involving an FGF scaffolding protein Heartbroken (Hbr, now known as Stumps) and an FGF negative regulator, Sprouty (Sty). How the Htl signalling becomes restricted to a particular set of founders and whether the same mechanisms operate in the thorax is not known (Dutta et al., 2005). It has been also suggested that the specification of founder cells depends on the segmental identity conveyed by *Hox* genes (see Chapter II) (Dutta et al., 2010).

The FCs for adult muscles localise at specific positions along the epidermis, at positions where the adult muscles will be located. AMPs thus need to migrate to these sites prior to their specification. How this is achieved remains elusive. For abdominal AMPs, by 13 h APF AMPs start to spread along the nerves and migrate along nerve growth cones and histoblasts (that will create adult epidermis), to create three final muscle groups (dorsal, lateral and ventral) and at 30h APF cells already organise in characteristic parallel rows (Currie and Bate, 1991).

For thoracic muscles, it is known that myoblasts leave the wing disc during the disc evertion around 6 h APF and that they migrate collectively in a swarm (Fernandes et al., 1991). They seem to follow a particular path along the nerves like in the abdomen (J. Fernandes and VijayRaghavan, 1993), but denervation does not hinder their migration (J. J. Fernandes and Keshishian, 2005). Nevertheless, innervation seems to be important for thoracic myoblast proliferation and differentiation (J. J. Fernandes and Keshishian, 1998). Similarly to larval FCMs, DLM myoblasts could be attracted towards larval scaffolds by their Duf expression (Ruiz-Gómez et al., 2000). How DVM myoblasts find their appropriate position is not known, but could possibly involve signals from the epidermis and/or the nerves (Dutta, 2004). It was suggested that flight myoblast migration may also involve the FGF receptor Htl (Michelson et al., 1998) and that DFM-contributing myoblast migration could involve secreted DWnt-2 (Kozopas and Nusse, 2002).

3.3.3 *Adult myoblast fusion*

After their migration, selected FCs enter the fusion process with the rest of AMPs (or larval templates for DLMs), for flight muscles spanning from around 12 h to 30 h APF and for abdominal muscles from 28 h APF up to 65 h APF (Currie and Bate, 1991).

In the case of DLMs, myoblast fusion is concomitant and required for the splitting of each of the three larval templates into two, which starts around 15 h APF and is completed by 20 h APF (Fernandes et al., 1991) **(Fig. 12)**. It is known that the splitting process involves the precise alignment of nuclei into rows, allowing for the fibre to separate in the middle by vacuolation, however how this process occurs at the molecular level is largely unresolved (Fernandes and Keshishian, 1996; Roy and VijayRaghavan, 1998).

Studies of genes involved in the pupal myoblast fusion have been hindered by the fact that their loss-of-function (LOF) mutations often lead to early lethality, because of their involvement in the larval muscle fusion. Nevertheless, similar molecular and cellular mechanisms seem to operate during larval and adult fusion, such as the presence and requirement of Duf/Rst-Sns/Hbs adhesion molecules (Gildor et al., 2012), the presence of F-actin-rich foci in FCMs, thin actin sheath in FCs, and the involvement of the same actin cytoskeleton regulators (Mukherjee et al., 2011).

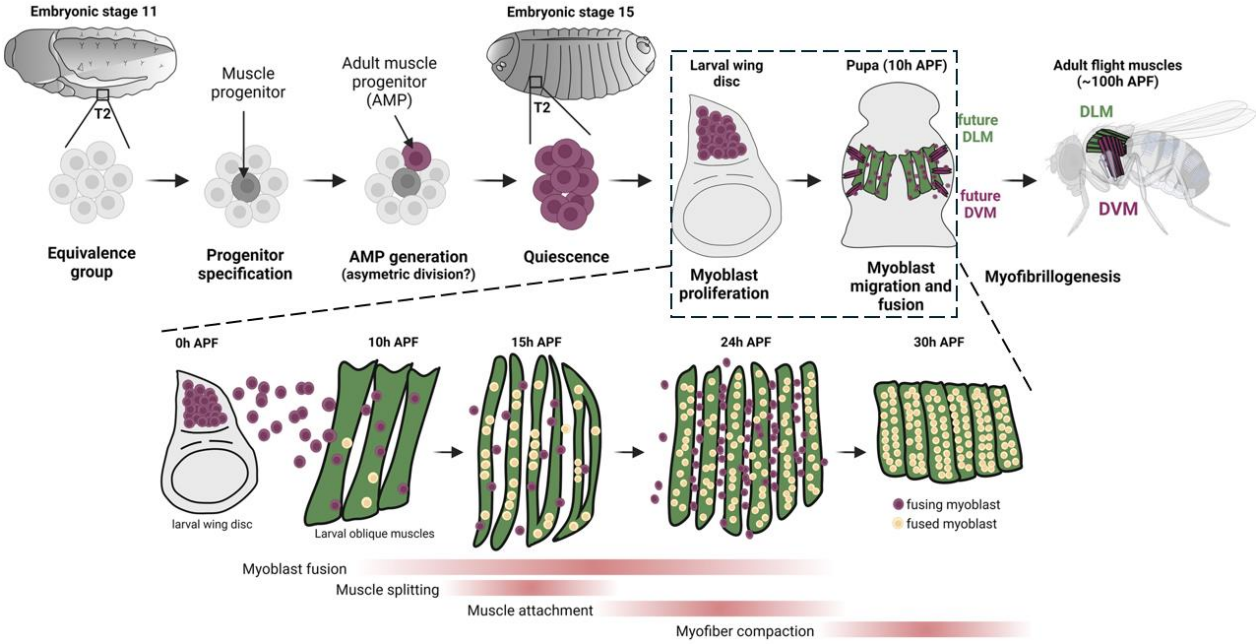

Figure 12. The development of *Drosophila* indirect flight muscles. Schematic representation of main steps of adult flight muscle development, starting with the AMP specification in the second thoracic segment (T2) at stage 12, association of AMPs with the wing imaginal disc, proliferation during larval stages, subsequent migration and fusion with larval scaffolds during early pupal development, splitting of three larval scaffolds into six myofibers around 15 h APF, that undergo compaction required for correct DLM myofibrillogenesis (in green). The zoomed view represents a detailed view of the steps and timing of larval muscle splitting. DVMs do not require a positional scaffold for their development, they fuse between each other and create seven adult fibres *de novo* (in magenta).

Thanks to the large size and easy accessibility for ultrastructural analysis, the fusion giving rise to IFMs was described in large detail (Dhanyasi et al., 2015; Segal et al., 2016). These studies showed that an initial tight cell apposition between myoblasts and larval templates (20 to 50 nm) is followed by flattening of the myoblast membrane towards the myotube, leading to an even tighter apposition (10-20 nm), requiring actin cytoskeleton, creating multiple point contacts, presumably initiating the fusion. This process, like in the case of larval fusion, requires WASp and SCAR/WAVE. In contrast to larval muscle fusion, where a single fusion pore seems to be created between fusing cells, multiple membrane discontinuities seem to be observed in the IFM fusion (Dhanyasi et al., 2015). The fusion is facilitated by a dense array of dynamic, actin-based filopodia that emanate from larval templates, that seem to direct myoblasts for fusion (Segal et al., 2016).

A very exciting, but not easily observable aspect of adult fusion is the dynamics of transcriptional changes that occur just prior to the fusion. While proliferating and migrating, DLM myoblasts are kept in a semi-differentiated state by a combined action of N and Twi (Anant et al., 1998; Bernard et al., 2006, 2010; Caine et al., 2014; Gildor et al., 2012). In the case of N conditional mutation in pupal AMPs, there is a premature loss of Twi expression and subsequent differentiation and conversely, Twi maintenance in pupal AMPs prevents differentiation and leads to muscle degeneration (Anant et al., 1998). Furthermore, besides its known role in cell fate determination, N has been shown to directly regulate genes that coordinate cell morphology (Pezeron et al., 2014).

During their migration, myoblasts seem to maintain the N signalling active and their transit-amplifying state by providing the Dl ligand to each other. There needs to be a fine balance in levels of Dl available, since both downregulation and upregulation of Dl in myoblasts lead to an increase of Sns, in the first case by premature differentiation and in the second likely via cis-inhibition (inhibition of N when the same cell presents the ligand and the receptor) (Gildor et al., 2012). Then, by an unknown mechanism, the N pathway and thus Twi expression is switched off, only when myoblasts reach the close proximity of the larval template, and molecules required for fusion, such as Sns and dWIP (Bernard et al., 2006; Gildor et al., 2012), but also additional regulators such as Erect-wing (Ewg) (DeSimone et al., 1996) start to be expressed. This is in sharp contrast with larval myogenesis, where Sns is expressed by all FCMs prior to fusion (Bour et al., 2000), whereas, in DLMs, Sns is expressed only in myoblasts closest to the fibres (Gildor et al., 2012). Interestingly, while the presence of filopodia on the larval template surface is required for fusion, it is not required for the initiation of Sns or dWIP expression in myoblasts, leaving the nature of the myotube-provided differentiation signal unresolved (Segal et al., 2016).

3.3.4 Adult myofibrillogenesis

Similarly to larval muscles, during and after fusion, myotubes undergo terminal differentiation, attach to the cuticle forming MTJs and are contacted by neurons, forming NMJs and the contractile apparatus.

Like during larval muscle differentiation, Mef2 is the major differentiating factor in the adult fly, described best in the case of IFM differentiation. Mef2 is activated in differentiating IFMs at least in part by Twi (Cripps et al., 1998) and Ecdysone (Lovato et al., 2005), but its function

is inhibited by interactions with Him and Zfh1 (Liotta et al., 2007; Postigo et al., 1999). Mef2 hypomorphic mutations resulted in weak IFM phenotypes, namely defaults in patterning due to improper muscle splitting and reduced fibre number (Baker et al., 2005; Cripps and Olson, 1998; T. Nguyen et al., 2002; Ranganayakulu et al., 1995). Using the RNA interference (RNAi) approach, it was shown that Mef2 knock-down (KD) in myoblasts leads to massive loss of virtually all somatic muscles, due to impaired myoblast fusion and activation of muscle structural genes. Downregulating Mef2 at the end of the fusion process led to mild phenotypes, suggesting that the majority of muscle differentiation post-fusion proceeds independently of Mef2 activity (Bryantsev, Baker, et al., 2012; Soler et al., 2012). Mef2 was shown to regulate fusion by directly regulating the MARVEL domain-containing fusion gene *singles bar* (*sing*), required both in FCs and FCMs (Brunetti et al., 2015) and to regulate some muscle structural genes, such as *tropomyosin* (Lin et al., 1996) and *paramyosin* (Arredondo et al., 2001).

It was proposed by a series of in vitro and in vivo experiments that Mef2 promotes IFM differentiation at least in part by inhibiting N signalling, by directly binding and activating, together with Scalloped (Sd) (requiring Vg for its TF function), the Dl enhancer in developing IFMs (Caine et al., 2014). Similarly, Vg was shown to promote differentiation via the regulation of a glycosyltransferase Fringe (Fng), leading to the inhibition of the N pathway (Bernard et al., 2006). IFM differentiation thus involves complex cross-regulations between negative signals, such as N, Twi and Him and positive signals such as Mef2 and Sd/Vg.

The formation of MTJs is completed in DLMs by 30h APF, followed by extensive muscle growth (Weitkunat et al., 2014), in the abdomen by 40 h APF (Weitkunat et al., 2017) and in legs, the final pattern of muscles and tendons is visible at 55 h APF (Soler et al., 2004). A special role in myofibrillogenesis was assigned to the mechanical tension that builds while muscles attach to tendons, and that is crucial for correct sarcomere morphogenesis (reviewed in Lemke & Schnorrer, 2017). At least in DLMs and the abdomen, the sarcomere formation starts immediately after the muscle attachment is completed and the mechanical tension is high, synchronously across the entire fibre (Spletter et al., 2018; Weitkunat et al., 2014, 2017).

At the end of myogenesis, the adult fly possesses two major distinct muscle types, depending on the nature of the contractile apparatus, namely the tubular muscles, with laterally aligned sarcomeres and synchronous contraction and fibrillar muscles, in which myofibrils are not laterally aligned and that display a stretch-activated mechanism of contraction, allowing for very fast contractions required for flight. All adult fly muscles are of the tubular type, except the IFM muscles (Schönbauer et al., 2011; Smith, 1961).

Chapter II. How to create muscle diversity? – Hox genes and mesodermal patterning

Part 1. Muscle diversification

1.1 Larval muscle diversification

During larval muscle development, two distinct levels of diversity need to be achieved: first, in every abdominal segment there are 30 different muscles and second, there is a different number of muscles between different larval segments. What are the sources of this diversity?

It is believed that it is the constellation of iTFs (referred to as iTF code) expressed by each founder, inherited from the MP, which determines the unique properties of the muscle fibre it gives rise to (**Fig. 13**). The idea of a combinatorial expression stems from the fact there are less iTFs than larval muscles and that mutant embryos for a single iTF have often a low phenotypic expressivity (reviewed in Poovathumkadavil & Jagla, 2020).

Many iTFs are homeodomain-containing TFs, such Ap (Bourgouin et al., 1992), Araucan (Ara), Caupolican (Caup) (Carrasco-Rando et al., 2011), Eve (Fujioka et al., 2005; Knirr et al., 1999), Lb (Jagla et al., 1998), Lms (Müller et al., 2010), Msh/Dr (Nose et al., 1998), Ptx1 (Vorbrüggen et al., 1997), Slou/S59 (Knirr et al., 1999) and Tailup (Tup) (Boukhatmi et al., 2012). Other iTFs such as Nau (Keller et al., 1997) and Col/Kn (Crozatier and Vincent, 1999) belong to the bHLH TF family, Org-1 (Schaub et al., 2012) and Midline (Mid) (Kumar et al., 2015) to the T-box TF family. Other iTFs are Sd/Vg (Deng et al., 2010), Runt (Fujioka et al., 2005) and Poxm (Duan et al., 2007). The list of iTFs was recently enriched by Eyes-absent (Eya), Sine oculis (So), No Ocelli (Noc) and ETS-domain lacking (Edl) (Dubois et al., 2016).

That the expression of a specific iTF could convey a specific muscle fate was first demonstrated for *apterous*, where in *ap* mutant, there is a variable loss of *ap*-expressing muscles. Conversely, upon *ap* mesodermal overexpression, muscle duplication of *ap*-expressing muscles occurs (Bourgouin et al., 1992). This has been shortly after demonstrated in embryos with altered expression of *Kr* (Ruiz-Gómez et al., 1997), *muscle segment homeobox* (*msh*), now known as *drop* (*dr*) (Nose et al., 1998) and *lb* (Jagla et al., 1998).

This led to the hypothesis that by altering patterns of iTF expression in MP/FC one could induce predictable changes in muscle characteristics. This was first demonstrated in the case of ventral *Kr*-expressing muscles. The first progenitor singled out from cluster 10 expresses both *S59* and *Kr*, giving rise to two distinct FCs, only one retaining *S59/Kr* expression, becoming the VA2 muscle. Its sister FC loses the marker expression and differentiates into the VA1 muscle. In the *Kr* mutant condition, the expression of S59 even though initiated is not maintained in one of two FCs, and two VA1-like muscles are produced. Conversely, upon *Kr* mesodermal overexpression, the *S59* expression is maintained in both sibling founders, and two VA2-like muscles are produced (Ruiz-Gómez et al., 1997).

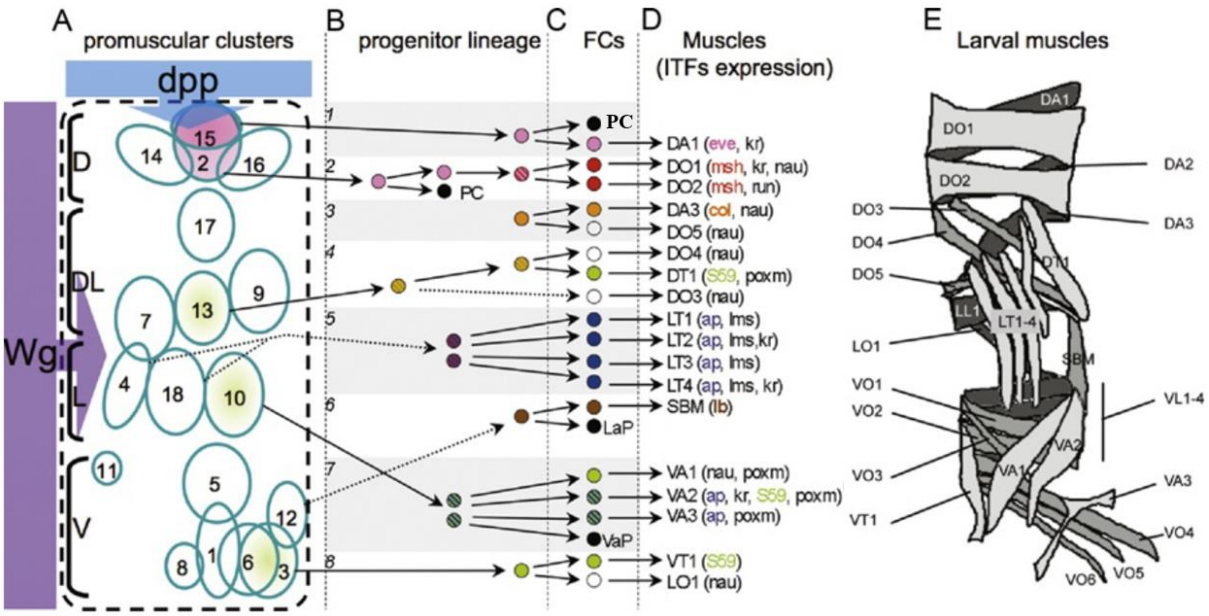

Figure 13. Schematic view of larval FC diversification. After promuscular cluster establishment in the somatic mesoderm (A) and MP division (B), each FC inherits a specific combinatorial code of iTFs it expresses (C, D), transiently, or during the whole differentiation process and in mature larval muscles (E). Illustration from (de Joussineau et al., 2012).

This data demonstrates that some iTFs can maintain the expression of other iTFs, thus determining the differential fate between two sibling FCs, without altering the muscle differentiation.

Expression of iTFs is dynamic, which was demonstrated in the case of the iTF *msh/dr*, involved in the specification of dorsal muscles DO1 and DO2 and lateral muscles LT1-LT4. Interestingly, the expression of *msh/dr* can be found in the dorsal progenitor, as well as in the differentiated DO1 and DO2 muscles. In contrast, the expression of *msh/dr* in the lateral progenitors is transient and disappears when FCs are formed. In the *msh/dr* mutant all these muscles show abnormalities, where muscle precursors do not form properly, and the subsequent fusion is also altered. Its overexpression in the mesoderm leads to a disruption of several dorsolateral somatic muscles. It was thus concluded that the function of *msh/dr* is in the realisation of the myogenic program required for the formation of a particular subset of muscle precursors (Nose et al., 1998).

The perturbation of other iTFs such as *nau* (Keller et al., 1997) and *collier* (*coe*), now known as *knot* (*kn*) (Crozatier and Vincent, 1999) does not lead to muscle transformations, but results in arrested FC differentiation and the absence of muscles they would normally form.

Interestingly, the loss of *S59/slou* leads to all above mentioned phenotypes, including abnormal differentiation and cell fate transformations (Knirr et al., 1999). Complex interactions between distinct iTFs are at the origin of these phenotypes. In the *S59/slou* mutant embryos, the muscles VA2 and VA3 form one, aberrant, syncytial muscle, with mixed characteristics. In the wild-type condition, the muscle VA3 expresses *S59/slou*, *Kr*, *nau* and *ap*. In the *S59/slou* mutant, the expression of *Kr* and *nau* is maintained, while the expression of *ap* is lost in the VA2/VA3 mixed muscle. As mentioned previously, the mutation of *Kr* leads to the duplication of the VA2

muscle and loss of *S59/slou* expression, meaning that *Kr* is, in this case, acting upstream of *S59/slou*. In the *S59/slou* mutant, the muscle transformation is thus not complete, and the resulting muscle adopts an intermediate phenotype.

On the other hand, *S59/slou* mutation leads also to the absence of muscles LO1 and VT1, correlated with the duplication of the SBM muscle. In this case, it is *lb*, normally expressed in the SBM muscle (Jagla et al., 1998), that extends its expression to LO1 and VT1 founders, that now become a supernumerary SBM. *S59/slou* is thus a repressor of *lb* expression in the LO1/VT1 progenitor, acting upstream of *lb* (Knirr et al., 1999). The output of iTF mutation thus seems to be determined by the presence of other iTFs in the same FC and their respective hierarchical relationships. Indeed, cross-repressive interactions were shown to be an important component in cell fate specification of adjacent populations of dorsal cardiac and muscle cells (Jagla et al., 2002). There are also positive mutual interactions, e.g. Org-1 activates the expression of Slou/S59 and Lb in LO1/VT1 and SBM progenitors (Schaub et al., 2012).

In the efforts to identify how the selection timing of PC links with muscle identity, an iTF Tailup (Tup), involved in the diversification of DA2 and DA3 muscles was identified. While Tup is a part of the iTF code instructing the DA2 muscle, Col instructs the DA3 muscle. The MP for the DA2 muscle is born at stage 10, at the intersection of Col and Tin expression, representing the spatial constraint in DA2 specification. Tup expression in the DA2 MP is under the control of Tin. Importantly, at stage 11, *col* expression is repressed by Tup repression, representing the temporal constraint for DA2 selection. During muscle differentiation Tup maintains its own expression, using a distinct enhancer than the one used by Tin for its early expression in DA2 MP (Boukhatmi et al., 2012). (Dubois et al., 2016)

Overall, it seems that during muscle development, several iTFs are expressed at the progenitor stage, some transiently, some inherited by FCs. Integrating positional, temporal and homeotic (see Part 3) information, extensive cross-regulatory interactions occur amongst iTFs, leading to a final FC-specific iTF expression pattern, which then propagates to the muscle fibre after fusion. This seems to depend on the usage of distinct iTF enhancers, active during the early, progenitor stage or late, differentiation stage of development (Boukhatmi et al., 2012; Dubois et al., 2016; Enriquez et al., 2010). The competence of muscle cells to respond to iTFs was shown to depend, at least in part on the expression of a chromatin regulator Sin3A. Muscle diversification thus also depends on the MP chromatin landscape, which contributes to cross-regulatory interactions between iTFs (Dobi et al., 2014).

In the effort to understand the final muscle pattern, one must thus consider several concomitant sources of information: 1, Signalling cues coming from the ectoderm that pre-pattern the mesoderm. 2, The asymmetric division of progenitors regulated by the Notch/Numb pathway, giving rise to distinct sibling FCs. 3, The autonomous expression by MPs and FCs of a specific array of iTFs and their cross-regulatory actions among them. 4, The input from *Hox* genes, which segregates progenitors along the AP axis. 5, Innervation patterns influencing the FC segregation.

1.2 Adult muscle diversification

In the adult fly, another level of muscle diversification needs to be achieved compared to the larval muscles. While the larval muscles mainly support the feeding and crawling movements, the adult fly requires muscles to perform more diverse tasks, such as walking, jumping, flying, oviposition and mating.

Several iTFs promoting adult muscle diversification were identified, such as Ewg (DeSimone et al., 1996), Extradenticle (Exd), Homothorax (Hth) (Bryantsev, Duong, et al., 2012), Spalt major (Salm) (Schönbauer et al., 2011) and Vg/Sd (Bernard et al., 2006; Sudarsan et al., 2001), involved in IFM development, Ct (Sudarsan et al., 2001), Lms (Müller et al., 2010) and Ap (Bernard et al., 2003) involved in DFM development and Lb (Maqbool et al., 2006) involved in leg muscle development (reviewed in Poovathumkadavil & Jagla, 2020).

A major diversification event that occurs during adult myogenesis is the choice between tubular (all adult muscles except IFMs) and fibrillar (IFMs) muscle types. As mentioned previously, tubular and fibrillar muscles differ highly in their ultrastructure (e.g. mitochondrial content, mode of contraction, sarcomere alignment and nuclei positioning), but they also strongly diverge in their transcriptome. They express different actin isoforms such as Act88F in IFMs, Act79B in the legs and the jump muscle and Act57A in abdominal muscles (Fyrberg et al., 1983). Some other IFM-specific proteins are Flightin (Fln) (Vigoreaux et al., 1993) and Troponin C4 (TpnC4), and tubular-specific proteins are TpnC41C (jump) and TpnC73F (abdomen) (Herranz, 2004). For some proteins, such as Myofilin (Mf) (Qiu et al., 2005) and Stretchin (Strn-Mlck) (Spletter et al., 2015), it is a different isoform that is expressed in fibrillar versus tubular muscles.

The choice between fibrillar and tubular fibre type was shown to depend on a member of the Spalt TF family, *salm*. Salm is expressed in developing flight myotubes and not in fusing myoblasts, and weakly in the jump muscle (Bryantsev, Duong, et al., 2012; Schönbauer et al., 2011). While *salm* downregulation during myogenesis leads to a transformation of fibrillar flight muscles towards tubular fate, its upregulation leads to the opposite effect in the leg and abdominal muscles. Interestingly, Vg was shown to be required for Salm expression in post-fusion myotubes, but its overexpression along with its partner Sd is not sufficient to induce Salm ectopic expression in wing disc-associated myoblasts (Schönbauer et al., 2011). During myogenesis, Salm is responsible for the transcriptional upregulation of many fibrillar sarcomeric components (Spletter et al., 2018) and also instructs the fibrillar muscle-specific mitochondrial morphology (Avellaneda et al., 2021).

Alongside Salm, *Hox* gene cofactors, Exd and Hth were shown to be involved in the choice between tubular and fibrillar muscle fate (Bryantsev, Duong, et al., 2012). Exd and Hth are highly expressed in IFMs, weakly in abdominal and leg muscles and no expression is detected in jump muscles. Exd or Hth downregulation leads to a transformation of fibrillar flight muscles towards tubular jump muscle fate and their overexpression to a partial opposite transformation. This study suggested that Exd and Hth would act upstream of Salm in the adult fibre type specification. Binding sites for Exd/Hth, but not for Salm, were found in the enhancer of the actin, fibrillar-specific gene, *Act88F* and Exd/Hth were shown to directly activate its expression. Furthermore, upon Exd/Hth binding, *Act88F* can be bound in vitro by Ubx, leading to *Act88F* repression (Bryantsev, Duong, et al., 2012; Roy and Raghavan, 1997). It was thus

concluded that the tubular fate would be achieved in the absence of Exd/Hth or when a *Hox* gene is co-expressed with them (Bryantsev, Duong, et al., 2012).

At the individual muscle level, the best studied is the diversification of flight muscles. Wing disc-associated myoblasts were shown to comprise two distinct populations, one expressing high Vg levels and low Ct levels, destined to become IFM muscles and the second smaller population, closer to the wing pouch, expressing high Ct and low Vg levels, that will give rise to DFMs. How the initial Ct and Vg expression is established in embryogenesis is not known, but high Vg expression in future flight myoblasts is maintained through Wg signalling coming from the disc epithelium. The maintenance of these two populations is reinforced by a mutually repressive loop between Vg and Ct (Sudarsan et al., 2001). The DFM specification was shown to be dependent on Ap, expressed in DFM-forming myoblasts starting from 12 h APF, most likely in a Wg-dependent manner. This contrasts with Ap expression in the embryo, where it is expressed in FCs, and not in FCMs, like in the case of DFMs. Ap also contributes to the specification of IFM non-autonomously, by activating the expression of Stripe (Sr) in muscle attachment sites, which is necessary for their establishment (Ghazi et al., 2000). Ectopic expression of Ap and Ct was observed in *vg* mutant pupal IFMs, suggesting that in the absence of *vg* the IFM development program switches to the DFM program instead. The choice between DFM and IFM fates was proposed to occur only at the beginning of the pupal stage, with Ap and Vg being key players in this process (Bernard et al., 2003). Additional factors, Lms (Müller et al., 2010) and Ewg (DeSimone et al., 1996) were shown to be required for DFM and IFM development, respectively.

The recent avenue of single-cell RNA-sequencing (scRNA-seq) allowed for the identification of a larger number of flight myoblast populations (Everetts et al., 2021; Zappia et al., 2020). Based on Vg and Ct expression, Zappia et al. identified 5 IFM clusters and 2 DFM clusters in the wing disc-associated myoblast population, at different stages of differentiation. Many novel markers for DFM myoblasts were identified, some with a known role in myogenesis such as *duf/kirre*, *midline* (*mid*), *Anaplastic lymphoma kinase* (*Alk*), *wing blister* (*wb*) and *sprout* (*sty*) and other genes with yet unidentified muscle function such as *arginine kinase* (*Argk*), *Neurotactin* (*Nrt*), *Amalgam* (*Ama*) and *Tenascin accessory* (*Ten-a*). Similarly, novel IFM markers were identified, such as *naked cuticle* (*nkd*) and *nop5*. A significant role in myoblast proliferation and flight muscle differentiation was assigned to Ama (Zappia et al., 2020).

Everetts et al. detected seven IFM clusters and 1 DFM cluster, sequencing at two developmental time points, allowing for a more accurate developmental analysis. This study reinforced the implication of the FGF signalling in myoblast proliferation and survival, detecting the expression of FGF ligands, Thisbe (Ths) and Pyramus (Pyr) (Stathopoulos et al., 2004) in wing-disc notum epithelium, below myoblast population that expresses the FGF receptor Htl (Everetts et al., 2021). Interestingly, ectopic expression of *pyr* or *ths* using a dpp-Gal4 driver caused an expansion of the myoblast population towards dpp-Gal4 expression domain, namely under the wing pouch epithelium. This is an important observation indicating that the FGF ligands instruct the myoblast position on the wing disc epithelium. This study also introduced a role for the Hedgehog (Hh) signalling in DFM specification, where DFM myoblasts express the Hh receptor Patched (Ptc) (Everetts et al., 2021) and uptake the Hh signal from underlying ectoderm via cytonemes (Hatori and Kornberg, 2020). A decrease in Hh signalling disturbs DFM organisation, leading to an outstretched wing phenotype, while its increase perturbs DVM

development. Furthermore, *Nrt* and *mid*, novel DFM markers described by Zappia et al. were shown to be under the control of the Hh pathway in wing myoblasts and involved in DFM development (Everetts et al., 2021).

Using advanced confocal imaging methods, allowing for deep axial resolution, it was shown that myoblasts differ in their polarity and shape along the proximo-distal axis, with respect to the wing disc epithelium (Patel et al., 2022). Myoblasts located closer to the disc epithelium (proximal myoblasts) are polarised towards the epithelium, sending orthogonal, actin-rich cytonemes towards adherens junctions of disc epithelial cells. Myoblasts located further away from the epithelium (distal myoblasts) do not extend orthogonal cytonemes towards the epithelium, they polarise parallelly with respect to the disc and seem to adhere to each other with lateral cytonemes. Proximal myoblasts uptake FGF ligands, Ths and Pyr, via Htl-expressing cytonemes, which is important for maintaining their proximo-distal polarity since distal myoblasts do not activate the FGF pathway and show hallmarks of differentiation. Interestingly, while the FGF ligand Ths is expressed by epithelial cells below Vg-positive, future IFM myoblasts, Pyr is expressed below Ct-positive, future DFM myoblasts, creating two distinct epithelial niches. The FGF asymmetric signalling thus promotes diverse niche-specific AMP organisations on the wing disc (Patel et al., 2022).

In summary, the proper specification of direct versus indirect flight muscles depends on a regionalised activation and integration of Wg, Hh and FGF signalling pathways in myoblasts, using signals from underlying wing disc epithelium and a specific combination of iTFs expressed in myoblasts at both larval (such as Vg/Sd, Lms and Ct) and pupal stages (such as Ap, Ewg, Exd, Hth and Salm).

In leg muscles, *lb* contribute to myoblast diversity within the leg. The most proximal myoblasts of the leg disc express Vg and do not express Lbe, while conversely, more distal myoblasts express Lbe under the control of Wg signalling. In the DV axis, myoblasts located ventrally express higher levels of Lbe than dorsal myoblasts and respond differently to *lbe* overexpression. Interestingly, Lbe and Htl expression prefigures the expression of the FC-marker Duf (Maqbool et al., 2006).

Similarly to larval muscle diversification, adult muscle diversification depends on the specific and regionalised expression of an array of iTFs, often under the control of niche-derived signals such as Wg and FGF pathways.

Part 2. Hox genes

2.1 Hox gene discovery and function

In the efforts to understand how evolution arises, Walter Bateson defined the term “homeosis” to account for dramatic variations that could naturally occur in species. He defined this term as “something has been changed into the likeness of something else” (Bateson et al., 1894). A few decades later C. Bridges and T. H. Morgan described the first homeotic mutation in *Drosophila*, *bithorax* (*bx*), resulting in a partial transformation of the third thoracic segment into the second, bearing a pair of small wings instead of halteres (Bridges et al., 1923). Homeotic genes were identified through extensive studies of pseudoallelic series (clusters of two or more closely linked and functionally related genes) on the third *Drosophila*

chromosome. A seminal work by Ed Lewis described in detail the *bithorax* pseudoallelic series comprised of several groups of mutants. He named a cluster of these pseudoallelic genes the Bithorax complex (BX-C) and defined the collinearity principle inherent to homeotic genes, where the order of genes on the chromosome reflects the order of their expression patterns in the body (E. B. Lewis, 1963, 1978). The BX-C was shown to impose specific segmental identities to the posterior thorax and abdominal segments (E. B. Lewis, 1978).

More than 15 years later a second homeotic complex in *Drosophila* was described, named the Antennapedia complex (ANT-C). This complex was also discovered by a careful analysis of a series of mutations having homeotic phenotypes that map to the proximal region of the third chromosome (Denell, 1973; Kaufman et al., 1980; R. A. Lewis, Kaufman, et al., 1980; R. A. Lewis, Wakimoto, et al., 1980). The function of this complex was proposed to be the development of anterior segments, in a way analogous to the BX-C that regulates the posterior segments (Kaufman et al., 1980). In the BX-C, three transcription units were described, *Ultrabithorax* (*Ubx*), *iab-2* and *iab-7*, now known as *abdominal-A* (*abd-A*) and *Abdominal-B* (*Abd-B*) (Regulski et al., 1985). The ANT-C contains *Deformed* (*Dfd*), *proboscipedia* (*pb*), *labial* (*lab*), *Sex-combs-reduced* (*Scr*) and *Antennapedia* (*Antp*) genes (Kaufman et al., 1990). Collectively, homeotic genes were proposed to provide a unique identity to each body segment and became a paradigm for studying how genes control development.

Thanks to the endorsement of DNA recombinant techniques, the DNA of the *bithorax* locus was cloned, spanning over 195 000 base pairs (bp). By doing so, one intriguing property of homeotic complexes was discovered, the presence of very large cis-regulatory sequences, in the case of BX-C representing 95% of the complex (Bender et al., 1983). Shortly after, a groundbreaking discovery in the laboratory of W.J. Gehring showed the existence of the homeobox, a sequence encoding a helix-turn-helix, 180 bp homeodomain (HD) motif. This motif was found present in both Ubx and Antp (McGinnis, Levine, et al., 1984), displaying homology to yeast mating-type genes (Shepherd et al., 1984). This led to the proposition that both homeotic complexes must have arisen from a common origin and that genes clustered in these complexes are functionally related. The HD was found to contain a helix-turn-helix motif, mediating the binding to DNA (Desplan et al., 1985; Qian et al., 1989). Several other laboratories confirmed this discovery and defined homeobox as a highly conserved family of sequences, associated with homeotic and segmentation genes (Laughon and Scott, 1984; Scott and Weiner, 1984). Very quickly, the homeobox was found in other invertebrate species, Xenopus, mice and the human genome (Levine et al., 1984; McGinnis, Hart, et al., 1984; Shepherd et al., 1984), but also in plants (Williams, 1998) and funghi (Son et al., 2020). Not all genes containing a homeobox lead to homeotic transformations, in which case they are not considered homeotic genes. Based on these studies it was postulated that homeotic genes are transcriptional regulators able to bind DNA, acting on a plethora of downstream, developmental genes.

Hox genes are highly conserved in all bilaterians, presenting variable numbers in distinct species (reviewed in Hajirnis & Mishra, 2021). In vertebrates, where genetic tools were sparse, the discovery of *Drosophila* homeobox allowed the identification and cloning of vertebrate homeotic genes, contributing to the entry of experimental developmental biology in these species. Genome duplication events led to the acquisition of four Hox clusters in vertebrates (HOXA, B, C and D), encoding 39 *Hox* genes, categorised into 13 paralog groups, that still

respect the collinearity principle (Duboule and Dollé, 1989; Graham et al., 1989). Based on the conservation of their sequences, their relative position on the chromosomes and their roles in the patterning, *Hox* genes can be partitioned into an anterior block (*lab*, *pb*, *Dfd*, and *Scr* in *Drosophila* and Hox1-5 in vertebrates), a central block (*Antp*, *Ubx*, and *abd-A* in *Drosophila* and Hox6-8 in vertebrates), and a posterior block (*Abd-B* in Drosophila and Hox9-13 in vertebrates) **(Fig. 14)** (Hueber et al., 2010; Mark et al., 1997).

The complex pattern of *Hox* gene expression along the A-P axis is achieved by many regulatory inputs, explaining the very long non-coding regulatory sequences present in these genes. Some main regulatory inputs are their regulation by segmentation genes, expressed prior to *Hox* genes, by repressing and activating actions of the Polycomb and Trithorax groups, respectively, and by the cross-regulatory interactions occurring between *Hox* genes themselves (reviewed in Mallo & Alonso, 2013).

This year marks the 40th anniversary of the homeobox discovery. During these 40 years, many examples of Hox "canonical" functions were described, where Hox allocate distinct spatial coordinates along the A-P axis during embryogenesis and help in maintaining cellular identities during post-embryonic development. Besides these canonical functions, Hox play also "non-homeotic" roles during organogenesis, regulating virtually all basic cellular processes, such as differentiation, proliferation and cell death (Sánchez-Herrero, 2013). More recently, a distinction was made between Hox-specific and Hox-generic functions, the former referring to functions performed by a single Hox that cannot be assumed by any other Hox and the latter to functions that can be assumed by several Hox proteins (Saurin et al., 2018).

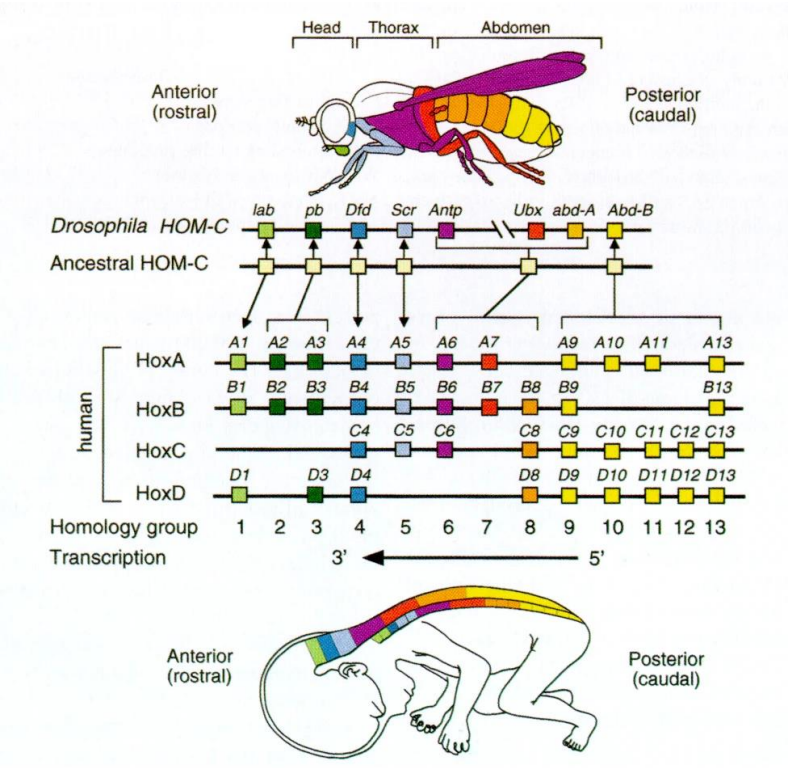

Figure 14. Genomic organisation and expression of *Drosophila* and vertebrate *Hox* genes. Expression of each *Hox* gene, depicted by a coloured box is shown in the adult fly and in the human embryo, extrapolated from the mouse data. For clarity, each colour shows the anterior-most expression domain of a given gene/subfamily and overlaps in gene expression between neighbouring *Hox* genes are not represented. Scheme from (Mark et al., 1997).

2.2 *Hox gene cofactors*

The most intriguing aspect of homeotic gene TFs is the discrepancy between their high specificity and their poorly selective DNA-binding motifs, rich in "AT" (TAAT motif in most cases) (Desplan et al., 1988), for *Antp* occurring in the genome once every kilobase (kb) of DNA (Mann and Chan, 1996). This phenomenon was named the Hox specificity paradox and is one of the main reasons why our understanding of molecular mechanisms underlying Hox function is still largely elusive.

This paradox was partially explained by the identification of so-called Hox cofactors, Pre-B-Cell Leukemia Transcription Factor (PBC) proteins (Exd in *Drosophila*) (Mann and Chan, 1996; Peifer and Wieschaus, 1990) and Myeloid Ecotropic Viral Integration Site (MEIS) proteins (Hth in *Drosophil*a) (Pai et al., 1998), that also encode for homeodomain TFs. The PBC proteins bind to Hox via the hexapeptide (HX) motif located upstream of the HD. The cooperative binding of Hox with cofactors increases the selectiveness of the Hox DNA-binding motif, providing additional specificity (Merabet and Mann, 2016; Ortiz-Lombardia et al., 2017; Ryoo et al., 1999; van Dijk and Murre, 1994). However, this paradox is still largely unresolved, since a large number of Hox functions are PBC/MEIS independent (reviewed in Rezsohazy et al., 2015). Many distinct elements of the Hox-cofactor binding were found to have an impact on target gene expression. For example, small changes in amino acids in DNA binding motifs can change the specificity from one Hox to another and recruit distinct co-activators/repressors, the specificity of binding via HD and HX can be modified by adjacent low-affinity sites, *Hox* genes were proposed to have a latent specificity, revealed upon a cofactor binding etc **(Fig. 15)** (reviewed in De Kumar et Darland 2021).

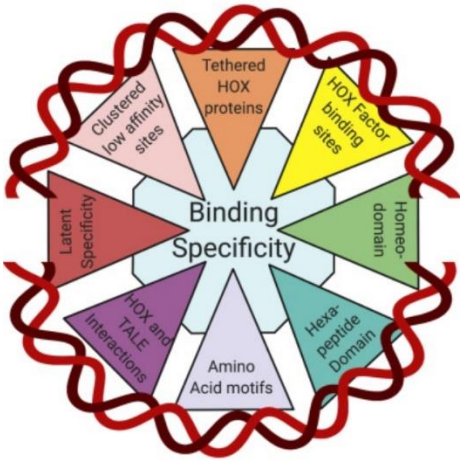

Figure 15. Schematic representation of factors modulating Hox-cofactor specificity. Image from (De Kumar and Darland, 2021).

In summary, large efforts are put into the field of Hox proteins to identify their downstream regulatory networks as well as their binding partners, accounting for the remarkable morphological diversity they regulate.

2.2.1 *M1BP, a novel Hox cofactor*

In efforts to enlarge our understanding of molecular mechanisms underlying Hox function, our group identified a novel Hox cofactor, Motif 1 binding protein (M1BP) (Zouaz et

al., 2017). M1BP was first identified as an RNA-polymerase II (Pol II) pausing factor, binding to a large number of genes with housekeeping functions, establishing distinct degrees of their poised Pol II state (J. Li and Gilmour, 2013). Its name comes from its ability to bind the so-called Motif 1, a core promoter element, identified as the most significantly overrepresented motif that lies within 100 bp of the transcription starting site (TSS) in *Drosophila* (Ohler et al., 2002). M1BP is an ubiquitous, 55 kDa zinc-finger TF, containing five C2H2 zinc-fingers in its C-terminal domain. It was later shown to activate the transcription of ribosomal proteins (Baumann and Gilmour, 2017), to contribute to the regulation of Topologically Associated Domains (TAD) boundaries (Bag et al., 2021) and to promote eye fate in *Drosophila* (Raj et al., 2020). The functional homologue of M1BP in vertebrates is ZKSCAN3 (Barthez et al., 2020).

Our group identified that M1BP collaborates with Hox proteins in the process of gene regulation. M1BP was shown to physically interact with Abd-A and Ubx in the embryo, and Hox binding to M1BP target genes to alleviate their poised Pol II state and increase transcriptional efficiency (Zouaz et al., 2017). In the fat body, the Hox-mediated autophagy repression (Banreti et al., 2014) requires the presence of M1BP (Zouaz et al., 2017).

2.3 Hox gene Antennapedia

2.3.1 Antennapedia, a "giant" gene

Thanks to the cytological data of different *Antp* mutant alleles, *Antp* was cloned using chromosome walking by the group of W.J. Gehring and its locus was found to span over 100 kb of genomic distance (Garber et al., 1983), leading to name *Antp* a "giant gene" (Scott et al., 1983). For a long time, the field considered the vertebrate orthologues of Antp the Hox6 proteins (Malicki et al., 1990), nevertheless more recent evidence suggests it rather being the proteins from the Hox7 paralog group (Hueber et al., 2010, 2013).

The *Antp* gene contains eight exons and very large introns, the largest spanning around 60 kb. The open reading frame comprises exons 5 to 8, the 8th exon containing the HD. Distinctive features of this locus are multiple polyadenylation sites, unusually long 5' UTR sequences, where only 1% of the 103 kb *Antp* gene is protein coding, and the presence of two internal promoters, P1 and P2. The first promoter is located in front of the exon 1 and the second in front of the exon 3, the two promoters being separated by approximately 70 kb **(Fig. 16)** (Garber et al., 1983; Laughon et al., 1986; Schneuwly et al., 1986; Scott et al., 1983; Stroeher et al., 1986).

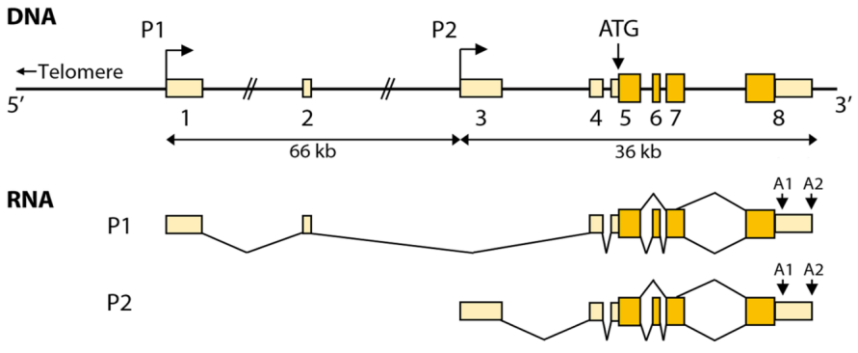

Figure 16. Antp gene displays a complex structure. Schematic view of the Antp gene and transcripts, with coding exons depicted in dark yellow and non-coding exons in light yellow, smaller boxes. P1 and P2 are two distinct promoters, A1 and A2 two alternative polyadenylation sites.

The presence of two promoters was an exciting discovery, providing an explanation for distinct portions of the *Antp* locus displaying different functions (see below) (Abbott and Kaufman, 1986). According to the current classification, P1 is a dispersed promoter, containing four non-canonical TSS, while P2 is a focused promoter with a Downstream Protein Element (DPE) box (reviewed in Rosales-Vega, Reséndez-Pérez, et Vázquez 2024).

Antp gene can produce an incredible number of 11 transcriptional isoforms via alternative splicing and differential promoter usage. The exon 6 (E6) is subject to an alternative splicing and can be omitted by an exon skipping mechanism. It contains three acidic residues in a neutral environment that could provide a new site of interaction with other proteins. Additionally, there are two different splicing donors present in the exon 7 (E7), one longer that includes (E7L) and one shorter that omits (E7S) a 4 aa linker located between HX and HD. Interestingly, this linker contains an additional cysteine and knowing that Antp protein contains three cysteines, the presence of this residue could change drastically the form of the protein. The combination of these alternative splicings can create four groups of peptides, the longest form of 378 aa (containing the E6 and E7L), the second of 374 aa (containing the E6 and E7S), the third form of 365 aa (lacking E6 and E7L) and the fourth form of 361 aa (lacking E6 and E7S). Transcripts giving rise to these peptides can be produced by both *Antp* promoters, leading to a very large number of 11 predicted transcript isoforms **(Fig. 17)** (Bermingham and Scott, 1988; Stroeher et al., 1986).

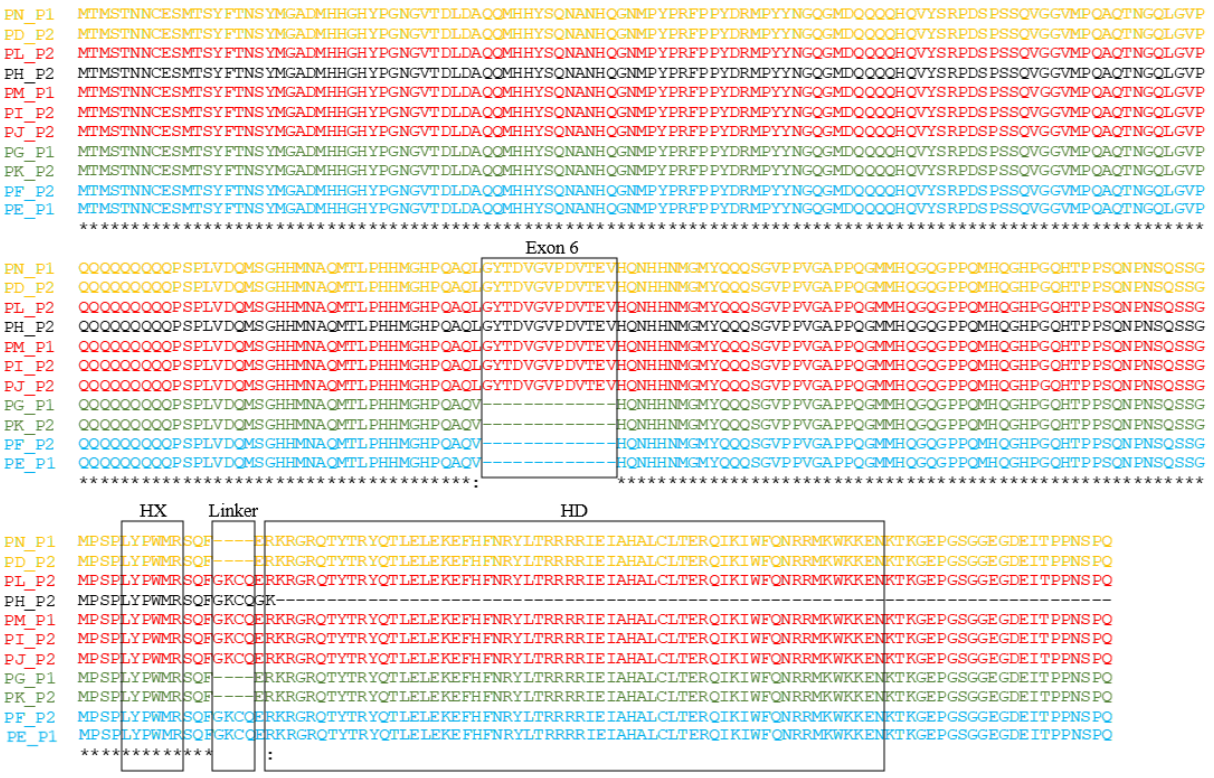

Figure 17. Structure of Antp gene products. Peptide alignment of all Antp peptides, produced from transcripts from the two Antp promoters, depicted P1 and P2. Four distinct types of peptides can be produced, the first group depicted in yellow contains the E6 and misses the linker region (PD and PN; 374 aa), the second group in red contains both the E6 and the linker region (PI, PJ, PL, PM; 378 aa), the third group in green lacks both the E6 and the linker region (PG and PK; 361 aa) and the last group in blue (PE, PF; 365 aa) contains the linker region but not the E6. One predicted transcript from the P2 produces a peptide lacking the HD (PH), but whether this form is produced in vivo is unknown. HX - hexapeptide, HD – homeodomain

Even though both *Antp* promoters can produce all four isoforms, there is a temporal, probably developmentally regulated, difference in splicing. In the embryo, the predominant form of transcripts contains E6 and later, in larvae in pupa both forms, with or without exon 6 are produced. A similar developmental profile was observed for the alternative donor at the 3' end of the exon 7 (generating E7L), where the longer form is predominant during embryogenesis and the shorter form is favoured later during development. Intriguingly, analysing in detail different larval tissues showed that there is a clear difference in transcripts derived from brain and gut tissues, compared to leg, wing and humeral discs.

While the brain and gut express the longer form containing E6, wing discs express the shorter form lacking this exon. Based on these data it was proposed that this mechanism could thus allow Antp to subdivide the thoracic region into subregions/tissue domains (Stroeher et al., 1988). It was later shown that the E7L isoforms, containing the linker region, favour transcriptional activation of Antp target genes whereas the E7S forms favour transcriptional repression of Antp targets (Papadopoulos et al., 2011), which also holds true for the autoregulation of Antp expression (Papadopoulos et al., 2019). Interestingly, it was shown that the E7S form binds stronger and longer to the chromatin, compared to the longer E7L form (Papadopoulos et al., 2019).

Antp gene encodes a 361 to 378 amino acid (aa) protein (approx. 43 kDa) with the HD at its C-terminus and an unusually rich composition in proline (10%) and glutamine (18%), suggesting that outside the homeobox, Antp protein is largely hydrophilic with an extended structure (Laughon et al., 1986).

2.3.2 Antennapedia expression

Antp can be first detected in the *Drosophila* embryo shortly after the formation of the cellular blastoderm, in clusters of nuclei constituting thoracic and abdominal primordia. After the germ band extension, Antp transcripts localise mainly to thoracic segments of the ventral nerve cord and after the band retraction, in a subpopulation of the ganglion cells of each abdominal segment (Levine et al., 1983). Even though Antp transcripts can be detected at the cellular blastoderm stage, the protein can be first detected only at the onset of germ band retraction, mainly in the epidermis of the three thoracic segments but also in the neuromeres of the head region and abdominal segments (S. B. Carroll et al., 1986; Wirz et al., 1986).

When studying *Antp* expression, it is useful to consider the expression from both promoters separately, as they drive *Antp* expression in distinct localisations/tissues **(Fig. 18)**. At the cellular blastoderm stage, P1 drives *Antp* expression in parasegments (PS) 4 to 6 (a parasegment

being constituted by a P part of one segment and the A part of the adjacent one), corresponding to the P part of T1 to the A part of A1. The P2 drives *Antp* expression in sharp stripes in the PS4, a ventral part of the PS6 and PS14 (Bermingham et al., 1990; Ingham and Martinez-Arias, 1986). During germ band elongation, Antp from the P1 promoter is expressed in the ectoderm of the PS4, the ectoderm and mesoderm of the PS5 and anterior PS6 and more weakly in the ectoderm of the posterior PS6 to 12 (Bermingham et al., 1990; Martinez-Arias, 1986). The P2 expression is detected in the ectoderm and mesoderm of the PS4, and mesoderm of the PS6. There is also weaker expression in PS5 and in the ectoderm of PS6 to PS14. The strongest mesodermal P2 expression is PS4 and PS6. At the end of the germ band extension, expression from P1 and P2 decreases in the epidermis and increases in the nervous system, with the P2 expressed in small clusters of epidermal cells in each PS from 4 to 14, likely contributing to sensory organs. At the shortened germ band stage, all somatic muscles of T3 express *Antp* from the P1 and somatic muscles of T2/T3 express Antp from the P2 (Bermingham et al., 1990; Engström et al., 1992; Irish et al., 1989; Riley et al., 1991). Antp expression in the mesoderm of the T2 and T3 segments (weaker in T2 compared to T3) was also detected at the protein level (Capovilla et al., 2001). Antp is also expressed and required in the visceral musculature, since in *Antp* mutant embryos the first midgut constriction does not form (Reuter and Scott, 1990).

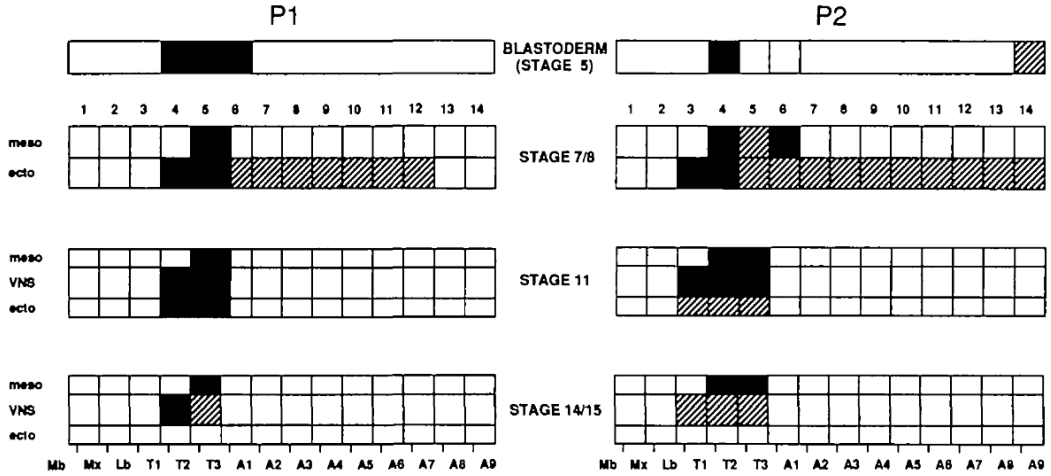

Figure 18. Complex distribution of *Antp* transcripts from its two promoters. Schematic summary of *Antp* expression during embryogenesis in the mesoderm, ectoderm and the ventral nervous system. Solid pattern depicts a strong expression and hatched pattern low expression levels.

By labelling promoter-specific exons in larval imaginal tissues, it was shown that in the wing disc, P1 drives *Antp* expression in the A columnar epithelium and the peripodial membrane, while P2 drives its expression in myoblasts attached to the notum part (Jorgensen and Garber, 1987). Antp expression in the wing disc epithelium was also detected at the protein level (Papadopoulos et al., 2019; Paul et al., 2021; Roy et al., 1997). Transcripts from both promoters were also detected in leg discs, in the P part of the T1 disc, several parts of the T2 disc and all throughout the ectoderm of the T3 disc. Antp is also expressed in the haltere disc and its myoblasts (Roy et al., 1997). In agreement with previous reports, no transcripts were detected in the eye-antennal disc (see below). Interestingly, it was shown that ectopic *Antp* transcripts in the antennal part of the disc, visible in several *Antp* dominant mutants (e.g., $Antp^{W}$, $Antp^{Ns}$,

Antp^{73b}), which are responsible for antenna-to-leg transformations, originate from the P2 (Engström et al., 1992; Jorgensen and Garber, 1987). In the adult, P1 was proposed to express *Antp* in the CNS, at the periphery of the thoracic ganglions, in neurons that innervate the IFMs and muscles of mesothoracic legs. In the thorax, the staining was present in nerves innervating DVMs and DLMs as well as T2 leg muscles, with some muscles in the metathorax and the T3 coxa also showing *Antp* expression (Engström et al., 1992).

2.3.3 Antennapedia function

Antp was first identified by a series of dominant mutations leading to a transformation of the antenna into a second thoracic leg in heterozygous individuals (Falk, 1964; Gehring, 1966; Le Calvez, 1948; E. B. Lewis, 1956). The most famous example of such a transformation is the *Nasobemia* (*Ns*) mutant identified by W.J. Gehring (Gehring, 1966) and only later unambiguously proven as an allele of *Antp* (Denell, 1973). Another dominant mutation identified was *Humeral* (*Hu*), leading to the appearance of extra bristles in the humerus (Lindsey and Grell, 1968). To better understand the genetic organization of the *Antp* locus, R. E. Denell generated by X-rays several revertants of *Ns* lines and by cytological and complementation studies mapped the *Antp* gene to the 84B1-2 location (Denell, 1972, 1973). The revertants of the *Ns* mutation and the majority of dominant *Antp* mutations share a recessive lethality when homozygous or combined with each other (Denell, 1973; Kaufman et al., 1980; R. A. Lewis, Kaufman, et al., 1980; R. A. Lewis, Wakimoto, et al., 1980). Knowing that *Ns* phenotype could be reverted by a deletion, Denell suggested that *Ns* is a neomorph, together with other *Antp* dominant alleles (Denell, 1973).

What would thus be the function of *Antp* wild-type product? Inspections of recessive lethal *Antp* mutant embryos and larvae from different complementation groups showed meso-to-prothorax (T2 to T1) transformation phenotypes, suggesting that in the wild-type condition, *Antp* regulates the development of the mesothorax and the second pair of legs (Martinez-Arias, 1986; Wakimoto and Kaufman, 1981). More recently, Antp was shown to regulate the development of the wing blade in *Drosophila* (Paul et al., 2021) as well as in other insects (Fang et al., 2022). No evidence was found suggesting that *Antp* would be involved in the development of the head or antenna, even though many *Antp* mutations lead to a transformation of the antenna to legs. It was thus suggested that *Antp* adult dominant phenotypes are due to the alteration of cis-regulatory regions repressing *Antp* in the antennal primordia (Denell et al., 1981). This was later confirmed by an ectopic overexpression of *Antp* using a heat-shock promoter that indeed led to an antenna-to-leg transformation (Schneuwly et al., 1987). These studies were supported by the isolation of *Antp* null alleles that displayed a transformation of the second leg into an antenna, the opposite phenotype to the known dominant *Antp* mutations, without disrupting the normal antenna development (Struhl, 1981).

Based on these complementation studies, several genetic subfunctions were postulated for the *Antp* gene. One subfunction would be the discrimination between distinct thoracic segments, which when disrupted leads to recessive lethality (Wakimoto and Kaufman, 1981). The second subfunction would be the choice between the antennal versus leg fate in imaginal discs, a function inappropriately activated in the head of individuals carrying *Antp* dominant mutations

(Kaufman and Abbott, 1984). The former subfunction when disrupted leads to the embryonic/larval lethality and the latter to the pupal lethality (Abbott and Kaufman, 1986).

To perform its function of imposing the mesothoracic identity, Antp can form transcriptional complexes with multiple TFs and proteins from the basal transcription machinery (Baëza et al., 2015). The most studied interaction of Antp occurs with Exd or both Exd and Hth, recognising distinct chromatin sites in both cases (Kribelbauer et al., 2020). Sites of poor chromatin accessibility are better recognised by Antp when Exd/Hth are present, supporting the idea that Hox cofactors do not bind to DNA with high affinity unless cofactors are present (Porcelli et al., 2019). Antp can further interact with a TATA-binding protein-associated factor Bric-à-brac interacting protein 2 (BIP2) through the YPWM motif present in the HX (Prince et al., 2008), a protein of the mediator complex Med19 via the HD (Boube et al., 2014), TFIIEβ via the HD (Altamirano-Torres et al., 2018), TATA-binding protein (TBP) via its polyQ stretches, forming a trimeric complex Antp-TBP-Exd (Jiménez-Mejía et al., 2022) and Ubx via the HD (Villarreal-Puente et al., 2024). Trimeric complexes between Antp-Ubx-Exd or Antp-Ubx-TBP were also identified, leading to a reduction in Antp transcriptional activity (Villarreal-Puente et al., 2024). By interacting with the basal transcription machinery Hox proteins are thought to integrate cell-specific information, leading to the transcription of a few selected target genes.

In summary, the function of Antp in the acquisition of the mesothoracic identity thus encompasses several regulatory layers. First, the Antp expression pattern during embryogenesis is dynamic and complex, suggesting a large number of regulatory inputs refining Antp expression, explaining the unusually large 5' UTR sequence of Antp. Second, the presence of two promoters refines Antp expression within its broader thoracic expression domain, allowing for distinct regulatory inputs for both promoters. Third, both promoters can produce four distinct protein isoforms, containing or not a linker region that can potentially change Antp conformation, and or an additional exon that can likely serve as a hub for additional interactors. Additionally, these splicing events are temporally regulated, allowing for a gradual refinement of Antp expression in certain tissues during development. Fourth, Antp can interact with several TFs and proteins, linking it to the general transcriptional machinery, where depending on the cofactor present, distinct chromatin sites become available. With the avenue of new genomic tools requiring less and less dissected tissue, more knowledge will be gained about how this complex spatio-temporal pattern of Antp expression arises and how distinct Antp transcriptional complexes allow for selective regulation of target genes.

Part 3. The role of Hox genes in mesodermal patterning

Best known for their involvement in the patterning of the ectoderm, there is increasing evidence for the role of *Hox* in the patterning of distinct mesodermal derivatives. We have reviewed the role of *Hox* in the patterning of all mesodermal derivatives in both flies and vertebrates (Poliacikova et al., 2021) (see Annexe), I will thus focus here solely on the involvement of *Hox* genes in the patterning of the *Drosophila* somatic musculature.

3.1 The role of Hox genes in larval muscle patterning

An important aspect of the *Hox* gene function in the somatic mesoderm is that the Hox pattern of expression is shifted posteriorly in the mesoderm in comparison to the ectoderm (Enriquez et al., 2010; Michelson, 1994). In this context, the loss (Hooper, 1986; Lawrence and Johnston, 1984) and gain (Michelson, 1994) of *Hox* function leads to larval muscle transformations from one segment into the likelihood of another (P into A structures for loss, and A into P structures for gain-of-function). Ubx was shown to be expressed in the abdominal, but not thoracic progenitors of the LO1/VT1 muscles alongside S59/Slou, seemingly under the control of Org-1 (Schaub et al., 2012). This difference in expression could account for the fact that in the thorax these founders do not fuse and these muscles do not form (Frasch, 1999). A mutation of *Ubx* resulting in the production of only one of its splicing isoforms specifically perturbs the formation of a subset of abdominal muscles in the embryo (Reed et al., 2010). Another study showed that Antp directly binds to and activates a muscle-specific *ap* enhancer, contributing to the specification of LT1-LT4 muscles, representing the first example of how Hox contribute to larval myogenesis at the molecular level (Capovilla et al., 2001).

Important insight about how iTF and Hox codes integrate came from the seminal work in the laboratory of A. Vincent, where it was shown that *Hox* genes intervene at several steps of larval myogenesis. Taking the Col and Nau-expressing, DA3/DO5 MP as an example, it was shown that this progenitor and its resulting muscles show segment-specific variations, where only one such MP forms in the T2 and T3, none in T1 and two in A1-A7 segments. Furthermore, the DA3 muscle possesses 6 nuclei in the thorax and 8 nuclei in the abdomen. At stage 11, a pan-mesodermal overexpression of *Hox* results in an ectopic Col/Nau-expressing progenitor formation in the T1, one MP when *Antp* is used and two MPs when *Ubx* or *abd-A* are used. Conversely, *Antp* LOF leads to no Col-positive DA3 muscle in the thorax, due to a failure of maintaining Col expression in the DA3/DO5 MP, at the precise moment where the *col* expression switched from an early-to-late *col* enhancer. Interestingly, to activate *col* expression, Antp and Ubx/Abd-A directly bind to distinct *col* "late" enhancer sequences. This data clearly demonstrates that by activating the expression of a combination of iTFs at the progenitor stage, Hox superimpose the segment-specific information they carry on the information from segmentation and D-V patterning genes. Later during development, Hox collaborate with iTFs to allocate a segment-specific number of FCMs to the DA3 muscle, regulating the final muscle size (Enriquez et al., 2010; Enriquez and Vincent, 2010). In summary, *Hox* genes have an important function in the diversification of larval muscles by activating and collaborating with some of the iTFs, a function that remains largely unexplored.

3.2 The role of Hox genes in adult muscle patterning

In the adult progenitors, the expression of Hox is still under debate. The current picture is that the three leg discs as well as some adult leg muscles express Scr (Glicksman and Brower, 1988) and Antp (Engström et al., 1992; Simpson, 2016), but their precise expression in leg disc-associated AMPs was not established. The haltere disc-associated myoblasts in the T3 express Antp, but the consequence of *Antp* mutation on haltere muscle formation is not known. The wing disc-associated myoblasts were first shown to contain Antp transcripts from the P2 (Jorgensen and Garber, 1987), but not the Antp protein and the development of flight muscles

is thought to occur without Hox input (Roy et al., 1997). These results were challenged by both older (Capovilla et al., 2001) and recent stainings (Paul et al., 2021), suggesting that Antp is expressed in wing disc-associated myoblasts an could play a role in flight myogenesis. Up to date, no staining of Hox in abdominal AMPs was published.

An important insight about the regulation of adult muscle patterning came from the laboratory of M. Akam, where it was shown that the mesodermal overexpression of *abd-A* converts the thoracic AMP pattern into abdominal AMP pattern (**Fig. 19**).

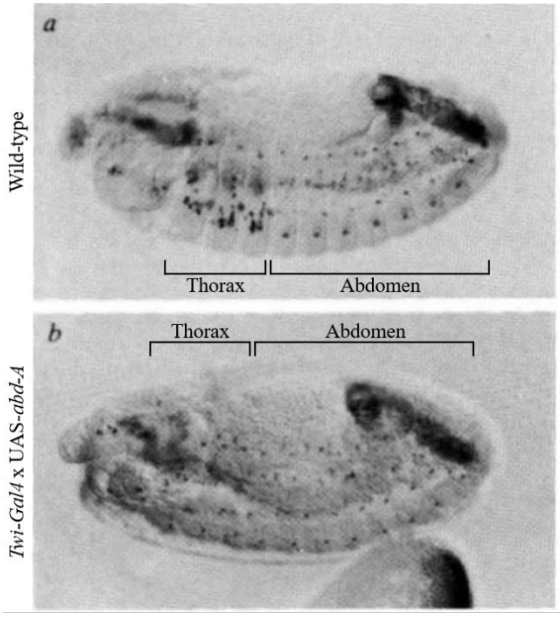

Figure 19. Hox genes specify the embryonic AMP pattern. (a) Wild-type stage 14 embryo labelled with anti-Twi antibody, showing the pattern of AMPs. Thoracic segments present a larger number of AMPs than abdominal segments. **(b)** Stage 14 embryo, labelled with anti-Twi antibody, where abd-A was overexpressed in the whole mesoderm using Twi-Gal4 driver. In this condition, there is no visible distinction between thoracic and abdominal AMP patterns. Image adapted from (Greig and Akam, 1993).

This suggested that like in the embryo, Hox could be involved in the specification of AMPs in the segment-specific manner. Ubx overexpression in the mesoderm (Roy and Raghavan, 1997) or motoneurons (Dutta et al., 2010) perturbs the development of adult flight muscles, suggesting that the patterning of adult precursors involves both autonomous and non-autonomous cues. The studies of Hox functions in adult muscles were for a long time hampered by the embryonic lethality of *Hox* gene mutants. Nevertheless, many genetic tools are now available for distinct adult muscles (Lavergne et al., 2017; Morriss et al., 2012; Weitkunat and Schnorrer, 2014), as well as CRISPR and/or RNAi Hox lines (Dietzl et al., 2007; Perkins et al., 2015; Viswanatha et al., 2018), promising more insights into the role of Hox in adult muscle patterning, a topic of high interest for novel muscle regeneration strategies.

Chapter III. How do flies have the energy to fly? – Muscle mitochondria

Part 1. Mitochondrial development

1.1 The biology of mitochondria

Mitochondria are organelles present in eukaryotic cells, well known for their involvement in cellular bioenergetics through (adenosine-5'-triphosphate) ATP production. Even though considered a "powerhouse" of the cells (reviewed in Vakifahmetoglu-Norberg et al., 2017), their functions extend beyond metabolism, such as the production of ROS involved in the cell signalling, regulation of the immune system (reviewed in Jin et al., 2017) and apoptosis (reviewed in Orrenius et al., 2003). The deficit of mitochondrial integrity was proposed to contribute to the pathogenesis of many human diseases and ageing (Harrington et al., 2023).

Mitochondria, unlike other organelles, have their own mitochondrial genome (mtDNA), a circular double-stranded molecule of 16,569 kb, encoding 37 genes in humans. These genes encode proteins involved in the mitochondrial respiratory function, ribosomal RNAs and transfer RNAs that synthesise mitochondrial proteins (reviewed in Heuer, 2021).

A high complexity of metabolic processes performed efficiently by mitochondria suggested that a high degree of molecular organisation exists in this organelle. In 1952, a seminal work by G. Palade provided the first high-resolution TEM images of mitochondria, demonstrating the existence of the mitochondrial membrane and mitochondrial ridges, emanating from the membrane to the interior of mitochondria, named mitochondrial cristae **(Fig. 20)**. The space inside of mitochondria was referred to as mitochondrial matrix (Palade, 1952).

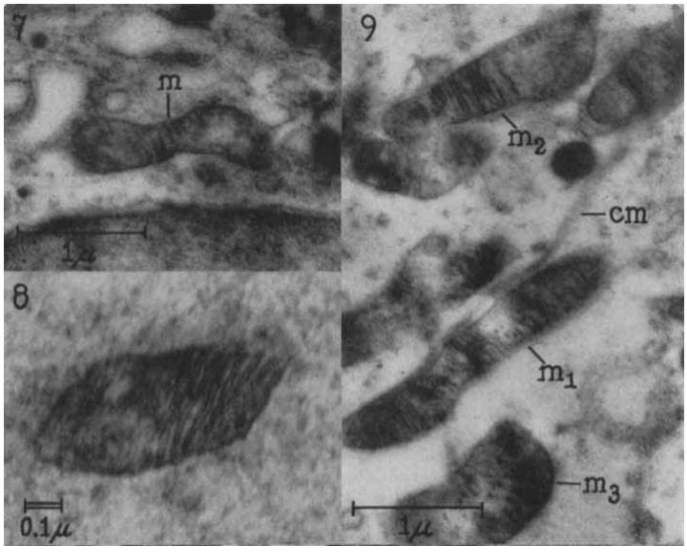

Figure 20. First high-resolution TEM micrographs of the mitochondrial membrane. Micrographs of mitochondria in a glandular cell of the rat pituitary gland (7), of mitochondria in nephrons of rat embryo (8) and mitochondria in adult rat kidney (9).

In the initial cristae description, it was noted that the number and spacing of cristae vary between cell types, with thin cristae in cells with low energetic requirements such as fibroblasts and endothelial cells, while mitochondria in metabolically active cells, such as skeletal muscle cells and nephrons have a higher concentration and regularity of cristae. Knowing the complexity of oxidative processes carried out by mitochondria *in vitro*, it was suggested that

enzymes involved in these processes are maintained in “definite spatial relationships”, that could be organised in chains using mitochondrial cristae (Palade, 1952). We now distinguish an inner mitochondrial membrane (IMM) that encompasses the matrix, an outer mitochondrial membrane (OMM) facing the cytoplasm and between them the intermembrane space (IMS). Cristae are formed from the invagination of the IMM and bear the respiratory chain (reviewed in Cogliati et al., 2016).

1.2 Mitochondrial respiratory chain

The most “famous” mitochondrial function is the mitochondrial respiration process, yielding 90% of all ATP the cell uses (Bottje, 2019). During oxidative metabolism, the oxidation of glucose in a process called glycolysis generates the pyruvate, which is imported into mitochondria, converted into acetyl-CoA and enters the Krebs cycle, also referred to as Tricarboxylic Acid (TCA) cycle. The TCA cycle generates electron donors for OXPHOS, namely Nicotinamide adenine dinucleotide (NADH) and succinate. Electrons provided by those carriers are used by the electron transfer chain (ETC) to drive ATP synthesis via oxidative phosphorylation (OXPHOS) (Mitchell, 1961). For one glucose molecule, oxidative metabolism theoretically yields 36-38 molecules of ATP (Harrington et al., 2023).

OXPHOS system consists of five multi-protein complexes, the first four composing the ETC and the fifth driving the synthesis of ATP. These complexes are Complex I (CI: NADH:ubiquinone oxidoreductase); Complex II (CII: succinate dehydrogenase), Complex III (CIII: cytochrome bc_1 oxidoreductase), Complex IV (CIV: cytochrome c oxidase) and Complex V (CV: ATP synthase, FoF1-ATPase). OXPHOS system comprises also two freely mobile electron carriers, the membrane-embedded ubiquinone and the soluble cytochrome c (cyt c) **(Fig. 21)** (Green and Tzagoloff, 1966; Sousa et al., 2018). In the following section mammalian complexes and assembly factors will be discussed.

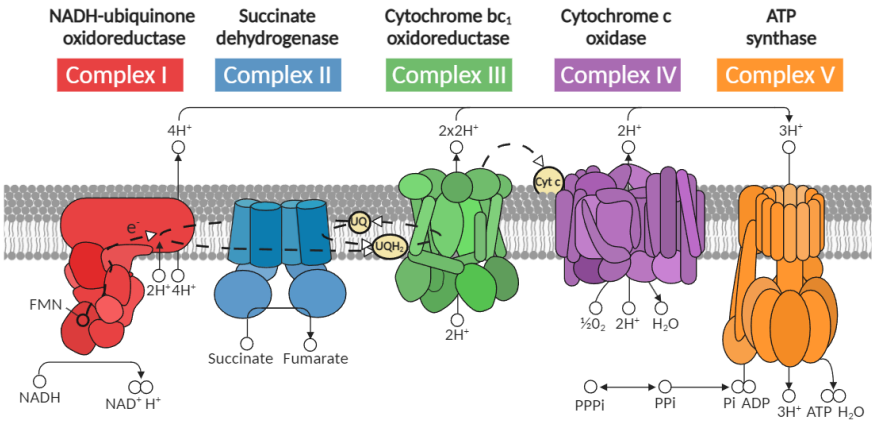

Figure 21. Complexes of the mitochondrial respiratory chain. Schematic structure of the ETC and the ATP synthase. Electrons donated to CI and CII via NADH and succinate, respectively, generate an electrochemical proton gradient, used by ATP synthase to drive ATP production, by adding inorganic phosphate (Pi) to ADP. Adapted from the KEGG pathway database (Kanehisa and Goto, 2000).

CI is the largest complex in the ETC, with approximately 1 MDa mass in mammals, whose role is to transfer electrons from NADH to ubiquinone, in mammalian cells displaying an L-shape with two domains, the membrane arm embedded in the IMM and the matrix arm. There are 45 identified proteins forming the CI, from which 14 are core subunits and 31 supernumerary subunits (J. Carroll et al., 2006; Fiedorczuk et al., 2016; Zhu et al., 2016). The membrane arm contains 7 subunits that are encoded by the mtDNA (Chomyn et al., 1985, 1986). The matrix arm contains cofactors, the primary electron acceptor flavin mononucleotide (FMN) and 7-9 iron-sulfur (Fe-S) clusters and the final electron-accepting Fe-S cluster N2 that delivers electrons to ubiquinone (Q) (Hunte et al., 2010). FMN accepts electrons from NADH, produced by the Krebs cycle in the matrix, oxidising it into NAD^+. Two electrons then travel the chain of Fe-S clusters from low to high potential. Upon receiving the pair of electrons, ubiquinone (Q) is reduced to ubiquinol (QH_2) and the energy released by this transfer leads to the pumping of four protons into the IMS, via proton translocation channel forms (E-channel) in the membrane arm (Berrisford and Sazanov, 2009; Jones et al., 2017; Tan et al., 2015).

CII, being 120 kDA in size, is the smallest complex and has the particularity of being a component of both the Krebs cycle, where it catalyses the oxidation of succinate to fumarate, and of the ETC, where it reduces Q to QH_2 (Rasheed and Gabor, 2018). Similarly to CI, CII can donate electrons to Q via Fe-S clusters. In both eukaryotes and prokaryotes, it consists of 4 subunits, 2 membrane-anchored proteins that contain the Q binding site and 2 other subunits on the matrix side that contains an iron-sulfur protein with three Fe-S clusters and a flavoprotein, covalently bound to a FAD cofactor, the primary electron acceptor (Sun et al., 2005). After receiving electrons from the succinate, FAD is reduced to $FADH_2$, transferring the electrons to Fe-S clusters that transfer them to Q reduced to QH_2. CII is the only ETC component that does not pump protons across the IMM (Iverson, 2013; Rasheed and Gabor, 2018). There is confusion in the literature concerning CII, where NADH together with $FADH_2$ are considered as electron donors for the ETC. While NADH provides electrons to CI by its oxidation, FAD is reduced by CII to FADH2 during the oxidation of succinate, which is the true donor of electrons for the CII (Gnaiger, 2023).

CIII transfers the electrons from the QH_2 generated by CI and CII to cyt c. It is an obligatory symmetrical dimer, containing 11 subunits per monomer (Schägger et al., 1986). It contains three catalytically active, conserved subunits: cytochrome c1 (cyt c1), a high potential Fe-S cluster enclosed in Rieske iron-sulfur protein (ISP) and the only mtDNA-encoded subunit cytochrome b (cyt b). Cyt b contains two heme groups (also referred to as haem), heme b_L and heme b_H, constituting the low-potential chain and 8 accessory subunits (Gao et al., 2003; Yang and Trumpower, 1986). The transfer of electrons in the CIII happens via Q-cycle **(Fig. 22)**. It defines two reaction sites, a QH_2 oxidation site (Q_P or Q_O) near b_L heme, located near IMS and a Q reduction site, site (Q_N or Q_i) near b_H heme, located closer to the matrix. The first electron is separated from QH_2, bound at the Q_P the site and transferred to the high-potential chain, constituted of the Fe-S cluster, the cyt c1 and the mobile cyt c. The second electron is concomitantly passed through the low-potential chain, hemes b_L and b_H, to the Q_N site, reducing Q to ubisemiquinone, releasing two protons. The second QH_2 is oxidised at the Q_P site in the same way, this time the low-potential chain reducing the ubisemiquinone to QH_2, which is released, transferring an additional two protons. In total, four protons are pumped to the IMS and two molecules of cyt c are reduced (Trumpower, 1990, 2002; Xia et al., 2013).

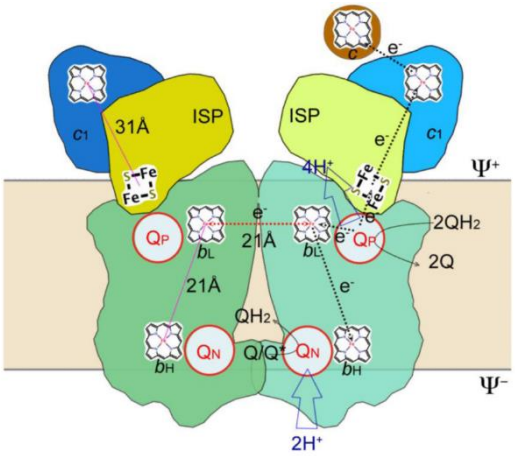

Figure 22. Schematic representation of the Q-cycle occurring in the CIII. The important aspect is the electron bifurcation point occurring at the Q_P site, from where an electron either reduces cyt c or reduces the Q molecule at the Q_N site.

CIV transfers electrons from cyt c to the terminal electron acceptor, the oxygen (O_2) to generate water (H_2O). It contains 14 subunits, three encoded by mDNA and four redox-active metal centres (2 heme and 2 copper), used to reduce O_2 to H_2O. In many crystal structures, it appears as a dimer (Kadenbach and Hüttemann, 2015; Timón-Gómez et al., 2018; Tsukihara et al., 1996). In the CIV, four electrons are transferred, one by one, from cyt c via four metal centres to O_2, which is then reduced into H_2O (Shimada et al., 2017). CIV pumps one proton to the IMS for each oxidised cyt c molecule, 4 protons in total for each functional cycle, with four additional protons used to create two H_2O molecules (Wikstrom, 1977). The pumping occurs via the D-channel (Maréchal et al., 2020).

CV, called ATP synthase consists of two functional domains, F_0 with a c-ring and F_1 and is composed of 17 subunits. F_0 is in the IMM, referred to as a rotor, and F_1 is in the mitochondrial matrix. As mentioned previously, during electron transfer in the ETC, protons are pumped from the matrix to the IMS by CI, CIII and CIV. These protons are pumped back to the matrix via the F_0 domain, transferring the potential energy created by the proton electrochemical gradient to the F1 domain, causing its conformation change, leading to the phosphorylation of ADP to ATP (Jonckheere et al., 2012; Spikes et al., 2020). Dimers of CV were shown to regulate cristae biogenesis (Blum et al., 2019) and interestingly, to be involved in the process of cell death, via the formation of permeability transition pores (PTPs) (Mnatsakanyan et al., 2019; Pinke et al., 2020).

1.2.1 Roles of assembly factors

The assembly of mitochondrial complexes is a mammoth task since these complexes are composed of dozens of subunits (except for CII), encoded by both mtDNA and nuclear DNA, which need to be imported inside mitochondria (Donati et al., 2018; Harbauer et al., 2014) and contain several cofactors, such as the heme and Fe-S clusters (Cogliati et al., 2018; Priesnitz and Becker, 2018). With increasing organism complexity the number of subunits also increases, where we can distinguish core subunits, conserved in simpler organisms and supernumerary subunits, likely regulating the stability and assembly of complexes (Pierron et al., 2012; Stroud et al., 2016). It is thus not surprising that the assembly of the respiratory complex involves many assembly factors (that I will refer to here as AFs), ranging from 4 for

CII up to 50 for CIV, which is even higher than the number of CIV subunits (Vercellino and Sazanov, 2022).

Very briefly, the assembly of CI requires around 20 AFs and involves the formation of six independent modules (Formosa et al., 2018). The assembly of CII involves 4 AFs, where two membrane subunits dimerise, and the remaining two matrix subunits are associated with cofactors and bind to the membrane dimer (Bezawork-Geleta et al., 2017). The assembly of CIII involves three intermediate states and 8 AFs, with the dimerisation occurring early during its assembly (Ndi et al., 2018). The assembly of CIV seems by far the most complex, involving almost 50 AFs, during which three subcomplexes are assembled first, each one containing one of the core subunits (Timón-Gómez et al., 2018). The assembly of CV involves the independent formation of 5 subcomplexes, assisted by 5 AFs (Signes and Fernandez-Vizarra, 2018)

A further layer of complexity was added to this system by the characterisation of supercomplexes in the year 2000 (Schägger and Pfeiffer, 2000), structurally resolved more than 15 years later (Gu et al., 2016; Letts et al., 2016). Supercomplexes were shown to regulate the assembly of individual complexes and regulate OXPHOS efficiency (Protasoni et al., 2020). They are referred to as quaternary structures and currently, we distinguish 5 types: 1. CI-$CIII_2$-CIV also known as respirasome, 2. CI-$CIII_2$, 3. $CIII_2$-CIV, 4. CI-CII-CIII-CIV and 5. CII-CIII-CIV supercomplexes (reviewed in Guan et al., 2022).

For the proper assembly of complexes, subunits need to be in correct localisation and topology, to have specific post-translational modifications and interact with correct subunits. AFs thus fulfil a variety of roles, regulating transcription and translation, insertion of subunits into membrane, proteolysis and clearance of fragments, association of subunits with cofactors, acting as chaperons etc (Vercellino and Sazanov, 2022; Watson and McStay, 2020).

1.2.2 Drosophila respiratory chain

In *Drosophila*, the structure and function of the respiratory chain are largely conserved with vertebrates, with a similar number of subunits and AFs (Tripoli et al., 2005). As in mammals, *Drosophila* CI contains 14 core subunits, 7 encoded by the nuclear DNA and 7 by the mtDNA (Rhooms et al., 2020). The number of accessory subunits of the CI remains unclear. The mass-spectrometry performed in flight muscle mitochondria proposed the presence of 38 subunits (Garcia et al., 2017), while the Flybase database predicts 43 subunits in total (Gramates et al., 2022). The Complex II is conserved and consists of four subunits (Tripoli et al., 2005). The CIII has 10 known identified subunits, from which one is mtDNA-encoded, missing one subunit compared to vertebrates. CIV is also conserved, having 14 subunits, from which three are mtDNA-encoded (Brischigliaro et al., 2022). CV contains 16 subunits, missing one subunit compared to vertebrates, with two being mtDNA-encoded (Tripoli et al., 2005) (**Table 1**).

The number of assembly factors is not precisely determined in *Drosophila*, many of them being predicted in the Flybase database, but never tested. According to Flybase, the CI involves 13, CII 5, CIII 6, C IV 22 and CV 6 assembly factors.

CI		CII	CIII	CIV	CV
ND-B8	ND-24	SdhC	UQCR-11	COX7C	ATPsynE
ND-AGGG	ND-B14.7	SdhB	ox	levy	ATPsynB
ND-13B	ND-15	SdhD	UQCR-C1	COX5A	ATPsynG
ND-B18	ND-B15	SdhA	Cyt-c1	COX4	ATPsynD
NP15.6	ND-19		RFeSP	COX6B	ATPsynO
ND-MWFE	ND-42		UQCR-Q	cype	sun
ND-B16.6	ND-B22		UQCR-C2	COX5B	ATPsyngamma
ND-13A	ND-B17		UQCR-6.4	COX8	ATPsynbeta
ND-B14.5B	ND-39		UQCR-14	COX7A	ATPsynCF6
ND-B14.5A	ND-ASHI		mt:CYTB	COX7B	ATPsyndelta
ND-51	ND-SGDH			ND-MLRQ	ATPsynF
ND-B12	ND-49			mt:COX1	ATPsynC
ND-B17.2	ND-75			mt:COX2	blw
ND-20	ND-30			mtCOX3	Neb-cGP
ND-23	ND-B14				mt:ATP6
ND-PDSW	CG11752				mt:ATP8
ND-18	CG40472				
ND-ACP	ND-MNLL				
mt:ND1	mt:ND5				
mt:ND2	mt:ND6				
mt:ND3	mt:ND4				
mt:ND4L					

Table 1. List of *Drosophila* genes encoding subunits of the respiratory chain.

1.3 Mitochondrial quality control

1.3.1 Ubiquitin-proteasome

Mitochondrial quality control (MCC) is the ensemble of mechanisms that remove damaged and misfolded mitochondrial proteins, components or even entire mitochondria. As mentioned above, for proper mitochondrial function, the majority of proteins operating in mitochondria are imported from the nucleus in an unfolded state by various importing systems (Donati et al., 2018; Harbauer et al., 2014). In mammals, 1200-3200 such proteins are currently annotated (Leyfer and Fetterman, 2023; Rath et al., 2020). In *Drosophila*, at least 1064 genes were annotated as having a mitochondrial function (Poliacikova et al., 2023; Yim et al., 2020). Since such a vast quantity of proteins are imported from the cytosol, protein quality in the cytosol is the first layer of protection of the mitochondrial function (Quiles and Gustafsson, 2020).

To ensure protein quality control the cell uses a protein degradation machinery called ubiquitin-proteasome system (UPS). It is a dynamic multi-protein complex that exists in several variants. Its central part is the barrel-shaped 20S core particle possessing proteolytic activity. Upon binding of the 20S core particle with the 19S regulatory particle that brings target specificity, a 26S proteasome forms, that specifically degrades ubiquitinated proteins (Livneh et al., 2016). Ubiquitination of proteins is a stepwise process, in which the ubiquitin-activating E1 enzyme activates ubiquitin (Ub) and transfers it to the ubiquitin-conjugating enzyme E2, which together with E3 ubiquitin ligase transfers the Ub to the substrate protein (Finley, 2009).

The fact that the cytosol protein quality impacts mitochondria can be demonstrated upon inhibition of the proteasome, where protein aggregates that accumulate in the cytosol are enriched in proteins destined for mitochondria (Sung et al., 2016). In line with this are observations showing that proteins imported in mitochondria seem to be constantly degraded by the cytosolic proteasome, seemingly competing with the mitochondrial import machinery

(Bragoszewski et al., 2013; Margineantu et al., 2007; X. Wang and Chen, 2015). Others found an increase of ubiquitinated proteins in the IMM upon proteasome inhibition (Lavie et al., 2018), suggesting that UPS dysfunction leads to the accumulation of protein aggregates both inside and outside of mitochondria (Quiles and Gustafsson, 2020).

In the respiratory chain, an additional layer of possible damage arises from the fact that many subunits composing the respiratory complexes are embedded in the IMM and contain thus transmembrane domains (TMDs), which render them insoluble and prone to aggregation. Many mitochondrial proteins are so-called metastable, meaning that when a critical concentration of the protein is achieved, they tend to aggregate (Bragoszewski et al., 2017; Ciryam et al., 2015). In line with this is the observation that various proteasome stresses lead to a consistent and irreversible aggregation of respiratory chain complexes in the cytosol, due to the presence of so-called low-complexity regions in their N-terminus region, rendering many complex subunits unstable (Rawat et al., 2019). Furthermore, since respiratory complexes require both nuclear-encoded and mtDNA-encoded subunits for their assembly, a proper quantity and stoichiometry of each component needs to be maintained to avoid aggregation (C. M. Brennan et al., 2019; Houtkooper et al., 2013).

1.3.2 Mitochondrial proteases

The first layer of protection against misfolding damage inside mitochondria is the protection afforded by chaperons and proteases, historically viewed as guardians of protein quality (Leonhard et al., 1999), now known to contribute to many mitochondrial physiological functions (Deshwal et al., 2020). There are at least 45 proteases in mitochondria, 23 located exclusively in the mitochondria and others shuttling between mitochondria and cytosol. They harbour an independent proteolytic system that allows them to degrade polypeptides into amino acids. We distinguish processing peptidases, ATP-dependent proteases, oligopeptidases, and other mitochondrial peptidases.

Mitochondrial peptidases remove signals from the newly imported proteins, such as mitochondrial importing sequence and other peptides, a crucial step for their maturation, action and localisation (Poveda-Huertes et al., 2017). ATP-dependent proteases form multimeric, cylinder-shaped complexes, that use ATP hydrolysis to unfold substrates, translocate them in the proteolytic chamber and process them into oligopeptides (Gerdes et al., 2012). Oligopeptidases then cleave the oligopeptides into amino acids (Teixeira and Glaser, 2013). In *Drosophila*, there are at least 10 mitoproteases (Poliacikova et al., 2023), the best characterised being the conserved Lon protease (Lon) (Pareek et al., 2018) and Caseinolytic protease proteolytic subunit (ClpP) (Matsushima et al., 2017) proteases. Besides its role in degrading misfolded or oxidised proteins (Van Melderen and Aertsen, 2009), studies in Drosophila showed that Lon is involved in the regulation of mtDNA maintenance (Matsushima et al., 2010) and its downregulation triggers a stress response leading to the inhibition of mitochondrial translation (Pareek et al., 2018). As Lon, ClpP is a serine, ATP-dependent protease, degrading misfolded and damaged proteins and is additionally involved in the regulation of mtRNA biogenesis (Matsushima et al., 2017).

1.3.3 Mitochondrial unfolded protein response

If levels of misfolded damage in mitochondria exceed the capacity of chaperones and proteases, the mitochondrial unfolded protein response (UPR^{mt}) is activated. Similarly to the endoplasmic reticulum UPR (UPR^{ER}), UPR^{mt} is triggered by an accumulation of misfolded proteins and activates the transcription of nuclear genes, even though their target genes differ (Quiles and Gustafsson, 2020). UPR^{mt} thus involves a retrograde mitochondria-to-nucleus signalling, leading to inhibition of the translation of new proteins and activation of chaperone proteins, proteases and proteins involved in ROS detoxification (Muñoz-Carvajal and Sanhueza, 2020). UPR^{mt} can be triggered by various stresses often leading to protein damage, such as the impairment of the ETC, increase in ROS levels, alteration of mitochondrial dynamics and deletion of mtDNA. UPRmt includes cytosolic and mitochondrial chaperones, heat shock proteins (Hsp), the leading families being Hsp40, 60, 70, 90, Hsp100/Clp and small Hsp (sHsp), named by their estimated molecular mass.

The molecular mechanism of UPR^{mt} was first described in *Caenorhabditis elegans*, where upon sustained protein damage, there is a nuclear translocation of activating transcription factor associated with stress-1 (ATFS-1), which in conjunction with ubiquitin-like protein 5 (Ubl5) and defective proventriculus-1 (DVE-1) trigger the expression of chaperon proteins, proteases, mitochondrial import proteins and other proteins to restore homeostasis. Interestingly, ATFS-1 has both a nuclear and mitochondrial localisation sequence, and in stress-free conditions is degraded in the mitochondrial matrix by the Lon protease (Nargund et al., 2012).

1.3.4 Mitophagy

Mitophagy is defined as a selective autophagy of mitochondria and constitutes another level of mitochondrial network protection (Lemasters, 2005). During autophagy, portions of cytoplasm are sequestered into double-membrane vesicles (autophagosomes) and delivered to lysosomes for degradation (Dikic and Elazar, 2018). During mitophagy, mitochondria are sequestered into autophagosomes via specific receptor proteins, linking mitochondrial OMM to the autophagy membrane. Depending on the requirement of the kinase Phosphatase and tensin homolog (PTEN)-induced putative kinase 1 (PINK1), and Ub E3 ligase Parkin, we can distinguish PINK1/Parkin-dependent and PINK1/Parking-independent mitophagy. Many triggers for mitophagy were proposed, such as mitochondrial depolarisation, matrix acidification, hypoxia, iron chelation, Listeria infection, high glucose levels, and accumulation of misfolded proteins (Killackey et al., 2020).

In the PINK1/Parkin-dependent mitophagy, the main trigger is believed to be the loss of mitochondrial potential. The proposed mechanism is the following. In healthy mitochondria with a negative membrane potential, PINK1 is translocated into the matrix, where it is processed by proteases and retro-translocated to the cytosol for degradation (Greene et al., 2012; Whitworth et al., 2008). In contrast, if mitochondria depolarise, the import of proteins into mitochondria is stalled and PINK1 accumulates at the OMM, promoting the recruitment of Parkin (Narendra et al., 2010). PINK1 phosphorylates Ub present on OMM proteins and Parkin to potentiate its Ub E3 ligase activity, creating an amplification loop (Kane et al., 2014; Koyano et al., 2014; Shiba-Fukushima et al., 2014). The presence of poly-Ub chains on OMM proteins recruits autophagy receptors leading to mitochondrial degradation (Lazarou et al., 2015). This

mechanism was described in harsh laboratory conditions, in which mitochondria were treated with depolarising agents and OXPHOS inhibitors. Studies in both *Drosophila* (Lee et al., 2018) and mice (McWilliams et al., 2018) showed that the loss of PINK1 or Parkin does not affect the basal level of mitophagy, leaving the role these proteins play in physiological conditions elusive.

The PINK1/Parkin-independent pathways, also referred to as mitophagy receptor pathways, use mitochondria proteins containing a LIR motif enabling the direct recruitment of the autophagy machinery to mitochondria, such as BNIP3 (Quinsay et al., 2010) and FUNDC1 (Liu et al., 2012).

Part 2. Transcriptional control of mitochondrial respiration

Mitochondrial content and respiratory capacities are highly dynamic to accommodate the energetic requirements of different tissues during their development and adult life. The precise transcriptional control of genes encoding components of oxidative metabolism is essential for the proper mitochondrial function (Ploumi et al., 2017; Scarpulla, 2008; Scarpulla et al., 2012; Scholtes and Giguère, 2022; van Waveren and Moraes, 2008).

Among the first identified nuclear TFs regulating mitochondrial respiration is the nuclear respiratory factor 1 NRF1 (*Drosophila* Erect wing (Ewg)) (Fazio et al., 2001; Rai et al., 2014), first identified as a cyt c regulator (Chau et al., 1992). NRF1 activates the transcription of several respiratory genes as well as regulators of the mtDNA replication and transcription machinery (Evans and Scarpulla, 1989, 1990; Satoh et al., 2013), notably the mitochondrial transcription factor A (TFAM) (Dairaghi et al., 1995). GA-binding protein transcription factor (GABPA), also known as NRF2 (*Drosophila* Ets97/Delg) (Baltzer et al., 2009), similarly to NRF1 regulates mtDNA expression and some OXPHOS genes (Bruni et al., 2010; Yang et al., 2014), the best known being COX subunits (Ongwijitwat et al., 2006). Nuclear factor erythroid 2-like 1 NFE2L1 (*Drosophila* Cap-n-collar (Cnc)) (Sykiotis and Bohmann, 2008), mainly known to regulate detoxification response is also involved in the regulation of respiratory genes (Zhao et al., 2024).

Transcriptional coactivator peroxisome proliferator-activated receptor gamma coactivator-1 PGC1-α (Drosophila Spargel (Srl)) (Tiefenböck et al., 2010) is known to interact with NRF1, NRF2 and oestrogen-related receptor alpha (ERRα), stimulating the expression of several OXPHOS genes (Shao et al., 2010; Vega et al., 2000). Host cell factor 1 (Hcf-1) was shown to act with PGC1-α and NRF2 to regulate respiratory gene expression (Vercauteren et al., 2008). Cyclic-AMP response element-binding protein B (CREB) (Drosophila CrebB) (Yin et al., 1995) can induce PGC1-α expression (Herzig et al., 2001) and is mainly involved in the regulation of mitochondrial metabolism in the liver (Pardo et al., 2017). Both CREB and Specificity protein 1 (Sp1) were proposed to regulate cyt c expression (Evans and Scarpulla, 1989). In *Drosophila*, Sp1 was shown to activate the expression of cyt c1 (Zaid et al., 1999) and a few other respiratory genes in vertebrates (Kelly and Scarpulla, 2004). Ying yang 1 (YY1) (*Drosophila* Pleiohomeotic (Pho)) (Brown et al., 1998) was shown to regulate the COX subunits (Seelan and Grossman, 1997) and other respiratory genes (Cunningham et al., 2007; B. Li et al., 2022). The conserved Myocyte enhancer factor 2 (Mef2) (Bour et al., 1995) was shown to activate some COX subunits in muscles (Wan and Moreadith, 1995), under the control of NRF1

(Ramachandran et al., 2008). The E2F and retinoblastoma protein (pRb) were shown in addition to their role in the cell cycle regulation to regulate the switch between glycolytic and oxidative metabolism (Benevolenskaya and Frolov, 2015; Blanchet et al., 2011).

In summary, the high number of OXPHOS proteins and distinct energetic requirements of different tissues and organs call for the existence of large upstream GRNs. A large array of TFs regulating distinct components of the respiratory chain allows for a fine-tuned modulation of oxidative capacities in space and time.

Part 3. Mitochondrial changes during muscle development

Muscles are highly metabolically active tissues, containing large amounts of mitochondria to sustain their function. Several fibre types can be distinguished according to their metabolic properties and requirements. With decreasing oxidative capacity, we can distinguish, slow-twitch, type I fibres which exhibit high resistance to fatigue and are enriched in postural muscles and fast-twitch, type II fibres, which are quickly fatigable with high power outputs, enriched in directional muscles. With lower oxidative capacities we can further distinguish fast-oxidative (IIA), fast-intermediate (IIX) and fast-glycolytic (IIB) fibres (Talbot and Maves, 2016).

All these metabolically distinct fibre types are sustained by various mitochondrial networks, in which mitochondrial content, dynamics and orientation vary. Oxidative fibres display higher individual mitochondrial volume, a grid-like mitochondrial network and higher fusion rates, glycolytic fibres show a perpendicular orientation to the contraction axis and less connectivity and cardiac fibres have a parallel mitochondrial network (Bleck et al., 2018; Mishra et al., 2015; Ogata and Yamasaki, 1985; Willingham et al., 2019). One of the key questions in muscle mitochondrial biology is how these different networks are regulated to support the distinct metabolic requirements of the muscles they fuel and how these organisations arise during development.

Due to the inaccessibility for imaging of mouse muscle mitochondria during in-utero development, very few studies focused on mitochondrial changes during muscle development (Kim et al., 2019; Mishra et al., 2015). These studies showed that the mitochondrial dynamics and the orientation of the mitochondrial network change during muscle development, accompanied by an increase in OXPHOS protein levels during postnatal development in mice, but how these processes are regulated remains unclear.

Similarly to vertebrate muscles, distinct mitochondrial networks operate in different *Drosophila* muscles, where fibrillar, flight muscles display a parallel mitochondrial network and tubular muscles a grid-like network, except one fibre type in leg muscles (Fibre I), jump muscles and DFMs that present parallel mitochondrial networks, nevertheless with smaller mitochondrial volume compared to fibrillar muscles (Avellaneda et al., 2021; Katti et al., 2022). Due to the largely characterised muscle development and accessibility for imaging of all development stages (Fernandes et al., 1991; Lemke and Schnorrer, 2018), developing flight muscle mitochondria are the most studied (Avellaneda et al., 2021; Rai et al., 2014; Sauerwald et al., 2019). During myoblast fusion, mitochondria are first small and thin, around 45 h APF they start to extensively elongate and then become larger and rounder (Rai et al., 2014; Sauerwald

et al., 2019). Similarly to data obtained in postnatal mice muscles (Kim et al., 2019), a large transcriptional increase of OXPHOS protein-encoding genes was described during flight muscle development (Spletter et al., 2018).

During flight myogenesis, there is mechanical feedback between mitochondria and myofibrils, where strikingly, the perturbation of mitochondrial dynamics can change the muscle fate. Increasing mitochondrial fusion, or decreasing mitochondrial fission in myofibrils post-fusion leads to the transformation of fibrillar fibres to tubular fate (Avellaneda et al., 2021). Furthermore, this study emphasised that during development, mitochondria are largely excluded from developing myofibrils and rapidly intercalate between them around the time of sarcomere assembly. The master regulator of the switch between fibre types, Salm, was proposed to also mediate the distinction between mitochondrial networks in these fibre types (Avellaneda et al., 2021). Indeed, Salm and its downstream target TF H15 were shown to promote the parallel mitochondrial network in flight muscles. H15 was shown to also regulate the parallel network in the jump muscle and one leg fibre type and Ct to regulate the leg muscle mitochondrial network (Katti et al., 2022).

Concerning the regulation of flight muscle mitochondrial metabolism, Salm was proposed to at least in part mediate the large transcriptional increase of OXPHOS-genes during flight muscle development, even though its binding to the promoters of these genes was not demonstrated (Spletter et al., 2018). The Retinoblastoma-family protein (Rbf) was shown to bind to promoters of OXPHOS genes in flight muscles at the pharate stage, but the consequences of Rbf loss on mitochondrial morphology and function were not studied. Interestingly, looking for genes downstream of Rbf in the regulation of muscle development, it was shown that the most significantly enriched motif in genes activated by Rbf is the Motif 1 (Zappia et al., 2019), bound by M1BP (Li and Gilmour, 2013). Since M1BP, was already shown to regulate metabolism in the fat body (Barthez et al., 2020), and its expression is ubiquitous (Li and Gilmour, 2013), it can potentially also do so in the flight muscles. Even though more data about mitochondrial changes during muscle development are available in *Drosophila*, the picture of how these changes are transcriptionally regulated during development remains incomplete.

Thesis objectives

During my thesis I had the chance to work on two distinct projects, both focusing on different aspects of the transcriptional regulation of adult flight muscle development.

Objective 1. Characterising the timing and mechanism of mitochondrial metabolism regulation in flight muscles by M1BP

Looking for molecular mechanisms of Hox function, the group identified M1BP as a novel cofactor of *Hox* genes in the regulation of autophagy (Zouaz et al., 2017). Following this study, the group showed that the downregulation of *M1BP* in the fat body leads to a deregulation of many metabolic genes (~25%), suggesting that *M1BP* function in the regulation of metabolism extends far beyond autophagy (Barthez et al., 2020).

Preliminary work of M. Barthez (former PhD student in the group and the co-first author of Article 1) in the fat body showed that *M1BP* KD leads to a widespread downregulation of genes associated with mitochondrial oxidative metabolism, genes that are directly bound by M1BP in this tissue. Downregulation of *M1BP* also leads to an appearance of electron-dense inclusions in the fat body mitochondria, visible using TEM. The work of M. Barthez thus established M1BP as a direct regulator of mitochondrial oxidative metabolism in the fat body (Thesis of M. Barthez, 2019).

Knowing that M1BP was described as a ubiquitous protein (J. Li and Gilmour, 2013), the group wondered how widespread the M1BP function of regulating mitochondrial metabolism is. Choosing another highly metabolic tissue for the analysis, the adult flight muscle, M. Barthez showed that upon muscle-specific *M1BP* KD, large mitochondrial inclusions also appear in adult flight muscle mitochondria. Adult flies lacking *M1BP* in muscles display a flightless phenotype (Thesis of M. Barthez, 2019).

Upon my arrival in the laboratory, I continued this work, performing a genetic, transcriptomic and biochemical analysis of the M1BP function in developing flight muscle mitochondria, resulting in Article 1, published in *Nature Communications* in May 2023.

Objective 2. Characterising the potential role of Hox in the regulation of mitochondrial metabolism in flight muscles

We showed that M1BP is an activator of oxidative mitochondrial metabolism in the adult flight muscles (Poliacikova et al., 2023). The laboratory previously demonstrated that M1BP collaborates with Hox proteins in the process of autophagy regulation (Zouaz et al., 2017). Building on these observations we thus wondered whether the transcriptional activation of oxidative metabolism in flight muscles by M1BP involves Hox.

As a candidate, we selected the *Antp* gene, as its domain of expression spans the T2 segment where flight muscles develop (Levine et al., 1983; Martinez-Arias, 1986). Antp was shown to regulate larval lateral muscle development, by directly activating iTF *ap* (Capovilla et al., 2001). Furthermore, a transcriptomic study of flight myogenesis detected the expression of both *Antp* and *M1BP* in wing disc-associated myoblasts (Spletter et al., 2018). Based on this

evidence we hypothesised that the activation of mitochondrial oxidative metabolism in flight muscles could be a result of a cooperation between *M1BP* and *Antp*.

This hypothesis proved false, as we did not detect any effect of *Antp* KD on the mitochondrial metabolism **(Fig. 23)**. Labelling mitochondria using a mitochondrially-directed fluorescent protein Dendra2 allows for live visualisation of large adult DLM mitochondria. While in the *M1BP* KD condition mitochondria display severe disorganisation, inhomogeneous labelling and a presence of large zones devoid of Dendra2 staining, upon *Antp* KD mitochondria resemble the wild-type condition, except for being smaller in size (**Fig. 23A**). Furthermore, the quantity and integrity of IFM mitochondrial complexes upon muscle-specific *Antp* KD is unperturbed (**Fig. 23B**), concluding that *Antp* does not regulate oxidative metabolism in flight muscle mitochondria with *M1BP*.

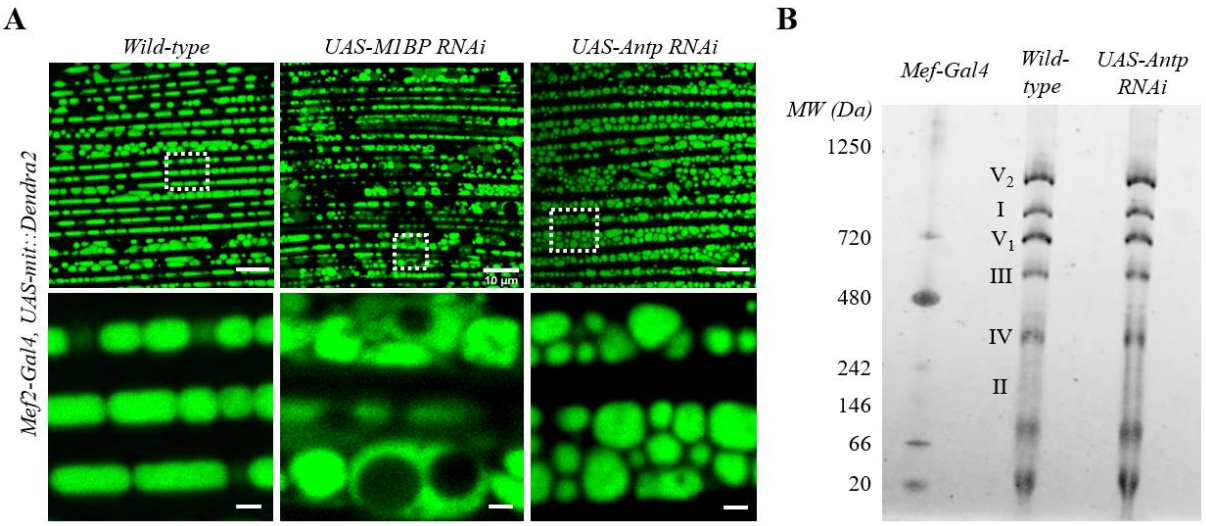

Figure 23. Antp does not regulate oxidative metabolism in flight muscles with M1BP. (A) Adult female DLM mitochondria visualised using UAS-mit::Dendra2 transgene, driven by the muscle ubiquitous *Mef2*-Gal4 driver. Zoomed views of individual mitochondria are depicted by white dashed rectangles. Scale bars are 10 µm for large views and 1 µm for zoomed views. Efficient KD of *M1BP* occurs at 25°C and of *Antp* at 29°C **(B)** Native-PAGE on adult mitochondria isolated from adult thoraces, allowing to visualise the complexes of the mitochondrial respiratory chain (depicted here in italic numbers, V1 and 2 referring to a monomer of dimer of the complex V). Flies were kept at 29°C prior to dissection for optimal RNAi expression. My unpublished data.

While considering the cooperative role of *M1BP* and *Antp* in the flight muscle mitochondria, we co-labelled wing disc-associated myoblast at the L3 stage and detected both Antp and M1BP expression in these cells. This results was in contradiction with previous reports stating that Antp is not expressed in flight myoblasts and that the development of flight muscles occurs independently on Hox (reviewed in Laurichesse and Soler, 2020; Roy et al., 1997). Furthermore, we observed that upon muscle-specific *Antp* KD adult flies displayed an outstretched wing position and were flightless, suggestive of a default in flight muscle development. In the second part of my thesis, I thus decided to change the second objective and to characterise the role of *Antp* in the transcriptional regulation of adult flight myogenesis, the results of which are presented in the Article 2, currently resubmitted after revision in *Science Advances*.

Results

Article 1. M1BP is an essential transcriptional activator of oxidative metabolism during *Drosophila* development

nature communications

Article

https://doi.org/10.1038/s41467-023-38986-5

M1BP is an essential transcriptional activator of oxidative metabolism during *Drosophila* development

Received: 26 July 2022

Accepted: 23 May 2023

Published online: 02 June 2023

Check for updates

Gabriela Poliacikova[1,2], Marine Barthez[1,2], Thomas Rival[1], Aïcha Aouane[1], Nuno Miguel Luis[1], Fabrice Richard[1], Fabrice Daian[1], Nicolas Brouilly[1], Frank Schnorrer[1], Corinne Maurel-Zaffran[1], Yacine Graba[1] & Andrew J. Saurin[1]

Oxidative metabolism is the predominant energy source for aerobic muscle contraction in adult animals. How the cellular and molecular components that support aerobic muscle physiology are put in place during development through their transcriptional regulation is not well understood. Using the *Drosophila* flight muscle model, we show that the formation of mitochondria cristae harbouring the respiratory chain is concomitant with a large-scale transcriptional upregulation of genes linked with oxidative phosphorylation (OXPHOS) during specific stages of flight muscle development. We further demonstrate using high-resolution imaging, transcriptomic and biochemical analyses that Motif-1-binding protein (M1BP) transcriptionally regulates the expression of genes encoding critical components for OXPHOS complex assembly and integrity. In the absence of M1BP function, the quantity of assembled mitochondrial respiratory complexes is reduced and OXPHOS proteins aggregate in the mitochondrial matrix, triggering a strong protein quality control response. This results in isolation of the aggregate from the rest of the matrix by multiple layers of the inner mitochondrial membrane, representing a previously undocumented mitochondrial stress response mechanism. Together, this study provides mechanistic insight into the transcriptional regulation of oxidative metabolism during *Drosophila* development and identifies M1BP as a critical player in this process.

Mitochondria, the energetic hubs of the cell, are best known for harbouring pathways required for efficient ATP synthesis through the tricarboxylic acid (TCA) cycle and oxidative phosphorylation (OXPHOS). These essential, evolutionary conserved organelles are at the core of cellular metabolism[1] and as such their dysfunction lies central to a plethora of chronic human diseases, including myopathies, multiple encephalopathies and neuropathies, diabetes, epilepsy and cancer (reviewed in ref. 2).

The OXPHOS system consists of the respiratory chain complexes I to IV and the mitochondrial F_1F_o-ATP synthase, herein referred to as Complex V. Mitochondrial content and the expression of genes encoding the OXPHOS complex system are highly dynamic to adapt to the metabolic and energetic demands of the different tissues of an organism[3]. The timely transcriptional control of nuclear genes encoding proteins of various metabolic pathways is essential for proper mitochondrial biogenesis and function, since mitochondria

[1]Aix-Marseille Univ, CNRS, Developmental Biology Institute of Marseille (IBDM), UMR 7288, Case 907, Turing Center for Living Systems, Parc Scientifique de Luminy, 13288 Marseille Cedex 09, France. [2]These authors contributed equally: Gabriela Poliacikova, Marine Barthez. e-mail: andrew.saurin@univ-amu.fr

import the vast majority of their proteins from the cytoplasm[4–6]. Numerous transcription factors and transcriptional co-activators have been identified that regulate the transcription of nuclear-encoded mitochondrial genes implicated in mitochondrial function, biogenesis and OXPHOS (herein referred to as mito-genes[7]) (reviewed in refs. 8–10). The role these factors play in mitochondrial adaptation to environmental cues, stresses or disease has been extensively studied, yet how this is coordinated in a developmental context is less well known.

Muscles are one of the most energetically demanding tissues in the body, requiring large amounts of ATP for their contraction and proper function[11]. Several fibre types can be distinguished according to their contractile and metabolic properties. Slow-twitch, type I fibres exhibit high resistance to fatigue, are enriched in postural muscles and are largely oxidative. Fast-twitch, type II fibres, are quickly fatigable with high power outputs and are enriched in directional muscles. With a decreasing oxidative capacity, we can further distinguish fast-oxidative (IIA), fast-intermediate (IIX) and fast-glycolytic (IIB) fibres (reviewed in ref. 12). Mitochondria dynamics, orientation and content vary between different fibre types, with oxidative fibres displaying higher individual mitochondrial volume, a grid-like mitochondrial network and higher fusion rates, while mitochondria in glycolytic fibres show a perpendicular orientation to the contraction axis and less connectivity[13–15].

Studies conducted in vitro and in postnatal muscles have demonstrated that proteins associated with mitochondrial biogenesis and respiration increase sharply during muscle differentiation[16–19]. Even though several factors regulating mitochondrial metabolism have been identified, their requirement at different stages of muscle development and between different muscle fibre types are poorly understood.

In *Drosophila*, adult muscle development has been extensively studied, the most prominent adult muscles being the highly oxidative indirect flight muscles (IFMs) oscillating at 200 Hz during flight[20]. A second muscle type is present in the adult legs or abdomen mediating locomotion or mating. Remarkably, the mitochondrial morphology between both muscle types is strikingly different with flight muscle mitochondria containing very dense cristae and being in very close contact with the contractile myofibrils, in contrast to the more complex shapes of leg muscle mitochondria that locate more sparsely in the middle and at the periphery of myofibrils[21].

Indirect flight muscles are formed from myoblasts that are attached to the notum region of the larval wing disc. During early pupation, myoblasts migrate and fuse with surviving larval muscle scaffolds, the larval oblique muscles (LOMs), to form the dorsal longitudinal flight muscles (DLMs). In contrast, dorso-ventral flight muscles (DVMs) form de novo, without any larval scaffolds. DLMs and DVMs form collectively the adult indirect flight muscles[22,23], that we will for simplicity herein refer to as flight muscles. Since mitochondrial flight muscle development takes place during the accessible pupal stage[22], *Drosophila* is an excellent model to study the molecular control of mitochondrial biogenesis and dynamics during muscle development.

Current data suggest that several transcription factors and coactivators are involved in mitochondrial oxidative metabolism control during flight muscle development. The transcription factor Spalt-major (encoded by the *salm* gene), known for its role in muscle fibre identity[24] has been shown to regulate the expression of both sarcomeric and mitochondrial genes during myogenesis[7,21]. Specifically, Spalt is involved in the upregulation of TCA and OXPHOS protein coding genes after 30 h after puparium formation (APF) in flight muscles, although it is unclear whether it is directly or indirectly activating the expression of these genes[7,21]. Retinoblastoma-family protein (Rbf) has been shown to directly activate the transcription of both sarcomeric and mitochondrial respiratory chain-encoding genes, but the functional consequences on mitochondria development upon Rbf loss of function were not studied[25].

Interestingly, it was shown that a motif enriched in genes activated by Rbf is a motif bound by Motif-1 binding protein (M1BP)[25,26]. M1BP is an RNA polymerase II pausing factor, binding to the promoters of genes involved in basic cellular processes such as cell cycle and metabolism. We have previously shown that M1BP plays an important role in the control of metabolism since one-quarter of all metabolic genes are downregulated upon fat body-specific M1BP knock-down[27]. These data prompted us thus to ask whether M1BP function in metabolism control is important in *Drosophila* muscles.

In this study, we performed an ultrastructural imaging description and detailed transcriptional and biochemical analyses of mitochondrial oxidative metabolism during the course of *Drosophila* flight muscle development. This work identifies an essential role for M1BP in activating the transcription of nuclear-encoded OXPHOS-related genes and in controlling mitochondrial respiratory chain assembly. This approach provides a detailed analysis of *Drosophila* flight muscle mitochondrial development and identifies a critical player in the regulation of muscle mitochondrial oxidative metabolism.

Results

M1BP loss leads to ultrastructural defects in mitochondria

It had been shown that OXPHOS genes activated by Rbf in flight muscles contain Motif-1[25], which is bound by Motif-1 binding protein[26]. M1BP is a transcription factor that regulates the transcription of metabolic genes in the larval fat body[27] and in in vitro cell culture systems[26,28]. Based on these observations, we wished to determine whether M1BP is involved in the regulation of mitochondrial metabolism in the flight muscles.

Throughout flight muscle development, transcriptome data demonstrate that *M1BP* expression is relatively stable (data analysed from[7] and represented in the Supplementary Fig. 1a), which we confirmed by immunolabelling in both wing disc-associated myoblasts (labelled by a *twi*::*GFP* transgene[29]) and adult flight muscle nuclei (Supplementary Fig. 1b, c). Driving UAS-M1BP RNAi construct by the muscle-specific *Mef2-GAL4* driver (Mef2 > *M1BP*-RNAi), expressed during all myogenic stages[30], we knocked down *M1BP* expression by ≈40–60% in myoblasts and in the adult muscle (Supplementary Fig. 1b′, c′, c″). It has been previously reported that expressing *M1BP* RNAi in in vitro cell culture conditions leads to the eventual cell cycle arrest following few days of RNAi expression[26,31]. We thus wanted to test whether M1BP knockdown (KD) in myoblasts will affect their proliferation. To count the number of wing disc-associated nuclei, we developed a machine learning-based, 3D nuclei counting technique that allowed us to estimate the number of myoblasts on the wing disc notum region at 0 h APF to approximately 1500 cells. As we did not detect any significant decrease in myoblast number upon *M1BP* RNAi driven by *Mef2-GAL4*, we thus conclude that M1BP does not regulate myoblast proliferation (Supplementary Fig. 1d).

To test whether M1BP plays a role in the regulation of flight muscle metabolism, we first assessed the muscle function after M1BP downregulation by a standard flight assay[32]. Flight muscles depleted of M1BP during development do not support flight, with 50–100% of adult males (depending on the RNAi line used), being flightless (Fig. 1a). For *M1BP* RNAi #1 we further showed that even though a milder percentage of adults are flightless, the flight muscles in this condition are less resistant to fatigue compared to the WT (Supplementary Fig. 2a). To identify the origin of these phenotypes, we performed an immunolabelling of adult DLMs. *M1BP* RNAi driven by *Mef2-GAL4* results in no visible perturbation of adult sarcomeric integrity and size (Fig. 1b, b′). Mitochondria in *M1BP*-depleted muscles, stained with an anti-Complex V antibody (ATP5A subunit, encoded by the *bellwether* gene), are present in between myofibrils, although they display a severe defect in their shape (Fig. 1b, bottom panels) that prompted us to investigate the mitochondria further.

https://doi.org/10.1038/s41467-023-38986-5

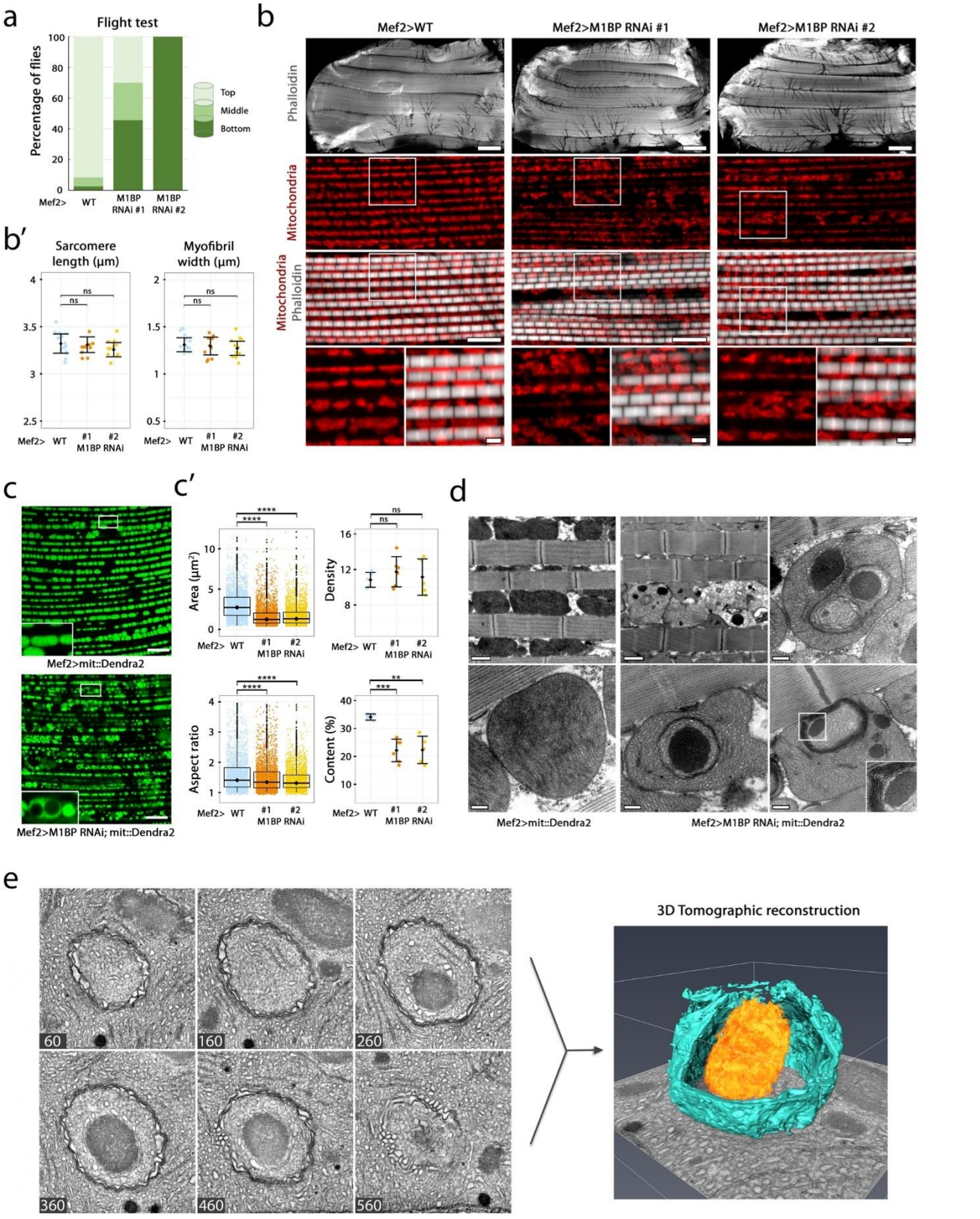

Knowing that the *Mef2-GAL4* transgene can drive expression in a subset of neurons[33] and that *Mef2* is expressed also in the fat body[34], we wished to verify that the muscle mitochondrial phenotypes we observed upon *M1BP* KD are not due to perturbation of *M1BP* expression in these other tissues. This is particularly important for the fat body, given the known intercommunication between fat body and muscle[35–37] and that transcription factor perturbation in one can result in a phenotype in the other[38]. To this end, we downregulated *M1BP* with either a pan-neural *elav-GAL4* driver or a fat body-specific *cg-GAL4* driver, yet observed no sarcomeric or mitochondrial phenotypes in the flight muscles (Supplementary Fig. 2b, c). Furthermore, we confirmed the muscle paralysis and mitochondrial morphology defects upon

Fig. 1 | M1BP downregulation in flight muscles leads to mitochondrial ultrastructural defaults. a Flight ability was scored as a mean percentage of male flies landing on column segments, from two independent biological replicates ($n_{WT} = 150$, $n_{\#1} = 90$ and $n_{\#2} = 20$). **b** Confocal sections of female wild-type (left) and M1BP-depleted DLMs with two different RNAi lines, (#1 and #2) driven by *Mef2*-GAL4. White rectangle represents an enlarged view. Myofibrils are stained with phalloidin (grey) and mitochondria with anti-ATP5A antibody (red). The scale bar is 100 μm (top), 10 μm (middle) and 2 μm (bottom views). **b'** Quantification of muscle parameters, each dot corresponding to one animal ($n_{WT} = 15$, $n_{\#1} = 10$ and $n_{\#2} = 11$ flies). Mean and standard errors are indicated. After applying Shapiro–Wilk test for normality, two-sided Mann–Whitney test was applied (p-values (length) = 0.87 and 0.1 and p-values (width) = 0.53 and 0.44). **c** Confocal sections of live 2-days-old female adult wild-type (left) and M1BP-depleted (right) DLM mitochondria labelled with mit::Dendra2, driven by *Mef2-GAL4*. Scale bars represent 10 μm. **c'** For area and aspect ratio quantification, data are represented in boxplots (median and quartiles) with whiskers (minimum to maximum), where each point represents one mitochondrion ($n_{WT} = 2464$, $n_{\#1} = 3196$ and $n_{\#2} = 2535$ mitochondria). Outliers are depicted with black circles. Two-sided Mann–Whitney test was applied (*p* values (area) = 2×10^{-16} **** and (aspect ratio) = 2.9×10^{-9} and 2.8×10^{-9} ****). For density and content quantification mean and standard errors are indicated, where each point represents one confocal section ($n_{WT} = 5$, $n_{\#1} = 6$ and $n_{\#2} = 6$ sections). After applying Shapiro–Wilk test for normality an unpaired two-sided Student's test was applied (*p* values (density) = 0.28 and 0.76 and (content) = 0.0005 *** and 0.005 ***). **d** TEM micrographs of male adult WT (left) and *M1BP*-depleted (middle, right) DLM mitochondria. Scale bars represent 1 μm (larger views) and 200 nm (individual mitochondria). **e** Tomographic reconstruction of an inclusion (orange) and the IMM (blue) (to visualise the inclusion a part of the IMM was computationally removed). Six of the 633 slices from the reconstructed tomogram stack are shown with their respective stack position. Source data are provided as a Source data file.

M1BP KD with another myoblast-specific driver, *Him-GAL4*, that in our hands downregulates *M1BP* expression until the adult stage to a similar level as the *Mef2-GAL4* driver (Supplementary Fig. 2d, e), demonstrating that the phenotypes we observe in flight muscle are due to M1BP function in this tissue.

To better characterise the mitochondrial morphology defects we observed, we used a mitochondrially localised fluorescent protein, mit::Dendra2, enabling live mitochondrial imaging in *Drosophila* tissues[39]. While wild-type mitochondria display the well described regular ellipsoid shapes[21], *M1BP*-depleted mitochondria are severely disorganised and display heterogeneous fluorescent intensity (Fig. 1c). We quantified a number of mitochondrial parameters: area, aspect ratio (ratio of major to the minor axis), density (number of mitochondria per 100 μm^2) and mitochondrial content (mitochondrial area with respect to total area), on live mitochondria to avoid fixation artefacts (Fig. 1c'). We observed that mitochondria in muscles from *M1BP* RNAi are smaller than WT mitochondria (the area median of 2.8 μm^2 in WT compared to 1.29 μm^2 and 1.36 μm^2 in two distinct *M1BP* RNAi expressing lines) and slightly rounder (WT median aspect ratio of 1.4 compared to 1.3 in both *M1BP* RNAi-expressing lines). Furthermore, we detected a significantly lower mitochondrial content upon *M1BP* KD (mean of 34% in WT and 22% in both *M1BP* RNAi-expressing lines), with no significant change in the mitochondrial density (mean of 11 mitochondria per 100 μm^2 in WT vs 11.7 and 11.1 in *M1BP* KD). Together, this suggests that mitochondria are smaller due to a decrease in their biogenesis rather than an increase in their fission. Importantly, we observed many mitochondria containing large circular zones devoid of mit::Dendra2 staining (see Fig. 1c inset).

Transmission electron microscopy (TEM) confirmed that the adult sarcomere ultrastructure is unperturbed by M1BP RNAi, as assayed by longitudinal (Fig. 1d) and cross-sections (Supplementary Fig. 3a) of adult flight muscles. While wild-type adult flight muscle mitochondria display dense, parallel, lamellar cristae spanning the mitochondria, *M1BP* downregulation leads to widespread mitochondrial ultrastructural defects (Fig. 1d): while we observed several instances of translucid mitochondria that are likely being eliminated (Fig. 1d, top middle panel), the most prominent, widespread defects were large, amorphous, electron-dense inclusions in the mitochondrial matrix. We noticed that in adult mitochondria, these inclusions were often encircled by several rounds of inner mitochondrial membrane (IMM), with the mitochondrial matrix enclosed within being more electron-lucent (Fig. 1d, middle bottom and right panels). We hypothesise that the inclusions either represent a spatial constraint on developing cristae that end up by encircling them during cristae development or that mitochondria actively attempt to isolate the inclusions from the remaining mitochondrial matrix, which could account for the more electron-lucent matrix surrounding the inclusions and correspond to the observed mit::Dendra2-excluded zones in live imaging. To test whether IMM encirclement could serve for compartmentalisation of inclusions we performed serial electron tomography 3D-imaging. The reconstruction showed that the inner mitochondrial membrane completely encompasses the electron-dense structures, thereby isolating it from the rest of the matrix (Fig. 1e and Supplementary Movie 1), which is suggestive of an active mitochondrial process to isolate the inclusion using the IMM that has not yet been described.

We confirmed the presence of mitochondrial inclusions in the flight muscles upon *M1BP* KD with another muscle-specific driver, *Him-GAL4* (Supplementary Fig. 3b). Furthermore, mitochondrial inclusions can also be observed upon *M1BP* KD in the tubular leg muscles upon *Mef2-Gal4* KD (Supplementary Fig. 3c) and in the highly metabolically active fat body upon *cg-GAL4* KD (Supplementary Fig. 3d). Of note here, like for the flight muscle mitochondrial inclusions that result in flight defects, leg muscle function is severely perturbed, which we attribute to the mitochondrial defects observed since *M1BP* KD results in flies that are unable to climb and are severely restricted in the speed at which they walk (Supplementary Fig. 3c'). This mitochondrial phenotype thus includes both fibrillar and tubular muscle types and even spans to other metabolically active tissues.

Overall, these data demonstrate that M1BP downregulation in the muscle leads to widespread adult mitochondrial morphological defects, ultimately resulting in muscle paralysis as observed through a flightless and climbing phenotype.

OXPHOS transcription is concomitant with cristae biogenesis

Having shown that flight muscle mitochondria upon *M1BP* KD contain large inclusions in their matrix, we wished to determine the developmental origin of this phenotype. It is widely accepted that mitochondria undergo regulated changes during the muscle differentiation process[13,17]. Several studies imaged mitochondrial dynamics during flight muscle development using fluorescence microscopy that does not allow for proper cristae visualisation[21,40,41], while a study focusing on the trachea invasion of flight muscles used electron microscopy imaging but was limited to two developmental time points[42].

Given the little available ultra-structural data about mitochondrial development during flight myogenesis, we first decided to better describe this process in the wild-type situation, and second characterise the function that M1BP plays. To characterise mitochondrial morphological ultrastructural changes during flight myogenesis in more detail, we used high-resolution, transmission-electron microscopy. We performed a time-course of flight muscle mitochondrial development spanning from third instar larval myoblasts until the adult stage (Fig. 2a and Supplementary Fig. 4a). Wing disc-associated myoblasts give rise to flight muscles during pupation[22]. Their mitochondria at 0 h APF have few cristae (mean of 6.9 cristae per 500 nm), which does not change during early stages of myogenesis through to 48 h APF (mean density of 6.3 cristae; quantification of cristae at 34 h

https://doi.org/10.1038/s41467-023-38986-5

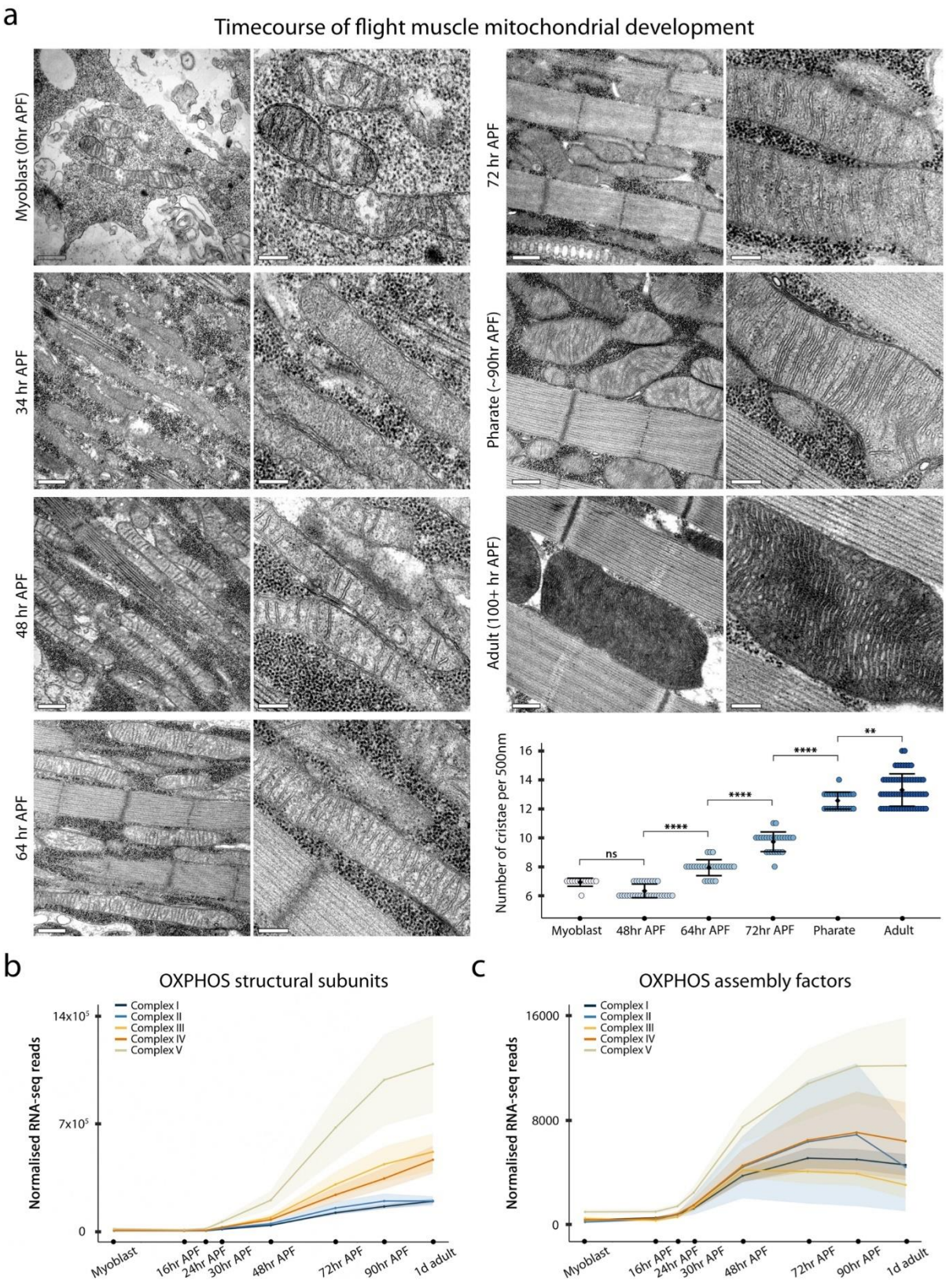

APF was not performed as they were poorly defined by TEM). The density of cristae starts to increase around 64 h APF (mean density of 7.9 cristae) and continues increasing throughout development to eclosion (mean density of 13.3 in 2-day-old adults) (Fig. 2a). The number of cristae appears to peak during the first week of adult life (mean density of 15.2 in 7 days-old adults), since the number of cristae in aged flies decreases to the values observed at eclosion (mean density of 13.3 in 30-day-old adults) (Supplementary Fig. 4b).

During the early stages of myogenesis, mitochondria intercalate between immature myofibrils and elongate into large tubules[21,41]. While cristae biogenesis has not yet started, we observed a sharp decrease in the mitochondrial circularity and increase in perimeter between 24 h

Fig. 2 | Large scale OXPHOS-related gene transcriptional upregulation and mitochondrial cristae biogenesis occur during flight muscle development. **a** Transmission electron microscopy micrographs of wild-type flight muscle development spanning from wing-disc associated myoblasts to 2 days-old adult DLM. For each time point, a larger view (left, scale bar of 500 nm) and a zoom on mitochondria cristae (right, scale bar of 200 nm) are represented. The quantification of the number of mitochondrial cristae per length unit (500 nm) is shown for each corresponding time point except for 34 h APF. Mean and standard deviation are shown with each point representing a value of a single mitochondrion (*n* (Myo) = 12, *n* (48 h) = 19, *n* (64 h) = 15, *n* (72 h) = 23, *n* (pharate) = 21 and *n* (adult) = 47 mitochondria). For statistical analysis, one-way analysis of variance (ANOVA) was performed, followed by Tukey's test for multiple mean comparisons (*p* values: Myo vs 48 h = 0.2; 48 h vs 64 h = 0 ****; 64 h vs 72 h = 0 ****; 72 h vs pharate = 0 ****; pharate vs adult = 0.002 **). **b**, **c** Transcriptional profile during flight muscle development of genes encoding structural subunits (**b**) and assembly factors (**c**) of the mitochondrial respiratory chain complexes. The solid lines represent the normalised mean of sequenced counts of all subunits/assembly factors of a given respiratory complex with shaded areas representing the standard error of the mean. Source data are provided as a Source data file.

and 34 h APF, which might be important for proper myofibril development (Supplementary Fig. 4c)[21]. Of note is that between the pharate and the adult stages, mitochondria increase significantly their area and perimeter to adopt their typical ellipsoid shape and squeeze densely into a single row in between adult myofibers[21] (Supplementary Fig. 4c).

Mitochondrial cristae bear the OXPHOS protein complex chain, comprised of five multimeric complexes that are comprised of numerous core enzymatic subunits, accessory subunits and proteins required for their assembly (reviewed in ref. 43). To complement our imaging analysis and provide further insight into mitochondrial metabolic states during flight muscle development, we performed a computational analysis of OXPHOS gene expression during flight myogenesis using available transcriptome data performed at similar developmental time points[7]. Using Flybase[44] and Gene Ontology (GO)[45] databases we manually curated a list of *Drosophila* nuclear genes encoding core and accessory subunits (herein called structural subunits; 73 genes) as well as genes encoding proteins required for complex assembly (termed assembly factors; 52 genes) of the *Drosophila* mitochondrial respiratory chain (that we will collectively refer to in this article as OXPHOS genes) (Supplementary Data 1). We observed that OXPHOS gene expression has two phases: first a basal expression phase that occurs from third instar larval myoblasts until 48 h APF (after puparium formation), followed by a large-scale transcriptional upregulation phase sustained until the adult stage (Fig. 2b, c and Supplementary Data 1). The transcriptional upregulation of these genes is complex-dependent: genes encoding subunits of Complex V are transcribed at the highest level, Complexes III and IV subunits have a similar transcriptional profile with a number of reads being approximately half than those of Complex V, and Complexes I and II have the lowest transcription levels, being approximately 20% of those of Complex V (Fig. 2b).

The transcriptional upregulation of OXPHOS assembly factors slightly precedes the upregulation of structural subunits and peaks between 70–90 h APF before showing trends of downregulation at the adult stage (Fig. 2c and Supplementary Fig. 5a). Similar to the structural subunits, the transcripts of genes encoding assembly factors of Complex V are the most abundant. Assembly factors of other complexes have similar expression profiles with approximately half the number of transcripts compared to Complex V.

Continuing our analyses of the developmental transcriptome data from Spletter and colleagues[7], we extended this to genes coding for other critical OXPHOS components: creatine kinases (in *Drosophila* arginine kinases), involved in ATP buffering[46], adenosine nucleotide translocases (ANTs), mediating ADP/ATP transport[47] and the mitochondrial phosphate carrier (PiC), involved in the inorganic phosphate transport across the IMM[48]. The expression of *Drosophila* orthologue of vertebrate creatine kinases, *Arginine kinase 1* (*Argk1*)[49] peaks at the mid-myogenesis (Supplementary Fig. 5b). Concerning *Drosophila* orthologues of vertebrate ANTs, *Ant1*, also called *stress sensitive B* (*sesB*) and *Ant2*[50], only *Ant1* transcripts were detected during flight myogenesis and its expression dynamics follows those of OXPHOS subunits and assembly factors (Supplementary Fig. 5c). Similarly, for the *Drosophila* orthologues of PiC, *Mitochondrial phosphate carrier proteins 1* (*Mpcp1*) and 2 (*Mpcp2*)[51], only *Mpcp1* expression was detected and its expression follows similar dynamics to *Ant1* and OXPHOS-related genes (Supplementary Fig. 5d).

The expression of genes involved in the TCA cycle and glycolysis follows very similar dynamics to OXPHOS genes, which is much less the case for genes involved in other mitochondrial processes such as amino acid metabolism or the pentose phosphate pathway (Supplementary Fig. 5e). Together, these data highlight a large-scale transcriptional response of genes required for mitochondrial energy metabolism that correlate with extensive cristae biogenesis.

M1BP regulates OXPHOS gene expression during myogenesis

The *GAL4/UAS* system is a temperature-sensitive system, with increased temperature driving more *UAS-transgene* expression[52]. We noticed that rearing flies expressing *Mef2-GAL4* driven *M1BP* RNAi at 29 °C was lethal at the pharate stage, whereas at 25 °C only a third of flies eclose likely due to an incapacity of the fly to break the pupal case required for eclosion. We thus used this lethality phenotype to determine when M1BP function is required during adult myogenesis. Temporal control of *M1BP* RNAi expression during myogenesis using the TARGET system, in which GAL4 is active at 29 °C and inactive at 18 °C[53], demonstrated an essential role for M1BP during early-to-mid pupation, since down-regulation of *M1BP* between ≈10–60 h APF leads to the pharate pupal lethality phenotype (Fig. 3a). This fits with stages at which the transcription of components involved in mitochondrial energy metabolism is increasing (see above).

To study the origin of mitochondrial defects in M1BP-depleted flight muscles we imaged mitochondria at three different time points, representative of distinct mitochondrial metabolic states we established earlier: myoblasts, in which the mitochondrial respiratory chain is poorly developed; 48 h APF, at which stage mitochondria are at the peak of their elongation and OXPHOS genes start to be transcriptionally upregulated; and 64 h APF when the process of cristae biogenesis is fully engaged (see Fig. 2 and Supplementary Figs. 4 and 5). We did not detect any major morphological changes in mitochondria in larval myoblasts or at 48 h APF upon *Mef2-GAL4* driven *M1BP* RNAi (Fig. 3b). In contrast, at 64 h APF, we observed that mitochondria in M1BP-depleted muscle display fewer cristae (mean density of 7.9 cristae in WT versus 6 upon *M1BP* KD) and contain small electron-dense, amorphous inclusions in their matrix, similar to those observed in adult *M1BP* KD mitochondria (Fig. 3b, bottom panels). We thus conclude that mitochondrial inclusions observed upon *M1BP* KD are of developmental origin, appearing around 60 h APF, at a time when we first observed an increase in the number of cristae in wild-type mitochondria (see Fig. 2).

Mitochondrial inclusions have been reported in patients suffering from myopathies[54] and cancer[55] but their origin has not been determined. Nevertheless, mitochondrial inclusions seem to be related to the mitochondrial respiratory chain defects since they have also been observed in mitochondria of rats fed with the respiratory toxin (cronotoxin)[56] and in yeast mutants for subunits of the Complex V[57]. We thus looked at transcriptomic changes in genes with mitochondrial function triggered by M1BP depletion in flight muscles that we reasoned could give us insight into the origin of mitochondrial inclusions we observed. We performed RNA-seq analyses at the same

https://doi.org/10.1038/s41467-023-38986-5

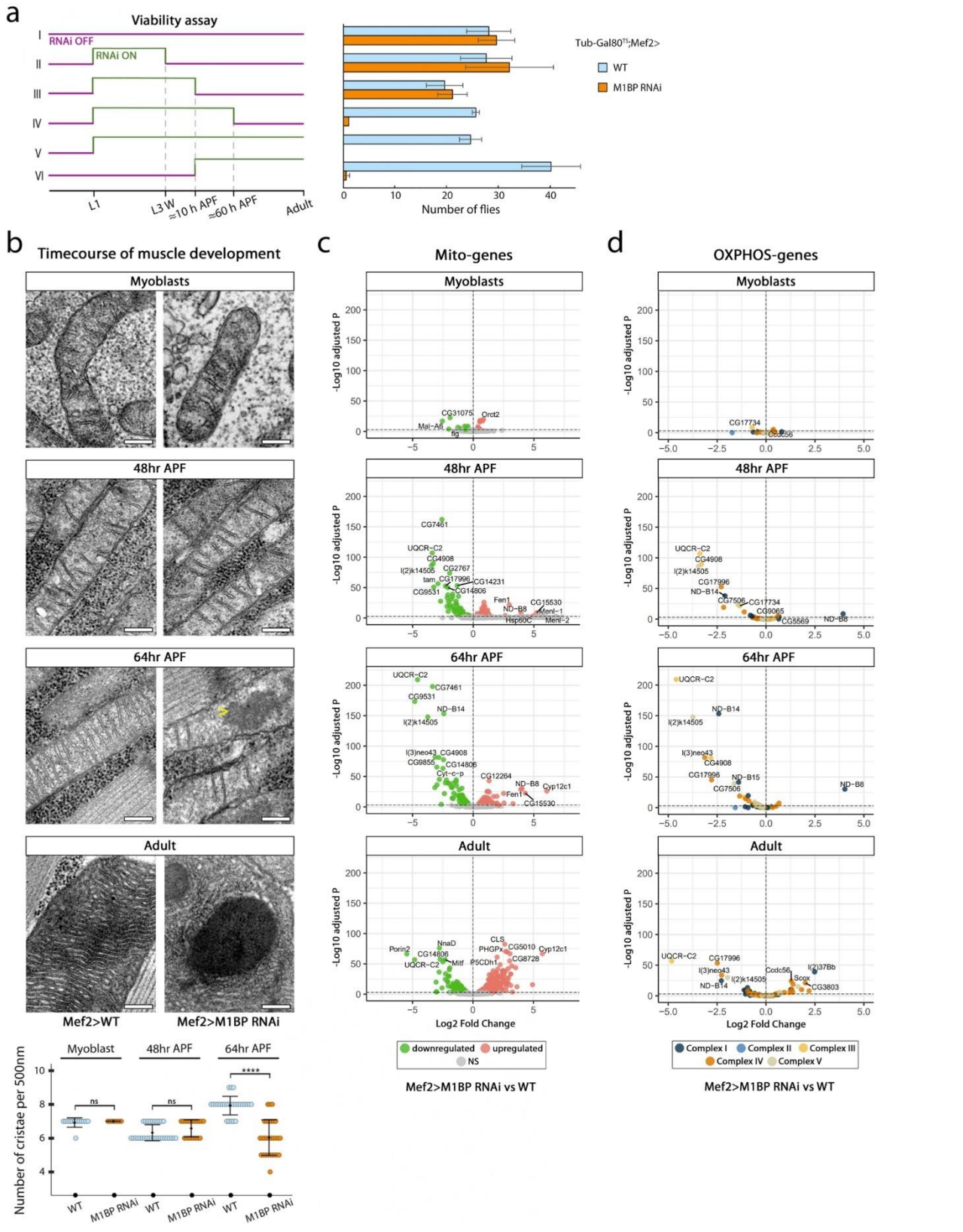

developmental time points as the electron microscopy analysis; on FACS-purified myoblasts to avoid contamination by wing disc epithelial cells and manually dissected flight muscles for pupal and adult stages. We first looked at the expression of all nuclear-encoded genes related to mitochondrial function from the curated MitoXplorer database[58] from which we excluded glycolysis-related genes and genes encoded by the mitochondrial genome (Mito-genes; $n = 1064$) (Fig. 3c). Using a highly stringent threshold ($padj \leq 0.001$), the differential gene expression (DGE) analyses showed that only 2% of Mito-genes were significantly deregulated upon *M1BP* RNAi in myoblasts, suggesting that M1BP is not involved in the transcriptional regulation of mitochondrial function in larval myoblasts (Supplementary Data 2),

Fig. 3 | M1BP regulates the expression of OXPHOS genes during flight muscle development. a *M1BP* downregulation was temporally controlled using *Mef2-GAL4* driven *tub-Gal80^{ts}* transgene. For each condition, the mean and standard deviation of the number of adult flies (both sexes included) is represented resulting from two independent biological replicates. **b** Transmission electron microscopy micrographs of mitochondria from WT (left) and M1BP-depleted (right) myoblast and pupal flight muscles at 48 h and 64 h APF, using *Mef2-GAL4* driver. Arrowhead highlights amorphous electron-dense inclusions visible in the matrix in 64 h APF preparations upon *M1BP* RNAi. Scale bars represent 200 nm. Quantification of cristae number per 500 nm is shown for each time point (n (Myo_{WT}) = 12, n (Myo_{RNAi}) = 8, n (48 h_{WT}) = 29, n (48 h_{RNAi}) = 15, n (64 h_{WT}) = 15, n (64 h_{RNAi}) = 28 mitochondria). After applying Shapiro-Wilk test for normality, two-sided Mann–Whitney test was applied (p values: Myo = 0.53; 48 h = 0.08; 64 h = 1.36×10^{-8} ****). **c**, **d** Volcano plots of all differentially expressed nuclear-encoded mitochondrial (**c**) or only OXPHOS-related (**d**) genes between Mef2>WT and Mef2 > *M1BP* RNAi at corresponding time points. For statistical analysis, the Wald test with Benjamini–Hochberg-correction was applied. Source data are provided as a Source data file.

confirming the electron microscopy data. At 48 h APF, 10% of Mito-genes become deregulated with approximate equal numbers being upregulated or downregulated (Supplementary Data 3). At 64 h APF nearly a quarter (22%) of all Mito-genes were differentially expressed upon *M1BP* RNAi, with more genes being significantly downregulated than upregulated (Supplementary Data 4). At the adult stage, we detected 41% differentially expressed Mito-genes upon *M1BP* KD (Supplementary Data 5).

At both pupal stages as well as the adult stage, the most downregulated genes, such as *UQCR-C2* and *l(2)k14505* are related to OXPHOS, whose expression levels were decreased by up to 30-fold. This prompted us to analyse separately genes related to OXPHOS using the updated list of OXPHOS-encoding genes we curated (Supplementary Data 1 and Fig. 3d). Interestingly, we observed a time-dependent increase in the number of OXPHOS-encoding genes that were significantly downregulated upon *M1BP* muscle-specific RNAi: whereas only two OXPHOS genes were differentially expressed at the myoblast stage, this increased to 15 genes (12%) at 48 h, 40 genes (32%) at 64 h and 35 genes (28%) at the adult stage and nearly all of these were downregulated.

The mitochondrial genome (mtDNA) encodes 13 subunits contributing to all OXPHOS complexes, except Complex II. The dynamics of their expression during myogenesis generally follows those expressed in the nucleus (Supplementary Fig. 6a, b). While intriguingly we observed an increased expression of some of the 24 tRNAs encoded by mtDNA during myogenesis, with the exception of a transient decrease in expression in *ND4L*, none of the 13 OXPHOS subunits genes encoded by the mitochondrial genome were affected by *M1BP* RNAi (Supplementary Fig. 6c and Supplementary Data 6).

Altogether, these data suggest that M1BP is required for the expression of nuclear-encoded OXPHOS genes during a critical period of their transcriptional upregulation.

A regulatory network exists at the promoters of OXPHOS genes

Being a transcription factor, we wondered whether M1BP transcriptionally regulates the expression of other transcription factors and cofactors whose role in OXPHOS regulation in other tissues has been already established (reviewed in ref. 59), which could account for the observed downregulation of OXPHOS gene transcription following *M1BP* KD. These known OXPHOS transcriptional regulators are: Mitochondrial transcription factor A (TFAM), a transcriptional regulator of the mitochondrial genome[60], the Rbf/E2f pathway linked with muscle metabolism and development[25,61] and known OXPHOS activators such as Erect Wing (Ewg, homologue of vertebrate NRF1)[62], Ets97D/Delg (homologue of GABPA)[63], Cap-n-collar (Cnc, homologue of NFE2L1/NRF2)[64], Spargel (Srl, homologue of PGC1-α)[65], its target Oestrogen-related receptor (ERR, homologue of ERRα/Essrg), the conserved Myocyte enhancer factor 2 (Mef2, homologue of MEF2)[66], Cyclic-AMP response element-binding protein B (CrebB, CREB1)[67], Host cell factor (Hcf), Pleiohomeotic (Pho, homologue of YY1)[68] and Stimulatory Protein 1 (SP1). With the exception of *ets97D*, *pho*, and *ERR*, available developmental transcriptome data[7] show that all factors are expressed at the mid-pupa stage of flight muscle development at levels at least equal to or higher than *M1BP* (Supplementary Fig. 7a), suggesting they could all represent potential M1BP targets in this tissue. However, upon *M1BP* RNAi, we observed no significant change in the expression of any of these genes in myoblasts and pupal stages, except for a transient decrease of *srl* levels. At the adult stage, we detected a slight downregulation of *crebB*, *mef2*, *hcf* and *ewg* levels (Supplementary Fig. 7b). This suggests that M1BP does not regulate the expression of other transcription factors, but rather cooperates with these factors to induce the large transcriptional upregulation of OXPHOS-genes during flight myogenesis.

To ascertain the possible regulatory networks underlying OXPHOS gene regulation, we undertook an in silico analysis of DNA-binding motif occurrence in the promoters of OXPHOS-genes regulated by M1BP and other OXPHOS sequence-specific transcription factors for whose DNA binding motifs were known. This approach showed that amongst the ten sequence-specific transcription factors studied, the DNA binding motif of M1BP is the most significantly represented in the promoters of OXPHOS-genes, followed by the E2F1 motif (Fig. 4a and Supplementary Data 7). Furthermore, the motif of M1BP can be found at 79 OXPHOS gene promoters (63%) placing it, along with Mef2, as one of the most overrepresented motifs at OXPHOS-gene promoters (Supplementary Data 7). Studying DNA motif co-occurrences among these ten transcription factors demonstrate a complex, but potentially interesting transcription factor regulatory network underlying the expression of OXPHOS genes (Fig. 4b and Supplementary Data 7).

Altogether, these data show that the main M1BP function in developing flight muscle mitochondria is in the transcriptional activation of OXPHOS-protein coding genes and that M1BP likely acts through the global transcriptional control of OXPHOS genes in cooperation with other known OXPHOS regulators.

M1BP loss results in reduced OXPHOS complex assembly

We showed that *M1BP* KD in flight muscles leads on the one hand to a decrease in expression levels of OXPHOS genes and on the other, to ultrastructural abnormalities such as matrix inclusions and fewer mitochondrial cristae. Muscle mitochondrial cristae abnormalities and the presence of inclusions have both been linked with respiratory chain impairment[57]. Analysis of OXPHOS-encoding nuclear genes downregulated upon *M1BP* KD identifies both structural subunits and assembly factors of respiratory complexes, the latter being much more affected by *M1BP* KD (Fig. 5a and Supplementary Data 3–5). Indeed, the DGE analysis showed that at 48 h APF 6% of genes encoding structural mitochondrial subunits and 15% of genes encoding mitochondrial assembly factors are significantly downregulated upon *M1BP* KD (Fig. 5a, left panels). At 64 h, 27% of structural subunits and 35% of assembly factors are significantly downregulated (Fig. 5a, middle panels). At the adult stage, 11% of structural subunits are downregulated, and some 50% of assembly factors are deregulated, with 13% of genes that are downregulated and 37% upregulated (Fig. 5a, right panels). Interestingly, the structural subunits whose expression is the most significantly affected in all time points belong to Complex I except for UQCR-C2, belonging to Complex III. However, the affected assembly factors belong mainly to Complexes III, IV and V. We did not detect any major changes in the expression of OXPHOS genes (subunits or assembly factors) relating to Complex II. Together, these data demonstrate that M1BP is a major transcriptional regulator of genes

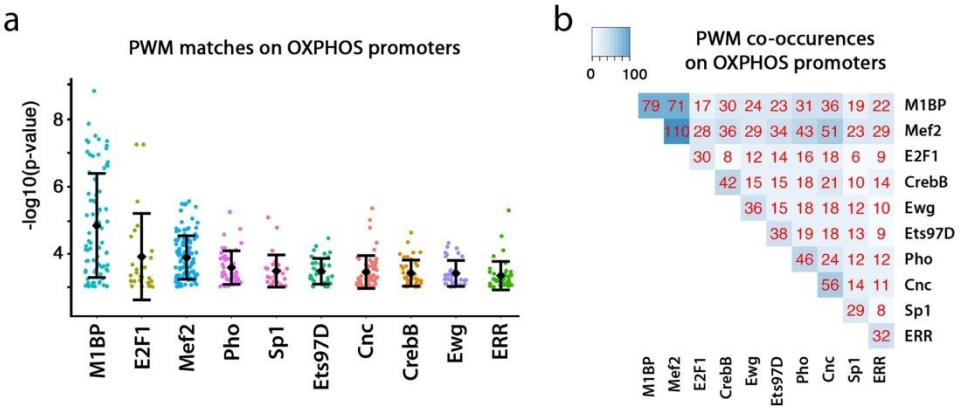

Fig. 4 | The promoters of OXPHOS genes contain DNA binding motifs of multiple transcription factors. a Motif occurrence analysis in promoters of OXPHOS genes of M1BP and other known OXPHOS transcriptional regulators. Each dot represents a binding motif found for a given factor in OXPHOS gene promoters (*n* (M1BP) = 80, *n* (E2F1) = 31, *n* (Mef2) = 111, *n* (Pho) = 47, *n* (Sp1) = 30, *n* (Ets97D) = 39, *n* (Cnc) = 57, *n* (CrebB) = 43, *n* (Ewg) = 37 and *n* (ERR) = 44 found motifs). The mean and standard deviation of −log10 (p-value) for each OXPHOS gene bound by a given factor is represented. *p* values, obtained using FIMO[113], are defined as the probability of a random sequence of the same length as the motif matching that position of the sequence with a score at least as good. **b** Motif co-occurrence analysis in promoters of OXPHOS genes of M1BP and other known OXPHOS transcriptional regulators, represented as a matrix, where each value corresponds to the number of genes bound by a single factor or in combination.

encoding respiratory chain assembly factors of Complexes I, III, IV, and V and structural subunits of Complexes I and III during flight muscle development.

The assembly and insertion in the inner mitochondrial membrane of OXPHOS complexes is a complex process, requiring the presence of assembly factors and a correct stoichiometry of structural subunits[69]. Having shown that M1BP KD affects the expression of numerous assembly factors and some structural subunits, we reasoned that this should lead to a decrease in the quantity of assembled OXPHOS protein complexes in the inner mitochondrial membrane (IMM). To test this, we performed Blue Native Polyacrylamide Gel Electrophoresis (BN-PAGE) on mitochondrial membrane-isolated complexes[70] which revealed that, with the exception of Complex II, for the same mitochondrial protein quantity loaded, the quantity of all mitochondrial complexes assembled in the IMM substantially decreases upon M1BP KD (Fig. 5b). Testing the in-gel enzymatic activities of Complexes I, II, IV and V (Complex III activity is incompatible with BN-PAGE[71]) demonstrated that while the assembly of Complex I, IV, and V was reduced, the assembled complexes were enzymatically active, where the difference in activity observed relative to wild type complexes is largely a reflection in the relative abundance of each assembled complex (Supplementary Fig. 8a). Interestingly, while the abundance of Complex II remained unchanged upon M1BP loss of function, the succinate dehydrogenase activity of this complex was consistently slightly higher, although the significance of this is unclear. To rule out the possibility of unequal protein loading, which could account for the observed differences, we performed the histochemical assays in a sequential manner, confirming the decreased activities of Complexes I, IV and V, while demonstrating that the increase in Complex II activity upon M1BP KD is consistent (Supplementary Fig. 8b). Altogether, these data show that the transcriptional downregulation of numerous OXPHOS assembly factors and/or structural subunits due to *M1BP* KD leads to largely reduced fully-assembled OXPHOS complexes in the adult.

Knowing that the dysfunction of the mitochondrial respiratory chain was linked with the appearance of mitochondrial inclusions[56,57], and that the subunits of OXPHOS complexes, destined to be inserted in the membrane are highly hydrophobic in nature, we hypothesised that the observed mitochondrial inclusions could contain misfolded, aggregated proteins, including OXPHOS complex components. To study this, we performed immunoblotting analyses of detergent soluble and insoluble protein fractions obtained from adult flight muscle-purified mitochondria. In line with the BN-PAGE data, using an antibody against a Complex V subunit, ATP5A we observed a decrease of ≈30% of ATP5A protein quantity in the soluble fraction upon M1BP KD. Interestingly, we observed a small amount of ATP5A in the detergent-insoluble fraction, solely in the M1BP KD condition (Fig. 5c). These data indicate that OXPHOS subunit solubility changes upon M1BP KD. Since the presence of an OXPHOS subunit in the insoluble-fraction does not demonstrate its presence in inclusions, we performed immuno-electron microscopy (Immuno-EM), allowing us to access mitochondrial inclusions on tissue sections. Quantification of ATP5A density in the cell cytosol, mitochondrial matrix or in mitochondrial electron-dense inclusions showed a significantly higher density of this subunit in mitochondrial inclusions compared to the mitochondrial matrix and outside of mitochondria (Fig. 5d). These results strongly suggest that the electron-dense inclusions represent protein aggregates, likely resulting from unassembled OXPHOS complex components.

M1BP KD triggers a mitochondrial protein quality control response

Since most proteins operating in mitochondria are imported from the cytosol, mitochondrial function depends on the correct folding and turnover of these proteins assured by mitochondrial protein quality control (reviewed in ref. 72). In line with our hypothesis that mitochondrial inclusions represent protein aggregates, amongst the most significantly upregulated genes upon *M1BP* KD in the adult flight muscles were genes linked to a proteotoxic response, such as ubiquitin-dependent catabolic process and cellular response to unfolded proteins (Supplementary Data 8). We thus performed a differential gene expression analysis upon *M1BP* KD using GO-based lists of genes related to the unfolded protein response (UPR, 93 genes), the ubiquitin-proteasome system comprising the catalytic subunit 20 S and the regulatory particle 19S (UPS, 35 genes), and mitochondrial proteases (Mitoproteases, 10 genes) (Supplementary Data 8). We detected significant upregulation of half of all UPR-related genes, all proteasome-related genes as well as all Mitoprotease-encoding genes (Fig. 6a, lower panels). Interestingly, we were able to detect changes in the expression of these genes already at the mid-pupa stage, when mitochondrial inclusions begin to appear (Fig. 6a, upper panels). These data demonstrate that M1BP KD elicits a strong transcriptional activation of protein quality control pathways.

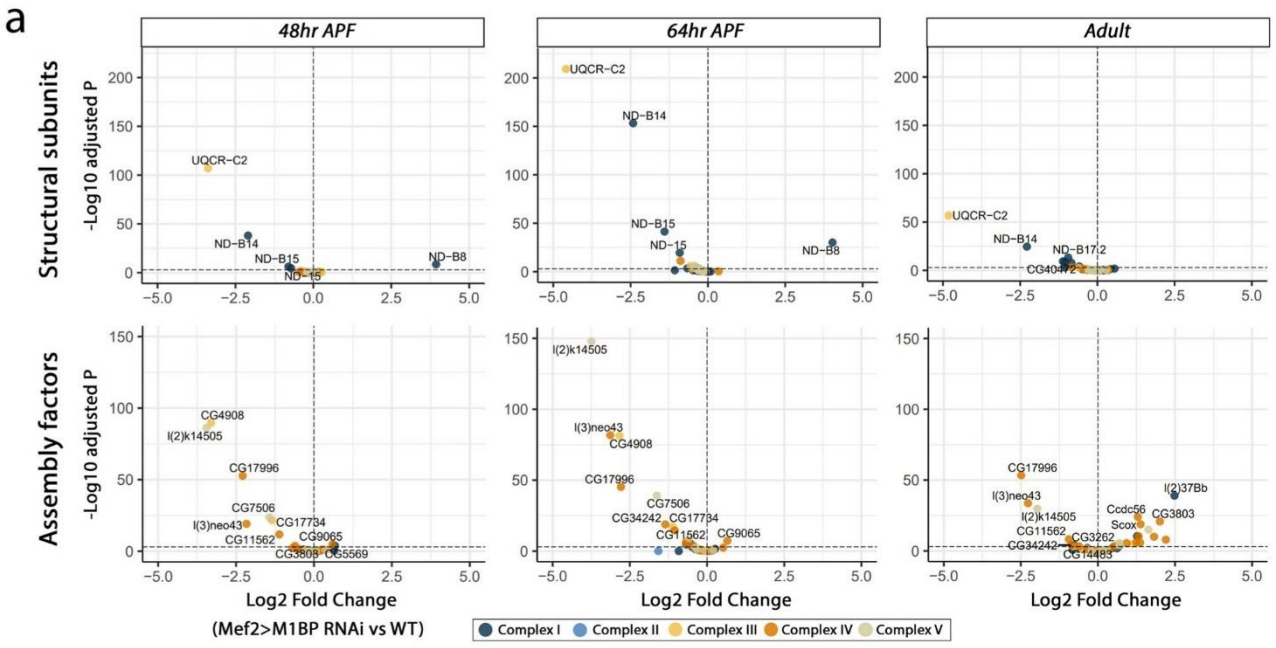

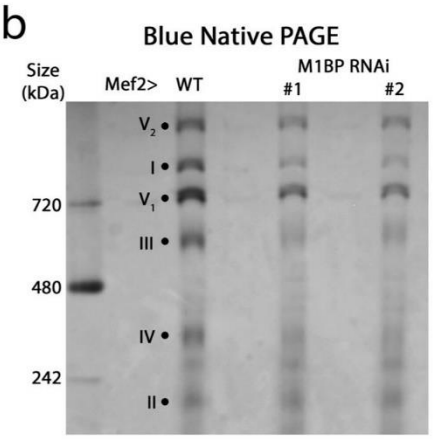

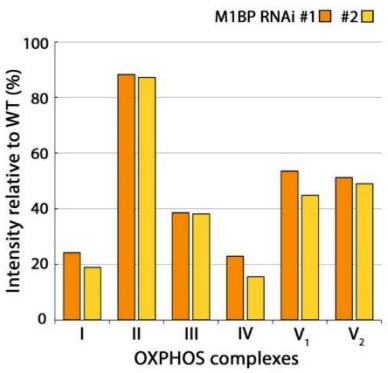

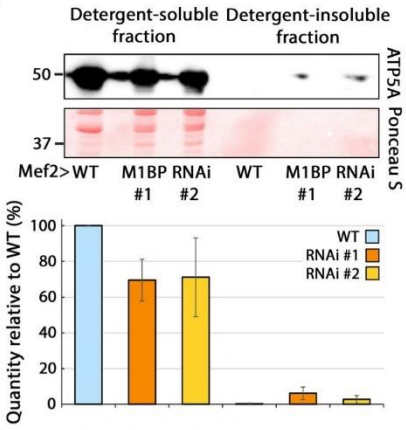

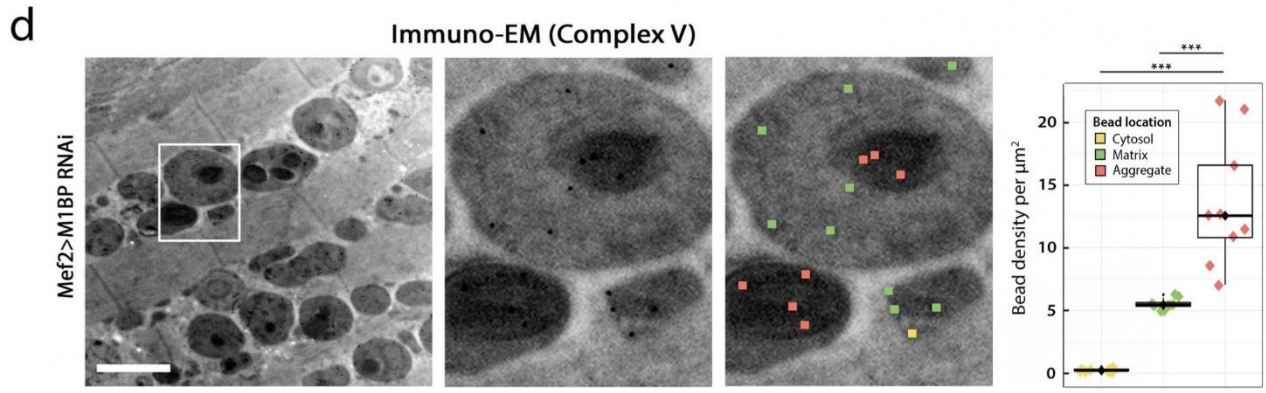

UPR is a cellular response to stress induced by the abnormal accumulation of unfolded or misfolded proteins either at the endoplasmic reticulum (UPR^{ER}) or in mitochondria (UPR^{mt}) (reviewed in[73,74]). While a large number of heat shock proteins, including Hsp70 family members, can localise to both the cytoplasm and mitochondria depending on the source of stress, we noticed among the most significantly upregulated genes the exclusively mitochondrial-localised small heat shock protein *Hsp22*[75] (Supplementary Data 6). This chaperonin interacts with mitochondrial-localised Hsp70 and Hsp60 family members[76], suggesting that the UPR observed upon *M1BP* KD is primarily of mitochondrial stress origin, which we sought to investigate in the flight muscle. Using mit::mKate2, a near far-red reporter line, to label mitochondria in fixed tissue, the Hsp70 stress response was shown to localise mainly to mitochondria (Fig. 6b), which together with the more than three-hundred-fold transcriptional increase in mitochondria-specific *Hsp22* demonstrates that *M1BP* KD leads primarily to a UPR^{mt}. Of note here is that like for mit::Dendra2 staining (Fig. 1c), large circular areas of the mitochondrial matrix were devoid

Fig. 5 | M1BP KD leads to reduced mitochondrial respiratory complex assembly. a Volcano plots of differential gene expression analyses between Mef2>WT and Mef2 > *M1BP* RNAi developing DLM. The top volcano plots represent genes encoding structural subunits and bottom plots assembly factors of mitochondria respiratory complexes. Genes are colour-coded accordingly to their complex membership. For statistical analysis, the Wald test with Benjamini–Hochberg-correction was applied. **b** Blue native polyacrylamide gel of mitochondrial complexes extracted from adult flight muscle mitochondria. Complexes are depicted by a black circle, V_1 and V_2 refer to the monomer and dimer of complex V, respectively. Quantifications of the intensity of bands, representative of the protein quantity for each complex are represented in the bar chart as a percentage relative to the WT. **c** Western Blot of ATP5A Complex V subunit on detergent-soluble and insoluble protein fractions from WT and M1BP-depleted adult purified mitochondria. The Ponceau S membrane staining is shown as a loading control. The mean band intensities are represented as histograms for each condition from two independent biological replicates. Protein size is indicated in kDa. **d** Representative transmission electron micrographs (with an enlarged view on the right, depicted by a white rectangle) of the ImmunoEM experiment using gold-conjugated secondary antibody targeting an anti-Complex V antibody. The gold conjugates were quantified with respect to their location. Data are represented in boxplots (median and quartiles) with whiskers (minimum to maximum), where each image gave rise to a single value of the density of beads for each of the three locations; $n = 9$ sections; total number of beads= 1048 in the matrix, 169 in the cytosol and 102 in aggregates. The scale bar corresponds to 2 μm. After applying non-parametric Kruskal–Wallis test the pairwise, two-sided Mann–Whitney test was used (p values = 0.0004 ***). Source data are provided as a Source data file.

of mit::mKate2 staining upon M1BP RNAi and these excluded areas did not contain Hsp70 protein (see Fig. 6b, enlarged area). It is thus possible that these areas, representing the electron-dense protein aggregates are likely inaccessible to the UPR^{mt}, reinforcing the notion that the observed aggregates are totally isolated from the remaining matrix by the IMM. These data showing a strong UPR^{mt} were confirmed by immunoblotting analyses on purified proteins from flight muscle mitochondria, using an anti-Hsp70 antibody (Fig. 6c). Interestingly, we observed upon M1BP KD several instances of ubiquitinylated proteins on mitochondria that are very lowly or not present in the WT condition (Fig. 6c, asterisk) as well as several proteins that were already poly-ubiquitinylated in the WT condition, but whose quantity strongly increase upon M1BP KD (Fig. 6c, dagger).

The UPR and UPS are the main transduction pathways that maintain protein homoeostasis under conditions of protein misfolding and aggregation and can result in the accumulation of poly-ubiquitinated proteins which are then either targeted for degradation by the proteosome or sequestered into insoluble protein aggregates (reviewed in ref. 77). To this end, analyses of the detergent soluble and insoluble protein fractions have proven useful in studying proteostasis. Since *M1BP* KD in flight muscles elicits such a large transcriptional proteotoxic response, we thus wished to analyse the general protein status in this condition. While we detected only minor changes in the detergent-soluble protein fraction between WT and M1BP-depleted adult flight muscles, in the detergent-insoluble protein fraction we detected several proteins appearing upon *M1BP* KD that are soluble in WT (Fig. 6d, asterisks) and several proteins whose insolubility increases upon *M1BP* KD (Fig. 6d, dagger). Similar to what we observed in the mitochondrial fraction, the insoluble protein fraction also showed increased ubiquitinated proteins (Fig. 6e).

Taken together, these data demonstrate that loss of M1BP function leads to widespread mitochondrial proteotoxic stress, resulting in the accumulation of insoluble protein aggregates in the mitochondrial matrix.

Discussion

M1BP transcriptionally regulates OXPHOS complex assembly

Relying on aerobic glycolysis for ATP generation, myoblasts, like all stem cells generally exhibit a fragmented mitochondrial network with underdeveloped cristae, yet maintaining a baseline of OXPHOS transcription and activity[19,78,79]. At this stage, we find that M1BP function is dispensable, as we see no modification to the transcription of OXPHOS-related genes through *M1BP* KD. However, at the onset of myofibrillogenesis, when OXPHOS transcription is normally upregulated together with mitochondrial cristae biogenesis, loss of M1BP function results in perturbed cristae biogenesis and loss of the transcriptional upregulation of numerous OXPHOS complex subunits and factors required for their assembly, with transcriptional defects affecting at least one major subunit or assembly factor of Complexes I, III, IV and V. Through biochemical analyses, we showed that these transcriptional defects resulted in vastly reduced assembly of these complexes in the IMM in adults (Fig. 5). Of note is that we observed neither transcriptional defects in factors related to Complex II nor in modification to the levels of assembled Complex II upon *M1BP* KD.

Concomitant with the loss of transcriptional upregulation of numerous OXPHOS complex subunits and assembly factors, the loss of M1BP function triggers an accumulation of electron-dense inclusions in the mitochondrial matrix, originating from the mid-pupa stage and persisting until the end of muscle differentiation (see Figs. 1d and 3b) which contain at least a subunit of the respiratory Complex V (see Fig. 5d). Knowing that the expression of numerous assembly factors is downregulated at least ten-fold upon *M1BP* RNAi, we believe this leads to a reduction in mitochondrial respiratory complexes assembly and the insoluble aggregation of their precursors. Numerous observations are in favour of this: first, subunits of the mitochondrial complexes are destined for integration in the inner mitochondrial membrane and thus contain transmembrane domains, which have hydrophobic properties rendering the proteins prone to misfolding damage. Second, many mitochondrial proteins are metastable, meaning that they aggregate when their critical concentration is achieved[80,81]. Third, in the transcriptomic time-course of flight muscle development, we observed that the transcription of OXPHOS complex assembly factors precedes the transcription of structural subunits (see Fig. 2b, c). The early presence of assembly factors in mitochondria thus seems critical to prevent misfolding and aggregation of subunits upon their arrival in mitochondria. Fourth, we observed a strong mitochondrial protein quality control response upon *M1BP* RNAi starting at the mid-pupa stage, correlating with the appearance of protein aggregates in mitochondria, as well as an increase in the amount of poly-ubiquitinylated proteins in the adult flight muscles (see Fig. 6). Fifth, it had been shown in yeast, that the failure to assemble Complex V can lead to the aggregation of structural subunits in inclusions bodies and a decrease in mitochondrial cristae quantity[57]. Based on these data we suggest that the aggregates present in the mitochondrial matrix upon M1BP downregulation contain misfolded OXPHOS complex subunits.

Apart from factors assuring protein complex assembly, the correct subunit stoichiometry is crucial for the proper complex assembly and function[82]. In mitochondria, a mismatch in the stoichiometry of nuclear-encoded and mitochondria-encoded OXPHOS subunits can lead to OXPHOS components accumulation[83]. *M1BP* KD in flight muscles leads to a decrease in expression levels of a few structural OXPHOS subunits of Complex I and III (see Fig. 5a). Namely, the UQCR-C2 subunit of Complex III was systematically the most significantly downregulated gene in our RNA-seq analyses (nearly 30-fold downregulated). Based on this evidence we believe that the perturbed OXPHOS subunit stoichiometry, together with decreased assembly factor expression levels, account for the phenotypes we observed in M1BP-depleted muscles. All these data point towards an important role for M1BP in oxidative metabolism control through the control of the transcriptional upregulation of genes required for respiratory complex assembly and integrity.

https://doi.org/10.1038/s41467-023-38986-5

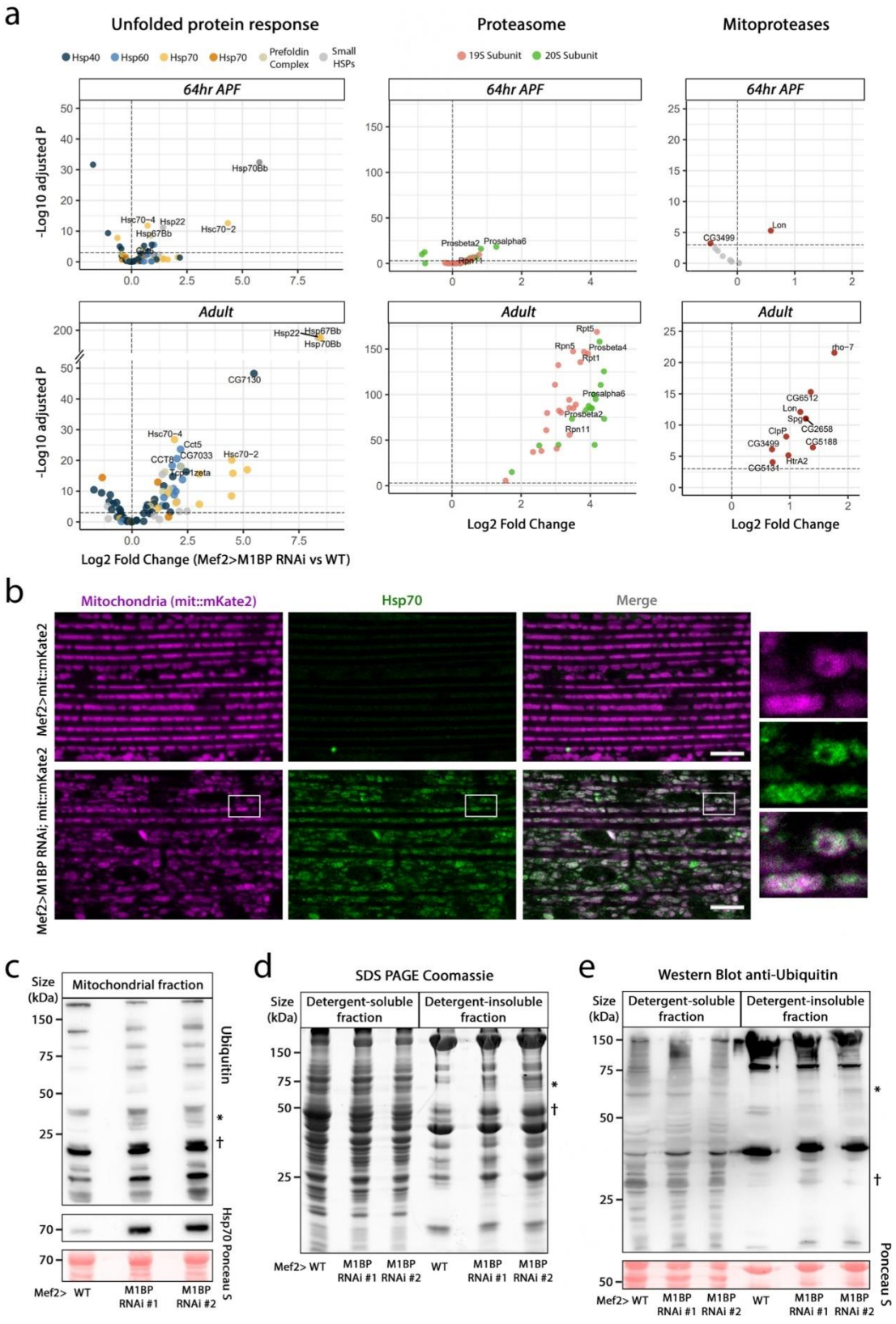

M1BP and the interplay with other OXPHOS regulators

M1BP likely plays a direct role in the transcriptional upregulation of OXPHOS-related gene expression at the middle of pupation, since none of the known OXPHOS transcriptional regulators are affected by M1BP loss of function (see Supplementary Fig. 7). Noteworthy here is the E2F/Rbf pathway, where in vertebrates E2F1 is a repressor of oxidative metabolism[84] and Rbf is an activator[85]. In *Drosophila*, while E2F is an activator of the myogenic programme in flight muscle development[61], its role in oxidative metabolism is less clear. Interestingly, we showed here that the motifs of M1BP and E2F1 are the most significantly enriched motifs in the promoters of the OXPHOS-genes (see Fig. 4a). Nonetheless, Rbf, a transcriptional co-regulator that does

Fig. 6 | M1BP KD in flight muscles triggers a widespread mitochondrial protein quality control response. a Volcano plots of differential gene expression analysis between Mef2>WT and Mef>*M1BP* RNAi adult flight muscles. Analysed genes belong to the mitochondrial quality control response: UPR-related genes, UPS-related genes, and mitochondrial proteases. For statistical analysis, the Wald test with Benjamini–Hochberg correction was applied. **b** Confocal sections of wild-type (top) and M1BP RNAi (bottom) mitochondria in adult flight muscles labelled with mit::mKate2 and anti-Hsp70 antibody, to visualise a part of the unfolded protein response. White rectangles depict an enlarged view of a single, aggregate-containing mitochondrion (right). The scale bar corresponds to 10 μm. **c** Western blot analysis of Ubiquitin and Hsp70 on proteins obtained from adult purified mitochondria. The Ponceau S membrane staining is shown as a loading control. The asterisk represents an example of proteins with very low or no ubiquitination in the WT condition compared to the M1BP KD and the dagger a protein whose ubiquitination further increased upon M1BP KD. **d** Coomassie Blue staining of detergent-soluble and insoluble fractions obtained from adult flight muscles. **e** Western Blot analysis of Ubiquitin on detergent-soluble and insoluble fractions obtained from adult flight muscles. The Ponceau S membrane staining is shown as a loading control. Source data are provided as a Source data file.

not bind DNA directly in a sequence-specific manner, is found enriched at promoters containing Motif-1, the DNA recognition sequence of M1BP, and activates OXPHOS gene expression during myogenesis[25], suggesting that Rbf may cooperate with M1BP in the activation of OXPHOS genes in this process. Furthermore, M1BP was identified in a screen as counteracting E2F activity, similar to Rbf[86]. Interestingly, the screen by Lu and colleagues[86] also identified GFZF, a known transcriptional M1BP co-activator[87] as counteracting E2F activity. Since *GFZF* RNAi in flight muscles with *Mef2-GAL4* leads to late pupal lethality[32], it will thus be of interest to now study in detail a potential M1BP/Rbf partnership in OXPHOS gene expression, which may implicate a possible transcriptional co-activator, GFZF, in this process.

Finally, the vast majority of OXPHOS genes are ubiquitously expressed from TATA-less promoters, a characteristic of metabolic genes usually not subject to large amplitudes in gene expression[3]. This has incorrectly conveyed the idea that transcriptional regulation is not key to plasticity in OXPHOS gene expression. Yet, stem cells increase OXPHOS gene expression upon differentiation[78], somatic dedifferentiation into induced pluripotent stem cells involves the transcriptional downregulation of OXPHOS expression[88] and changes to the expression of OXPHOS genes contribute to a wide and diverse range of human diseases[89], which demonstrates the importance in defining the transcriptional mechanisms underlying such plasticity. Here, we highlight the dynamic temporal transcriptional upregulation of OXPHOS genes during myogenesis and identify M1BP as playing a fundamental role in this process. Since M1BP is a major RNA Pol II pausing factor of plethora *Drosophila* genes[26] it will now be of interest to study the interplay between the chromatin landscape of nuclear-encoded OXPHOS components, the state of paused RNA Pol II at their promoters, and the role other transcription factors and/or co-activators play with M1BP in this process as potential mediators of oxidative metabolism transcriptional plasticity.

Similarities drawn between M1BP loss and human pathologies

The main steps and key players of muscle development are well conserved between *Drosophila* and vertebrates, and since flight muscle are not required for adult viability this makes *Drosophila* a valuable model organism for numerous human myopathies[90,91]. Flight muscles are structurally and mechanistically similar to vertebrate cardiac muscles and have been used to model human cardiomyopathies[92]. Our findings in muscle mitochondria are of clinical relevance since plethora human diseases, including multiple mitochondrial myopathies originate from mutations in genes encoding OXPHOS subunits or assembly factors[43,93]. Strikingly, some patients suffering from myopathies display mitochondrial inclusions, in some cases very similar to the phenotype triggered by *M1BP* RNAi (see[54] for examples). Mitochondrial inclusions have been also reported in patients with gastric adenocarcinomas[55]. Of interest is to note, that many patients cannot be diagnosed by light microscopy but electron microscopy is required to detect such ultrastructural mitochondrial defects[54,94].

Ultrastructural defects are due to perturbations in the highly dynamic membrane morphology of mitochondria (reviewed in refs. 95,96). While we did not observe any transcriptional changes in the components responsible for cristae dynamics upon *M1BP* KD during pupation, we did observe a delay in cristae remodelling and development that occurs at the onset of OXPHOS transcriptional regulation during mid-pupation (see Fig. 3b). Furthermore, by the adult stage, the rapidly developing IMM had completely isolated the large protein aggregates from the remaining matrix space (Fig. 1e). Isolation of protein aggregates in the matrix by the IMM represents a previously undocumented mitochondrial stress response mechanism. Understanding the molecular mechanisms driving this remodelling may be of therapeutic benefit in combating diseases resulting from mitochondrial-targeted protein aggregation-related neurodegenerative diseases, such as Parkinson's, Alzheimer's and Huntington's diseases. Indeed, such diseases often elicit a strong UPR^{mt}, which we also observed during myogenesis in the M1BP KD muscle (see Fig. 6). Like in these neurodegenerative diseases, we hypothesise this proteotoxic response is the consequence of the toxicity of protein aggregates present in the mitochondrial matrix, although in the case of *M1BP* KD, we favour this is due to the primary defects observed on OXPHOS complex assembly. Nonetheless, as in the case of yeast protein aggregates upon Complex V mis-assembly[57], it remains an open question as to why, despite a strong and early protein quality control response, the observed aggregates cannot be resolved and cleared.

Finally, mitochondrial proteases are not only central regulators of mitochondrial proteostasis but play a key role in the response to mitochondrial stress. We observed all mitoproteases transcriptionally upregulated upon *M1BP* KD, the first of which, Lon protease (see Fig. 6) is known to help mediate the turnover of non-assembled proteins in mitochondria (reviewed in ref. 97). In addition to its protease activity, Lon protease also exhibits chaperone-like activity, working with mitochondrial heat shock proteins to exhibit anti-aggregation activities[98,99]. The observed mitoprotease response, combined with heat shock protein UPR^{mt}, are thus likely to represent an initial anti-aggregation response, followed by a much later protein degradation response through mitoprotease activity and ubiquitin-dependent proteasome degradation (Fig. 6). Given that numerous mitoproteases are transcriptionally upregulated in human diseases, including highly aggressive metastatic cancers in the case of Lon (reviewed in refs. 100,101), it will be of benefit to use M1BP KD in flight muscle as a means to better study and characterise the mitoproteases in the mitochondrial stress response, particularly pertaining to human diseases.

Methods

Fly stocks

Flies were raised under standard conditions at 25°C, unless otherwise stated, in a 12 h light/12 h dark cycle. For *M1BP* downregulation, the following lines were used: *UAS-M1BP* RNAi #1 (110498/KK VDRC) and *UAS-M1BP* RNAi #2 (BL32858). All experiments were performed with both RNAi lines and if unspecified, including for RNA-seq experiments, data for the weaker RNAi #1 line are shown.

GAL4 drivers used in this study were muscle-specific *Mef2-GAL4* (BL27390) and *Him-GAL4*[7], pan-neuronal *elav-GAL4* line (BL458, C155) and fat body-specific *cg-GAL4* line (BL7011). For all experiments performed on myoblasts, we staged larvae to 0 h APF (white pupa), where the number of larval myoblast is the highest[102]. Myoblasts were visualised using a *twi*::*GFP* transgene (BL79615). Lines allowing

mitochondria imaging in flight muscles were *UAS-mit*::Dendra2[39] and *UAS-mit*::*mKate2* (chr. 2 and chr. 3) that was generated by P-element-mediated transgenesis using *pUASp* and contains the far-red fluorescent protein mKate2 (excitation 588 nm, emission 633 nm) fused at the N-terminus to human COXVIII mitochondrial target sequence (MSVLTPLLLRGLTGSARRLPV PRAKIHSL).

For conditional *M1BP* depletion, the TARGET system was used[53]. In this system, *TubGAL80^{TS}* is expressed at 18 °C, repressing *Mef2-GAL4* activity and is inactivated at 29 °C, allowing for *Mef2-GAL4* to be active, allowing *UAS-RNAi* expression. Females laid eggs for a period of 24 h at 18 °C and one hundred embryos per genotype and condition were collected. Eggs were kept at 18 °C during the whole embryogenesis and then RNAi activated through switching to 29 °C at either larval L1 or early pupa stage (≈10 h APF). RNAi was then either maintained until adult or removed by switching to 18 °C at L3 wandering, early (≈10 h APF) or mid-pupa (≈60 h APF) stages. Eggs kept at 18 °C during whole embryogenesis served as a control. The number of eclosed flies for each condition was quantified.

Immunofluorescence

Imaginal discs. White pupae (0 h APF) were dissected in PBS and fixed for 20 min in 4% formaldehyde in PBS, rinsed and washed three times in PBT (0.2% Triton X-100, PBS), 10 min each. Samples were blocked in 4% bovine serum PBT for at least 1 h and incubated with primary antibodies in 4% bovine serum in PBT overnight (ON) at 4°C. After three washes in PBT samples were incubated with secondary antibodies for 1h30 followed by washing six times in PBT for 10 min each. Imaginal wing discs were dissected using forceps (Fine Science Tools, Dumont #5), mounted in a Vectashield medium containing DAPI (H-1200, Vector Laboratories) and imaged using a confocal microscope (Zeiss LSM 880). All steps were performed at room temperature, using gentle agitation, unless otherwise stated. Primary antibodies were rabbit anti-M1BP (1/250, D. Gilmour) and chicken anti-GFP (1/1000, GFP-1010, AB_2307313, AvesLabs). Secondary antibodies were AlexaFluor 488, donkey anti-chicken A10039, Invitrogen, 1:500 and AlexaFluor 568, goat anti-mouse, Invitrogen, A11004, 1:500.

Indirect flight muscles. Adult females were quickly rinsed in ethanol, and wings, head and abdomen were removed in PBS. Thoraces were split in half using forceps and fixed in 4% formaldehyde in PBS for 20 min. Hemithoraces were rinsed and washed three times in PBT (0.5% Triton X-100, PBS) for 10 min each and blocked in 3% NGS (S26-M, Sigma-Aldrich) in PBT for at least 1 h. Samples were incubated ON with primary antibodies at 4 °C. Samples were rinsed and washed three times in PBT for 15 min each, incubated with secondary antibodies including Phalloidin (1/200, Phalloidin-Atto 647 N, Sigma-Aldrich) and Hoechst (1/1000) at RT for 1h30 and washed again in PBT six times for 10 min each. Hemithoraces were mounted in a Vectashield medium (Vector Laboratories) and imaged using a confocal microscope (Zeiss LSM 880). All steps were performed in a 24-well plate under agitation. Primary antibodies used were rabbit anti-M1BP (1/250, gift from D. Gilmour), and mouse anti-ATP5A (1/250, 15H4C4 Thermo Scientific 43-9800). In Fig. 6, mitochondria were visualised using *Mef2-GAL4* driven *UAS-mit*::*mKate2* line and UPR was visualised with mouse anti-HSP70 antibody (1/100, StressMarq Biosciences Cat# SMC-106, RRID: AB_2295500). Secondary antibodies were AlexaFluor 488, goat anti-rabbit, Invitrogen, A11034, 1:500 and AlexaFluor 568, goat anti-mouse, Invitrogen, A11004, 1:500.

Live flight muscle imaging

For adult flight muscle imaging, adult females expressing *UAS-mit*::*Dendra2* under the control of the *Mef2-GAL4* driver were briefly rinsed in ethanol and transferred to dissecting plate containing PBS. The head, abdomen, wings, legs and thorax ventral cuticle were gently removed using forceps. Thorax was split with forceps in two hemithoraces that were quickly transferred to a slide containing PBS. Three layers of double-sided tape were used to increase the slide height and prevent tissue deformation. Hemithoraces were imaged using a confocal microscope (Zeiss LSM 880).

Transmission electron microscopy

For myoblast imaging, wing discs of 0 h APF pupa were fixed for 2 h in a fixation solution (2.5% glutaraldehyde, 2% paraformaldehyde and 0.1 M sodium cacodylate pH 7.3), embedded in 4% low melting agarose (A9414, Sigma) and kept at 4 °C in the fixation solution until further processing. For pupal flight muscle visualisation, pupa were staged at 25 °C, removed from the pupal case and poked twice in the abdomen with a microneedle for the penetration of the fixation solution. The abdomen has been removed to allow for proper osmium penetration. For adult flight muscles, adult males were quickly rinsed in ethanol and dissected in PBS. The head, wings, abdomen and legs were removed, as well as the ventral thoracic cuticle. Thoraces were fixed in a fixation solution and kept at 4 °C until further processing. Samples were further processed according to the published protocol[21] and imaged on a Transmission Electron microscope FEI Tecnai G2 at 200 keV.

For tomographic reconstruction of mitochondrial aggregates, serial 350nm-thick sections were deposited on slot grids and contrasted in 2% uranyl acetate for 20 min and lead citrate for 8 min. Dual-axis tomographic acquisitions were carried out in an FEI Tecnai G2 at 200 keV using a Veleta camera (Olympus, Japan) for image collection from −60° to +60°. Tomographic reconstructions and tomograms joining were carried out in eTomo (IMOD, version 4.11), segmentation was carried out in Ilastik (version 1.4.0) and surface rendering in Amira (version 2022.2). Observed reconstructions represent 75% certainty, due to missing upper and lower wedges that are inherent in the protocol.

For the Immuno-EM experiments, 2-day-old females were processed as for transmission electron microscopy imaging above, until the dehydration step. Sample were embedded in epoxy resin and cut in 90 nm and deposited on nickel mesh grids. Grids were treated with a saturated solution of Sodium Meta-Periodate (S-1878, Sigma) for 2 min, washed with 1% Triton X-100 in TBS for 5 min, saturated 1 h in 5% BSA, 0.5% Fish Gelatine skin and incubated ON with mouse anti-ATP5A (1/100, 15H4C4 Thermo Scientific 43–9800). Grids were washed 4 times in TBS for 5 min each, incubated with an anti-mouse secondary antibody conjugated with 10 nm gold (1/30, Aurion) in TBS at 37 °C for 1 h, washed 4 times in TBS for 5 min each and postfixed in 2.5% glutaraldehyde, 0.05 M Sodium Cacodylate for 10 min. Acquisitions were carried out in an FEI Tecnai G2 at 200 keV using a Veleta camera (Olympus, Japan).

Muscle locomotor assays

To assess flight capacity, 20–30 3–4-day-old flies per genotype (of separated sex) were thrown into a Plexiglas cylinder (with the height of 1 m and a diameter of 8.4 cm), and the landing position in the cylinder (top, middle, bottom) was scored[103]. Flies landing at the top are considered as able to fly, in the middle as weak flyers and to the bottom as flightless. At least 90 flies were tested per genotype (except for *M1BP* RNAi #2 leading to significant adult lethality) and at least two independent biological replicates were performed. To test the flight muscle fatigability, flies were tapped 3 times and let to recover for a few seconds. This was repeated three times and directly after that, flies were subjected to the flight test. Negative geotaxis assay was performed as previously described in ref. 39. The walking speed was determined by scoring the distance travelled (in cm) in 10 s, repeated five times.

Mitochondria purification

Mitochondria purification was performed according to a modified procedure[104]. Flight muscles from 15–20 adult female flies were

dissected in ice-cold PBS and crushed with a Potter homogeniser in the mitochondrial isolation buffer containing 250 mM sucrose and 0.15 mM $MgCl_2$ in 10 mM Tris-HCl, pH 7.4, on ice. Muscle homogenate was centrifuged twice at 400 g for 5 min at 4 °C to remove insoluble material. The supernatant was centrifuged at 7000 × *g* for 5 min at 4 °C. The mitochondrial pellet was washed twice with the mitochondria isolation buffer and stored at −80 °C. Mitochondrial protein concentrations were determined using the Bradford method[105].

Blue native PAGE (BN-PAGE) analysis and in-gel activity assay

BN-PAGE was performed using NativePAGE Bis-Tris gels, following manufacturer protocol (Invitrogen). 20 μg of mitochondria was solubilised in a buffer containing native PAGE sample buffer (BN2003, Invitrogen) supplemented with 1% of digitonin (digitonin/protein (w/w) ratio of 8) (D5628, Sigma) and EDTA-free Protease inhibitors (11873580001, Sigma) and incubated on ice for 20 min. After centrifugation at 20,000 × *g* for 30 min at 4 °C, the supernatant was recovered and mixed with the 5% G-250 Sample Additive (BN2004, Invitrogen). The final volume was loaded in 3–12% Bis-Tris NativePAGE gels (BN2012BX10, Invitrogen) and the electrophoresis was performed using the NativePAGE Running buffer (BN2001, Invitrogen) as anode buffer, and the NativePAGE Running buffer containing the NativePAGE Cathode Additive (BN2002, Invitrogen), as cathode buffer. NativeMark Protein standard (LC0725, Invitrogen) was used as the molecular weight marker, and run with the samples. Following electrophoresis, the resulting gel was either stained with Coomassie Brilliant blue G 250 (1.15444, Sigma) or was subjected to in-gel activity assays as described below[106,107]. Complexes were optionally analysed on separate gel stripes or consecutively. Source data are provided as a Source Data File.

Complex I activity was performed by incubating the native gels in a solution containing 2 mM Tris-HCl (pH 7.4), 0.1 mg/ml NADH and 2.5 mg/ml Nitrotetrazolium Blue chloride for 20 min. After the appearance of violet bands, the reaction was stopped by the addition of 10% Acetic Acid. The Complex II in-gel activity assay was performed by incubating the gel in a solution containing 5 mM Tris-HCl (pH 7.4), 20 mM Sodium Succinate, 2.5 mg/ml Nitrotetrazolium Blue chloride and 0.2 mM Phenazine Methosulfate for 40 min. After the appearance of the violet colour indicative of Complex II activity, the reaction was stopped with 10% acetic acid.

The Complex IV in-gel activity assay was performed by incubating the gel in a solution containing 0.5 mg/ml 3,3′-diaminobenzidine (DAB), 1 mg/ml of the Complex IV substrate cytochrome *c* and 50 mM Phosphate buffer (pH 7.4) for 40 min. After the brown product appearance, the reaction was stopped with 10% acetic acid.

The Complex V in-gel activity assay was carried out by pre-equilibrating the gel in a solution containing 40 mM Tris-HCl (pH 8.5), 4 mM ATP, and 1.5 mM magnesium chloride supplemented with 30 mM of *N*-dodecyl-β-D-maltoside (DDM) for 3 h. After removal of the solution, the gel was washed for 1 min in water and incubated in a buffer consisting of 35 mM Tris-HCl, 270 mM glycine, 14 mM magnesium sulfate, 0.075% lead nitrate, and 0.8 mM ATP (pH 7.8) with 20% methanol for 40 to 60 min. Following the appearance of white bands, the reaction was stopped with 50% methanol. The activity of Complex III cannot be visualised on the Blue Native PAGE gel[71]. Source data for complex activities are provided In the Supplementary information file.

Protein solubility fractionation analyses

Detergent-soluble and insoluble protein fractions were obtained from adult flight muscles or purified mitochondria (see "Mitochondria purification" section) following a published protocol[108] with minor modifications. Adult thoraces/mitochondria were homogenised using 0.5 mm silica glass beads (Beadbug, Z763748-50EA) in a Precelyss 24 tissue homogeniser (Bertin technologies) at 5500 rpm, 2 × 25 sec with 40 sec pause. Protein fractions or purified mitochondria were mixed with Laemmli buffer, denatured for 5 min at 95 °C and run on two 12% SDS-polyacrylamide gels. One of the gels was stained with Coomassie Brilliant blue G 250 (1.15444, Sigma) and the other subjected to western blotting using standard protocols. Primary antibodies used were mouse anti-ATP5A (1/1000, 15H4C4 Thermo Scientific 43–9800), rabbit anti-Ubiquitin polyclonal antibody (1/100, U-5379 Sigma) and mouse anti-HSP70 antibody (1/1000, SMC-106). Secondary antibodies used were light chain-specific, conjugated to HRP, anti-rabbit-HRP (1/20,000, 211-032-171, Jackson ImmunoResearch) and anti-mouse-HRP (1/20,000, 115-035-174, Jackon ImmunoResearch). Source data are provided as a Source data file.

Real-time quantitative PCR

Total RNA was extracted from 10 adult females using Promega kit (ReliaPrep™ RNA Miniprep Systems, Z6111), according to the manufacturer specification, except the initial centrifugation step replaced by 1 min vortex and 5 min incubation at RT. Extracted RNA was reverse transcribed using Superscript Reverse Transcriptase IV kit (#18090010, Invitrogen). The relative mRNA level was quantified using SYBR Green qPCR Master Mix (#4472954, Invitrogen) in a CFX96 BioRad Detection system. The reference genes *pfk*, *ald*, and *gapdh* were validated as stable control genes. Two to three independent biological replicates per condition were performed. Primers used in the experiment are: for *pfk* (forward 5′-TCGATGCCATCTCCAGTACA-3′, reverse 5′-CCCATGACCTCCATGATGA-3′), for *ald* (forward 5′-AATGACGACCTACTTCAACTACCC-3′, reverse 5′-AACGATTTTCTGGGCGATT-3), for *gapdh* (forward 5′-AGCGAACTGAAACTGAACGAG-3′, reverse 5′-AATTCCGATCTTCGACATGG-3′) and for *M1BP* (forward (5′-CGCATGGCCTTTGAACTT-3′, reverse 5′-GAAGCGCGACTGACAGATT-3′).

Sample preparation for RNA-seq

For the wing disc-associated myoblasts dissociation was performed according to a modified protocol[109]. 0 h APF *Mef2-GAL4*, *UAS-GFP::Gma*/WT or *UAS-M1BP* RNAi #1 expressing larvae were washed in PBS, sterilised with 70% ethanol and dissected in Supplemented Schneider's Medium (SSM) containing 10% foetal bovine serum, 2% Penicillin/Streptomycin and 0.02 mg/ml Insulin. 30 to 35 wing discs were collected in ice-cold PBS and dissociated using preheated TrypLE 10× at 30 °C for 45 min at 300 rpm. The reaction was stopped by adding SSM and the cells were mechanically resuspended by gentle pipetting. Aggregates were removed by filtering cells in a cell strainer (30 μm, Miltenyi) and cells were sorted using a FACS AriaII Machine (BD), according to cell viability, size and GFP intensity. Myoblasts were sorted directly in the kit-provided Lysis buffer supplemented with 2-Mercaptoethanol (#M6250, Sigma) and kept at −80 °C until RNA extraction, which was preferentially performed the same day. RNA was isolated from the pure myoblast population of approximately 50,000 cells using RNA extraction Microkit (#74004, Qiagen).

For pupal flight muscle RNA-seq, *Mef2-GAL4*/WT or *UAS-M1BP* RNAi expressing pupa were staged at 25 °C and dissected in ice-cold PBS. The dissection was performed according to a published protocol[103]. Hand-isolated flight muscles from 6 to 8 pupa were directly collected in the kit-provided Lysis buffer supplemented with 2-Mercaptoethanol (#M6250, Sigma), homogenised with a small pestle and RNA was extracted using RNA extraction Microkit (#74004, Qiagen).

For adult flight muscles, RNA isolation was performed on hand dissected indirect flight muscles from 30, 2-days old females. The tissue was collected in batches of 15 flies at a time to minimise the time between samples and TRIzol treatment and transferred to Eppendorf tubes, then centrifuged at 2000 × *g* for 5 min at 4 °C. The flight muscle pellet was resuspended in TRIzol reagent (Thermofisher cat #15596026), shock froze in liquid nitrogen and kept at −80 °C. RNA was isolated directly from the TRIzol muscle samples using a tube-based purification kit from Zymo Research (Direct-zol RNA Microprep, Zymo Research, #R2060).

For all samples (myoblast, pupa and adult flight muscles) RNA quality was verified via Bioanalyzer (Agilent).

High-throughput sequencing analysis

The analyses of mito-gene and sarcomeric gene expression during flight muscle development presented in Fig. 2 and Supplementary Fig. 5 were performed on DESeq2-normalised RNA-sequencing data provided from ref. 7.

RNA sequencing was performed on libraries prepared from triplicate RNA preparations. Libraries for myoblast preparations were performed using the SMART-SeqX v4 UltraX Low Input RNA Kit for Sequencing (Takara Bio Europe, Saint Germain en Laye, France) according to manufacturer's instructions with 10 cycles of PCR for cDNA amplification by Seq-Amp polymerase. Six hundreds pg of pre-amplified cDNA were then used as input for Tn5 transposon tagmentation by the Nextera XT DNA Library Preparation Kit (96 samples) (Illumina, San Diego, USA). Libraries from DLM preparations were performed using the TruSeq stranded mRNA Sample Preparation Kit and TruSeq RNA Single Indexes kits A and B (Illumina, San Diego, CA) following the manufacturer's instructions. All library preparations were followed by 12 cycles of library amplification, further purified with SPRIselect beads to remove primer adaptors and size selection and validated for concentration and fragment size using Agilent DNA1000 chips. Sequencing was performed using a HiSeq 4000. Base calling performed using RTA (Illumina) and quality control performed using FastQC.

Differentially expressed genes were called using DESeq2[110] (version 1.34.0) using a false discovery rate (p-adjusted value in DESeq2) threshold of 0.001 and having a 1.5× fold change in expression upon *M1BP* RNAi. The lists of differentially expressed genes for all RNA-seq datasets are available in Supplementary Data 2–5. Gene ontology analyses were performed using FlyEnrichr[111] on differentially expressed genes, retaining the top ten ontologies having an adjusted p value of less than 0.01.

Identification of transcription factor binding sites on OXPHOS promoters

Position weight matrices (PWMs) of transcription factor binding sites were obtained from JASPAR[112]. For *Drosophila* transcription factors that have no identified PWM, we used the PWMs from the human or mouse homologues. The following position weight matrices were used: Drosophila M1BP (MA1459.1), human MEF2A (MA0052.4), human E2F1 (MA0024.3), human CREB1 (MA0018.4), human NRF1 (MA0506.1), human GABPA (MA0062.3), Drosophila Pho (MA1460.1, Drosophila cnc (MA0530.1), Human SP1 (MA0079.3), Mouse Essrg (MA0643.1). The obtained PWMs were used to scan OXPHOS gene promoters using FIMO (version 5.5.1)[113] using a p-value threshold of 0.001, and retaining the most significant occurrence in case of multiple matches. OXPHOS promoters (dm6 genome release) were defined as sequences encompassing 250 bp upstream and 50 bp downstream from the transcription start site.

3D nuclei counting

Automatic 3D nuclei counting from fluorescent images was achieved using the Python package Stardist[114,115], which implements a deep learning approach based on star-convex shape representations for object detection and comes along with different pre-trained 2D and 3D models. As the counting using the pre-trained Stardist 3D model was not accurate enough for our images, we trained a custom Stardist 3D model from scratch. We built an in-house dataset consisting of both a single volume of size 97 × 256 × 256 extracted from one of our fluorescent images and its corresponding manual annotation in 3D we created using Napari's labelling tool[116]. In order to increase the number of images, we tiled this volume into four non-overlapping sub-volumes of size 97 × 128 × 128 and used three of them for training the model and the remaining one for evaluation using the Intersection Over Union metrics.

The hyper-parameters of Stardist were left as default and 3D UNET architecture used as backend. Image normalisation (between 1 and 99.8) was applied by channel independently. Empirical object anisotropy estimations was calculated using Stardist function calculate_extents and the subsampling grid size (2,1,1) for prediction was inferenced from this anisotropy value. Ray value ($v = 96$) was left as default, train patch size (48x96x96) and train batch size ($n = 32$) was chosen accordingly with our dataset size and hardware memory constraints. Moreover, we used the data augmentation strategy proposed by Stardist consisting of random image flip, rotation and random image intensity variation. We trained the model for 80 epochs using an Nvidia GV100 GPU and monitored the training until it reached a plateau (IoU: 0.53 on validation set). Then, the optimised probability threshold was automatically inferenced by Stardist using different Non-Maximum-Suppression threshold (NMS 0.3, 0.4 and 0.5). A memory efficient inference pipeline was created to handle the prediction of 27 full stack images of size 2048 × 2048 and varying depth. All codes (training/inference) and trained models are available on github (https://doi.org/10.5281/zenodo.7695893)[117].

Statistics and reproducibility

All experiments were performed in three independent biological replicates unless otherwise stated in the figure legend. All image processing and quantifications were performed using Fiji software[118]. The intensity of M1BP staining in myoblasts was quantified as a ratio of the M1BP intensity in the myoblast area (labelled by *twi::GFP*) and in the disc epithelium, measured using ImageJ. In adult flight muscles, the intensity of M1BP staining was measured using ImageJ with ROI applied on nuclei. Muscle parameters, sarcomere length and myofibril width were estimated using the MyofibrilJ plugin for ImageJ (https://imagej.net/MyofibrilJ)[7]. For mitochondrial quantification from fluorescence images, the Watershed process was applied on by-default thresholded images. Analyze particles tool was applied to acquire mitochondrial area and aspect ratio (defined as ratio of the major to the minor axis). Mitochondrial density and content were quantified by dividing the number of mitochondria and total mitochondrial area, respectively, by the confocal section area. For mitochondria quantification from TEM images, mitochondria were manually outlined in ImageJ and Measure tool was applied to obtain Area, Aspect Ratio, Perimeter and Circularity (defined as $\frac{4\pi \times \text{Area}}{\text{Perimeter}^2}$) values. The number of cristae was quantified manually using ImageJ over a distance of 500 nm. All BN-PAGE gels and SDS-PAGE gels were quantified from scanned gels using ImageJ. The Immunogold experiment was quantified using the Cell counter plugin (https://imagej.net/plugins/cell-counter) as a density (the number of beads per μm^2) of mitochondrial matrix area, aggregate area or area outside of mitochondria. All statistical analyses applied can be found in figure legends. Statistical tests and charts were performed using R (version 4.1.0)[119,120].

Reporting summary

Further information on research design is available in the Nature Portfolio Reporting Summary linked to this article.

Data availability

All high-throughput sequencing data generated in this study have been deposited with the Gene Expression Omnibus (GEO) and are available under the accession number GSE207241. Source data are provided with this paper.

Code availability

All custom code for nuclei counting of larval myoblasts in 3D space described in this manuscript are made available as open source code under GNU General Public Licence v3.0 and are available on GitHUB and accessible at https://doi.org/10.5281/zenodo.7695893.

References

1. van der Bliek, A. M., Sedensky, M. M. & Morgan, P. G. Cell biology of the mitochondrion. *Genetics* **207**, 843–871 (2017).
2. Herst, P. M., Rowe, M. R., Carson, G. M. & Berridge, M. V. Functional mitochondria in health and disease. *Front. Endocrinol.* **8**, 296 (2017).
3. van Waveren, C. & Moraes, C. T. Transcriptional co-expression and co-regulation of genes coding for components of the oxidative phosphorylation system. *BMC Genomics* **9**, 18 (2008).
4. Donati, S., Sander, T. & Link, H. Crosstalk between transcription and metabolism: how much enzyme is enough for a cell? *WIREs Syst. Biol. Med.* **10**, e1396 (2018).
5. Harbauer, A. B., Zahedi, R. P., Sickmann, A., Pfanner, N. & Meisinger, C. The protein import machinery of mitochondria-a regulatory hub in metabolism, stress, and disease. *Cell Metab.* **19**, 357–372 (2014).
6. Pagliarini, D. J. et al. A mitochondrial protein compendium elucidates complex I disease biology. *Cell* **134**, 112–123 (2008).
7. Spletter, M. L. et al. A transcriptomics resource reveals a transcriptional transition during ordered sarcomere morphogenesis in flight muscle. *eLife* **7**, e34058 (2018).
8. Hock, M. B. & Kralli, A. Transcriptional control of mitochondrial biogenesis and function. *Annu. Rev. Physiol.* **71**, 177–203 (2009).
9. Kelly, D. P. & Scarpulla, R. C. Transcriptional regulatory circuits controlling mitochondrial biogenesis and function. *Genes Dev.* **18**, 357–368 (2004).
10. Scholtes, C. & Giguère, V. Transcriptional control of energy metabolism by nuclear receptors. *Nat. Rev. Mol. Cell Biol.* **23**, 750–770 (2022).
11. Moyes, C. D. Controlling muscle mitochondrial content. *J. Exp. Biol.* **206**, 4385–4391 (2003).
12. Talbot, J. & Maves, L. Skeletal muscle fiber type: using insights from muscle developmental biology to dissect targets for susceptibility and resistance to muscle disease. *Wiley Interdiscip. Rev. Dev. Biol.* **5**, 518–534 (2016).
13. Mishra, P., Varuzhanyan, G., Pham, A. H. & Chan, D. C. Mitochondrial dynamics is a distinguishing feature of skeletal muscle fiber types and regulates organellar compartmentalization. *Cell Metab.* **22**, 1033–1044 (2015).
14. Ogata, T. & Yamasaki, Y. Scanning electron-microscopic studies on the three-dimensional structure of mitochondria in the mammalian red, white and intermediate muscle fibers. *Cell Tissue Res.* **241**, 251–256 (1985).
15. Bleck, C. K. E., Kim, Y., Willingham, T. B. & Glancy, B. Subcellular connectomic analyses of energy networks in striated muscle. *Nat. Commun.* **9**, 5111 (2018).
16. Jahnke, V. E., Sabido, O. & Freyssenet, D. Control of mitochondrial biogenesis, ROS level, and cytosolic Ca2+ concentration during the cell cycle and the onset of differentiation in L6E9 myoblasts. *Am. J. Physiol. Cell Physiol.* **296**, C1185–C1194 (2009).
17. Kim, Y., Yang, D. S., Katti, P. & Glancy, B. Protein composition of the muscle mitochondrial reticulum during postnatal development. *J. Physiol.* **597**, 2707–2727 (2019).
18. Kraft, C. S. et al. Control of mitochondrial biogenesis during myogenesis. *Am. J. Physiol. Cell Physiol.* **290**, C1119–C1127 (2006).
19. Remels, A. H. V. et al. Regulation of mitochondrial biogenesis during myogenesis. *Mol. Cell Endocrinol.* **315**, 113–120 (2010).
20. Lehmann, F. O. & Dickinson, M. H. The changes in power requirements and muscle efficiency during elevated force production in the fruit fly Drosophila melanogaster. *J. Exp. Biol.* **200**, 1133–1143 (1997).
21. Avellaneda, J. et al. Myofibril and mitochondria morphogenesis are coordinated by a mechanical feedback mechanism in muscle. *Nat. Commun.* **12**, 2091 (2021).
22. Fernandes, J., Bate, M. & Vijayraghavan, K. Development of the indirect flight muscles of Drosophila. *Development* **113**, 67–77 (1991).
23. Roy, S. & VijayRaghavan, K. Patterning muscles using organizers: larval muscle templates and adult myoblasts actively interact to pattern the dorsal longitudinal flight muscles of drosophila. *J. Cell Biol.* **141**, 1135–1145 (1998).
24. Schönbauer, C. et al. Spalt mediates an evolutionarily conserved switch to fibrillar muscle fate in insects. *Nature* **479**, 406–409 (2011).
25. Zappia, M. P., Rogers, A., Islam, A. B. M. M. K. & Frolov, M. V. Rbf activates the myogenic transcriptional program to promote skeletal muscle differentiation. *Cell Rep.* **26**, 702–719.e6 (2019).
26. Li, J. & Gilmour, D. S. Distinct mechanisms of transcriptional pausing orchestrated by GAGA factor and M1BP, a novel transcription factor. *EMBO J.* **32**, 1829–1841 (2013).
27. Barthez, M. et al. Human ZKSCAN3 and Drosophila M1BP are functionally homologous transcription factors in autophagy regulation. *Sci. Rep.* **10**, 9653 (2020).
28. Zouaz, A. et al. The Hox proteins Ubx and AbdA collaborate with the transcription pausing factor M1BP to regulate gene transcription. *EMBO J.* **36**, 2887–2906 (2017).
29. Kudron, M. M. et al. The ModERN resource: genome-wide binding profiles for hundreds of *Drosophila* and *Caenorhabditis elegans* transcription factors. *Genetics* **208**, 937–949 (2018).
30. Ranganayakulu, G., Elliott, D. A., Harvey, R. P. & Olson, E. N. Divergent roles for NK-2 class homeobox genes in cardiogenesis in flies and mice. *Development* **125**, 3037–3048 (1998).
31. Bag, I. et al. M1BP cooperates with CP190 to activate transcription at TAD borders and promote chromatin insulator activity. *Nat. Commun.* **12**, 4170 (2021).
32. Schnorrer, F. et al. Systematic genetic analysis of muscle morphogenesis and function in Drosophila. *Nature* **464**, 287–291 (2010).
33. Blanchard, F. J. et al. The transcription factor Mef2 is required for normal circadian behavior in Drosophila. *J. Neurosci.* **30**, 5855–5865 (2010).
34. Clark, R. I. et al. MEF2 is an in vivo immune-metabolic switch. *Cell* **155**, 435–447 (2013).
35. Demontis, F. & Perrimon, N. Integration of insulin receptor/Foxo signaling and dMyc activity during muscle growth regulates body size in Drosophila. *Development* **136**, 983–993 (2009).
36. Zhao, X. & Karpac, J. Muscle directs diurnal energy homeostasis through a myokine-dependent hormone module in Drosophila. *Curr. Biol.* **27**, 1941.e6–1955.e6 (2017).
37. Demontis, F., Patel, V. K., Swindell, W. R. & Perrimon, N. Intertissue control of the nucleolus via a myokine-dependent longevity pathway. *Cell Rep.* **7**, 1481–1494 (2014).
38. Zappia, M. P. et al. E2F/Dp inactivation in fat body cells triggers systemic metabolic changes. *eLife* **10**, e67753 (2021).
39. El Fissi, N. et al. Mitofusin gain and loss of function drive pathogenesis in Drosophila models of CMT2A neuropathy. *EMBO Rep.* **19**, e45241 (2018).
40. Katti, P., Rai, M., Srivastava, S., Silva, P. D. & Nongthomba, U. Marf-mediated mitochondrial fusion is imperative for the development and functioning of indirect flight muscles (IFMs) in drosophila. *Exp. Cell Res.* **399**, 112486 (2021).
41. Rai, M., Katti, P. & Nongthomba, U. Drosophila Erect wing (Ewg) controls mitochondrial fusion during muscle growth and maintenance by regulation of the Opa1-like gene. *J. Cell Sci.* **127**, 191–203 (2014).
42. Sauerwald, J., Backer, W., Matzat, T., Schnorrer, F. & Luschnig, S. Matrix metalloproteinase 1 modulates invasive behavior of tracheal branches during entry into Drosophila flight muscles. *eLife* **8**, e48857 (2019).

43. Vercellino, I. & Sazanov, L. A. The assembly, regulation and function of the mitochondrial respiratory chain. *Nat. Rev. Mol. Cell Biol.* **23**, 141–161 (2022).
44. Gramates, L. S. et al. FlyBase: a guided tour of highlighted features. *Genetics* **220**, iyac035 (2022).
45. Mi, H., Muruganujan, A., Ebert, D., Huang, X. & Thomas, P. D. PANTHER version 14: more genomes, a new PANTHER GO-slim and improvements in enrichment analysis tools. *Nucleic Acids Res.* **47**, D419–D426 (2019).
46. Newsholme, E. A., Beis, I., Leech, A. R. & Zammit, V. A. The role of creatine kinase and arginine kinase in muscle. *Biochem. J.* **172**, 533–537 (1978).
47. Klingenberg, M. Membrane protein oligomeric structure and transport function. *Nature* **290**, 449–454 (1981).
48. Runswick, M. J., Powell, S. J., Nyren, P. & Walker, J. E. Sequence of the bovine mitochondrial phosphate carrier protein: structural relationship to ADP/ATP translocase and the brown fat mitochondria uncoupling protein. *EMBO J.* **6**, 1367–1373 (1987).
49. Wallimann, T. & Eppenberger, H. M. Properties of arginine kinase from *Drosophila melanogaster*. *Eur. J. Biochem.* **38**, 180–184 (1973).
50. Zhang, Y. Q. et al. Stress sensitive B encodes an adenine nucleotide translocase in *Drosophila melanogaster*. *Genetics* **153**, 891–903 (1999).
51. Sugahara, R. et al. Tissue-specific expression and silencing phenotypes of mitochondrial phosphate carrier paralogues in several insect species. *Insect Mol. Biol.* **26**, 332–342 (2017).
52. Southall, T. D., Elliott, D. A. & Brand, A. H. The GAL4 system: a versatile toolkit for gene expression in Drosophila. *Cold Spring Harb. Protoc.* **2008**, pdb.top49 (2008).
53. McGuire, S. E., Mao, Z. & Davis, R. L. Spatiotemporal gene expression targeting with the TARGET and gene-switch systems in Drosophila. *Sci. STKE Signal Transduct. Knowl. Environ.* **2004**, pl6 (2004).
54. Linda, S. et al. Mitochondrial diseases and myopathies: a series of muscle biopsy specimens with ultrastructural changes in the mitochondria. *Ultrastruct. Pathol.* **16**, 263–275 (1992).
55. Marinozzi, V., Derenzini, M., Nardi, F. & Gallo, P. Mitochondrial inclusions in human cancer of the gastrointestinal tract. *Cancer Res.* **37**, 1556–1563 (1977).
56. Shah, A. J., Sahgal, V., Muschler, G., Subramani, V. & Singh, H. Morphogenesis of the mitochondrial alterations in muscle diseases. *J. Neurol. Sci.* **55**, 25–37 (1982).
57. Lefebvre-Legendre, L. et al. Failure to assemble the α3 β3 subcomplex of the ATP synthase leads to accumulation of the α and β subunits within inclusion bodies and the loss of mitochondrial cristae in *Saccharomyces cerevisiae*. *J. Biol. Chem.* **280**, 18386–18392 (2005).
58. Yim, A. et al. mitoXplorer, a visual data mining platform to systematically analyze and visualize mitochondrial expression dynamics and mutations. *Nucleic Acids Res.* **48**, 605–632 (2020).
59. Scarpulla, R. C. Nuclear control of respiratory chain expression by nuclear respiratory factors and PGC-1-related coactivator. *Ann. NY Acad. Sci.* **1147**, 321–334 (2008).
60. Dairaghi, D. J., Shadel, G. S. & Clayton, D. A. Addition of a 29 residue carboxyl-terminal tail converts a simple HMG box-containing protein into a transcriptional activator. *J. Mol. Biol.* **249**, 11–28 (1995).
61. Zappia, M. P. & Frolov, M. V. E2F function in muscle growth is necessary and sufficient for viability in Drosophila. *Nat. Commun.* **7**, 10509 (2016).
62. Fazio, I. K., Bolger, T. A. & Gill, G. Conserved regions of the drosophila erect wing protein contribute both positively and negatively to transcriptional activity. *J. Biol. Chem.* **276**, 18710–18716 (2001).
63. Baltzer, C., Tiefenböck, S. K., Marti, M. & Frei, C. Nutrition controls mitochondrial biogenesis in the Drosophila adipose tissue through Delg and Cyclin D/Cdk4. *PLoS ONE* **4**, e6935 (2009).
64. Sykiotis, G. P. & Bohmann, D. Keap1/Nrf2 signaling regulates oxidative stress tolerance and lifespan in Drosophila. *Dev. Cell* **14**, 76–85 (2008).
65. Tiefenböck, S. K., Baltzer, C., Egli, N. A. & Frei, C. The Drosophila PGC-1 homologue Spargel coordinates mitochondrial activity to insulin signalling. *EMBO J.* **29**, 171–183 (2010).
66. Bour, B. A. et al. Drosophila MEF2, a transcription factor that is essential for myogenesis. *Genes Dev.* **9**, 730–741 (1995).
67. Yin, J. C. et al. A Drosophila CREB/CREM homolog encodes multiple isoforms, including a cyclic AMP-dependent protein kinase-responsive transcriptional activator and antagonist. *Mol. Cell. Biol.* **15**, 5123–5130 (1995).
68. Brown, J. L., Mucci, D., Whiteley, M., Dirksen, M. L. & Kassis, J. A. The Drosophila Polycomb group gene pleiohomeotic encodes a DNA binding protein with homology to the transcription factor YY1. *Mol. Cell* **1**, 1057–1064 (1998).
69. Signes, A. & Fernandez-Vizarra, E. Assembly of mammalian oxidative phosphorylation complexes I-V and supercomplexes. *Essays Biochem.* **62**, 255–270 (2018).
70. Schägger, H. & von Jagow, G. Blue native electrophoresis for isolation of membrane protein complexes in enzymatically active form. *Anal. Biochem.* **199**, 223–231 (1991).
71. Wittig, I., Karas, M. & Schägger, H. High resolution clear native electrophoresis for in-gel functional assays and fluorescence studies of membrane protein complexes. *Mol. Cell. Proteomics* **6**, 1215–1225 (2007).
72. Jadiya, P. & Tomar, D. Mitochondrial protein quality control mechanisms. *Genes* **11**, 563 (2020).
73. Hetz, C., Zhang, K. & Kaufman, R. J. Mechanisms, regulation and functions of the unfolded protein response. *Nat. Rev. Mol. Cell Biol.* **21**, 421–438 (2020).
74. Shpilka, T. & Haynes, C. M. The mitochondrial UPR: mechanisms, physiological functions and implications in ageing. *Nat. Rev. Mol. Cell Biol.* **19**, 109–120 (2018).
75. Morrow, G., Inaguma, Y., Kato, K. & Tanguay, R. M. The small heat shock protein Hsp22 of *Drosophila melanogaster* is a mitochondrial protein displaying oligomeric organization. *J. Biol. Chem.* **275**, 31204–31210 (2000).
76. Dabbaghizadeh, A. et al. Identification of proteins interacting with the mitochondrial small heat shock protein Hsp22 of *Drosophila melanogaster*: implication in mitochondrial homeostasis. *PLoS ONE* **13**, e0193771 (2018).
77. DiLoreto, R. & Murphy, C. T. The cell biology of aging. *Mol. Biol. Cell* **26**, 4524–4531 (2015).
78. Shyh-Chang, N. & Ng, H.-H. The metabolic programming of stem cells. *Genes Dev.* **31**, 336–346 (2017).
79. Tixier, V. et al. Glycolysis supports embryonic muscle growth by promoting myoblast fusion. *Proc. Natl Acad. Sci. USA* **110**, 18982–18987 (2013).
80. Bragoszewski, P., Turek, M. & Chacinska, A. Control of mitochondrial biogenesis and function by the ubiquitin–proteasome system. *Open Biol.* **7**, 170007 (2017).
81. Ciryam, P., Kundra, R., Morimoto, R. I., Dobson, C. M. & Vendruscolo, M. Supersaturation is a major driving force for protein aggregation in neurodegenerative diseases. *Trends Pharmacol. Sci.* **36**, 72–77 (2015).
82. Brennan, C. M. et al. Protein aggregation mediates stoichiometry of protein complexes in aneuploid cells. *Genes Dev.* **33**, 1031–1047 (2019).
83. Houtkooper, R. H. et al. Mitonuclear protein imbalance as a conserved longevity mechanism. *Nature* **497**, 451–457 (2013).

84. Blanchet, E. et al. E2F transcription factor-1 regulates oxidative metabolism. *Nat. Cell Biol.* **13**, 1146–1152 (2011).
85. Takebayashi, S.-I. et al. Retinoblastoma protein promotes oxidative phosphorylation through upregulation of glycolytic genes in oncogene-induced senescent cells. *Aging Cell* **14**, 689–697 (2015).
86. Lu, J., Ruhf, M.-L., Perrimon, N. & Leder, P. A genome-wide RNA interference screen identifies putative chromatin regulators essential for E2F repression. *Proc. Natl Acad. Sci. USA* **104**, 9381–9386 (2007).
87. Baumann, D. G., Dai, M.-S., Lu, H. & Gilmour, D. S. GFZF, a glutathione *S* -transferase protein implicated in cell cycle regulation and hybrid inviability, is a transcriptional coactivator. *Mol. Cell. Biol.* **38**, e00476-17–17 (2017).
88. Folmes, C. D. L. et al. Somatic oxidative bioenergetics transitions into pluripotency-dependent glycolysis to facilitate nuclear reprogramming. *Cell Metab.* **14**, 264–271 (2011).
89. Reinecke, F., Smeitink, J. A. M. & van der Westhuizen, F. H. OXPHOS gene expression and control in mitochondrial disorders. *Biochim. Biophys. Acta* **1792**, 1113–1121 (2009).
90. Kreipke, R. E., Kwon, Y. V., Shcherbata, H. R. & Ruohola-Baker, H. *Drosophila melanogaster* as a model of muscle degeneration disorders. *Curr. Top. Dev. Biol.* **121**, 83–109 (2017).
91. Taylor, M. V. In *Muscle Development in Drosophila* (ed. Sink, H.) 169–203 (Springer New York, 2006).
92. Kronert, W. A. et al. Prolonged cross-bridge binding triggers muscle dysfunction in a Drosophila model of myosin-based hypertrophic cardiomyopathy. *eLife* **7**, e38064 (2018).
93. Suomalainen, A. & Battersby, B. J. Mitochondrial diseases: the contribution of organelle stress responses to pathology. *Nat. Rev. Mol. Cell Biol.* **19**, 77–92 (2018).
94. Vincent, A. E. et al. The spectrum of mitochondrial ultrastructural defects in mitochondrial myopathy. *Sci. Rep.* **6**, 30610 (2016).
95. Eramo, M. J., Lisnyak, V., Formosa, L. E. & Ryan, M. T. The 'mitochondrial contact site and cristae organising system' (MICOS) in health and human disease. *J. Biochem.* **167**, 243–255 (2020).
96. Kondadi, A. K., Anand, R. & Reichert, A. S. Cristae membrane dynamics – a paradigm change. *Trends Cell Biol.* **30**, 923–936 (2020).
97. Deshwal, S., Fiedler, K. U. & Langer, T. Mitochondrial proteases: multifaceted regulators of mitochondrial plasticity. *Annu. Rev. Biochem.* **89**, 501–528 (2020).
98. Matsushima, Y. et al. Mitochondrial Lon protease is a gatekeeper for proteins newly imported into the matrix. *Commun. Biol.* **4**, 974 (2021).
99. Kao, T.-Y. et al. Mitochondrial Lon regulates apoptosis through the association with Hsp60-mtHsp70 complex. *Cell Death Dis.* **6**, e1642 (2015).
100. Bota, D. A. & Davies, K. J. A. Mitochondrial Lon protease in human disease and aging: including an etiologic classification of Lon-related diseases and disorders. *Free Radic. Biol. Med.* **100**, 188–198 (2016).
101. Gomez-Fabra Gala, M. & Vögtle, F.-N. Mitochondrial proteases in human diseases. *FEBS Lett.* **595**, 1205–1222 (2021).
102. Gunage, R. D., Reichert, H. & VijayRaghavan, K. Identification of a new stem cell population that generates Drosophila flight muscles. *eLife* **3**, e03126 (2014).
103. Weitkunat, M. & Schnorrer, F. A guide to study Drosophila muscle biology. *Methods* **68**, 2–14 (2014).
104. Garcia, C. J., Khajeh, J., Coulanges, E., Chen, E. I.-J. & Owusu-Ansah, E. Regulation of mitochondrial complex I biogenesis in Drosophila flight muscles. *Cell Rep.* **20**, 264–278 (2017).
105. Bradford, M. M. A rapid and sensitive method for the quantitation of microgram quantities of protein utilizing the principle of protein-dye binding. *Anal. Biochem.* **72**, 248–254 (1976).
106. Jha, P., Wang, X. & Auwerx, J. Analysis of mitochondrial respiratory chain supercomplexes using blue native polyacrylamide gel electrophoresis (BN-PAGE). *Curr. Protoc. Mouse Biol.* **6**, 1–14 (2016).
107. Yang, J.-H. et al. Purification and biochemical characterization of the ATP synthase from *Heliobacterium modesticaldum*. *Protein Expr. Purif.* **114**, 1–8 (2015).
108. Rai, M. et al. Analysis of proteostasis during aging with western blot of detergent-soluble and insoluble protein fractions. *STAR Protoc.* **2**, 100628 (2021).
109. Khan, S. J., Abidi, S. N. F., Tian, Y., Skinner, A. & Smith-Bolton, R. K. A rapid, gentle and scalable method for dissociation and fluorescent sorting of imaginal disc cells for mRNA sequencing. *Fly* **10**, 73–80 (2016).
110. Love, M. I., Huber, W. & Anders, S. Moderated estimation of fold change and dispersion for RNA-seq data with DESeq2. *Genome Biol.* **15**, 550 (2014).
111. Kuleshov, M. V. et al. Enrichr: a comprehensive gene set enrichment analysis web server 2016 update. *Nucleic Acids Res.* **44**, W90–W97 (2016).
112. Sandelin, A., Alkema, W., Engström, P., Wasserman, W. W. & Lenhard, B. JASPAR: an open-access database for eukaryotic transcription factor binding profiles. *Nucleic Acids Res.* **32**, D91–D94 (2004).
113. Grant, C. E., Bailey, T. L. & Noble, W. S. FIMO: scanning for occurrences of a given motif. *Bioinformatics* **27**, 1017–1018 (2011).
114. Schmidt, U., Weigert, M., Broaddus, C. & Myers, G. Cell detection with star-convex polygons. In *Medical Image Computing and Computer Assisted Intervention – MICCAI 2018* (eds. Frangi, A. F., Schnabel, J. A., Davatzikos, C., Alberola-López, C. & Fichtinger, G.) 265–273 (Springer International Publishing, 2018).
115. Weigert, M., Schmidt, U., Haase, R., Sugawara, K. & Myers, G. Star-convex polyhedra for 3D object detection and segmentation in microscopy. In *2020 IEEE Winter Conference on Applications of Computer Vision (WACV)* 3655–3662 (2020).
116. Sofroniew, N. et al. napari: a multi-dimensional image viewer for Python. zenodo https://doi.org/10.5281/zenodo.7276432 (2022).
117. Daian, F. & Saurin, A. J. andysaurin/3DL_NuCount: Used to count myoblast nuclei attached to Drosophila wing imaginal discs. zenodo https://doi.org/10.5281/zenodo.7695893 (2023).
118. Schindelin, J. et al. Fiji: an open-source platform for biological-image analysis. *Nat. Methods* **9**, 676–682 (2012).
119. R Core Team. *R: A Language and Environment for Statistical Computing* (R Foundation for Statistical Computing, 2021).
120. RStudio Team. *RStudio: Integrated Development Environment for R* (RStudio, PBC, 2022).

Acknowledgements

We thank Bloomington and Vienna Stock Centres for fly stocks, D. Gilmour for M1BP antibodies and the IBDM Imaging and *Drosophila* platforms. We acknowledge the PICsL-FBI Marseille imaging facility, member of the national infrastructure France-BioImaging supported by the French National Research Agency (ANR-10-INBS-04). We thank the GenomEast (IGBMC, France) sequencing platform for generation of the high-throughput RNA sequencing data. This work was supported by the Fondation ARC pour la recherche sur le cancer (PJA20181208014, A.J.S.), la Ligue Nationale Contre le Cancer (M.B.) and AFM-Téléthon (no. 23721, A.J.S.).

Author contributions

G.P., M.B. and A.J.S. conceived the project, G.P. and M.B. performed experiments and analysed data with support from T.R., who performed adult live mitochondrial imaging and Immuno-EM imaging and quantification. N.M.L. performed adult flight muscle dissection for RNA-seq. A.A. prepared all transmission electron-microscopy samples. N.B. performed tomography imaging and 3D reconstruction. F.R. performed the

Immuno-EM experiment. F.D. performed the machine-learning-based strategy for myoblast counting. C.M.-Z. performed cristae quantification for adult mitochondria. F.S. and Y.G. analysed data and provided expert experimental suggestions. A.J.S. and G.P. carried out the bioinformatics analysis of RNA-seq datasets. G.P. and A.J.S. wrote the manuscript with inputs from all authors.

Competing interests
The authors declare no competing interests.

Additional information
Supplementary information The online version contains supplementary material available at https://doi.org/10.1038/s41467-023-38986-5.

Correspondence and requests for materials should be addressed to Andrew J. Saurin.

Peer review information *Nature Communications* thanks Brian Glancy, Liam Hunt and the other, anonymous, reviewer(s) for their contribution to the peer review of this work. A peer review file is available.

Reprints and permissions information is available at http://www.nature.com/reprints

Publisher's note Springer Nature remains neutral with regard to jurisdictional claims in published maps and institutional affiliations.

Open Access This article is licensed under a Creative Commons Attribution 4.0 International License, which permits use, sharing, adaptation, distribution and reproduction in any medium or format, as long as you give appropriate credit to the original author(s) and the source, provide a link to the Creative Commons license, and indicate if changes were made. The images or other third party material in this article are included in the article's Creative Commons license, unless indicated otherwise in a credit line to the material. If material is not included in the article's Creative Commons license and your intended use is not permitted by statutory regulation or exceeds the permitted use, you will need to obtain permission directly from the copyright holder. To view a copy of this license, visit http://creativecommons.org/licenses/by/4.0/.

© The Author(s) 2023

Article 2. Antp orchestrates *Drosophila* adult flight muscle development

Science Advances
AAAS

Manuscript Template

Front Matter

Title

- **The Hox protein Antennapedia orchestrates *Drosophila* adult flight muscle development**
- **Antennapedia orchestrates flight myogenesis**

Authors

Gabriela Poliacikova[1], Aïcha Aouane[1], Nathalie Caruso[1], Nicolas Brouilly[1], Corinne Maurel-Zaffran[1], Yacine Graba[1], Andrew J. Saurin[1]*

Affiliations

[1]Aix-Marseille Univ, CNRS, Developmental Biology Institute of Marseille (IBDM), UMR 7288, Case 907, Parc Scientifique de Luminy, Marseille Cedex 09 13288, France

*Corresponding author. Email: andrew.saurin@univ-amu.fr

Abstract

Muscle development and diversity require a large number of spatially and temporally regulated events controlled by transcription factors (TFs). *Drosophila* has long stood as a model to study myogenesis due to the highly conserved key TFs involved at all stages of muscle development. While many studies focused on the diversification of *Drosophila* larval musculature, how distinct adult muscle types are generated is much less characterised. Here, we identify an essential regulator of *Drosophila* thoracic flight muscle development, the Hox TF Antennapedia (Antp). Correcting a long-standing belief that flight muscle development occurs without the input of Hox TFs, we show that Antp intervenes at several stages of flight muscle development, from the establishment of the progenitor pool in the embryo to myoblast differentiation in the early pupa. Furthermore, the precisely regulated clearance of Hox in the developing flight muscle fibres is required to allow for fibrillar muscle fate diversification, setting these muscles apart from all other adult tubular muscle types.

Teaser

The timely presence and absence of the Hox protein Antp is required for the correct adult flight muscle development.

MAIN TEXT

Introduction

Muscle development requires a network of transcription factors that diversify distinct muscle types. Studies in *Drosophila* larval somatic muscles have provided an extensive picture of the gene regulatory networks responsible for the muscle progenitor's specification. The current picture is that following muscle progenitor specification, dependent on Notch and RAS/MAPK signalling pathways, muscle diversity is achieved through a combinatorial expression of identity transcription factors (iTFs) and *Hox* genes, controlling the muscle identity, such as size, position, innervation, and attachment

(reviewed in *1*). In the case of embryonic/larval muscles, *Hox* genes have been shown to intervene at several steps of their development, providing specific identity to muscle precursors by the regulation of iTFs (*2–5*), regulating final progenitor number for a given muscle and later during development regulating final muscle size (*6*; reviewed in *7*).

In contrast to larval muscle precursors, the specification of adult muscle precursors (AMPs) is much less characterised (reviewed in *8*). In this context, it has been shown that mesodermal AbdA overexpression converts thoracic AMPs into abdominal AMPs (*9*), suggesting that *Hox* genes provide identity to both embryonic and adult muscle precursors. One particular adult muscle, the *Drosophila* flight muscle, was suggested to develop without any Hox input as precursors of this muscle associated with the larval wing disc do not express any *Hox* gene (*10*). However, both older and recent staining of the embryonic thoracic mesoderm and larval wing discs indicate that Antp, the *Hox* gene responsible for mesothoracic identity establishment (*11*), is expressed in territories that may correspond to flight muscle AMPs (*5*, *12–14*), leaving the role of whether and how Hox regulate adult flight muscle contentious.

Results

Antp is expressed in flight muscle myoblasts

At the end of embryogenesis, flight muscle precursors (myoblasts) attach to the larval wing imaginal discs, precursors of the adult wings (*15*). To unambiguously demonstrate that Antp is expressed in flight muscle myoblasts, we labelled larval wing discs with antibodies against Twist (Twi) (a marker of myoblasts) and Antp at the onset of pupation (0 h after puparium formation (APF)), where the number of myoblasts is the highest (*16*). We detected strong Antp expression in the anterior disc epithelium (Fig. 1A) (*14*, *17*) and we also observed weaker expression, approximately 75% lower compared to the disc epithelium (Fig. 1B), in the notum region colocalising with Twi expression, showing that Antp is expressed in flight muscle myoblasts. To demonstrate specificity of this staining, we downregulated Antp expression in myoblasts using three different *UAS-Antp* RNAi lines, driven by a muscle-specific *Mef2*-Gal4 driver, active in wing disc-associated myoblasts from the third instar larval stage (*18*) and observed reduction of Antp expression (Fig. 1C, D). We additionally confirmed Antp expression in myoblasts with a second distinct antibody against Antp, with a GFP-reporter driven by an *Antp*-Gal4 line, and a GFP insertion into the *Antp* locus, fusing GFP to Antp (fig. S1A, B, C).

The locus of the *Antp* gene is large, spanning over 100 kb of genomic distance and contains two internal promoters, promoter 1 (P1) and promoter 2 (P2), that drive *Antp* expression in spatially different locations (*19–21*) (schematised in Fig. 1E). To determine which promoter drives Antp expression in flight muscle myoblasts, we used a *P1*-Gal4 line and constructed a *P2*-Gal4 line using minimal regulatory elements of the P2 promoter described in (*22*). In agreement with previous reports (*13*, *14*), we found that the P1 promoter drives the reporter expression in the anterior disc epithelium and the wing pouch (Fig. 1F). The P2 promoter on the other hand, shows strong expression in the majority of myoblasts and no expression in the disc ectoderm, being thus in the wing disc, a mesoderm-specific promoter (Fig. 1G). Altogether, these data demonstrate that Antp is expressed in wing disc-associated myoblasts, precursors of adult flight muscles and this expression is driven by the P2 promoter.

Antp loss leads to the absence of adult flight muscle precursors

Having established that Antp is expressed in wing disc-associated myoblasts we asked what role Antp plays during adult flight myogenesis. *Antp* homozygous null mutations are lethal during embryogenesis resulting from homeotic transformation of the mesothorax (second thoracic segment T2) towards a prothorax identity (first thoracic segment T1) (*23*). However, this transformation and lethality can be rescued by providing a single dose of Antp from the P1 promoter: when a P2-specific mutant line $Antp^{s1}$ is heterozygous with a null mutation of *Antp* ($Antp^{ns\text{-}rvc3}$), embryos and larvae develop normally giving viable animals until the late pupal stage (*24*). We thus used this genetic combination, which we refer to as $Antp^{P2\text{-}null}$ for simplicity, to study Antp function driven from the P2 promoter and its role in flight myogenesis.

Drosophila somatic myogenesis is a two-stage process where larval muscles are generated during embryogenesis and AMPs, specified in the embryo from a common lineage of cells to larval muscle, proliferate in the larvae and differentiate into adult muscles during pupal stages (Fig. 2A). AMPs in the embryo are distinguished from larval muscle precursors by persistent Twi expression from stage 14 onwards (*15*). Flight AMPs develop in T2, where they are mixed with leg muscle precursors and are visible as a patch of Twi-positive cells at the ventral side of the embryo at stage 15 onwards. At this stage, Antp expression can be found in T2 and T3 AMPs, with a lower expression in the T2 segment (Fig. 2B). Strikingly, in the $Antp^{P2\text{-}null}$ mutant, embryos showed a drastically reduced number of T2 AMPs (Fig. 2C), while heterozygous flies for any of the *Antp* mutant alleles showed no visible phenotype (fig. S2A). AMPs in the T3 segment were not affected in the $Antp^{P2\text{-}null}$ mutant, suggesting that the expression of Antp in the T3 AMPs is driven by the P1 promoter, which has been previously reported (*12*, *25*) and confirmed by our staining (fig. S2B). These results suggest that in the absence of *Antp* expression from the P2 promoter in the embryonic T2 mesoderm, flight muscle AMPs are not specified or are eliminated shortly after their specification.

Flight muscles are composed of indirect flight muscles (IFM) that power wing stroke and direct flight muscle (DFM) that regulate the wing angle. The IFM, which we will for simplicity refer to as “flight muscles”, are themselves composed of dorsal longitudinal muscle (DLM), which are responsible for wing depression, and dorsal-ventral muscle (DVM), which are responsible for wing elevation. Both direct and indirect flight muscles develop from wing disc-associated myoblasts (*26*), that themselves derive from T2 embryonic AMPs (*15*). We thus looked at myoblasts at the L3 larval stage, since if AMPs in the embryo are truly absent in the $Antp^{P2\text{-}null}$ mutant, the wing discs should be devoid of myoblasts at the larval stage.

While heterozygous larvae for any of the two *Antp* mutant alleles showed no visible phenotype (fig. S2C), in the $Antp^{P2\text{-}null}$ homozygous mutant wing discs the whole myoblast population, that would normally give rise to IFM and DFM muscles, was absent, as shown by a lack of Twi staining and a physical absence of the myoblast layer on the top of the notum epithelium (Fig. 2D, E). To permit adult muscle development, most larval muscles histolyse at the onset of pupation. The larval oblique muscles (LOM) 1,2,3 however persist and serve as scaffolds for DLM development, whereby wing disc myoblasts fuse with them in the early stages of pupation (*27*). However, these templates degenerate if there are no

fusing myoblasts (*28*) in the early pupa, which we also observe in the $Antp^{P2\text{-}null}$ mutant (Fig. 2F). This results in pharate animals whose thorax is completely devoid of any flight muscle (Fig. 2G). Heterozygous animals develop flight muscles normally (fig. S2D, E). Overall, these results show that the P2-specific loss of *Antp* leads to a complete absence of adult flight muscles due to lack of flight muscle AMPs and thus places *Antp* as a key player in early adult flight myogenesis.

Antp regulates flight muscle splitting and myoblast fusion

Following myoblast fusion with the larval templates in the early stages of pupation, the three LOM templates split to give rise to the final DLM pattern of six fibres ((*27*); see Fig. 3A). A transcriptional timecourse study of flight myogenesis detected *Antp* transcripts at the myoblast stage and up to 24 h APF when myoblast fusion is almost completed ((*29*), Fig. 3B). We confirmed these results at the protein level with antibody staining, showing that at 15 h APF Antp is expressed in myoblasts undergoing fusion, located outside the fibre, making contacts with the myotube membrane, and inside, at the fibre periphery (Fig. 3C). Antp expression is weaker in myoblasts located inside the myotube, and can no longer be detected at 24h APF, meaning that Antp is downregulated in myoblasts a few hours after their fusion.

In addition to its role in flight muscle AMP specification, we thus asked whether *Antp* has a role in these early stages of muscle differentiation. Since the $Antp^{P2\text{-}null}$ mutant condition results in absence of myoblasts at the larval stage, we used a UAS/Gal4 system to downregulate *Antp* expression during myogenesis using the *Mef2*-Gal4 driver (see Fig. 1D). Mef2 expression is absent in AMPs in the embryo (*30*), with expression turning on in myoblasts at larval third instar stages, allowing for *Antp* knockdown (KD) in proliferating myoblasts, without affecting their specification in the embryo. We observed that upon *Mef2*-Gal4 driven *Antp* KD, LOM splitting is markedly delayed and often incomplete with fewer muscle fibres at the end of the splitting process compared to control (Fig. 3D) accompanied by a decrease in the muscle compaction (fig. S3A, B). To gain more insight into the dynamics of this process we set up a live imaging of the muscle splitting using a *UAS-Gma::GFP* transgene (*31*) labelling actin, driven by the *Mef2*-Gal4 driver (*32*) (Movie S1). We observed that in this *Antp* KD condition the delay in the splitting is accompanied by a delay in myoblast fusion, where myoblasts appear to form the initial actin-rich patch but fail to complete the fusion for several hours (fig. S3C, ex.1; Movie S2). While the number of myoblasts prior (Fig. 3E) or post fusion (Fig. 3F) remains unchanged, we observed that nuclei were often improperly interspaced and often contained large hollow pockets (Fig. 3D, arrow). Furthermore, in an apparently stochastic manner, some muscle fibres became detached and were eliminated before the compaction stage, likely accounting for the decreased number of muscle fibres we observed in immunofluorescence experiments (fig. S3C, ex. 2; Movie S3).

At the adult stage, *Mef2*-Gal4-driven *Antp* KD results in numerous flight muscle phenotypes: 1) a held-out wing phenotype (fig. S4A) that does not support flight (fig. S4B), 2) a decrease of adult DLM fibre number, that nevertheless fill the whole thorax, and 3) phenotypes in sarcomeric compaction, fibre splitting and Z-line alignment (fig. S4C), with sarcomeres being significantly shorter and thicker (fig. S4D). The strongest RNAi line #3 led to a pharate lethality, displaying the same above-mentioned phenotypes (fig. S4E, F, G).

An incorrect adult fibre patterning, as well as defaults in sarcomeric integrity were also observed in the DVMs (fig. S4H). We confirmed these phenotypes with the *Him*-GAL4 line, active only until myoblast fusion (*29*), that in this case behaves similarly to *Mef2*-GAL4 line, in combination with *Antp* RNAi #2, leading to patterning defects (fig. S5A). We tested also another flight-muscle specific GAL4 line, *1151*-Gal4, which similarly to *Mef2*-Gal4 is active in larval myoblasts until the adult stage (*33*). This line in our hands has weaker expression, with only the strongest *Antp* RNAi #3 leading to patterning phenotypes (fig. S5B). As expected from Antp expression during early pupal stages, driving *Antp* KD post-fusion (starting at ~30h APF) with *Act88F*-Gal4 (*29*) does not perturb adult flight myogenesis (fig. S5C). These phenotypes generated by *Antp* RNAi are specific since they were rescued by simultaneously overexpressing Antp (fig. S6). Altogether, these results show that Antp expression in early pupal myoblasts is required for their correct fusion, muscle splitting and correct early sarcomerogenesis.

To gain molecular insights underlying the role of *Antp* in flight myogenesis we performed an RNA-seq analysis on FACS-sorted 0 h APF myoblasts (Data S1). Using a highly stringent significance threshold (p-adj < 0.001), we found 236 differentially expressed genes (DEGs) between *Mef2*-Gal4-driven *Antp* KD and the control condition, 56% of which were upregulated and 44 % downregulated (Fig. 3G). Interestingly, gene ontology (GO) analysis showed that upregulated genes, ie genes repressed by Antp in myoblasts, associate with cell-cell adhesion, muscle differentiation and fusion processes (Fig. 3H, Data S1). This suggests that *Antp* KD may lead to premature differentiation, likely accounting for the deficit in myoblast fusion and splitting we observed, which is similarly observed through perturbing the levels of many key genes responsible for muscle differentiation, such as *Notch*, *twi* and *Mef2* (*33–35*). Downregulated genes upon *Antp* KD, ie genes activated by Antp in myoblasts, were associated with BMP signalling and also cell-cell adhesion (fig. S7A, Data S1). Amongst the 236 DEGs, 15 encode for transcription factors (TFs) (Fig. 3I, Data S1), all linked with cell differentiation and/or specification, including TFs known to act in muscle development, such as *lame duck* (*lmd*) (*36*), *lateral muscle scarcer* (*lms*) (*37*), *optomotor blind-related-gene 1* (*org-1*) (*38*), *cut* (*ct*) (*26*) and *Kahuli* (*Kah*) (*39*). Antp thus controls a potential large gene regulatory network in adult flight muscle myoblasts.

To further endow functionality to our RNA-seq data set, we correlated them with data obtained from a functional flight test RNAi screen to identify factors involved in adult flight muscle development (*40*). This led to the identification of 17 genes downregulated upon *Antp* KD that have a phenotype in the flight screen (fig. S7B; Data S2). Towards a potential function in sarcomerogenesis, one gene whose downregulation caught our attention is the *Mlc2* gene, as its mutation was shown to cause flight muscle sarcomeric phenotypes highly similar to *Antp* KD (*41*) and recessive mutations of its vertebrate homologue, MYL2, were associated with infantile muscle fibre disease and cardiomyopathy, displaying similar sarcomeric phenotypes (*42*, reviewed in *43*). Certain sarcomeric phenotypes, notably the discontinuous Z-disk observed upon *Antp* KD can be rescued by *Mlc2* overexpression (fig. S7C).

Altogether, the study of Antp function in early pupal stages shows that besides its role in the establishment of flight muscle AMPs in the embryo (Fig. 2), Antp also plays a role at the early pupal stage, promoting myoblast transcriptional changes and controlling myoblast fusion, muscle splitting and correct early sarcomerogenesis.

Antp developmental clearance is necessary for fibrillar fibre type specification

Antp expression sharply decreases following myoblast fusion (Fig. 3B, C). To address if Antp clearance is functionally important, we maintained its expression post-fusion with a late, flight muscle-specific *Act88F*-Gal4 driver, active from around 24 h APF (*29*). Strikingly, using light and electronic microscopy we observed that Antp maintenance leads to sarcomeric perturbations (Fig. 4A, B, C, D). Adult *Drosophila* possesses two types of muscle fibre: stretch-activated fibrillar muscle composed of individual myofibrils and calcium-activated tubular muscle with laterally aligned myofibrils (reviewed in (*8*)), with IFM being the only fibrillar muscle type. In maintaining Antp expression, the IFM myofibrils seem to adopt a tubular-like fate, resembling morphologically leg muscles, with myofibrils aligning along the Z-disk and lesser mitochondrial volume and distribution (compare Fig. 4E with Fig. 4C bottom).

To molecularly study whether Antp maintenance alters muscle fibre fate, we performed RNA-seq analysis at 72 h APF, the earliest stage with a visible sarcomere perturbation (fig. S8A, B; Data S3). Maintaining Antp expression during late myogenesis led to a very large number of DEGs (4264 genes, p-adj < 0.001), from which 109 were related to sarcomere structure (*44*) (Fig. 4F, Data S3). Amongst the most significantly downregulated sarcomeric genes we found several fibrillar-specific genes, such as *Act88F,* whereas amongst the most significantly upregulated sarcomeric genes, we found several tubular-specific genes, such as *Act79B* (*45*, *46*) (fig. S8C). These data demonstrate that Antp maintenance prevents acquisition of the fibrillar fibre type. In favour of this is that amongst the repressed genes upon maintained *Antp* expression, we found *spalt major* (*salm)*, a master specifier of fibrillar muscle type (*47*), already reported as an Antp negative target in the antenna disc (*48*) (fig. S8D), which we show also holds true by immunofluorescence in the flight muscle (Fig. 4G, H). The activation of *salm* expression in post-fusion myoblasts was shown to be dependent on the transcriptional activator *vestigial* (*vg*) (*47*). We thus conducted an epistatic experiment between *vg* and *Antp*, showing that while *vg* overexpression alone does not seem to perturb IFM development (*26*), its simultaneous overexpression with *Antp* does not rescue *salm* repression nor the tubular-like IFM muscle fate caused by *Antp* GOF (fig. S8E). We thus conclude that *salm* repression by *Antp* is independent of *vg*. Interestingly, Salm expression starts in myotubes only after myoblast fusion is completed (*29*, *47*), at the time which coincides with Antp downregulation (see Fig. 3B). It is thus tempting to speculate that that *Antp* acts as direct or indirect repressor of *salm* expression, resulting in the tubular fibre muscle type in adult muscle whenever Antp expression is maintained. DFMs are of tubular muscle type and originate from myoblasts on the ventral side of the wing disc notum (*26*), that we showed express Antp at the larval stage (Fig.1). Unlike in the IFM, we detect persistent Antp expression in adult DFMs (fig. S8F), reinforcing our hypothesis that maintained Antp expression favours tubular muscle fate through lack of *salm* expression.

It has been reported that in the haltere disc, Ubx binds to *salm* promoter (*49*), where it negatively regulates a *salm* cis-regulatory element (*50*) and that Ubx overexpression in the thoracic mesoderm represses *Act88F* (*51*). We thus probed whether the expression of *Hox* genes in general also leads to similar muscle type transformation as observed using Antp. Strikingly, the expression of any *Hox* gene in the developing IFM led to various degrees of flight muscle transformation towards tubular-like fate as well as more or less strong *salm* repression (fig. S9), suggesting fibrillar fibre type suppression is shared by all Hox paralogs and can thus be considered as a Hox generic function (reviewed in (*52*)).

Discussion

The specification of different muscle fibre fates in *Drosophila* involves complex networks of transcription factors, amongst which iTFs and *Hox* genes. Challenging previously published results (*10*), in this study, we show that the specification of thoracic flight musculature is dependent on the *Hox* gene *Antp*. As suggested previously (*5*), we believe that the discrepancy in *Antp* expression in thoracic myoblasts results from the difficulty of detecting low Antp protein levels by immunostaining. How does Antp specify flight AMPs? Even though it was clearly demonstrated that the specification of embryonic abdominal AMPs depends on the Notch/Numb pathway, no studies addressed the specification of thoracic AMPs (*53–55*). Whether the thoracic AMP specification depends on *Notch* and how *Antp* intervenes in this process remains unknown.

An interesting point that stems from our findings is that the precise modulation of *Hox* gene expression in muscle precursors over time is crucial for the proper muscle fibre fate. It has been reported that ectopic *Antp* expression in wing myoblasts causes the absence of adult flight muscles, interpreted as *Hox* expression in flight muscle precursors being disruptive for flight myogenesis (*10*). We offer an alternative explanation by showing that while on the one hand Antp expression in flight muscle precursors is necessary for their specification, its clearance at the beginning of metamorphosis is also necessary for fibrillar vs tubular fate acquisition. Furthermore, while *vg* was shown to activate *salm* expression in post-fusion myoblasts, the overexpression of *vg* and its cofactor *scalloped* (*sd*) is not sufficient to induce ectopic Salm expression in wing disc myoblasts (*47*). We believe that this is caused by the concomitant repression of *salm* by Antp in these cells, even though we did not address whether Antp binds directly to the *salm* promoter in myoblasts due to their low number and a lack of ChIP-grade appropriate antibodies.

At the molecular level, we believe that the fate choice between thoracic tubular and fibrillary muscles is linked with the differential usage of the two *Antp* promoters in distinct thoracic segments. Indeed, while AMPs in the T2 segment express *Antp* from the P2 promoter, AMPs of the T3 segment express *Antp* from the P1 promoter, as they were not affected by the $Antp^{P2\text{-}null}$ mutant condition (see Fig. 2). As extensively suggested before (*11*), we believe that this differential promoter usage allows for distinct regulatory inputs between segments, allowing for the Antp T2-specific mesodermal clearance in the early pupa, necessary for the fibrillary muscle development.

In conclusion, this work corrects the long-accepted postulate stipulating that the establishment of thoracic muscles would be independent of *Hox* genes, and instead establishes a broad master regulatory role, orchestrating several key steps of adult muscle development: progenitor specification, myoblast fusion, muscle splitting, early sarcomerogenesis and fibrillar versus tubular fating.

Materials and Methods

Fly stocks

Flies were raised under standard conditions at 25°, unless otherwise stated, in a 12 h light/12 h dark cycle. For the manipulation of Antp expression the following lines were used: P2-mutant allele $Antp^{s1}$ (BL290), *Antp null-allele* $Antp^{ns\text{-}rvc3}$ (BL1829), Antp RNAi #1

(BL27675), Antp RNAi #2 (109547/KK, VDRC), Antp RNAi #3 (BL64926) and UAS-Antp (*56*). For Antp visualization, *Antp P1*-Gal4 (BL26817), *Antp P2*-Gal4 (this study, described below), *Antp*-Gal4 (*57*) and *Antp::GFP* (gift from S. Merabet) lines were used. With the exception of RNA-sequencing, all experiments were performed with all three RNAi lines.

Muscle-specific Gal4 lines used are *Mef2*-Gal4 (BL27390), *1151*-Gal4 (*45*), *Act88F*-Gal4 (*45*) and *Him*-Gal4 (*29*). UAS lines used are: *UAS-mCherry nls* (BL38424), *UAS-GFP nls* (BL4776), *UAS-Mlc-HA* (described below) and *UAS-GFP::Gma* where the actin-binding domain of Moesin is fused to GFP (*58*). Reporters used are the *weeP26* transgene *(Myosin-GFP)* containing an insertion of GFP in the *mhc* gene (*59*) and *salm::GFP* (*60*). Wild-type flies are the Oregon-R strain.

For myoblast counting and RNAseq analysis, larvae were staged to 0 h APF, where the number of myoblast is the highest (*16*). For optimal penetrance, all experiments with flies expressing *Mef2-GAL4* x *Antp RNAi* #1 and #2 were performed at 29°C. All other crosses were performed at 25°C.

Generation of UAS-Mlc2-HA line

The UAS-Mlc2 line was constructed by cloning the Mlc2 coding sequence obtained from the FlyBase database (*61*) in the pUAST plasmid containing the HA tag using standard cloning procedures. Briefly, the Mlc2 coding sequence was recovered from the clone RE01159 (DGRC Stock 1074315; https://dgrc.bio.indiana.edu//stock/1074315; RRID:DGRC_1074315) by PCR amplification, using primers : forward 5'-AAAAGAATTCATGGCCGATGAGAAGAAG-3' and reverse 5'-TTTTCTCGAGGGCGGCCTCCTCCTCCTC-3', adding EcoRI and XhoI restriction sites, respectively. The purified PCR product was digested using EcoRI (FD0278, Thermofisher Scientific) and XhoI (FD0698, Thermofisher scientific) restriction enzymes using the FastDigest protocol. The digested product was cloned into EcoRI-XhoI-digested pUASt vector using T4 ligase (M180A, Promega) with vector : insert ratio 1 : 3, overnight at 4°C. The ligated product was transformed into competent bacteria by heat-shock and verified by sequencing.

Generation of the Antp P2-Gal4 line

For the construction of the *Antp P2*-Gal4 *line,* a minimal sequence of approximately 6 kb (5738bp upstream of TSS plus 250 bp of exon 3), shown to drive expression from the Antp P2 promoter (*5.6d9,* described in (*22*)) was cloned in the pPTGAL vector (DGRC Stock 1225 ; https://dgrc.bio.indiana.edu//stock/1225 ; RRID:DGRC_1225) using Infusion cloning kit (639649, Takara). Briefly, the Antp P2 regulatory sequences were recovered from a BAC clone (CH321-43D16, BACPAC Resources center) by PCR. The sequence upstream of TSS plus 250 bp of exon 3 was amplified in two fragments using primers:

5'-GCTGAACAAGCTAAACAATCTGCAGGTACCATTCATTTTTCTTGACTATTT TGG-3'

5'-CACGGGAAATGAAACTGAAAAGGGAAAGGAAAC-3',

and

5'- CAGTTTCATTTCCCGTGCGCCCAAAGTTTCC-3'

5'-TTGGGCTGCAGCCTCGTCCTGAGCAGGCAGCGAA-3'

These fragments were inserted in the PstI site upstream the translation start site of Gal4.

Immunofluorescence

Embryos

Embryos were collected on agar plates, dechorionated using 50% bleach for 3min and fixed in 4% formaldehyde solution containing heptane. Embryos were dehydrated in a methanol wash followed by three ethanol washes, rehydrated in 50% ethanol/ 50% PBT (0.1 % Tween, PBS), washed for 15 min in PBT, saturated for 1 h in bovine serum albumin (BSA) 10% in PBT and incubated with primary antibodies in PBT overnight (ON) at 4°C. Embryos were washed three times in PBT, incubated with secondary antibodies for 1.5 h in PBT containing Hoechst (1:1000, H3570, Life Technologies) at room temperature (RT) and re-washed three times in PBT.

Imaginal discs

Larvae were dissected using forceps (Fine Science Tools, Dumont #5) in PBS and fixed for 20 min in 4% formaldehyde PBS, rinsed and washed three times in PBT (0.2 % Triton X-100, PBS), 10 min each. Samples were blocked in 2 % BSA in PBT (blocking solution) for at least 1 h and incubated with primary antibodies in blocking solution ON at 4°. After three washes in PBT samples were incubated with secondary antibodies in the blocking solution containing Hoechst (1:1000, H3570, Life Technologies) for 1.5 h followed by washing six times in PBT for 10 min each.

Indirect flight muscles

Pupal flight muscles were dissected as described in (*32*). Briefly, pupa were collected at 0 h APF and sticked to a slide using double-side tape for staging. Pupa were removed from the pupal case using forceps, poked at the thorax/abdomen junction and fixed in 4% formaldehyde in PBS for 20 min. Pupa were then pinned at the abdomen to a dissecting plate containing PBS and cut open using fine scissors (n°15003-08, Fine Science Tools), isolating flight muscles attached to the cuticle. Quarter thoraces were then washed in PBT (0.2% Triton X-100, PBS) for 10 min and saturated in BSA 2% for at least 1 h. Samples were incubated with primary antibodies in the blocking solution ON at 4°C, washed three times in PBT for 10 min each and secondary antibodies in PBT containing Hoechst (1:1000, H3570, Life Technologies) for 1.5 h at RT, followed by six washes in PBT. Pupa younger than 48 h APF were mounted as wing discs, for older pupa one or more layers of double side tape were used as spacers to prevent tissue deformation.

For adult flight muscles females were quickly rinsed in ethanol, and wings, head and abdomen were removed in PBS. For the visualisation of DLMs, thoraces were split in half using forceps, for dissection of DVMs, DLMs were removed using forceps and excess cuticle removed using fine scissors. For DFM dissection, DLMs, DVMs and the jump muscle (TDT) were removed using forceps and excess cuticle removed using fine scissors. Samples were fixed in 4% formaldehyde in PBS for 20 minutes, rinsed and washed in PBT (0.5% Triton X-100, PBS) three times, for 10 min each and blocked in 4% NGS (S26-M, Sigma-Aldrich) in PBT for at least 1 h. Thoraces were incubated ON with primary antibodies in PBT at 4°C. Samples were rinsed and washed three times in PBT for 15 min each, incubated with secondary antibodies in PBT including Phalloidin (1:500, Phalloidin-Atto 647N, Sigma-Aldrich) and Hoechst (1:1000, H3570, Life Technologies) at RT for 2 h and washed again in PBT six times for 10 min each. All steps were performed in a 24-well plate under agitation.

For all tissues samples were mounted in a Vectashield medium (Vector Laboratories) and imaged using a confocal microscope (Zeiss LSM 880). Primary antibodies used were anti-Antp (1:100 for embryos and discs and 1:20 for pupa, 8c11, DSHB), anti-Antp (1:50, 4c3, DSHB), anti-GFP (1:500, GFP-1010, AvesLabs), rabbit anti-Twi (1:200, gift from Eileen Furlong). Secondary antibodies were coupled to Alex Fluor 488, 568 or 647 (1:500, Life Technologies).

Live pupal IFM imaging

Live pupal flight muscle imaging was performed as described in (*32*) using spinning disc microscope (Spinning ROPER, Zeiss). Briefly, samples were taped on a slide using double side tape with three coverslips placed on each side to prevent tissue deformation. Pupa were covered in 50% glycerol and imaged overnight at 29°C every 10 minutes. Movies are available in Supplementary Materials.

Transmission electron microscopy

Pupal and adult flight muscle samples were processed as described in (*62*) and imaged on a Transmission Electron microscope FEI Tecnai G2 at 200 kV or FEI Tecnai T12 at 120 kV.

Flight assay

To assess flight capacity, 15, 3-4 days old males per genotype were thrown into a Plexiglas cylinder (with the height of 1m and a diameter of 8,4 cm), and the landing position in the cylinder (top, middle, bottom) was scored (*32*). Flies landing at the top are considered as able to fly, in the middle as weak flyers and to the bottom as flightless. At least 170 flies were tested per genotype and three independent biological replicates were performed.

Sample preparation for RNA-seq and high-throughput analysis

For FACS-sorted wing disc-associated myoblasts and pupal flight muscles samples were prepared and analysed as described previously (*62*). Differentially expressed genes were called using DESeq2 using a false discovery rate (p-adjusted value in DESeq2) threshold of 0.001. The lists of differentially expressed genes for all RNA-seq datasets are available in Supplementary Data files S1 to S3. Gene ontology analyses were performed using R Studio software (RStudio Team (2022). RStudio: Integrated Development Environment for R. RStudio, PBC, Boston, MA URL http://www.rstudio.com/) on differentially expressed genes, using the enrichGO function from clusterProfiler. For all samples RNA quality was verified via Bioanalyzer (Agilent).

Quantifications and statistical analysis

All image processing and quantifications were performed using Fiji software (*63*). The intensity of Antp staining in myoblasts was quantified as a ratio of the Antp intensity in the Twi-positive myoblast area and in the disc epithelium (the background fluorescence was subtracted). The number of wing disc associated-myoblasts was quantified in using 3D nuclei count tool (*64*) as described in (*62*). The number of pupal myoblasts was quantified manually in a defined volume of 14034 μm^3. The length of pupal fibres was quantified measuring the distance between two ends of the longest muscle fibre for each sample. Muscle parameters, sarcomere length and myofibril width were estimated using the MyofibrilJ plugin for ImageJ (https://imagej.net/MyofibrilJ) (*29*). In adult flight muscles, the intensity of Salm staining was measured with ROI applied on nuclei. Statistical tests and charts were performed using RStudio software. In the fig. 3E Anova test for multiple comparison was used followed by post-hoc Tukey test ($p\text{-value}_{y_RNAi\ vs\ \#1} = 0.42$, $p\text{-value}_{y_RNAi\ vs\ \#2} = 0.99$, $p\text{-value}_{y_RNAi\ vs\ \#3} = 0.79$). In the fig. 3F an unpaired Student's test was applied (p-value= 0.75). In the fig. S4D after applying Shapiro-Wilk test for normality, a non-parametric, Mann-Whitney test was applied (p-values (length) =0.007 and $0.4x10^{-8}$ and p-values (width) = 0.03 and $0.9x10^{-8}$). In the fig. S4F the same test as in fig. S4D was applied (p-value (length) = 0.02 and p-value (width) = 0.003). All experiments were performed in one technical replicate and three biological replicates except for the RNAseq analyses that were performed in three technical replicates and one biological replicate.

References

1. P. Poovathumkadavil, K. Jagla, Genetic Control of Muscle Diversification and Homeostasis: Insights from Drosophila. *Cells* **9** (2020).

2. A. M. Michelson, Muscle pattern diversification in Drosophila is determined by the autonomous function of homeotic genes in the embryonic mesoderm. *Development* **120**, 755–768 (1994).

3. P. A. Lawrence, P. Johnston, The genetic specification of pattern in a Drosophila muscle. *Cell* **36**, 775–782 (1984).

4. J. E. Hooper, Homeotic gene function in the muscles of Drosophila larvae. *EMBO J.* **5**, 2321–2329 (1986).

5. M. Capovilla, Z. Kambris, J. Botas, Direct regulation of the muscle-identity gene apterous by a Hox protein in the somatic mesoderm. *Dev. Camb. Engl.* **128**, 1221–1230 (2001).

6. J. Enriquez, H. Boukhatmi, L. Dubois, A. A. Philippakis, M. L. Bulyk, A. M. Michelson, M. Crozatier, A. Vincent, Multi-step control of muscle diversity by Hox proteins in the Drosophila embryo. *Development* **137**, 457–466 (2010).

7. G. Poliacikova, C. Maurel-Zaffran, Y. Graba, A. J. Saurin, Hox Proteins in the Regulation of Muscle Development. *Front. Cell Dev. Biol.* **9**, 2940 (2021).

8. Q. Laurichesse, C. Soler, Muscle development : a view from adult myogenesis in Drosophila. *Semin. Cell Dev. Biol.* **104**, 39–50 (2020).

9. S. Greig, M. Akam, Homeotic genes autonomously specify one aspect of pattern in the Drosophlla mesoderm. *Nature* **362**, 630–632 (1993).

10. S. Roy, L. S. Shashidhara, K. VijayRaghavan, Muscles in the Drosophila second thoracic segment are patterned independently of autonomous homeotic gene function. *Curr. Biol.* **7**, 222–227 (1997).

11. M. Rosales-Vega, D. Reséndez-Pérez, M. Vázquez, Antennapedia: The complexity of a master developmental transcription factor. *Genes. N. Y. N 2000*, e23561 (2023).

12. J. R. Bermingham, A. Martinez-Arias, M. G. Petitt, M. P. Scott, Different patterns of transcription from the two Antennapedia promoters during Drosophila embryogenesis. *Dev. Camb. Engl.* **109**, 553–566 (1990).

13. E. M. Jorgensen, R. L. Garber, Function and misfunction of the two promoters of the Drosophila Antennapedia gene. *Genes Amp Dev.* **1**, 544–555 (1987).

14. R. Paul, G. Giraud, K. Domsch, M. Duffraisse, F. Marmigère, S. Khan, S. Vanderperre, I. Lohmann, R. Stoks, L. S. Shashidhara, S. Merabet, Hox dosage contributes to flight appendage morphology in Drosophila. *Nat. Commun.* **12**, 2892 (2021).

15. M. Bate, E. Rushton, D. A. Currie, Cells with persistent twist expression are the embryonic precursors of adult muscles in Drosophila. *Development* **113**, 79–89 (1991).

16. R. D. Gunage, H. Reichert, K. VijayRaghavan, Identification of a new stem cell population that generates Drosophila flight muscles. *eLife* **3**, e03126 (2014).

17. D. K. Papadopoulos, K. Skouloudaki, Y. Engström, L. Terenius, R. Rigler, C. Zechner, V. Vukojević, P. Tomancak, Control of Hox transcription factor concentration and cell-to-cell variability by an auto-regulatory switch. *Development* **146**, dev168179 (2019).

18. C. Soler, M. V. Taylor, The Him gene inhibits the development of Drosophila flight muscles during metamorphosis. *Mech. Dev.* **126**, 595–603 (2009).

19. A. Laughon, A. M. Boulet, J. R. Bermingham, R. A. Laymon, M. P. Scott, Structure of transcripts from the homeotic Antennapedia gene of Drosophila melanogaster: two promoters control the major protein-coding region. *Mol. Cell. Biol.* **6**, 4676–4689 (1986).

20. S. Schneuwly, A. Kuroiwa, P. Baumgartner, W. J. Gehring, Structural organization and sequence of the homeotic gene Antennapedia of Drosophila melanogaster. *EMBO J.* **5**, 733–739 (1986).

21. V. L. Stroeher, E. M. Jorgensen, R. L. Garber, Multiple transcripts from the Antennapedia gene of Drosophila melanogaster. *Mol. Cell. Biol.* **6**, 4667–4675 (1986).

22. A. M. Boulet, M. P. Scott, Control elements of the P2 promoter of the Antennapedia gene. *Genes Dev.* **2**, 1600–1614 (1988).

23. B. T. Wakimoto, T. C. Kaufman, Analysis of larval segmentation in lethal genotypes associated with the antennapedia gene complex in Drosophila melanogaster. *Dev. Biol.* **81**, 51–64 (1981).

24. M. K. Abbott, T. C. Kaufman, The Relationship between the Functional Complexity and the Molecular Organization of the ANTENNAPEDIA Locus of DROSOPHILA MELANOGASTER. *Genetics* **114**, 919–942 (1986).

25. Y. Engström, S. Schneuwly, W. J. Gehring, Spatial and temporal expression of an Antennapedia/lac Z gene construct integrated into the endogenous Antennapedia gene of Drosophila melanogaster. *Rouxs Arch. Dev. Biol. Off. Organ EDBO* **201**, 65–80 (1992).

26. V. Sudarsan, S. Anant, P. Guptan, K. VijayRaghavan, H. Skaer, Myoblast Diversification and Ectodermal Signaling in Drosophila. *Dev. Cell* **1**, 829–839 (2001).

27. J. Fernandes, M. Bate, K. Vijayraghavan, Development of the indirect flight muscles of Drosophila. *Development* **113**, 67–77 (1991).

28. S. Roy, K. VijayRaghavan, Patterning Muscles Using Organizers: Larval Muscle Templates and Adult Myoblasts Actively Interact to Pattern the Dorsal Longitudinal Flight Muscles of Drosophila. *J. Cell Biol.* **141**, 1135–1145 (1998).

29. M. L. Spletter, C. Barz, A. Yeroslaviz, X. Zhang, S. B. Lemke, A. Bonnard, E. Brunner, G. Cardone, K. Basler, B. H. Habermann, F. Schnorrer, A transcriptomics resource reveals a transcriptional transition during ordered sarcomere morphogenesis in flight muscle. *eLife* **7**, e34058 (2018).

30. B. Lilly, B. Zhao, G. Ranganayakulu, B. M. Paterson, R. A. Schulz, E. N. Olson, Requirement of MADS Domain Transcription Factor D-MEF2 for Muscle Formation in Drosophila. *Science* **267**, 688–693 (1995).

31. K. A. Edwards, M. Demsky, R. A. Montague, N. Weymouth, D. P. Kiehart, GFP-Moesin Illuminates Actin Cytoskeleton Dynamics in Living Tissue and Demonstrates Cell Shape Changes during Morphogenesis inDrosophila. *Dev. Biol.* **191**, 103–117 (1997).

32. M. Weitkunat, F. Schnorrer, A guide to study Drosophila muscle biology. *Methods* **68**, 2–14 (2014).

33. S. Anant, S. Roy, K. VijayRaghavan, Twist and Notch negatively regulate adult muscle differentiation in Drosophila. *Dev. Camb. Engl.* **125**, 1361–1369 (1998).

34. C. Soler, J. Han, M. V. Taylor, The conserved transcription factor Mef2 has multiple roles in adult Drosophila musculature formation. *Development* **139**, 1270–1275 (2012).

35. R. M. Cripps, B. L. Black, B. Zhao, C.-L. Lien, R. A. Schulz, E. N. Olson, The myogenic regulatory gene Mef2 is a direct target for transcriptional activation by Twist during Drosophila myogenesis. *Genes Dev.* **12**, 422–434 (1998).

36. H. Duan, J. B. Skeath, H. T. Nguyen, Drosophila Lame duck, a novel member of the Gli superfamily, acts as a key regulator of myogenesis by controlling fusion-competent myoblast development. *Development* **128**, 4489–4500 (2001).

37. D. Müller, T. Jagla, L. M. Bodart, N. Jährling, H.-U. Dodt, K. Jagla, M. Frasch, Regulation and Functions of the lms Homeobox Gene during Development of Embryonic Lateral Transverse Muscles and Direct Flight Muscles in Drosophila. *PLoS ONE* **5**, e14323 (2010).

38. C. Schaub, H. Nagaso, H. Jin, M. Frasch, Org-1, the Drosophila ortholog of Tbx1, is a direct activator of known identity genes during muscle specification. *Development* **139**, 1001–1012 (2012).

39. P. Mendoza-Garcia, S. Basu, S. K. Sukumar, B. Arefin, G. Wolfstetter, V. Anthonydhason, L. Molander, E. Uçkun, H. Lindehell, C. Lebrero-Fernandez, J. Larsson, E. Larsson, M. Bemark, R. H. Palmer, DamID transcriptional profiling identifies the Snail/Scratch transcription factor Kahuli as an Alk target in the Drosophila visceral mesoderm. *Dev. Camb. Engl.* **148**, dev199465 (2021).

40. F. Schnorrer, C. Schönbauer, C. C. H. Langer, G. Dietzl, M. Novatchkova, K. Schernhuber, M. Fellner, A. Azaryan, M. Radolf, A. Stark, K. Keleman, B. J. Dickson, Systematic genetic analysis of muscle morphogenesis and function in Drosophila. *Nature* **464**, 287–291 (2010).

41. J. Warmke, M. Yamakawa, J. Molloy, S. Falkenthal, D. Maughan, Myosin light chain-2 mutation affects flight, wing beat frequency, and indirect flight muscle contraction kinetics in Drosophila. *J. Cell Biol.* **119**, 1523–1539 (1992).

42. M. A. J. Weterman, P. G. Barth, K. Y. van Spaendonck-Zwarts, E. Aronica, B.-T. Poll-The, O. F. Brouwer, J. P. van Tintelen, Z. Qahar, E. J. Bradley, M. de Wissel, L. Salviati, C. Angelini, L. van den Heuvel, Y. E. M. Thomasse, A. P. Backx, G. Nürnberg, P. Nürnberg, F. Baas, Recessive MYL2 mutations cause infantile type I muscle fibre disease and cardiomyopathy. *Brain J. Neurol.* **136**, 282–293 (2013).

43. F. Sheikh, R. C. Lyon, J. Chen, Functions of Myosin Light Chain-2 (MYL2) In Cardiac Muscle and Disease. *Gene* **569**, 14–20 (2015).

44. M. L. Spletter, C. Barz, A. Yeroslaviz, C. Schönbauer, I. R. S. Ferreira, M. Sarov, D. Gerlach, A. Stark, B. H. Habermann, F. Schnorrer, The RNA-binding protein Arrest (Bruno) regulates alternative splicing to enable myofibril maturation in Drosophila flight muscle. *EMBO Rep.* **16**, 178–191 (2015).

45. A. L. Bryantsev, P. W. Baker, T. L. Lovato, M. S. Jaramillo, R. M. Cripps, Differential requirements for Myocyte Enhancer Factor-2 during adult myogenesis in Drosophila. *Dev. Biol.* **361**, 191–207 (2012).

46. E. A. Fyrberg, J. W. Mahaffey, B. J. Bond, N. Davidson, Transcripts of the six Drosophila actin genes accumulate in a stage- and tissue-specific manner. *Cell* **33**, 115–123 (1983).

47. C. Schönbauer, J. Distler, N. Jährling, M. Radolf, H.-U. Dodt, M. Frasch, F. Schnorrer, Spalt mediates an evolutionarily conserved switch to fibrillar muscle fate in insects. *Nature* **479**, 406–409 (2011).

48. J. T. Wagner-Bernholz, C. Wilson, G. Gibson, R. Schuh, W. J. Gehring, Identification of target genes of the homeotic gene Antennapedia by enhancer detection. *Genes Dev.* **5**, 2467–2480 (1991).

49. S. W. Choo, R. White, S. Russell, Genome-Wide Analysis of the Binding of the Hox Protein Ultrabithorax and the Hox Cofactor Homothorax in Drosophila. *PLOS ONE* **6**, e14778 (2011).

50. R. Galant, C. M. Walsh, S. B. Carroll, Hox repression of a target gene: extradenticle-independent, additive action through multiple monomer binding sites. *Dev. Camb. Engl.* **129**, 3115–3126 (2002).

51. S. Roy, K. V. Raghavan, Homeotic genes and the regulation of myoblast migration, fusion, and fibre-specific gene expression during adult myogenesis in Drosophila. *Development* **124**, 3333–3341 (1997).

52. A. J. Saurin, M. C. Delfini, C. Maurel-Zaffran, Y. Graba, The Generic Facet of Hox Protein Function. *Trends Genet.* **34**, 941–953 (2018).

53. A. Carmena, B. Murugasu-Oei, D. Menon, F. Jiménez, W. Chia, inscuteable and numb mediate asymmetric muscle progenitor cell divisions during Drosophila myogenesis. *Genes Dev.* **12**, 304–315 (1998).

54. A. Carmena, M. Bate, F. Jiménez, Lethal of scute, a proneural gene, participates in the specification of muscle progenitors during Drosophila embryogenesis. *Genes Dev.* **9**, 2373–2383 (1995).

55. M. R. Gómez, M. Bate, Segregation of myogenic lineages in Drosophila requires Numb. *Development* **124**, 4857–4866 (1997).

56. S. Merabet, M. Saadaoui, N. Sambrani, B. Hudry, J. Pradel, M. Affolter, Y. Graba, A unique Extradenticle recruitment mode in the Drosophila Hox protein Ultrabithorax. *Proc. Natl. Acad. Sci. U. S. A.* **104**, 16946–16951 (2007).

57. J. H. Simpson, Rationally subdividing the fly nervous system with versatile expression reagents. *J. Neurogenet.* **30**, 185–194 (2016).

58. J. W. Bloor, D. P. Kiehart, zipper Nonmuscle Myosin-II Functions Downstream of PS2 Integrin in Drosophila Myogenesis and Is Necessary for Myofibril Formation. *Dev. Biol.* **239**, 215–228 (2001).

59. Z. Orfanos, J. C. Sparrow, Myosin isoform switching during assembly of the *Drosophila* flight muscle thick filament lattice. *J. Cell Sci.* **126**, 139–148 (2013).

60. X. Zhang, W. H. Koolhaas, F. Schnorrer, A versatile two-step CRISPR- and RMCE-based strategy for efficient genome engineering in Drosophila. *G3 Bethesda Md* **4**, 2409–2418 (2014).

61. L. S. Gramates, J. Agapite, H. Attrill, B. R. Calvi, M. A. Crosby, G. Dos Santos, J. L. Goodman, D. Goutte-Gattat, V. K. Jenkins, T. Kaufman, A. Larkin, B. B. Matthews, G. Millburn, V. B. Strelets, FlyBase: a guided tour of highlighted features. *Genetics* **220**, iyac035 (2022).

62. G. Poliacikova, M. Barthez, T. Rival, A. Aouane, N. M. Luis, F. Richard, F. Daian, N. Brouilly, F. Schnorrer, C. Maurel-Zaffran, Y. Graba, A. J. Saurin, M1BP is an essential transcriptional activator of oxidative metabolism during Drosophila development. *Nat. Commun.* **14**, 3187 (2023).

63. J. Schindelin, I. Arganda-Carreras, E. Frise, V. Kaynig, M. Longair, T. Pietzsch, S. Preibisch, C. Rueden, S. Saalfeld, B. Schmid, J.-Y. Tinevez, D. J. White, V. Hartenstein, K. Eliceiri, P. Tomancak, A. Cardona, Fiji: an open-source platform for biological-image analysis. *Nat. Methods* **9**, 676–682 (2012).

64. F. Daian, A. J. Saurin, andysaurin/3DL_NuCount: Used to count myoblast nuclei attached to Drosophila wing imaginal discs, Zenodo (2023); https://doi.org/10.5281/zenodo.7695893.

Acknowledgments

We thank Bloomington and Vienna Stock Centres for fly stocks, Drosophila Genomics Resource Center (NIH Grant 2P40OD010949) for cDNA clones, BestGene Inc for injection services, BACPAC Resources center for the BAC clone, Eileen Furlong for Twi antibodies, the GenomEast (IGBMC, France) sequencing platform for generation of the high-throughput RNA sequencing data, Frank Schnorrer for useful discussions, and the IBDM Imaging and Drosophila platforms. Immunofluorescence and electron microscopy imaging were performed on the PICsL-FBI core imaging facility, member of the France-BioImaging national research infrastructure supported by the French National Research Agency (ANR-10-INBS-04) and member of the Marseille Imaging Institute, an Excellence Initiative of Aix Marseille University A*MIDEX, a French "Investissements d'Avenir" programme (AMX 19 IET 002).

Funding:

This study was made possible through financial support from the following funding agencies:
AFM-Téléthon grant 23721 (AJS)
AFM-Téléthon grant 24928 (AJS)
Fondation pour la Recherche Médical fellowship EQU202403018061 (AJS)
Fondation pour la Recherche Médical fellowship FDT202304016709 (GP)

Author contributions:

Conceptualization: GP, AJS

Methodology: GP, AJS, NC, CMZ, FD, AA

Investigation: GP, AJS

Visualization: GP, AJS, AA, NB

Funding acquisition: AJS, GP

Project administration: AJS, YG

Supervision: GP, CMZ, YG, AJS

Writing – original draft: GP, AJS

Writing – review & editing: GP, AJS, CMZ, YG

Competing interests: Authors declare that they have no competing interests.

Data and materials availability: All data needed to evaluate the conclusions in the paper are present in the paper and/or the Supplementary Materials. The high throughput sequencing data have been deposited with the Gene Expression Ombudsman (GEO) and are available under the accession number GSE268583.

Table of contents for supplementary materials

Figs. S1 to S9:

Fig.S1 Antp is expressed in larval flight muscle precursors
Fig.S2 Heterozygous *Antp* mutations do not perturb flight muscle development
Fig.S3 *Antp* KD perturbs pupal flight muscle development
Fig.S4 *Antp* KD perturbs adult flight muscle myofibrillogenesis
Fig.S5 *Antp* early pupal, but not late pupal downregulation perturbs adult flight myogenesis
Fig. S6 Defaults in pupal flight muscle development in the *Antp* KD can be rescued with Antp overexpression
Fig. S7 Defaults in pupal flight muscle development in the *Antp* KD can be rescued with Mlc2 overexpression
Fig. S8 *Antp* overexpression prevents fibrillar fibre fate
Fig. S9 Fibrillar fate and Spalt repression are shared *Hox* functions

Movie S1 to S3 (separate files):

Movie S1 Spinning disc movie of developing flight muscles at 29°C, expressing *UAS-y RNAi* driven by the *Mef2*-Gal4 *driver,* with the *UAS-GFP-Gma* transgene added to visualise actin.

Movie S2 Spinning disc movie of developing flight muscles at 29°C, expressing *UAS-Antp RNAi #2* driven by the *Mef2*-Gal4 *driver,* with the *UAS-GFP-Gma* transgene added to visualise actin, corresponding to example 1.

Movie S3 Spinning disc movie of developing flight muscles at 29°C, expressing *UAS-Antp RNAi #2* driven by the *Mef2*-Gal4 *driver,* with the *UAS-GFP-Gma* transgene added to visualise actin, corresponding to example 2.

Data S1 to S3 (separate files):

Data S1 Excel file containing differential gene expression analysis of RNA-sequencing following *Antp* RNAi #2 expression in myoblasts, driven by the *Mef2*-Gal4 driver.

Data S2 Excel file containing the comparison of differential gene expression analysis of RNA-sequencing following *Antp* RNAi #2 in myoblasts, driven by the *Mef2*-Gal4 driver, with the screen from *Schnorrer et al. 2010.*

Data S3 Excel file containing differential gene expression analysis of RNA-sequencing following Antp overexpression driven by the *Act88F*-GAL4 driver in 72 h APF pupa at 25°C.

Figures and Tables

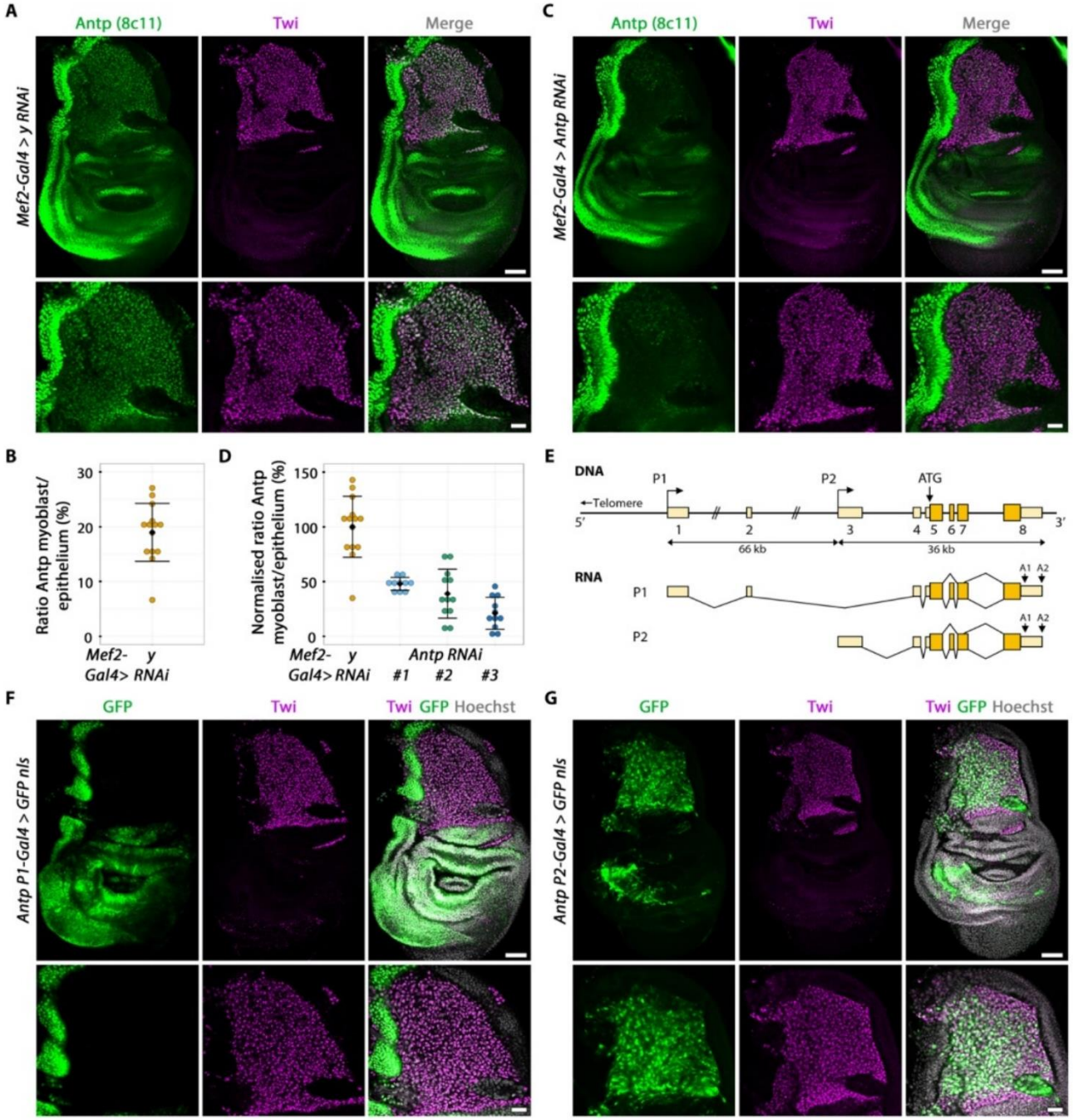

Fig. 1. Antp is expressed in flight muscle myoblasts from the promoter 2.
(A) Confocal sections of 0 h APF wing discs expressing *UAS-y RNAi* driven by *Mef2-Gal4*, stained with anti-Antp (8c11) and anti-Twi. **(B)** Ratio of Antp intensity in the myoblast area versus anterior epithelium. The mean and standard deviation are shown. Each dot represents a value from one disc (n = 14 discs from at least 7 animals). **(C)** As (A) with *Mef2-GAL4* driving *UAS-Antp RNAi #1*. **(D)** Normalised Antp intensity in *Antp RNAi* conditions (each RNAi line is depicted by with a #). Each dot represents a value from one disc (n_{WT} = 14, $n_{\#1}$ = 10, $n_{\#2}$ = 12 and $n_{\#3}$ = 11 wing discs from at least 5 animals). **(E)** *Antp* gene and transcripts (coding exons are dark yellow and non-coding exons are light yellow smaller boxes). P1 and P2 represent two distinct promoters and A1, A2 two alternative polyadenylation sites. **(F, G)** Confocal sections of 0 h APF wing discs expressing *UAS-GFP nls* driven by *Antp P1-Gal4* (F) or *Antp P2-Gal4* (G), stained with anti-GFP and anti-Twi. The scale bar is 50 µm for the top and 20 µm for the bottom views.

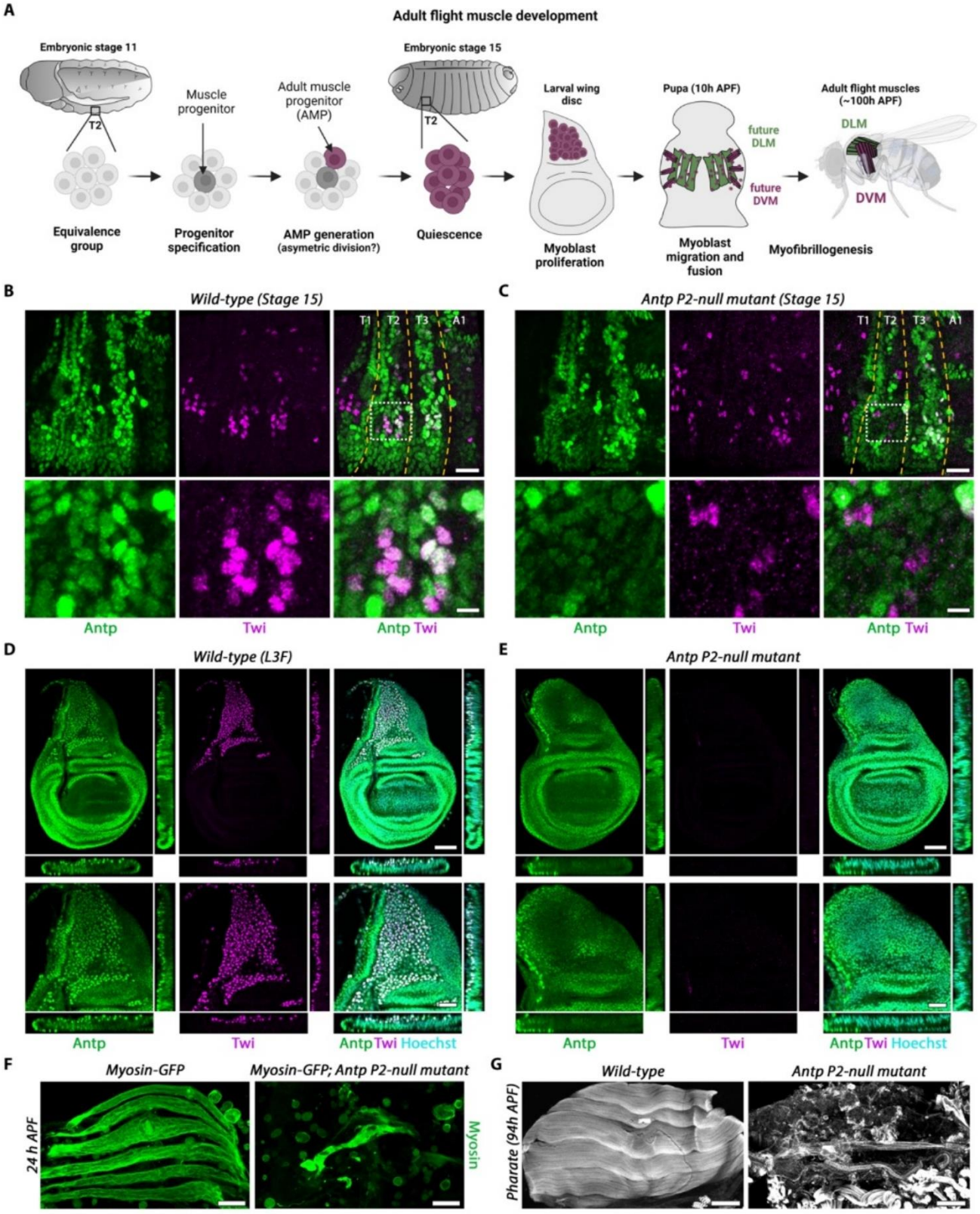

Fig. 2 *Antp* mutation leads to the absence of adult flight muscles

(A) Schematic representation of adult flight myogenesis. **(B, C)** Confocal sections of stage 15 embryos labelled with antibodies against Antp and Twi. Genotypes are: (B) wild-type and (C) $Antp^{P2\text{-}null}$ mutant: $Antp^{nsrv\text{-}c3}$ (null mutation) over $Antp^{s1}$ (P2 mutation). T1, T2, T3 depict the three thoracic segment and A1 the first abdominal segment. Scale bar is 20 µm and 5µm for zoomed views on T2 AMPs. **(D, E)** Confocal sections of wing discs at the L3 feeding stage labelled with antibodies against Antp and Twi. Genotypes are identical to (B, C). Scale bar is 50 µm and 25 µm for zoomed views. **(F)** Confocal projections of 24 h APF

pupal IFMs labelled with GFP to visualise myosin. Genotypes are identical to (B, C) with *weeP26* transgene (Myosin-GFP) added. The scale bar is 50µm. **(G)** Confocal sections of pupal IFM at the pharate stage, labelled with phalloidin. Genotypes are identical to (B, C). The scale bar is 100 µm. DLM (Dorsal longitudinal muscles), DVM (Dorsal ventral muscles).

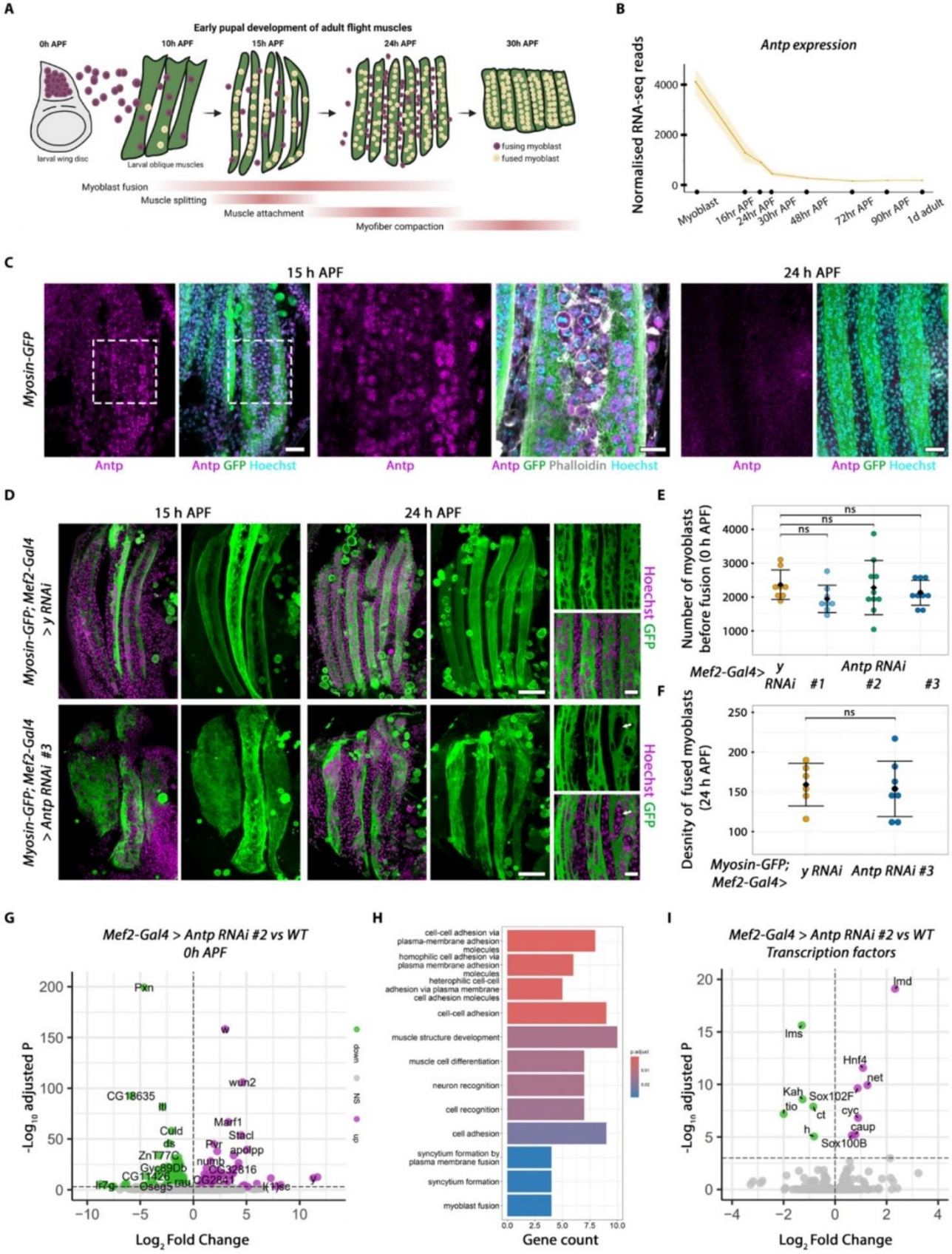

Fig. 3 *Antp* regulates flight muscle differentiation.

(A) Schematic representation of pupal flight myogenesis. **(B)** *Antp* mRNA normalised expression, analysed from (*29*). **(C)** Confocal sections of 15 h and 24 h APF flight muscles expressing *Myosin-GFP*, stained with anti-Antp, anti-GFP (to visualise myosin), Phalloidin and Hoechst. Scale bar is 20 µm for large views (left) and 10 µm for zoomed views (right),

depicted by the white triangle. **(D)** Confocal sections (left) and projections (right) of 15 h and 24 h APF flight muscles expressing *Myosin-GFP*; *Mef2-Gal4* driving *UAS-y RNAi* as control (top) or *UAS-Antp RNAi #3* (bottom), stained with anti-GFP and Hoechst. Scale bar is 50 µm for large sections and 15 µm for zoomed views. Arrow depicts zones of high nuclei density. **(E)** Quantification of number of myoblasts in 0 h APF wing disc upon *Antp* KD. Mean and standard deviation are shown, each dot represents a value from one disc (n_{WT} = 8, $n_{\#1}$ = 8, $n_{\#2}$ = 10 and $n_{\#3}$ = 10 wing discs from at least 5 animals). **(F)** The same as in (E) at 24h APF (n_{WT} = 6, $n_{\#3}$ = 8 animals). **(G)** Volcano plot of DEG between WT and *UAS-Antp RNAi #2* driven by *Mef2-Gal4* driver. **(H)** GO analysis using significantly upregulated genes. **(I)** Volcano plot of TFs, the same conditions as (G).

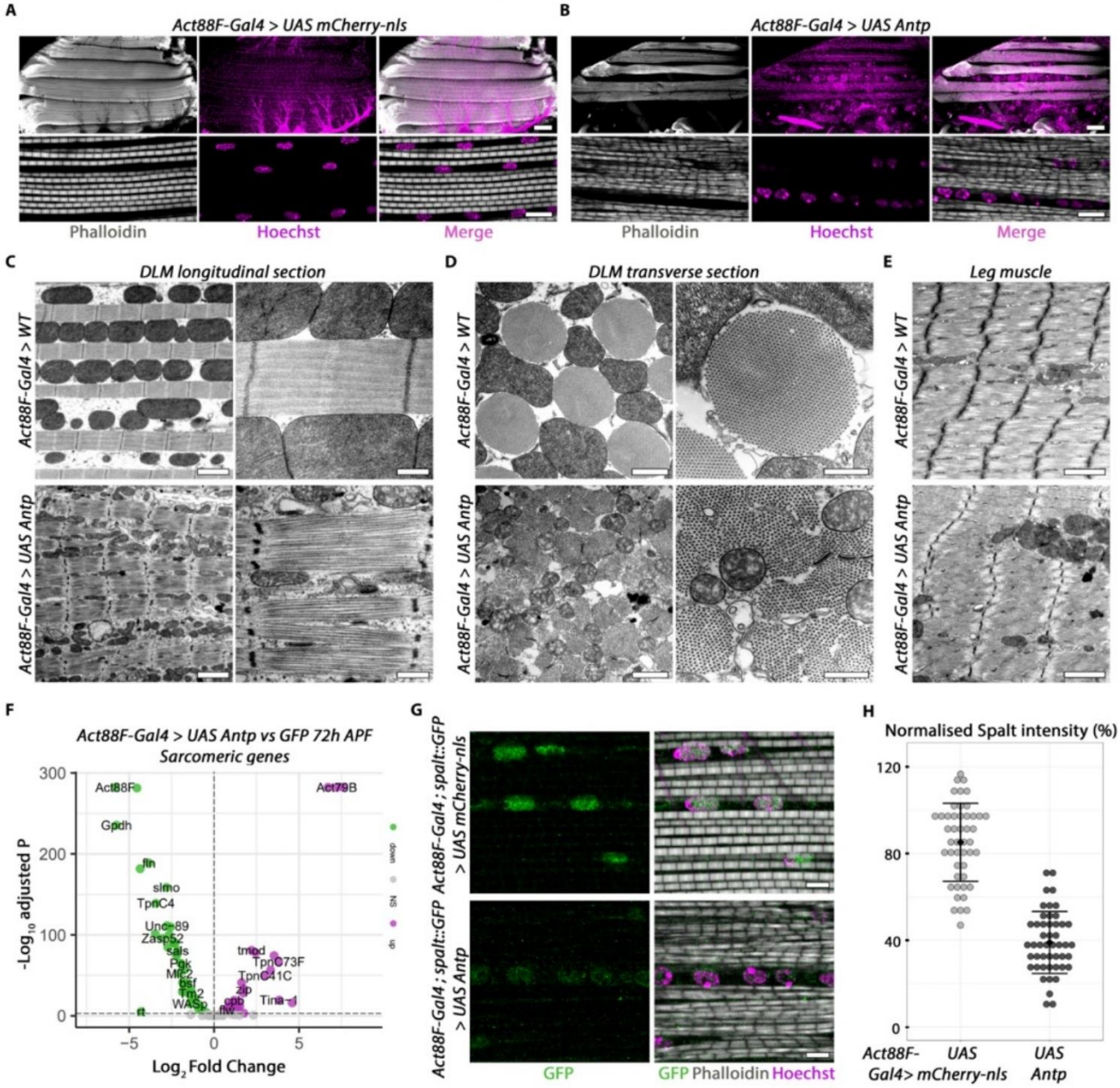

Fig. 4 *Antp* overexpression suppresses fibrillary muscle fate.

(A, B) Confocal sections of adult female DLM stained with phalloidin and Hoechst (Top), with zoomed views on sarcomeres (Bottom). Scale bars are 100 µm and 10 µm for zoomed views. Genotypes are: *UAS-mCherry-nls* (A) and *UAS-Antp* (B) driven by the *Act88F-Gal4* driver. **(C)** TEM micrographs of adult DLM, cut in longitudinal section. Scale bars are 2 µm and 500 nm for zoomed views. **(D)** The same as (C), cut in cross sections. Scale bars are 1 µm and 500 nm for zoomed views. **(E)** TEM micrographs of leg muscles, the scale bar is 2 µm. For (C-E) genotypes are: Wild-type (Top) and *UAS-Antp* (Bottom) driven by the *Act88F-Gal4* driver. **(F)** Volcano plot of sarcomeric DEG between *UAS-GFP* and *UAS-Antp* driven by *Act88F-Gal4* driver. **(G)** Confocal sections of adult female DLM stained with anti-GFP (to visualise Salm), Phalloidin and Hoechst. Scale bar is 5 µm. **(H)** Quantification of normalised Salm intensity, represented is the mean and standard deviation where each point represents a value of a single nucleus ($n_{mcherry\text{-}nls}$ = 60 nuclei and n_{Antp} = 48 nuclei from at least 3 animals). Genotypes in (G, H) are identical to (A, B), with the *spalt::GFP* transgene added.

Discussion and perspectives

Part 1. M1BP is an essential transcriptional activator of oxidative metabolism during *Drosophila* development

In Article 1 we showed that M1BP is an activator of oxidative metabolism during flight muscle development. Downregulation of *M1BP* during flight myogenesis leads to a flightless phenotype, a decrease in the quantity of mitochondrial respiratory complexes, mitochondrial inclusions containing at least one subunit of the respiratory chain complexes and a large mitochondrial unfolded protein response, all this without perturbing the myofibril organisation. Even though distinct types of vertebrate muscles depending on their metabolic requirements and capacities have been identified a long time ago (reviewed in Talbot and Maves, 2016), our understanding of how this is achieved at the molecular level is poor. The developing flight muscles proved to be an excellent tissue for studying the transcriptional regulation of mitochondrial metabolism since it undergoes a large transcriptional upregulation of genes participating in various mitochondrial processes in a span of three days (Spletter et al., 2018). Furthermore, this tissue is large enough to be easily used for transcriptomic analyses and accessible for in vivo imaging (Lemke and Schnorrer, 2018).

Mitochondria undergo drastic changes in their shape and transcriptome during flight muscle development

To provide a resource for future studies, we quantified numerous parameters describing the mitochondrial shape and the number of mitochondrial cristae during flight muscle development. We extensively analysed the publicly available transcriptomic data, focusing on genes involved in mitochondrial oxidative metabolism. These data showed the large extent of mitochondrial changes during myogenesis. After myoblast fusion, between 24 and 34 h APF mitochondria start to elongate, increasing their perimeter up to 12 µm. This process occurs just prior to the simultaneous appearance of the first immature sarcomeres in the muscle fibres at around 34 h APF (Spletter et al., 2018). Mitochondria were proposed to intercalate in between myofibrils at this time point, using very likely microtubules to do so (Avellaneda et al., 2021). Up to 48 h APF, the mitochondria cristae number remains the same as in the muscle precursor's mitochondria. Between 30 h and 48 h APF, the transcription of genes encoding assembly factors of mitochondrial respiratory complexes starts to increase drastically, which is followed by the upregulation of genes encoding complexes of the respiratory chain at 48 h APF. Between 48 h and 64 h APF the number of mitochondria cristae starts to increase, likely to accommodate for the newly synthesised respiratory complexes, to reach its final number 7 days after the fly eclosion. A second major shape transition starts at 72 h APF, where mitochondria become rounder, and increase their area to tightly fill the space in between myofibrils. The proper regulation of mitochondrial dynamics during myofibril assembly is crucial for the flight myogenesis, as an increase in the mitochondrial fusion, or a decrease in fission, leads to a switch from the fibrillar to the tubular fate (Avellaneda et al., 2021). We were surprised to see the extent of changes occurring just prior to and after the eclosion, where mitochondria double their

area before the eclosion and continue to incorporate new cristae during the first days of life (see Fig. 2, Suppl. Fig. 4).

Understanding the role mitochondria play in the regulation of muscle development is an extensive topic of research in both *Drosophila* and vertebrates. *Drosophila* fibrillar muscles display a parallel mitochondrial network and tubular muscles either a parallel (jump) or a grid-like network (leg) (Katti et al., 2022). In vertebrate striated muscles, mitochondria network organisation also differs between fibres, such as glycolytic, oxidative and cardiac muscles have perpendicular, grid-like and parallel orientations, respectively, showing distinct levels of mitochondrial connectivity, to fulfil distinct energetic requirements of these muscles (Bleck et al., 2018; Willingham et al., 2019). A critical question is how the establishment of these different mitochondrial networks is regulated during development.

Few studies focused on mitochondrial changes during mouse muscle development, accessible for imaging only after birth (Kim et al., 2019, 2024; Mishra et al., 2015). In this context, it was shown that the glycolytic tibialis anterior (TA) muscle mitochondria in mice during the first week of their life display a parallel mitochondrial network that changes towards a perpendicular network between P7 to P21. In a similar manner to what we described during flight myogenesis, in parallel to changes in mitochondrial shape, there is an increase of OXPHOS protein levels during postnatal mice development, suggestive of higher oxidative capacities, accommodating for the increasing hindlimb activity. Similarly to what we observed, mitochondrial elongation was detected during the early postnatal period preceding the increase in OXPHOS proteins (Kim et al., 2019).

Even though occurring at distinct phases of their life cycles, in both flies and mice there seems to be an early phase of muscle mitochondrial development involving changes in mitochondrial dynamics, followed by a second phase of mitochondrial specialisation for the particular energy metabolism required in a given fibre. How the regulation of OXPHOS-gene expression varies during development in distinct fibre types remains elusive. More work is needed to determine how mitochondrial biogenesis changes during muscle development to accommodate for energetic requirements of various fibre types, with a direct implication in ageing and muscle diseases.

M1BP activates the transcription of OXPHOS genes

The group previously showed that *M1BP* downregulation in the fat body affects 25% of all metabolic genes, the most significantly impacted genes being genes related to oxidative metabolism (Barthez et al., 2020). We showed that this is also the case in flight muscles, where the situation is a bit more complex, which is likely due to the extent of mitochondrial changes during flight myogenesis. By tracking M1BP function during different stages of flight muscle development, we determined that M1BP contributes to the large transcriptional activation of OXPHOS-genes (genes encoding both subunits of mitochondrial complexes and their assembly factors), starting between 30 and 48 h APF (see Fig. 3). Even though only a few genes encoding subunits of the respiratory chain were affected, many assembly factors were downregulated upon *M1BP* KD, starting from 48 h APF, resulting in a decrease in the quantity of mitochondrial complexes in the adult flight muscle mitochondria (see Fig. 5). This transcriptional deregulation was followed by an apparition of electron-dense mitochondrial inclusions, first detected at 64

h APF (see Fig. 3). These data show that M1BP is a part of the TF GRN responsible for the abrupt upregulation of mitochondrial metabolic genes occurring during mid-pupal development. Knowing that M1BP is expressed already in myoblasts during larval stages and that its downregulation affects only a portion of OXPHOS-genes, there are additional factors that are required for this switch.

The E2F TF, its co-regulator Retinoblastoma-family protein (Rbf) (Zappia et al., 2019) and Salm TF (Spletter et al., 2018) were shown to transcriptionally regulate OXPHOS genes in flight muscles, likely participating in the transcriptional upregulation of these genes with M1BP. In line with this is the fact that the most overrepresented motif in genes activated by Rbf is the M1BP motif 'GGTCACACTG' (Zappia et al., 2019). Knowing that all these factors are expressed prior to 48 h APF when the transcriptional upregulation occurs, other signals are required for the activation of mitochondrial genes. Our bioinformatics analysis showed that many TFs known for regulating mitochondrial biogenesis (such as TFAM, Ewg and Spargel) are expressed during flight myogenesis (see Fig. 4 and Suppl. Fig. 7). Using in silico approach, we could show that M1BP motif is the most significantly overrepresented in the promoters of OXPHOS-genes, largely co-occurring at these promoters with Mef2 (see Fig. 4). These data suggest that an intricate network of several TFs is involved in the large upregulation of OXPHOS-genes in developing flight muscles.

M1BP involvement in this process is unique in a way that it is the only one of these factors that do not regulate simultaneously sarcomeric and mitochondrial genes. M1BP was first identified as a Pol II pausing factor. The release of the promoter-proximal pausing can result in a very fast initiation of transcription, the best described during the heat-shock response (Lis, 1998). Knowing that the most significantly represented motif in promoters of OXPHOS genes is the M1BP motif, this suggests the intriguing possibility that these genes could be subject to promoter-proximal pausing, allowing for their dynamic upregulation during flight muscle development.

A missing point in our analysis is the genomic data of M1BP binding to the promoters of OXPHOS genes. We extensively attempted to perform a Chip-seq in the adult muscle following the protocol used in the flight muscle pharate muscles (Zappia et al., 2019). In our hands, even 200 dissected adult flight muscles were not sufficient to immunoprecipitate M1BP. We ignore whether there is a difference between nuclei accessibility in pharate versus adult muscles or whether our inability to obtain enough DNA for sequencing is due to technical issues.

Mitochondrial KD leads to the appearance of mitochondrial inclusions

An intriguing phenotype we observed in our analyses was the appearance of large, highly electron-dense inclusions in the mitochondrial matrix, that have a developmental origin, appearing around 64 h APF (see Fig. 1 and 3). While looking for similar phenotypes in the literature, we found that they always seem to arise from a perturbation of the mitochondrial respiratory chain, like in the yeast mutant for a subunit of the CV **(Fig. 24A)** (Lefebvre-Legendre et al., 2005) and in rats fed with a rattlesnake venom crotoxin **(Fig. 24B)** (Shah et al., 1982). This phenotype was also reported in biopsies of patients presenting mitochondrial myopathies (**Fig. 24C**) (Linda et al., 1992) and in gastric carcinoma patients (**Fig. 24D**) (Marinozzi et al., 1977). Interestingly out of these four cases, two are present in the

metabolically active muscle mitochondria, further suggesting they are related to mitochondrial metabolism.

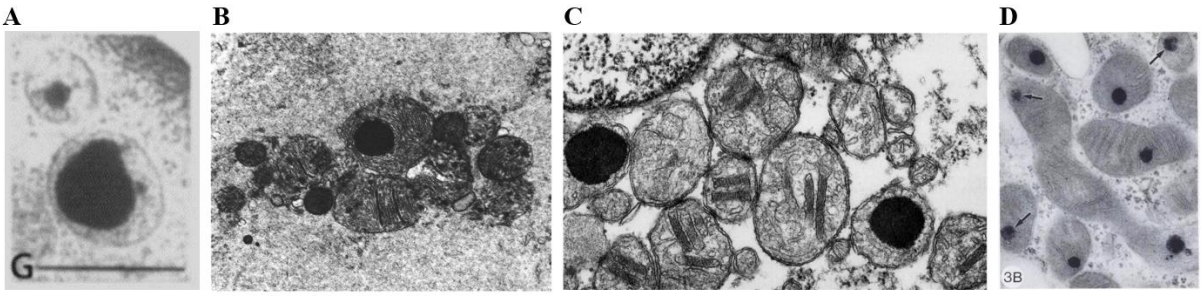

Figure 24. Presence of mitochondrial inclusions in various pathological conditions. (A) Mitochondrial inclusions observed in yeast mitochondria mutant for a subunit of the CV. (B) Mitochondria of the quadriceps muscle of a rat injected with a crotoxin 24 h prior. (C) Muscle biopsy of a human patient presenting mitochondrial myopathy. (D) Mitochondria of a metastatic tumour in a liver from gastric adenocarcinoma. References are indicated in the text.

We believe that the inclusions we observed also originate from the perturbations of mitochondrial metabolism, more particularly, oxidative metabolism. There is multiple evidence for this, such as the transcriptional deregulation of OXPHOS-genes occurring just prior to the appearance of this phenotype (see Fig. 3), the presence of a subunit of the CV in the insoluble protein mass of the muscle, while the overall quantity of OXPHOS complexes on the membrane decreases (see Fig. 5) and the large UPR^{mt} response we observed upon *M1BP* KD (see Fig. 6).

The most intriguing question is indeed what is contained in these large, electron-dense inclusions. We showed that *M1BP* KD leads to a deregulation of many assembly factors of the respiratory chain and a few subunits. Furthermore, many proteins encoding subunits of respiratory complexes are destined to the IMM and contain thus hydrophobic domains, rendering them to prone to aggregation. Indeed, many mitochondrial proteins are metastable, meaning that they aggregate when a critical concentration is achieved (Bragoszewski et al., 2017; Ciryam et al., 2015). A proper stoichiometry between nuclear-encoded and mtDNA-encoded subunits is crucial for the proper respiratory complex assembly (C. M. Brennan et al., 2019; Houtkooper et al., 2013). Based on all this evidence we believe that upon *M1BP* KD, there is an improper mitochondrial complex assembly, mitochondrial subunits stall in the mitochondrial matrix, leading to their aggregation. Despite the large mitochondrial quality control response we observed, mitochondria cannot resolve these aggregates and flight muscles do not manage to produce enough energy for flight. One way to analyse the composition of aggregates would be the energy dispersive X-ray analysis (EDX), allowing to determine the chemical composition of materials and was already applied to biological samples (Pirozzi et al., 2021).

In conclusion, we described in detail mitochondrial changes occurring during flight muscle development and identified a critical role for M1BP in regulating oxidative metabolism during this process. This data expanded the current knowledge about the regulation of mitochondrial functions during muscle development and identify a novel player in this process.

Part 2. Antp orchestrates *Drosophila* adult flight muscle development

In Article 2, we established a role for Antp in orchestrating adult flight myogenesis. We showed that Antp intervenes at several early stages of muscle development, in the specification of MPs in the embryo, in the regulation of muscle differentiation and in the choice of the muscle fibre type. This study challenges the longstanding belief that the development of adult muscles of the second thoracic segment does not require Hox input. Of this fact, this study is largely descriptive, and many open questions remain.

Antp is expressed in adult flight muscle precursors

We established using different antibodies and reporter lines that Antp is expressed in flight muscle precursors in the embryo, during larval stages until myoblast fusion, after which its expression is downregulated (see Fig. 1 and 3). There results confirm previous reports detecting *Antp* transcripts from the P2 in adepithelial cells (myoblasts) of the wing disc (Jorgensen and Garber, 1987) and Antp protein in the same region (Paul et al., 2021). Joining Capovilla et al., we believe that the seeming absence of Antp expression in flight muscle myoblasts described before (Roy et al., 1997) stems from the very low expression of Antp in these cells in comparison to the T3 mesoderm in the embryo or the wing disc epithelium in the larvae (Capovilla et al., 2001). All these examples suggest that the P1 drives *Antp* expression at higher levels compared to the P2. Detecting Antp expression in flight muscle myoblasts allows us to rethink the way we viewed the development of adult muscles in the T2 segment, in which it does not depend solely on non-autonomous cues.

The fact that Antp expression decreases in myoblast post-fusion around 24 h APF also explains why we failed to detect defaults in the mitochondrial respiratory chain upon *Antp* KD since mitochondrial biogenesis starts only 30 h later (Poliacikova et al., 2023).

Antp mutation leads to the absence of flight AMPs

Mutations affecting the P1 promoter when heterozygous with *Antp* deletion, die as embryos/early larvae. However, mutations affecting the P2, when heterozygous with a complete deletion of *Antp* survive until the pharate stage (Abbott and Kaufman, 1986). Since we established that the P2 promoter drives *Antp* expression in the T2 mesoderm, this mutations combination allowed us to study flight muscle development in this segment in the absence of *Antp*, without perturbing *Antp* expression in the ectoderm, which would lead to homeotic mutations and lethality. One caveat of this is that the P2 mutant allele we used, generated by X-rays, is not homozygous viable, but it is viable over a complete *Antp* deletion, suggesting that the P2 allele presents some other recessive lethal mutation. We are currently constructing a P2 mutant allele using CRISPR, to confirm our mutant data.

We showed that *Antp* P2 mutation leads to the absence of T2 AMPs (see Fig. 2). We offer two possible explanations for this result. First, AMPs could be specified in the absence of *Antp* but could be eliminated by apoptosis shortly after birth, in which case Antp would be responsible for the maintenance of AMP survival. In favour of this hypothesis Antp was shown to be responsible for the survival of MNs in the thoracic segments (Baek et al., 2013). This could be

tested by overexpressing an inhibitor of apoptosis, such as Diap1 (Hay et al., 1995), using the *Twi*-Gal4 line, in the *Antp* P2 mutant condition. A second hypothesis, that we favour, is that Antp could be involved in the specification of T2 AMPs. In support of this is the data showing that Antp is involved in the specification of the hematopoietic progenitors (Mandal et al., 2007).

How are AMPs specified in the thorax?

The issue with the hypothesis of Antp regulating AMP specification is that all the knowledge about this process we have comes from studies conducted in abdominal segments. In the abdomen it was shown that AMPs arise as sister cells of FCs through Notch/Numb mediated asymmetric division, where AMPs keep the N pathway active and the sibling FC inherits Numb, leading to its differentiation (Carmena et al., 1995; Carmena, Murugasu-Oei, et al., 1998; Ruiz Gómez and Bate, 1997). It is not known whether the same applies in the thorax, where each segment contains 3 times more AMPs compared to the abdomen (Bate et al., 1991). Interestingly, while comparing the number of embryonic muscles and the number of AMPs, there is an inverse correlation between the two. Indeed, the thoracic segments display fewer embryonic muscles (e.g. VA1/2/3, DA5 and VT1 are missing) or smaller muscles (such as LT muscles) and more AMPs (15-18 per segment), while abdominal segments have more embryonic muscles and fewer AMPs (6 per segment) (**Fig. 25**) (Bate, 1990; Bate et al., 1991). It is thus an interesting possibility, nevertheless never tested, that the greater number of AMPs generated in the thorax would be at the expense of larval FCs, ultimately allowing to have more adult muscles in the thorax than in the abdomen.

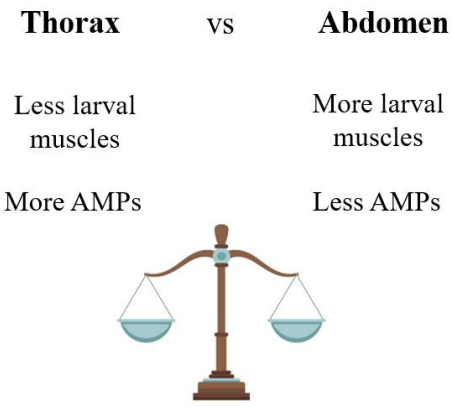

Figure 25. Inverse correlation between the number of larval and adult muscle progenitors along the A-P axis.

In favour of this hypothesis is the fact that upon overexpression of some iTFs important for AMP specification, surrounding progenitors can switch their fate to produce ectopic AMPs. This was demonstrated in the case of the SBM and lAMPs specification by *lb*. Lb-expressing progenitor produces three progeny and divides twice. The first division is asymmetric and produces a smaller SBM FC and the second division produces two lAMPs, all of which retain

Lb expression. Interestingly, when *lb* is overexpressed, some neighbouring *Kr*-expressing lateral progenitors become Lb-positive and switch their fate to produce surnumery lAMPs and giant SBMs (Jagla et al., 1998). This could thus constitute a general mechanism by which more AMPs can be produced at the expense of some larval muscles. The initial description of promuscular clusters already mentioned a segment-specific difference in cluster 18, expressing higher levels of L'sc in the thoracic versus abdominal segment, cluster 19 being present only in thoracic segments and a larger number of L'sc-expressing cells appearing in the thorax at stage 11 with an unknown lineage (Carmena et al., 1995).

Given the inverse correlation between the numbers of larval and adult muscle progenitors in the thorax and abdomen it is highly likely that the Notch/Numb-driven asymmetric division operates also in the thoracic AMPs like in the abdomen. This can be tested by manipulating the Notch pathway in the embryo and analysing the consequence on thoracic AMPs. For example, the overexpression of Numb using *Twi*-Gal4 leads to the absence of AMPs in the abdomen while ectopic larval muscles appear (Ruiz Gómez and Bate, 1997). The same experiment can be repeated with a focus on thoracic AMPs.

At least three possible mechanisms could operate, one where more AMP-giving progenitors would be specified in the abdomen or if MPs are the same between thorax and abdomen, the asymmetric division in the thorax could occur in favour of AMPs, meaning that more MPs in the thorax would divide asymmetrically compared to the abdomen. Another possibility is that the same number of AMPs would be generated during the initial MP division, and then AMPs would undergo additional divisions in the thorax. This is not very likely since AMPs are thought to be quiescent until their reactivation during larval stages (Aradhya et al., 2015). Following the division of MPs known to give AMPs in the abdomen (e.g. MP10 for vAMPs), using FC markers such as *duf* could be a starting point for resolving these speculations.

AMP specification by Hox

Assuming that the Notch-driven asymmetric division is involved in the thoracic AMP specification, we speculate that Antp could be involved in this process via indirect Notch regulation. In favour of this statement is the fact that flight myoblasts, in which *Antp* was downregulated using muscle-specific RNAi showed an increased *numb* expression, as observed by RNAseq. This could mean that Antp acts as a Numb repressor in AMPs, allowing for their specification by tilting the balance towards AMP fate by Notch expression maintenance. The expression of both Antp and Notch decreases just prior to AMP fusion and differentiation, further suggesting that Antp could maintain AMPs in an undifferentiated stage by allowing the Notch signalling to remain active in these cells. Even though no reports show that Antp could act as a Numb repressor, Antp was shown to act in parallel to the Notch pathway in the wing development (Kurata et al., 2000).

This would imply that in the *Antp* P2 mutant condition, the balance between larval and adult progenitors is perturbed, which could lead to the appearance of ectopic larval muscles, like in the case of *numb* overexpression (Ruiz Gómez and Bate, 1997). This could be tested by carefully comparing T2 larval muscles between wild-type and *Antp* P2 mutant embryos, which can be visualised by Mhc staining, and by following the asymmetric division in the thorax, as suggested above.

To expand on this idea, *Hox* genes were already shown to differentially regulate the number of larval (Enriquez et al., 2010) and adult (Greig and Akam, 1993) muscle progenitors in the thorax versus abdomen. We thus believe that the Hox code could help to establish the differential number of larval vs adult progenitors in the fly embryo. This could be achieved by for example specifying a higher number of AMP-giving progenitors in the thorax versus the abdomen, or by tilting the balance of the asymmetric division towards AMP fate via Notch regulation.

Could thoracic myoblasts mix during development?

We observed that in some cases, in very late *Antp* P2 mutant L3 wing discs, at 0 h APF (white pupa), there is a re-appearance of flight myoblasts in the notum region (**Fig. 26A**). We refer to it as a re-appearance as we never observed myoblasts in *Antp* P2 mutant discs in the L2 or L3F stage. Interestingly, some of these repopulating cells are Twi-positive, while some are Antp-positive and not Twi-positive. These cells do not continue the muscular development program as we never observed flight muscles in the *Antp* P2 mutant pupa. Their Antp expression would suggest that they express Antp from the P1 and could thus originate from the neighbouring segment. There is indeed very close spatial proximity between wing, haltere and leg myoblasts during larval development (**Fig. 26B**).

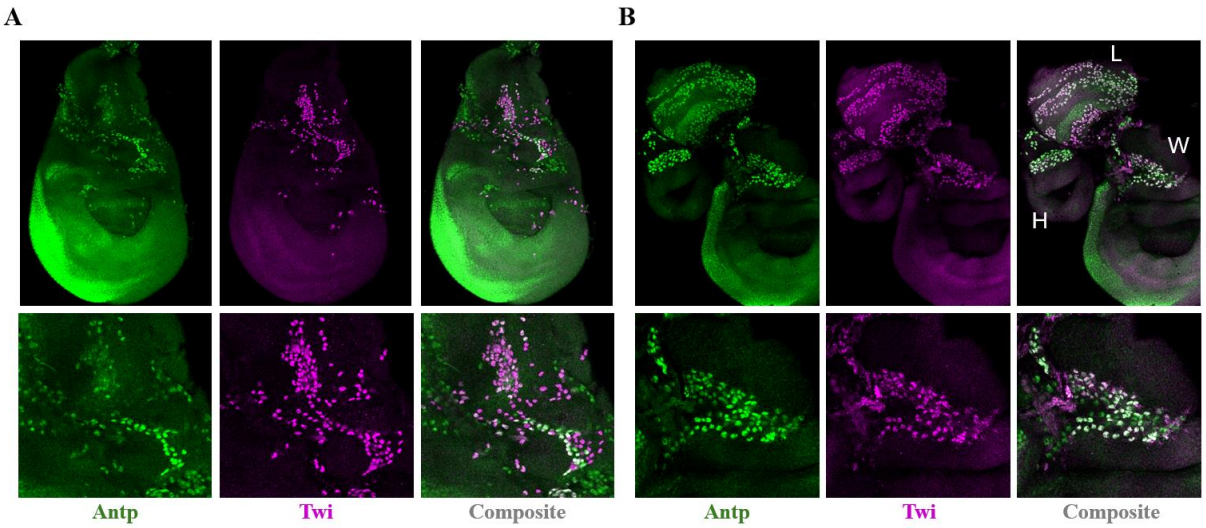

Figure 26. Myoblasts can re-appear in the *Antp* P2 mutant condition. **(A)** Confocal sections of 0 h APF wing discs, labelled with antibodies against Antp (in green) and Twi (in magenta). The notum region contains Antp and/or Twi-positive cells, which appear during the late L3W stage. **(B)** The same as A, with the wing disc (W), leg discs (L) and the haltere disc (H) shown. We note that the *Antp* P2 mutation does not alter Antp expression in haltere myoblasts or the T2 leg disc. The genotype in both panels is *Antp P2* mutation over *Antp* null deletion.

Myoblasts of the wing disc, when transplanted, can contribute indiscriminately to the development of the host abdominal muscles, suggesting that they are not committed to a flight muscle fate during larval stages. This would be in favour of the hypothesis that Antp prevents AMP differentiation, rather than providing them with a specific fate (Lawrence, 1982).

Molecular mechanisms underlying Antp function in larval myoblasts

We showed that Antp expression persists in flight myoblasts from their specification until their fusion (up to 15-20 h APF) (see Fig. 3). Downregulating Antp in these cells has consequences on myoblast fusion, muscle splitting and subsequent myofibrillogenesis. By our RNA-seq analysis, we showed that Antp potentially regulates a vast array of TFs, some of which have a function in muscle development (such as *kah*, *lmd*, *lms* and *org-1*). A study using a bimolecular fluorescence complementation (Bi-FC) assay showed that Antp can potentially interact with a variety of muscle-specific TFs, such as Eve, Kr, S59/Slou, Mef2, Twi and Salm in the embryo (Baëza et al., 2015).

It would be of great interest to obtain genomic data of Antp binding sites in flight myoblasts, to start to identify GRNs operating downstream of Antp in these cells. This task is hampered with several difficulties 1. There is a lack of a Chip-grade Antp antibody that could be used to immunoprecipitate Antp for a Chip-seq analysis. 2. Even if the antibody existed, Antp's high expression in the disc epithelium from the P1 would largely contaminate the myoblast samples. It would be required to proceed to cell-sorting prior to genomic analysis, which is incompatible with the high number of cells required for the Chip-seq. 3. Even though Cut & Run requires less initial material, we still lack an efficient antibody for Antp. The usage of an Antp-GFP reporter line coupled with cell sorting, or the creation of a Chip-grade antibody for Antp could help overcome these issues.

Regulation of Antp expression

A sharp decrease of Antp expression during myoblast fusion suggests a tight regulatory input operating at this stage. It was shown that *brahma* (*brm*) and *osa*, genes being a part of the Brahma complex (Brm; SWI/SNF in yeast and humans) activate Antp expression specifically from the P2. Interestingly, the heterozygous double mutation of *brm* and *osa* leads to held-out wings, phenocopying the muscle-specific *Antp* KD phenotype we observed. This phenotype was also observed in certain *Antp* mutants and can be significantly exacerbated by the heterozygous *brm* mutation, demonstrating a genetic interaction between them (Vazquez et al., 1999).

It was further shown by the team that *pontin* (*pont*), encoding a DNA helicase, associates with the Brm complex and regulates *Antp* expression in the wing disc (Diop et al., 2008). In the fat body, the loss of *pont* expression at the larval wandering stage results in the loss of Hox expression and the induction of developmental autophagy (Banreti et al., 2014). Given these results, we hypothesise that the Brm complex, comprising Osa and Pont, maintains Antp expression in myoblasts until their fusion at the beginning of the pupal stage. This could be tested by analysing Antp expression in larval myoblasts in the *brm*, *osa* and *brm*, *pont* mutants. Overexpression of Osa, Pont and Brm, if leading to the maintenance of Antp expression in flight myoblasts should result in a switch from fibrillar to tubular muscle fate as we observed in the case of Antp overexpression.

Role of Hox in leg muscle development

During my thesis, I co-supervised two Master 2 students, Océane Latagliata and Georges Delepine who worked on the expression of Hox in the leg discs. Unexpectedly, their work showed that both Antp and Scr are expressed in the myoblasts of all three thoracic leg discs, not respecting their mesodermal expression pattern (unpublished observations). In the ectoderm, they seem to obey their expression pattern, with Scr being expressed in the epithelium of the T1 disc, Antp in the T2 and Ubx in the epithelium of the T3 leg disc.

Interestingly, there seems to be a spatial distinction between Scr and Antp expressing myoblasts along the proximo-distal axis, with Scr being expressed in myoblasts in the centre of the leg disc, giving rise to more distal adult muscles (e.g. femur and tibia) while Antp is expressed at the disc periphery, in myoblasts that will give rise to proximal adult muscles (e.g. coxa and femur). Given that in the adult leg muscles, Antp is detected mainly in the T3 leg and Scr in the T1 leg (Simpson, 2016), there must be an extensive remodelling of Hox expression during morphogenesis. In the T2 the situation is even more intricate, as this disc contains also myoblasts contributing to the jump muscle, DFMs and possibly even DVM founders (Rivlin 2000). It would thus seem that leg myoblasts do not require a positional identity and the role Hox play in leg muscles stays elusive.

Differential promoter usage as a means of muscle diversification

Initial genetic studies of Antp function predicted that the P2 would be involved in the leg/antenna pathway choice in the imaginal discs and the P1 would be required for the thoracic segments discrimination, explaining their different lethality time points (Abbott and Kaufman, 1986; Laughon et al., 1986). Based on studies of their expression during development, it was proposed their function is rather spatial than temporal segregation, achieved through different posttranscriptional modifications (Laughon et al., 1986; Schneuwly et al., 1986; Stroeher et al., 1986).

In line with this, we showed that Antp is expressed in the mesoderm of the T2 and T3, using two distinct promoters, with the P2 driving Antp in the T2 and the P1 in the T3 (see Fig. 2 and S2). We believe that this configuration allows Antp to subdivide the thoracic domain into two distinct regions, with different regulatory inputs. Indeed, the T2 segment is specific in the fly in that it contains the precursors of flight muscles, the largest muscles in the fly, with a unique fibrillar morphology, not present elsewhere in the adult fly. We showed that Antp expression must decrease in the T2 segment to allow for the fibrillar fate acquisition (see Fig. 4). We hypothesise that the usage of the P2 to express Antp in the precursors of the fibrillar muscles allows for Antp downregulation specifically in these cells while maintaining its expression in tubular muscles, where Antp would be expressed presumably from the P1. In favour of this hypothesis, we observed that the *Antp P1*-Gal4 line drives Antp expression in the adult leg muscles in the T3 segment as well as in the haltere disc-associated myoblasts (unpublished results).

The situation nevertheless seems more complex, since we also detected Antp expression in the adult DFMs (see Fig. S8), that originate from myoblasts attached to the wing disc and from the T2 leg disc. How Antp expression is maintained in this muscle remains unclear.

While studying the transformation of muscle fibres from the fibrillar towards the tubular fate upon Antp overexpression, we observed that mitochondria also drastically change their shape (**Fig. 27**). Two distinct mitochondrial networks were described in tubular muscles, a grid-like network in the leg muscles (Fibers II and III) and a parallel network in the leg (Fiber I), DFMs and the jump muscle (Katti et al., 2022). Based on the parallel mitochondrial morphology we observed, we believe that Antp maintenance in the flight muscle myotubes post-fusion leads to their transformation towards a jump-like fate, DFM fate or towards the particular Fibre I type in the leg.

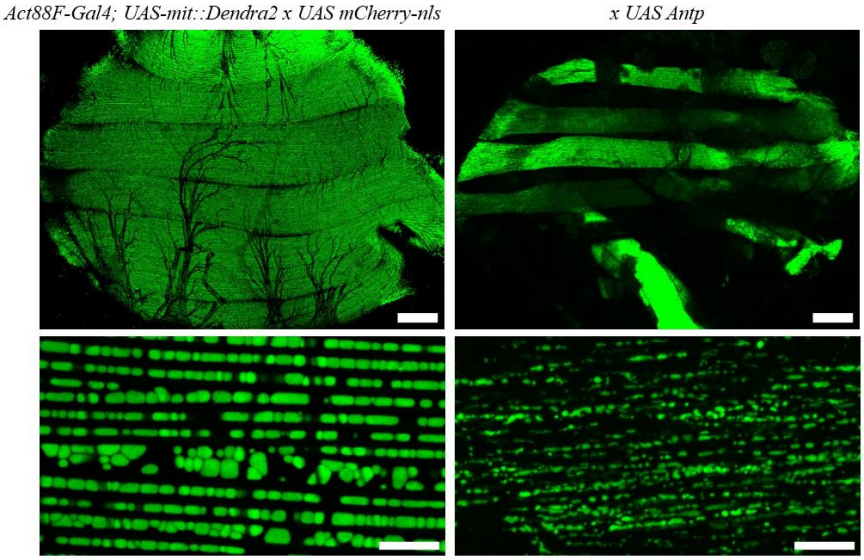

Figure 27. Antp overexpression leads to a parallel muscle mitochondria network organisation. Live confocal section of female, 2-day-old adult flight muscle mitochondria, labelled with mit::Dendra2, driven by *Act88F*-Gal4. Wild-type (right) and Antp overexpression (left) conditions are shown. The scale bar is 10 µm for large sections and 100 µm for zoomed views. My unpublished observations.

This would make sense in light of our observation that Antp seems to be expressed in adult DFMs and in the jump muscle. Even though many studies attributed to Antp the role in the development of the second pairs of legs, we believe that this function could be reserved only for the leg ectoderm. One interesting idea could be to examine whether the *Ns* mutant flies, exhibiting antenna-to-leg transformation (Gehring, 1966), contain muscles in their ectopic legs.

While we do not fully understand what the exact nature of muscle transformation upon Antp overexpression is, we believe that Antp is involved in the choice between the fibrillar and tubular fibre fate, by using its alternative P2 promoter, allowing for a precise downregulation of Antp at the critical timepoint of the decision between the fibre types. Antp and Ubx were both shown to repress Salm, the master regulator of the fibre fate choice (Choo et al., 2011; Galant et al., 2002; Roy and Raghavan, 1997; Wagner-Bernholz et al., 1991). We showed that all Hox genes have the capacity to repress Salm in developing flight muscles (see Fig. S9), in which Salm repression is a Hox generic function (Saurin et al., 2018). We thus believe that Antp clearance in flight myoblasts is necessary to allow for Salm expression. In support of this, while analysing the publicly available single-cell data of the adult fly (H. Li et al., 2022), we noticed that all adult muscles contain transcripts of *Hox* genes, except the flight muscles (**Fig. 28**). We

thus believe that *Hox* genes play a much greater role in the diversification of adult muscles than is currently appreciated.

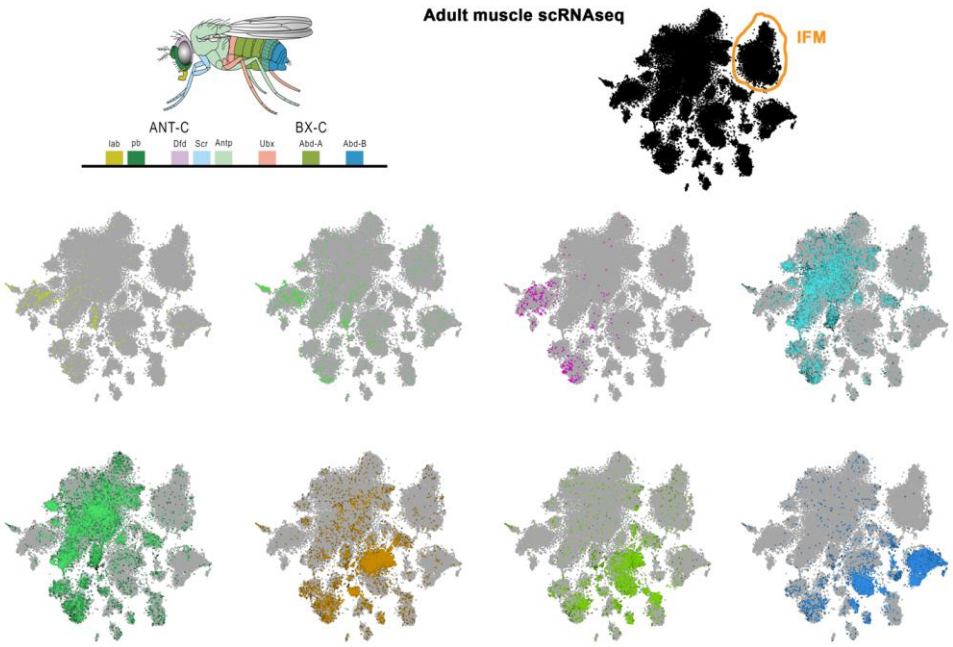

Figure 28. *Hox* gene expression in adult musculature at the single-cell level. Schematic representation of clusters of adult muscles, where the expression of each *Hox* gene is colour coded. Data analysed by A. Saurin, unpublished observation.

In summary, we propose a model **(Fig. 29)** where Antp regulates the specification of AMPs in the thorax, presumably via Notch regulation. After AMP specification, Antp maintains wing disc-associated myoblasts in an undifferentiated state during their proliferation. The decrease of Antp expression during myoblast fusion allows for flight myoblast differentiation and the acquisition of the fibrillar fibre fate, via Salm expression.

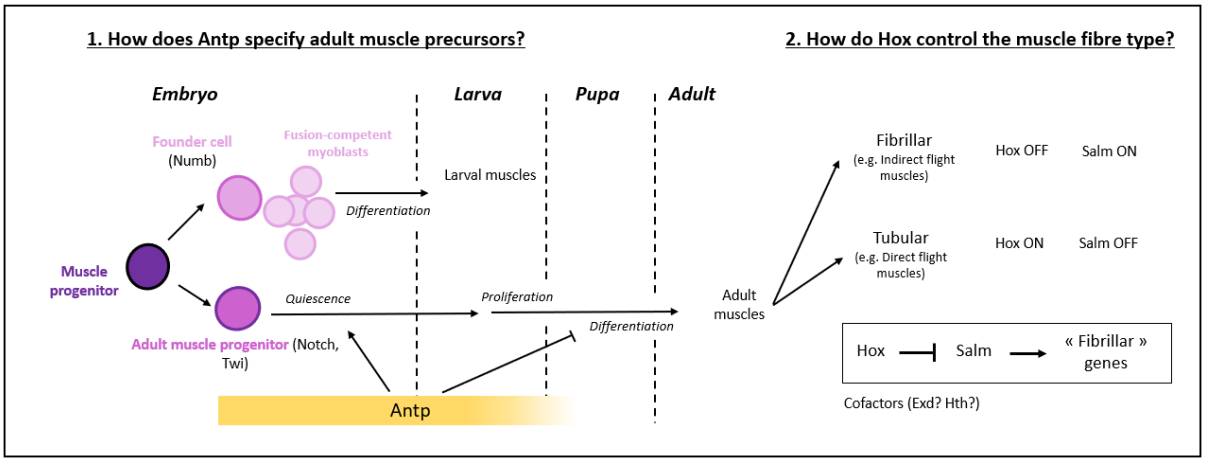

Figure 29. Model of Antp function during flight myogenesis.

In conclusion, this study allowed to re-evaluate the role Hox play in the regulation of adult thoracic muscle development and opens a Pandora's box of possibilities to test, to further elucidate the role Hox play in adult myogenesis.

Supplementary data

Supplementary data article *M1BP* is an essential transcriptional activator of oxidative metabolism during Drosophila development

Supplementary Information

Supplementary Figures

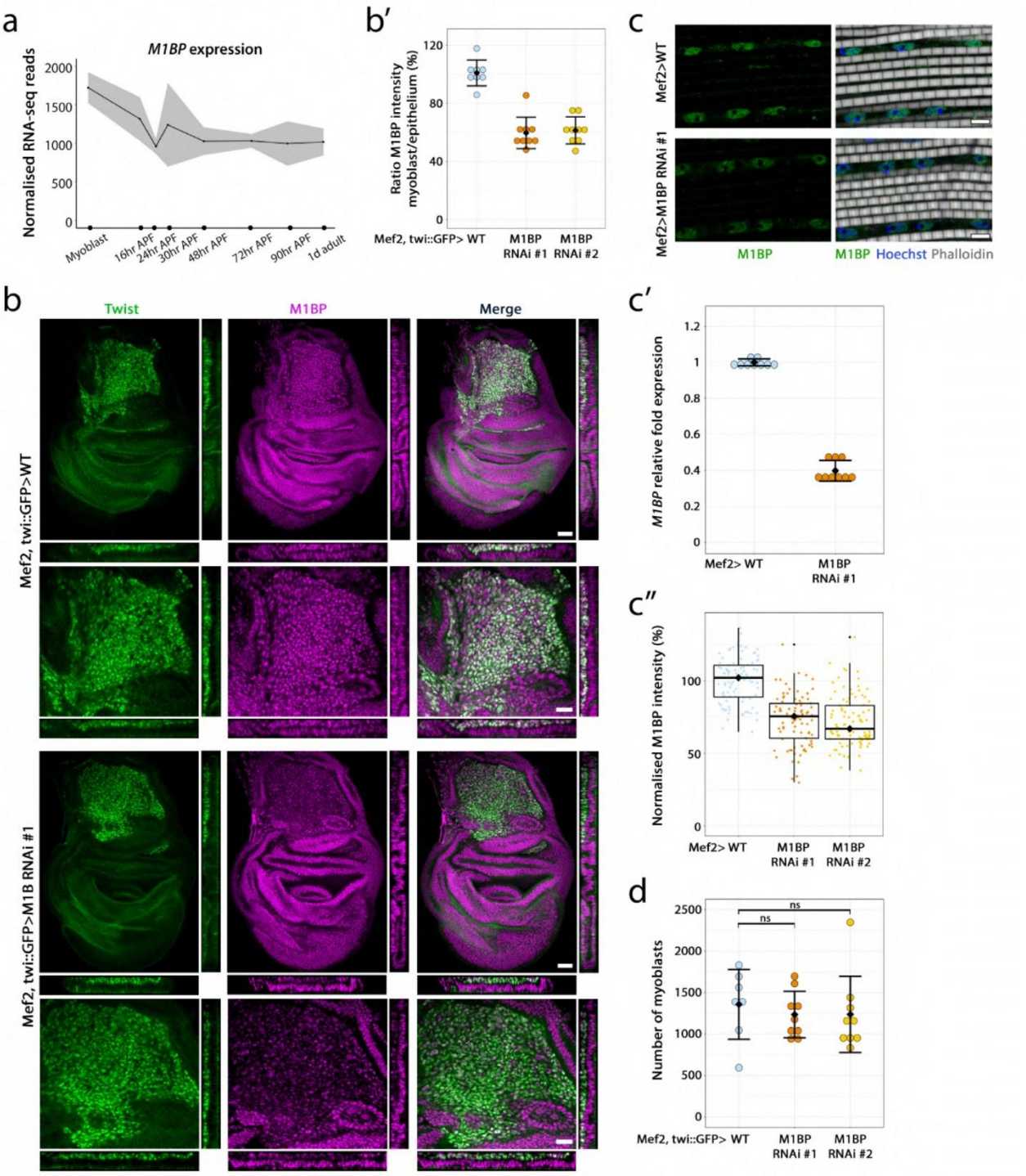

Supplementary Figure 1. M1BP-RNAi efficiently decreases M1BP protein levels during myogenesis

(a) *M1BP* mRNA expression levels during myogenesis. Mean and standard deviation are represented, data analysed from[7]. **(b)** Confocal sections of 0 h APF wild-type (Top) and *M1BP*-depleted (Bottom) wing discs stained with anti-M1BP antibody and anti-GFP to visualise myoblasts, labelled with a twist-GFP transgene. For each section, an enlarged view of the myoblast (GFP-positive) area and orthogonal views are represented. Scale bars correspond to 50 µm for large views and 20 µm for zoomed, bottom views. **(b′)** (Top) Quantification of M1BP intensity represented as a ratio of M1BP intensity in the myoblast area

compared to the epithelial area. The mean and standard deviation are shown. Each dot represents a value from one disc (n_{WT} = 9, $n_{\#1}$ = 8 and $n_{\#2}$ = 9 discs from at least 5 animals). **(c)** Confocal sections of WT (left) and M1BP-depleted (right) female adult DLM stained with an anti-M1BP antibody, phalloidin to visualise actin and Hoechst to stain nuclei. Scale bar represents 5µm. **(c')** Relative fold expression of *M1BP* mRNA levels assessed by quantitative RT-PCR in the WT and *M1BP* RNAi condition driven by *Mef-GAL4*. Mean and standard deviation are represented where each point represents a value from a single technical replicate (*n* = 9 replicates for both genotypes over three independent biological replicates). **(c'')** The intensity of M1BP staining is represented in boxplots (median and quartiles) with whiskers (minimum to maximum), where each point represents a value of a single nucleus (n_{WT} = 93, $n_{\#1}$ = 89 and $n_{\#2}$ = 101 nuclei from at least 3 animals). **(d)** Quantification of the number of myoblasts. The mean and standard deviation are shown. Each dot represents a value from one disc (n_{WT} = 7, $n_{\#1}$ = 9 and $n_{\#2}$ = 9 discs from at least 5 animals). After applying Shapiro-Wilk test for normality an unpaired, two-sided Student's-test was applied (p-values = 0.52 and 0.6). Source data are provided as a Source Data File.

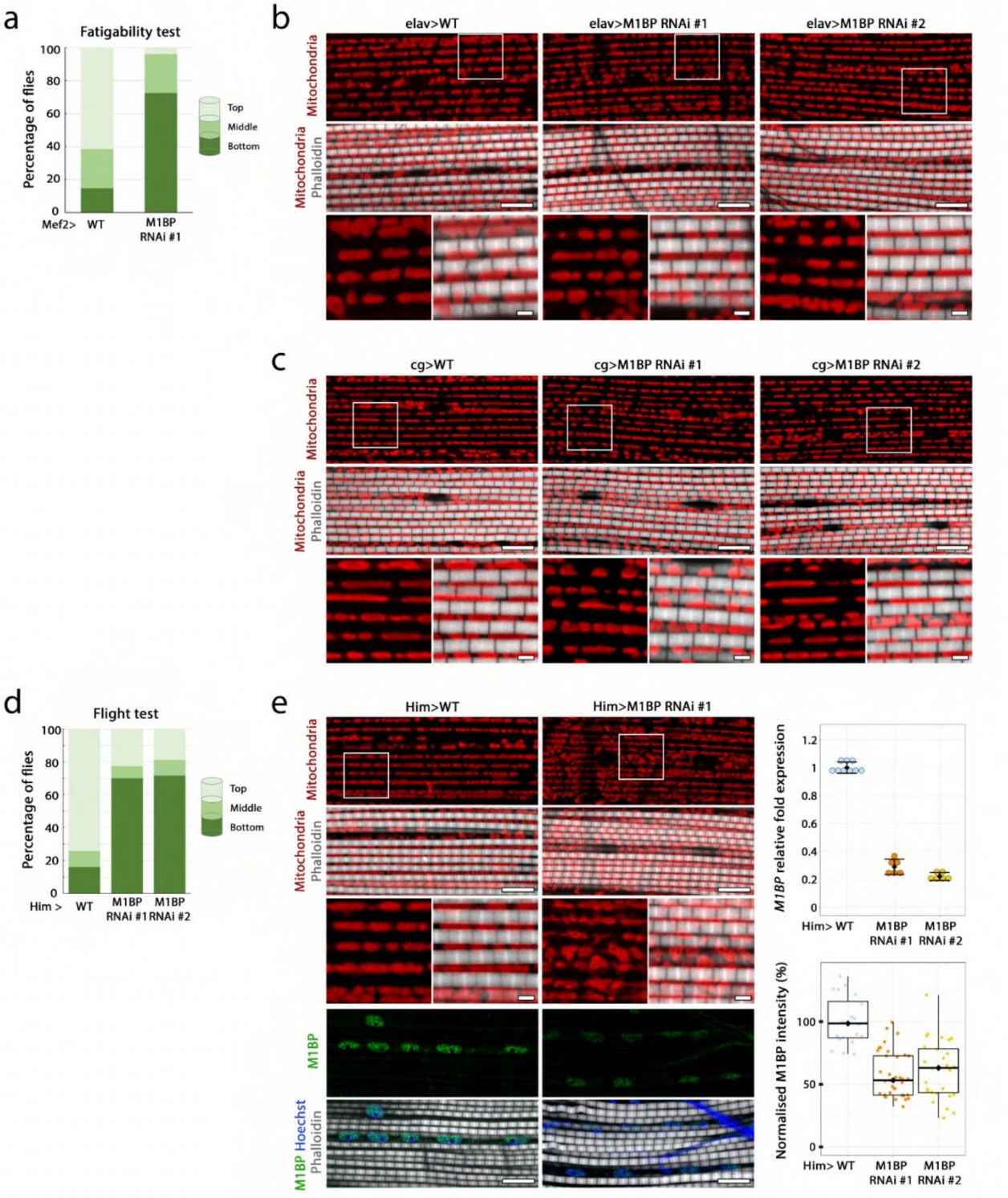

Supplementary Figure 2. Mitochondrial phenotypes observed upon M1BP KD are specific to its expression in the flight muscle.

(a) Flight muscle fatigability was scored as a percentage of male flies (Mef2>WT and Mef2>*M1BP-RNAi* #1) landing on each segment of the column. Represented is the mean of two independent biological replicates (n_{WT}= 204, $n_{\#1}$ = 135 flies). **(b)** Confocal sections of 2-days-old female adult wild-type (left) and *M1BP*-depleted (right) DLM mitochondria, driven by a neuron-specific *elav-GAL4* driver. Throughout the whole figure, for each section, an enlarged view of the individual mitochondrion (depicted by a white rectangle) is

shown. Myofibrils are stained with phalloidin (grey) and mitochondria with an anti-ATP5A antibody (red). Scale bars represent 10 µm for top images and 2 µm for zoomed, bottom views. **(c)** Identical staining and scale bars as **(b)**, with *M1BP-RNAi* being driven by a fat body-specific, *cg-GAL4* driver. **(d)** Flight ability was scored as a percentage of male flies landing on each segment of the column. Tested flies are Him>WT and Him>*M1BP* RNAi. Represented is the mean of three independent biological replicates (n_{WT} = 180, $n_{\#1}$ = 240 and $n_{\#2}$ = 210 flies). **(e)** (Left) Confocal sections of WT (left) and *M1BP*-depleted (right) female adult DLM, driven by *Him-GAL4*. Myofibrils were stained with phalloidin (grey) and mitochondria with an anti-ATP5A antibody (red). Scale bar is 10 µm for top and 2 µm for zoomed, bottom views. M1BP expression in adult female DLM was visualised with anti-M1BP antibody (green), nuclei stained with Hoechst (blue) and myofibrils with phalloidin (grey). Scale bar is 10 µm. (Right) Relative fold expression of *M1BP* mRNA levels assessed by quantitative RT-PCR in the WT and *M1BP* RNAi condition driven by *Him-GAL4*. Mean and standard deviation are represented where each point represents a value from a single technical replicate (*n* (WT) = 9 and *n* (both RNAi) = 6 technical replicates over two independent biological replicates). The intensity of anti-M1BP immunostaining is represented in boxplots (median and quartiles) with whiskers (minimum to maximum), where each point represents a value of a single nucleus, *n*= 5 animals per genotype. Source data are provided as a Source Data File.

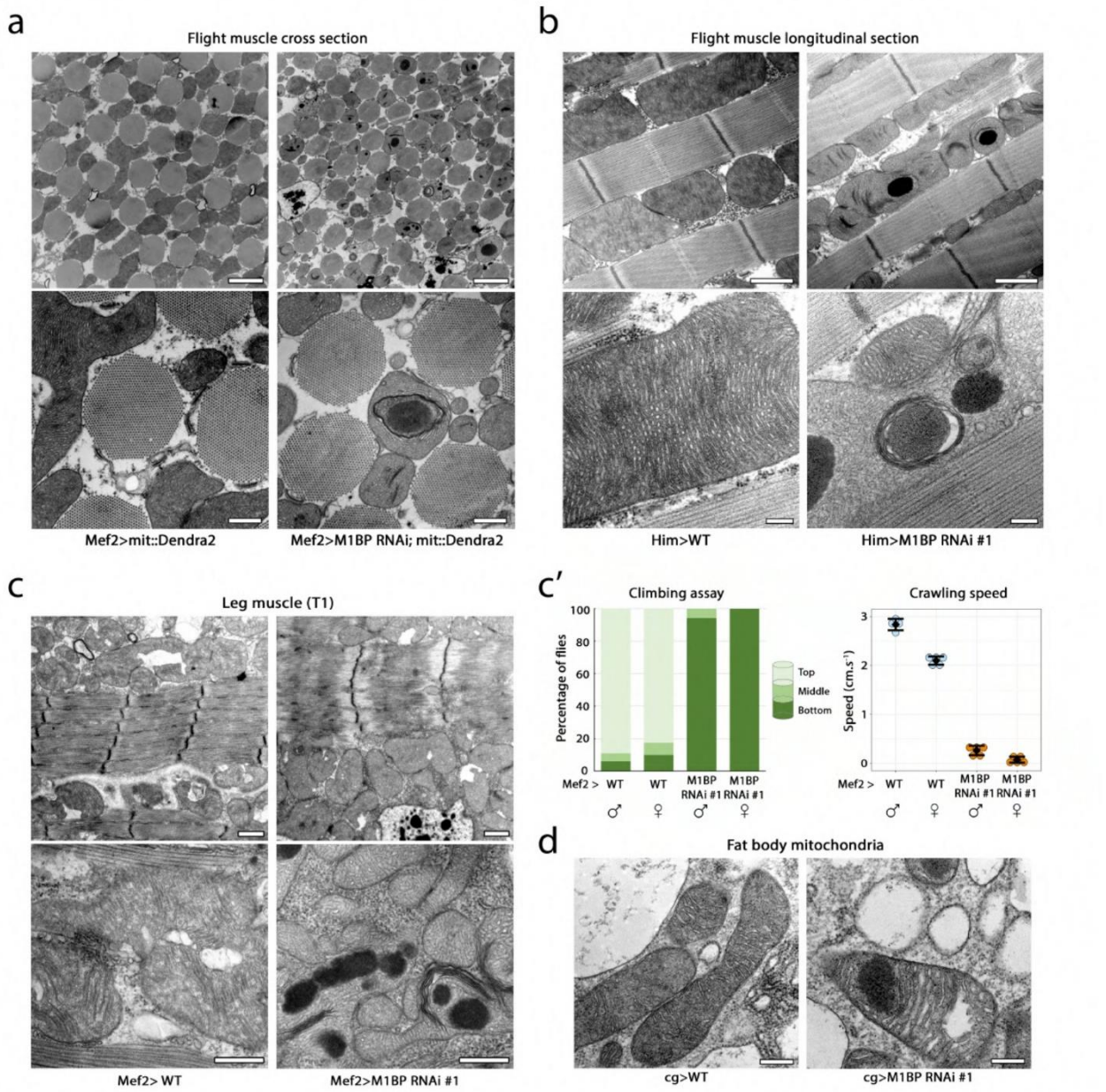

Supplementary Figure 3. M1BP inhibition leads to ultrastructural defects in muscle and fat body mitochondria

(a) Transmission electron microscopy micrographs of male adult WT (left) and *M1BP*-depleted (right) DLM mitochondria using *Mef2-GAL4* driver, cut in cross sections. Scale bars represent 2 µm for top images and 500 nm for larger bottom views. **(b)** Transmission electron microscopy micrographs of male adult WT (left) and *M1BP*-depleted (right) DLM mitochondria driven by *Him-GAL4*. Scale bars represent 1 µm for top images and 200 nm for larger bottom views. **(c)** Transmission electron microscopy micrographs of male adult WT (left) and *M1BP*-depleted (right) mitochondria in T1 adult coxa leg muscles, driven by *Mef2-GAL4*. Scale bars represent 1 µm for top images and 500 nm for larger bottom views. **(c')** Negative geotaxis climbing ability was scored as the mean percentage of flies present in each section of the column (*n* = 50 flies for each condition examined from five biological replicates). Crawling speed was quantified as the distance travelled during a fixed time, where each dot corresponds to a mean speed value of a biological

replicate (*n* = 5 flies for each condition examined from five biological replicates). Error bars represent standard deviation of the mean. **(d)** Transmission electron microscopy micrographs of 3rd instar larval fat body mitochondria in WT (top) or *M1BP* KD (bottom) condition, driven by *cg-GAL4*. Scale bar is 250 nm. Source data are provided as a Source Data File.

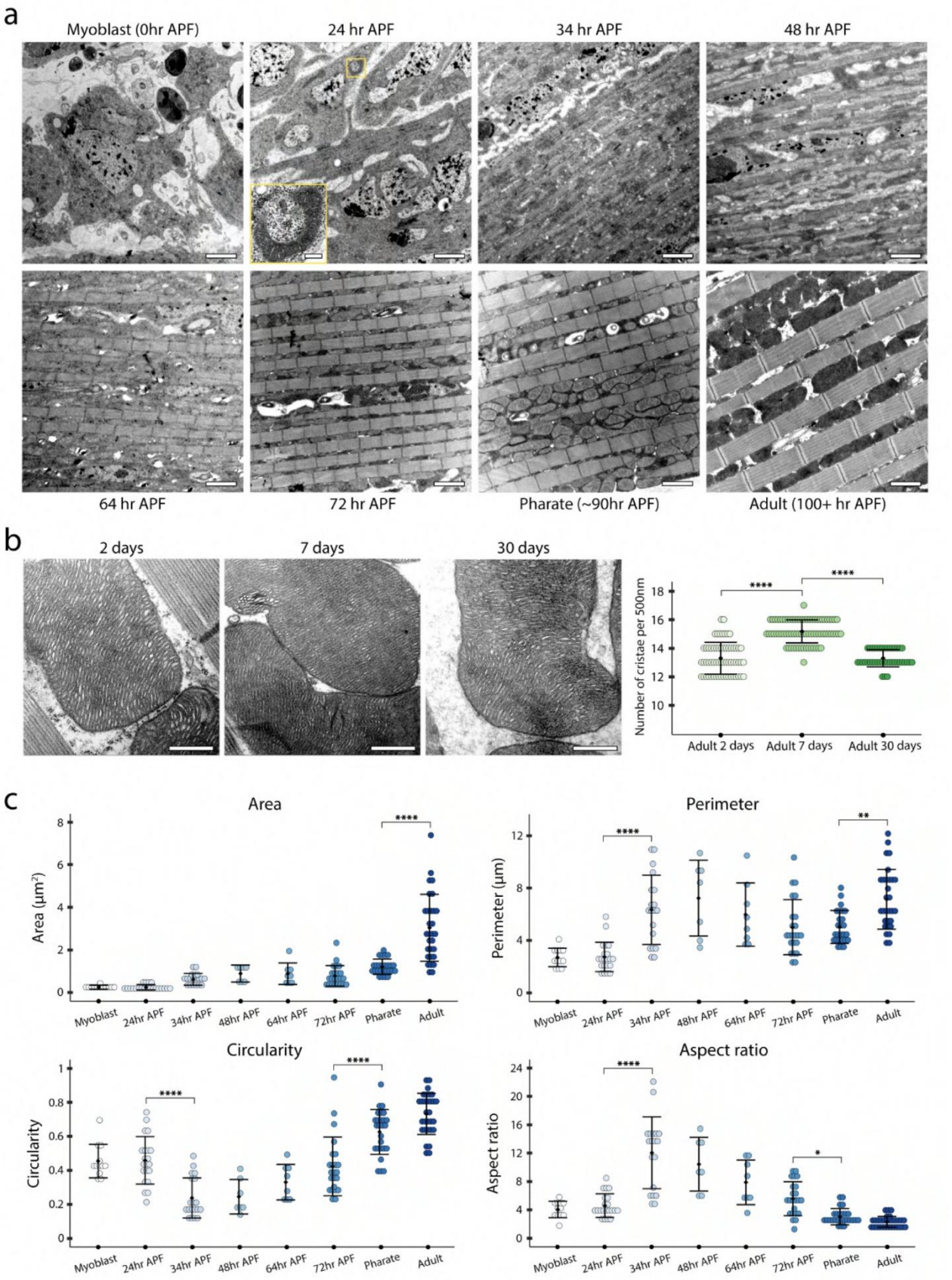

Supplementary Figure 4. Large mitochondrial cristae biogenesis occurs during flight muscle development

(a) Transmission electron microscopy micrographs of wild-type flight muscle development. Scale bars correspond to 2 µm. For 24 h APF a zoomed view of a single mitochondrion, depicted by a yellow rectangle is shown (scale bar is 200 nm). **(b)** Transmission electron microscopy micrographs of wild-type flight

muscles at 2, 7 and 30 days of adult development. Scale bar is 500 nm. The quantification of the number of mitochondrial cristae per length unit (500 nm) is shown. Mean and standard deviation are shown with each point representing a value of a single mitochondrion ($n_{2\ days}$ = 44, $n_{7\ days}$ = 46 and $n_{30\ days}$ = 28 mitochondria). For statistical analysis, one-way analysis of variance (ANOVA) was performed, followed by Tukey's test for multiple mean comparisons, p-values (2 days vs 7 days = 0 and 7 days vs 30 days = 0). **(c)** Quantification of mitochondrial parameters during flight muscle development. Mean and standard deviation are shown with each point representing a value of a single mitochondrion (for all parameters *n* (Myo) = 12, *n* (24 h) = 21, *n* (34 h) = 19, *n* (48 h) = 7, *n* (64 h) = 8, *n* (72 h) = 23, *n* (pharate) = 26 and *n* (adult) = 30 mitochondria). For statistical analysis, one-way analysis of variance (ANOVA) was performed, followed by Tukey's test for multiple mean comparisons. For area p-values (Myo vs 24 h = 1, 24 h vs 34 h = 0.8, 34 h vs 48 h = 1, 48 h vs 64 h = 1, 64 h vs 72 h = 1, 72 h vs pharate = 0.53 and pharate vs adult = 0). For perimeter p-values (Myo vs 24 h = 1, 24 h vs 34 h = 1.3*10^-6, 34 h vs 48 h = 0.97, 48 h vs 64 h = 0.92, 64 h vs 72 h = 0.93, 72 h vs pharate = 1 and pharate vs adult = 0.0026). For circularity p-values (Myo vs 24 h = 1, 24 h vs 34 h = 1.3*10^-5, 34 h vs 48 h = 1, 48 h vs 64 h = 0.91, 64 h vs 72 h = 0.68, 72 h vs pharate = 0 and pharate vs adult = 0.06). For aspect ratio p-values (Myo vs 24 h = 1, 24 h vs 34 h = 0, 34 h vs 48 h = 0.83, 48 h vs 64 h = 0.5, 64 h vs 72 h = 0.34, 72 h vs pharate = 0.01 and pharate vs adult = 0.96). Source data are provided as a Source Data File.

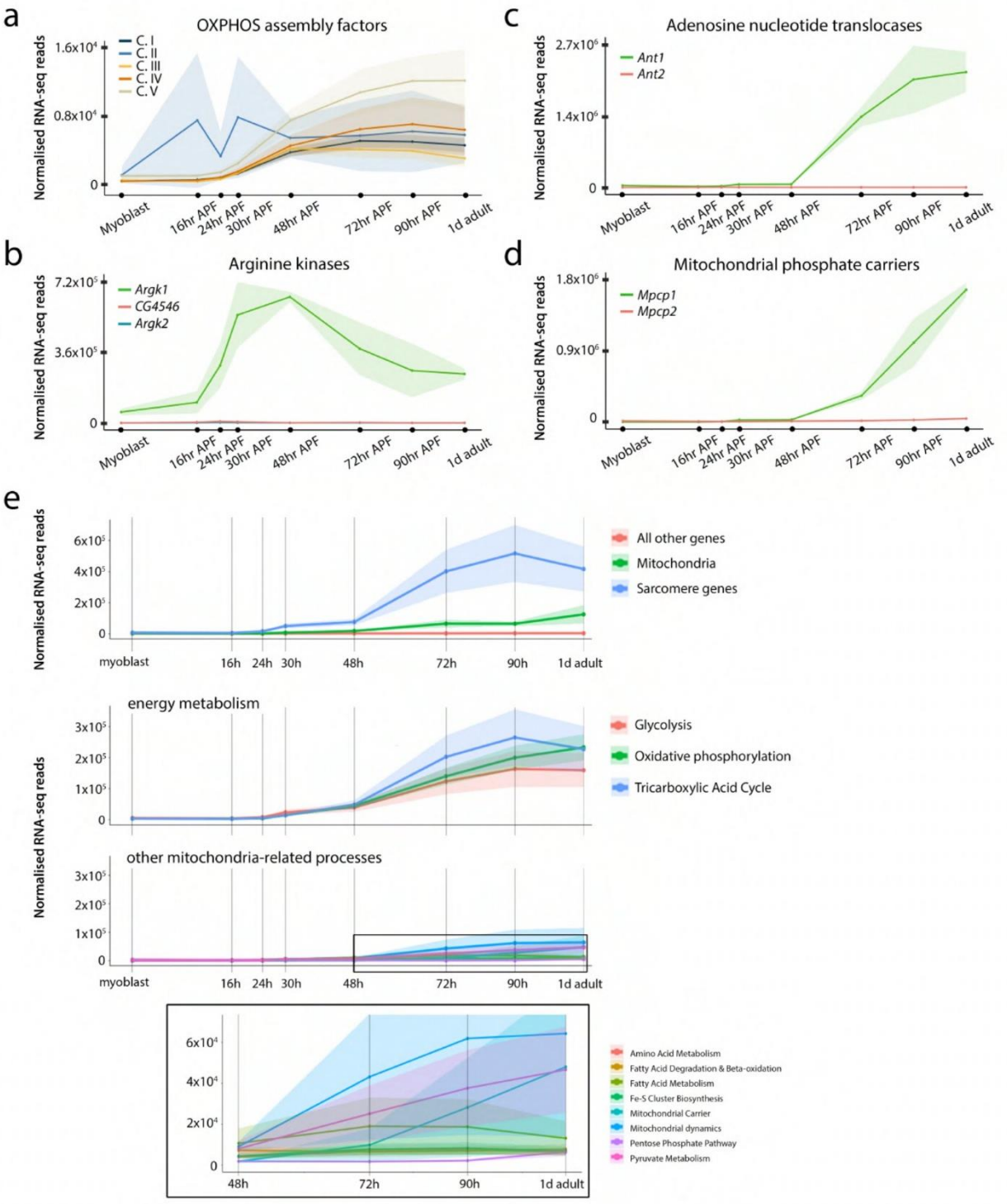

Supplementary Figure 5. Large-scale mitochondrial and sarcomeric gene transcriptional upregulation occurs during flight muscle development

(a) Transcriptional profile during flight muscle development of genes encoding assembly factors of the mitochondrial respiratory chain complexes. These data are the same as those presented in Figure 2c but with the addition of Complex II assembly factor Sirup that was omitted from the main data due to its oscillatory expression during early stages of pupation, which is likely a sequencing artefact. The solid line represents the normalised mean of sequenced counts of all assembly factors of a given respiratory complex

with shaded areas representing the standard error of the mean. **(b, c, d)** The transcriptional profile during flight muscle development of genes encoding arginine kinases **(b)** adenosine nucleotide translocases **(c)**, and mitochondrial phosphate carriers **(d)**. In all cases the solid lines represent the normalised mean of sequenced counts of a given gene with shaded areas representing the standard deviation of the mean. **(e)** Transcriptional profile of sarcomeric, mitochondrial and all other genes during IFM development. For mitochondrial genes, the transcriptional profile of genes related to energy metabolism and other mitochondrial processes (with a zoomed view in the bottom) are represented. In all cases the solid lines represent the normalised mean of sequenced counts of a given gene with shaded areas representing the standard error of the mean. Source data are provided as a Source Data File.

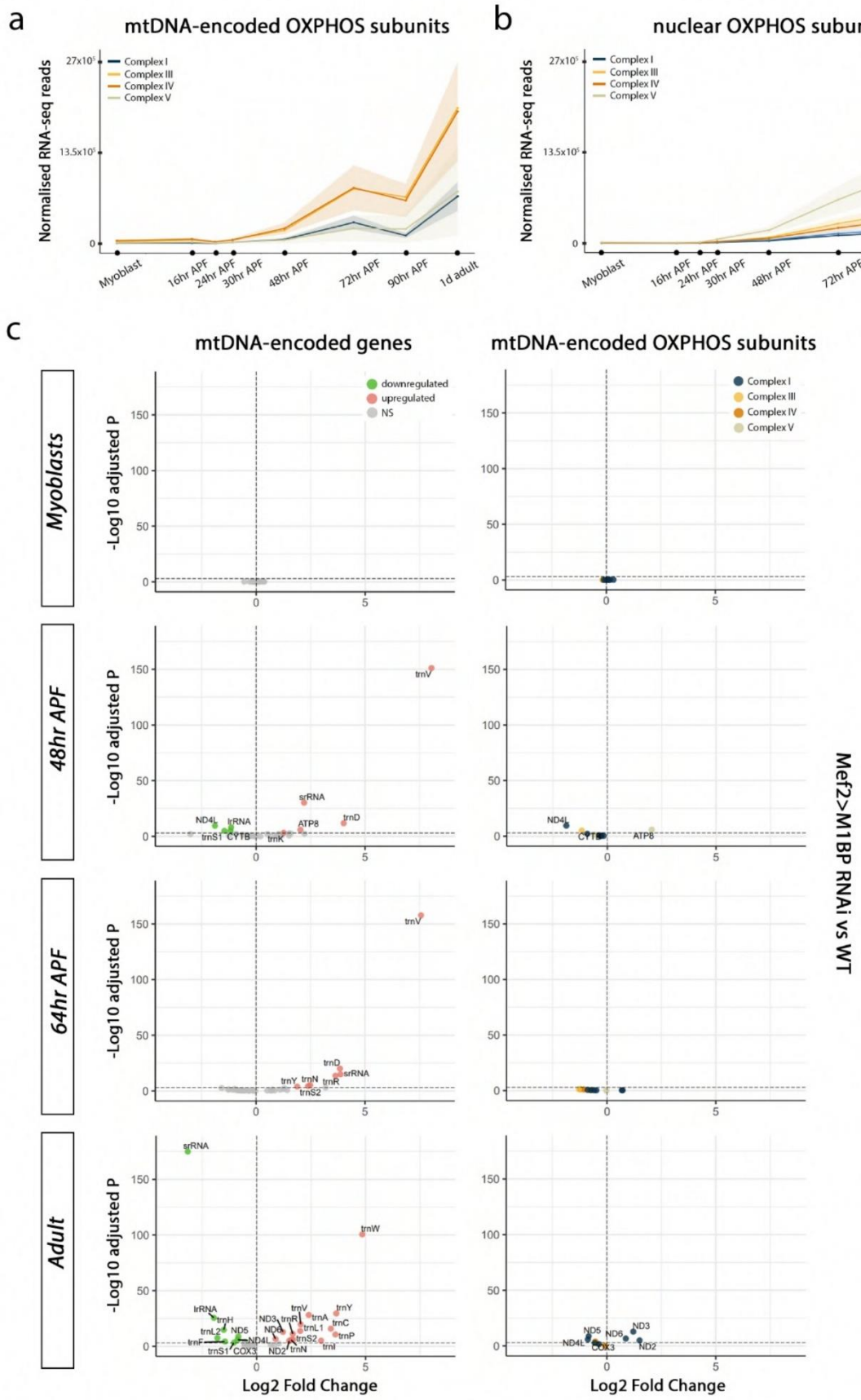

Supplementary Figure 6. M1BP does not transcriptionally regulate mtDNA-encoded OXPHOS subunits

(a,b) Transcriptional profiles using the same ordinate scale during flight muscle development of genes encoded by mtDNA **(a)** and nuclear DNA **(b)** that constitute the mitochondrial respiratory chain complexes.

The solid line represents the normalised mean sequenced counts of all subunits of a given respiratory complex with the shaded areas representing the standard error of the mean. **(c)** Volcano plots of all differentially expressed mtDNA-encoded genes (left) or only mtDNA-encoded, OXPHOS-related (right) genes between Mef2>WT and Mef>*M1BP* RNAi at time points corresponding to analyses in Figure 3. For statistical analysis, the Wald test with Benjamini-Hochberg-correction was applied.

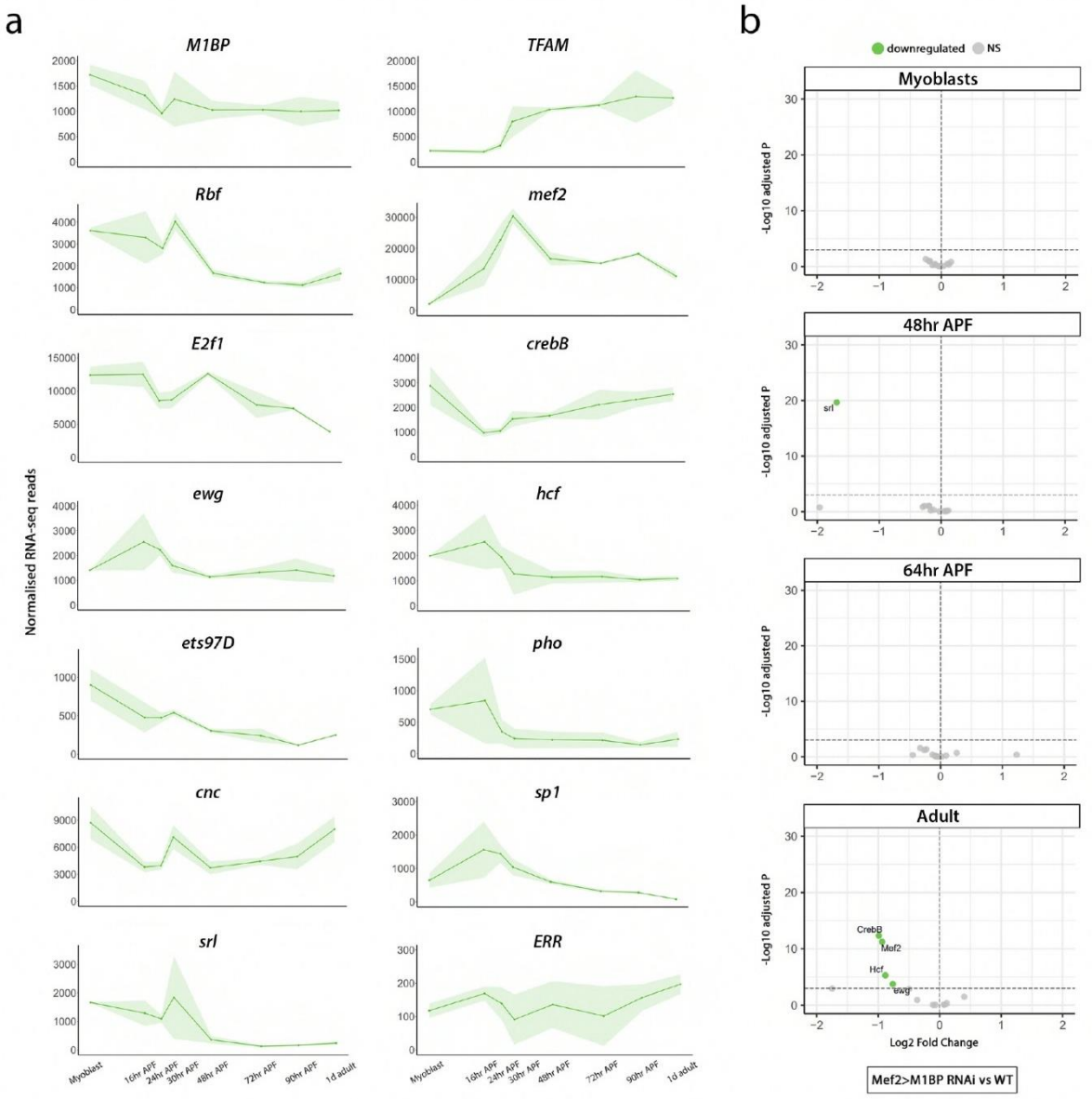

Supplementary Figure 7. M1BP does not transcriptionally regulate known OXPHOS activators

(a) Transcriptional profiles during flight muscle development of known OXPHOS transcriptional regulators. Mean and standard deviation are represented, data analysed from[7]. **(b)** Volcano plots of differential expression analysis of known OXPHOS transcriptional regulators between Mef2>WT and Mef>*M1BP* RNAi developing muscles. Significantly deregulated genes are depicted in green. For statistical analysis, the Wald test with Benjamini-Hochberg-correction was applied.

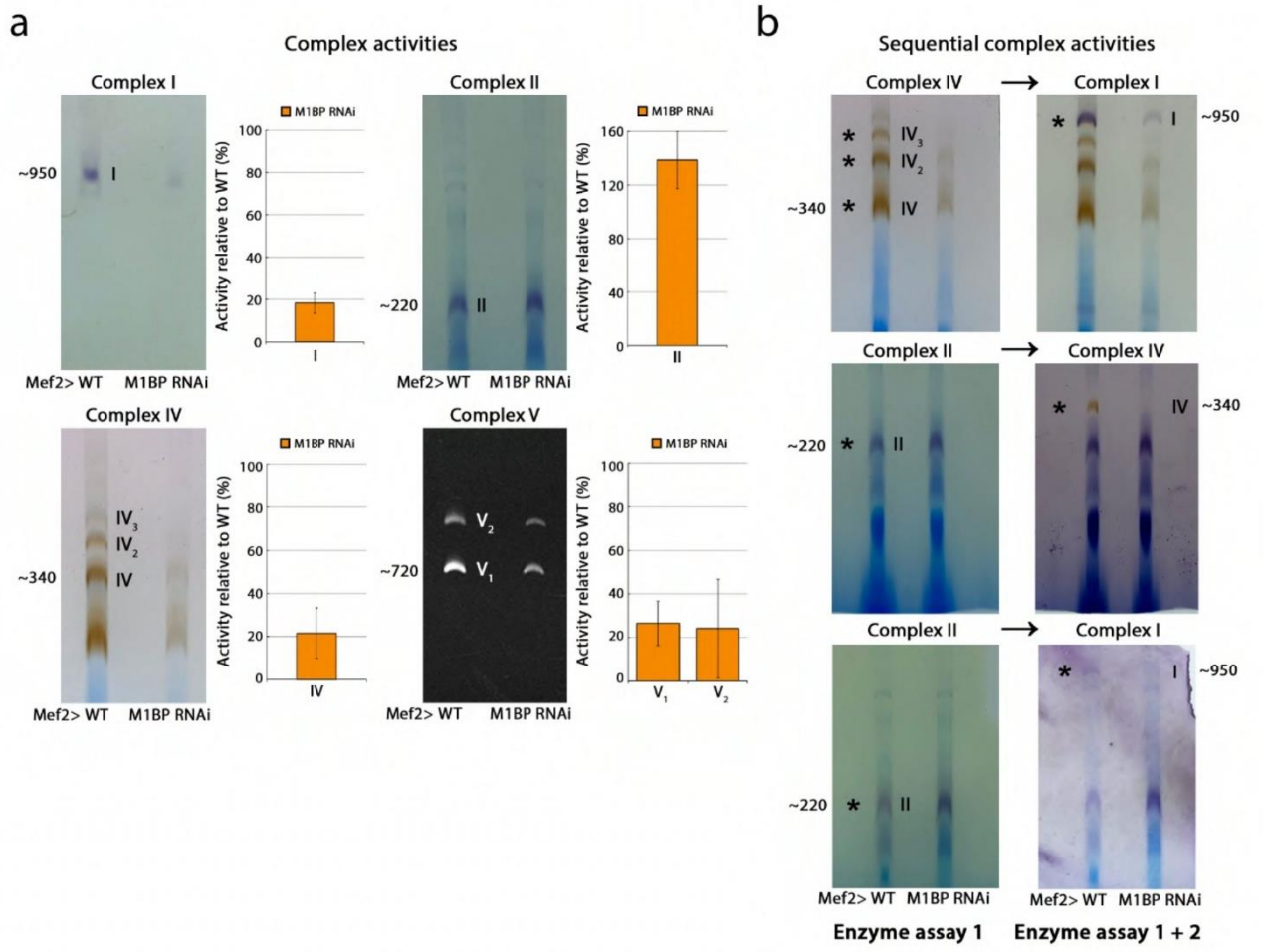

Supplementary Figure 8. OXPHOS complexes retain their enzymatic activities upon M1BP KD

(a) The activity of mitochondrial complexes upon M1BP KD was assayed following BN-PAGE separation of membrane-bound complexes. The intensity of the band representative of the complex activity after the incubation with a substrate was quantified for each complex. The intensity values are depicted as a percentage relative to the WT and represent a mean of two independent biological replicates. Approximate protein size is indicated in kDa. **(b)** The activity of mitochondrial complexes upon M1BP KD using *Mef2-GAL4* driver was assayed by BN-PAGE in a sequential manner, where the first tested activity is shown on the left, followed by the second activity test shown on the right. Approximate protein size is indicated in kDa. The experiment was performed in two independent biological replicates. Source data are provided as a Source Data File. Uncropped versions of the gels shown are provided at the end of the Supplementary Information.

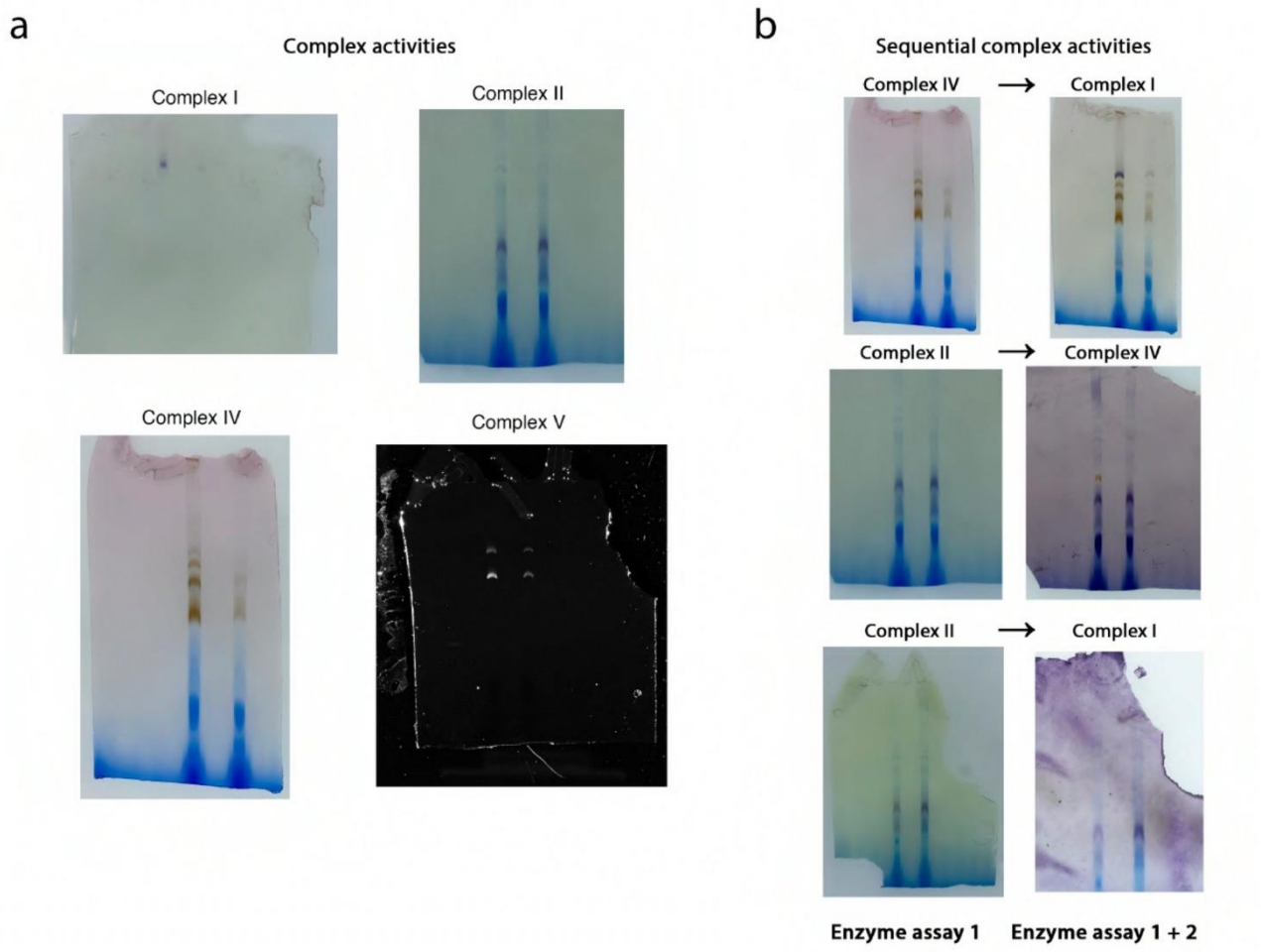

Source Data for Supplementary Figure 8.

The uncropped source data gels used in Supplementary Figure 8 are shown. The same layout as in Supplementary Figure 8 is used.

Description of Additional Supplementary Files

File Name: Supplementary Data 1
Description: Genes encoding proteins required for OXPHOS complex formation

File Name: Supplementary Data 2
Description: Differential gene expression analysis of M1BP RNAi in myoblasts

File Name: Supplementary Data 3
Description: Differential gene expression analysis of M1BP RNAi in 48 h APF DLMs

File Name: Supplementary Data 4
Description: Differential gene expression analysis of M1BP RNAi in 64 h APF DLMs

File Name: Supplementary Data 5
Description: Differential gene expression analysis of M1BP RNAi in adult DLMs

File Name: Supplementary Data 6
Description: Differential gene expression of mitochondrial DNA-encoded genes

File Name: Supplementary Data 7
Description: Identification of transcription factor binding sites in promoters of nuclear-encoded OXPHOS complex components

File Name: Supplementary Data 8
Description: Differential gene expression of genes involved in a cellular proteotoxic response

File Name: Supplementary Movie 1
Description: The inner mitochondrial membrane encompasses and isolates an aggregate. Tomographic reconstruction of a mitochondrial aggregate taken from dual-axis tomographic serial sections. Tomogram was joined and segmented with surface rendering showing the aggregate in gold and the encompassing inner mitochondrial membrane in cyan. Source data are provided as a Source Data File

Supplementary data article *Antp* orchestrates Drosophila adult flight muscle development

ScienceAdvances
AAAS

Supplementary Materials for

The Hox protein Antennapedia orchestrates *Drosophila* adult flight muscle development

Gabriela Poliacikova[1], Aïcha Aouane[1], Nathalie Caruso[1], Nicolas Brouilly[1], Corinne Maurel-Zaffran[1], Yacine Graba[1], Andrew J. Saurin[1]*

*Corresponding author. Email: andrew.saurin@univ-amu.fr

This PDF file includes:

Figs. S1 to S9
Legend for Movies S1 to S3
Legend for Data S1 to S4

Other Supplementary Materials for this manuscript include the following:

Movies S1 to S3
Data S1 to S4

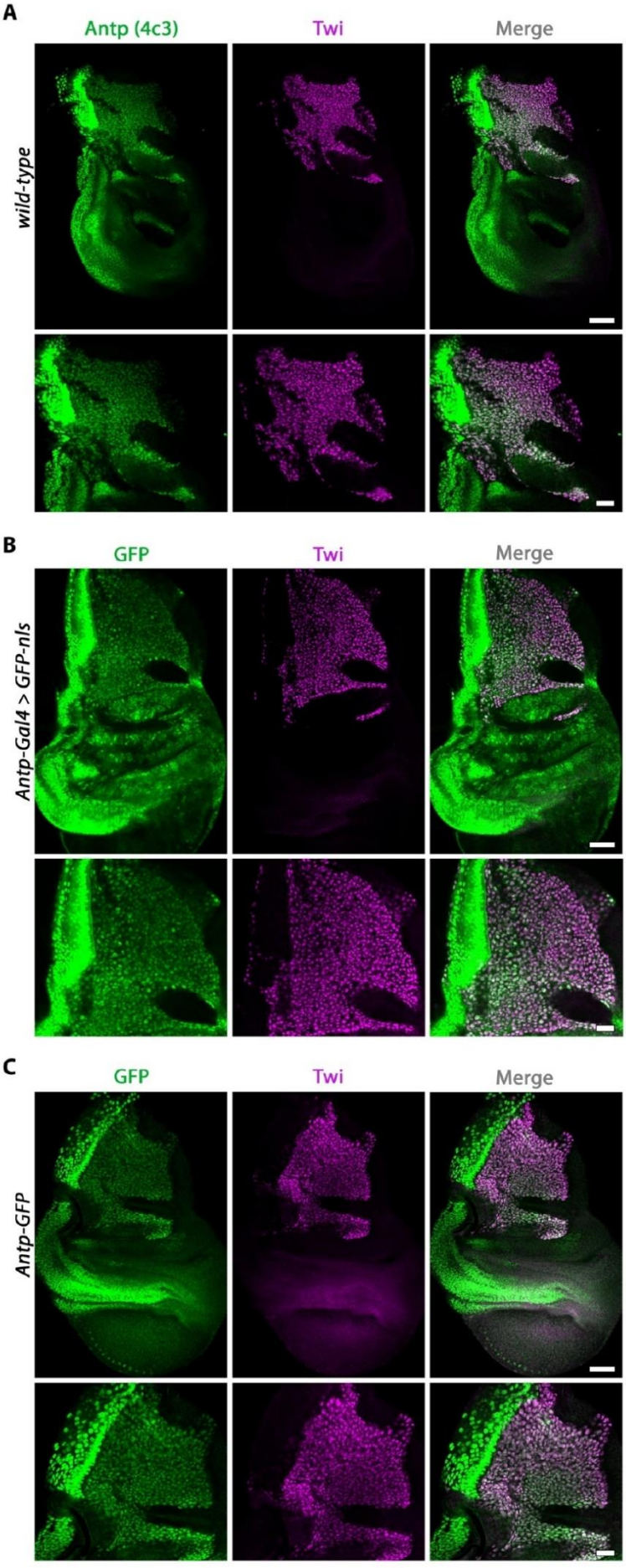
A
Antp (4c3)
Twi
Merge
wild-type
B
GFP
Twi
Merge
Antp-Gal4 > GFP-nls
C
GFP
Twi
Merge
Antp-GFP

Fig. S1. Antp is expressed in larval flight muscle myoblasts.

(A) Confocal sections of wild-type wing discs at the L3 wandering stage, stained with antibodies against Antp (4c3) and Twi. **(B)** Confocal sections of 0 h APF wing discs expressing *UAS-GFP nls* driven by *Antp*-Gal4, stained with antibodies against GFP and Twi. **(C)** Confocal sections of 0 h APF wing discs expressing *Antp-GFP*, stained with antibodies against GFP and Twi. The scale bar is 50 μm for the top and 20 μm for the bottom views in all panels.

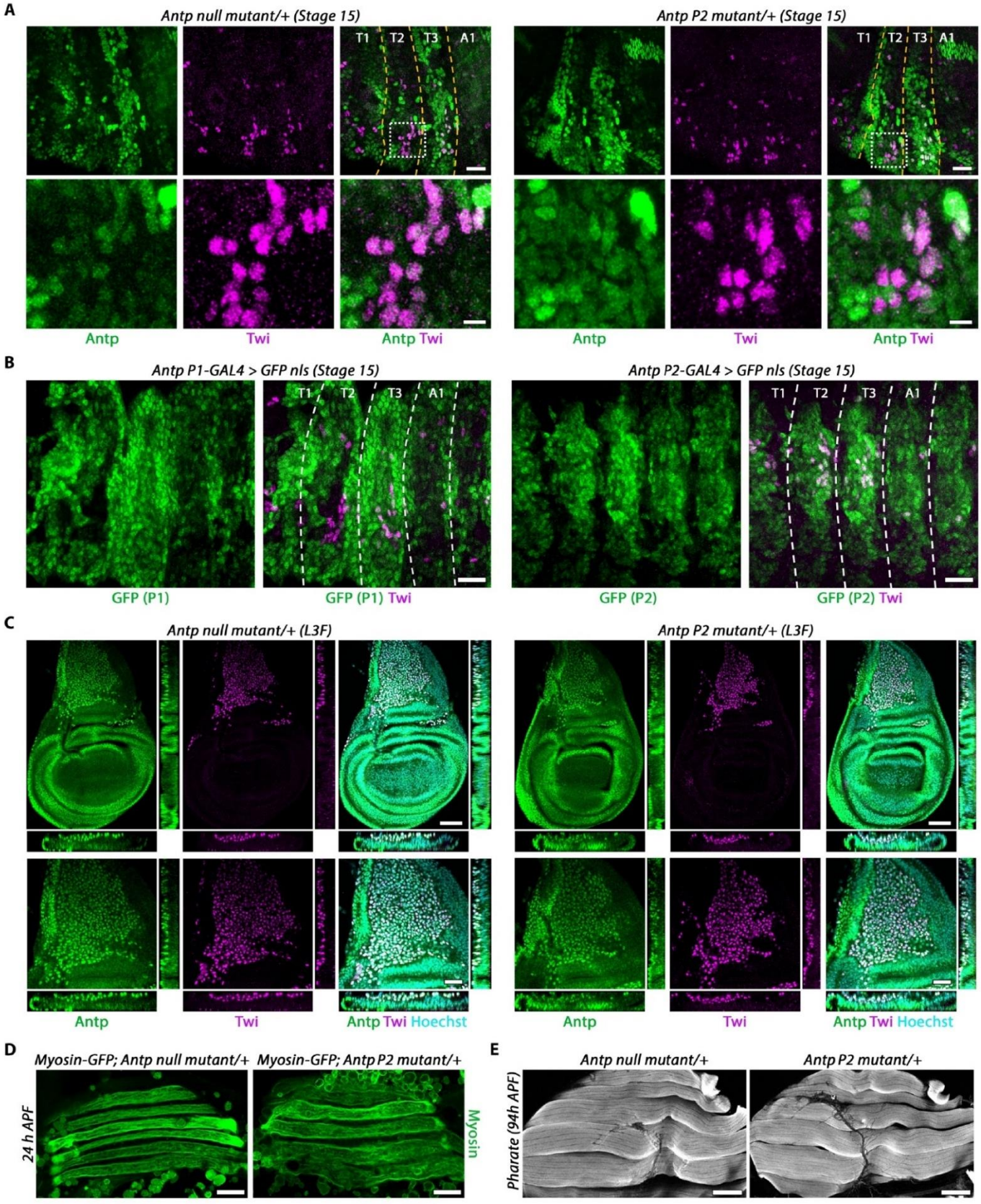
A
Antp null mutant/+ (Stage 15)
Antp P2 mutant/+ (Stage 15)
T1
T2
T3
A1
Antp
Twi
Antp Twi
B
Antp P1-GAL4 > GFP nls (Stage 15)
Antp P2-GAL4 > GFP nls (Stage 15)
GFP (P1)
GFP (P1) Twi
GFP (P2)
GFP (P2) Twi
C
Antp null mutant/+ (L3F)
Antp P2 mutant/+ (L3F)
Antp Twi Hoechst
D
Myosin-GFP; Antp null mutant/+
Myosin-GFP; Antp P2 mutant/+
24 h APF
Myosin
E
Antp null mutant/+
Antp P2 mutant/+
Pharate (94h APF)

Fig. S2. Heterozygous *Antp* mutations do not perturb flight muscle development.

(A) Confocal sections of stage 15 embryos labelled with antibodies against Antp and Twi. Genotypes are heterozygous $Antp^{ns\text{-}rvc1}$ (null mutation) (Left) and heterozygous $Antp^{s1}$ (P2 mutation) (Right). The scale bar is 20 µm for top views and 5µm for zoomed, bottom views on T2 AMPs, depicted by the white dashed square. **(B)** Confocal sections of stage 15 embryos expressing *UAS GFP-nls* driven by the *Antp P1*-Gal4 (Left) and *Antp P2*-Gal4 (Right), stained with anti-GFP and anti-Twi antibodies. The scale bar is 20µm. In (A) and (B) T1, T2, T3 depict the three thoracic segments and A1 the first abdominal segment. **(C)** Confocal sections of wing discs at the L3 feeding stage labelled with antibodies against Antp and Twi. Genotypes are identical to (A). The scale bar is 50 µm for large and 25 µm for zoomed views. **(D)** Confocal projections of 24 h APF pupal IFMs labelled with GFP to visualise myosin. Genotypes are identical to (A) with *weeP26* transgene (Myosin-GFP) added. The scale bar is 50µm. **(E)** Confocal sections of pupal IFM at the pharate stage, labelled with phalloidin. Genotypes are identical to (A). The scale bar is 100 µm.

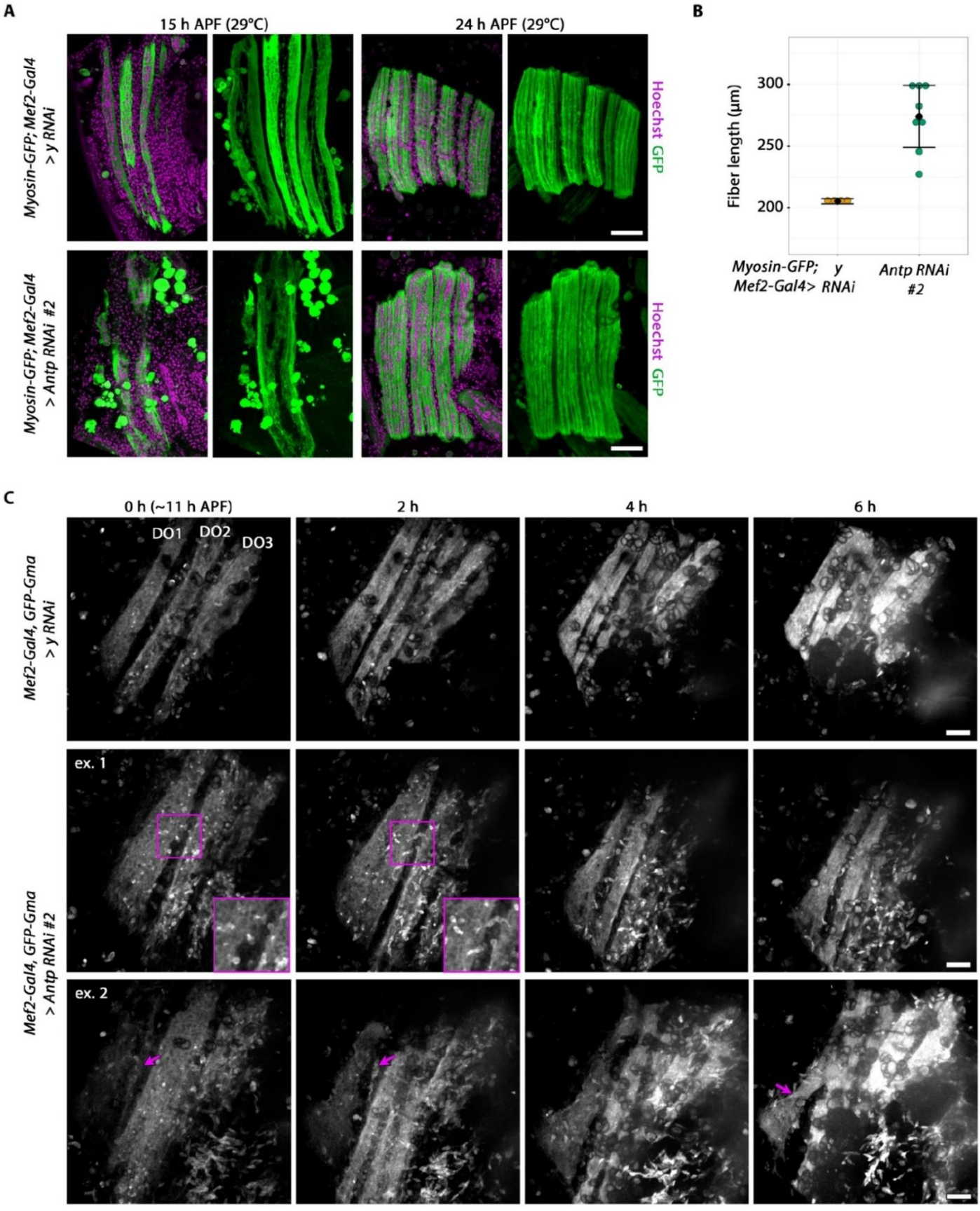
A
15 h APF (29°C)
24 h APF (29°C)
Myosin-GFP; Mef2-Gal4 > y RNAi
Myosin-GFP; Mef2-Gal4 > Antp RNAi #2
Hoechst GFP
B
Fiber length (µm)
300
250
200
Myosin-GFP; Mef2-Gal4> y RNAi
Antp RNAi #2
C
0 h (~11 h APF)
2 h
4 h
6 h
DO1
DO2
DO3
Mef2-Gal4, GFP-Gma > y RNAi
Mef2-Gal4, GFP-Gma > Antp RNAi #2
ex. 1
ex. 2

Fig. S3. *Antp* KD perturbs pupal flight muscle development.

(A) Confocal sections of 15 h and 24 h APF flight muscles expressing *weeP26; Mef2*-GAL4 driving *UAS-y RNAi* as a control (top) or *UAS-Antp RNAi #2* (bottom). Flight muscles are stained with an anti-GFP antibody to visualize myosin and Hoechst. Scale bar is 50 µm. **(B)** Quantification of flight muscle fibre length at 24 h APF, genotypes are identical to (A). Mean and standard deviation are shown, each dot represents a value from one animal ($n_{WT} = 4$, $n_{\#2} = 9$ animals). **(C)** Spinning disc, timecourse sections of developing pupal flight muscles. Genotypes are *UAS-y RNAi* (control condition) and *UAS-Antp RNAi #2* driven by the *Mef2*-GAL4 driver, with the *GPF-Gma* transgene added, labelling actin. Two examples of the RNAi condition are shown (Middle and Bottom). Zoomed views show myoblasts delayed in their fusion (ex. 1) and arrows point to detaching muscle fibres (ex. 2). DO – dorsal oblique muscles

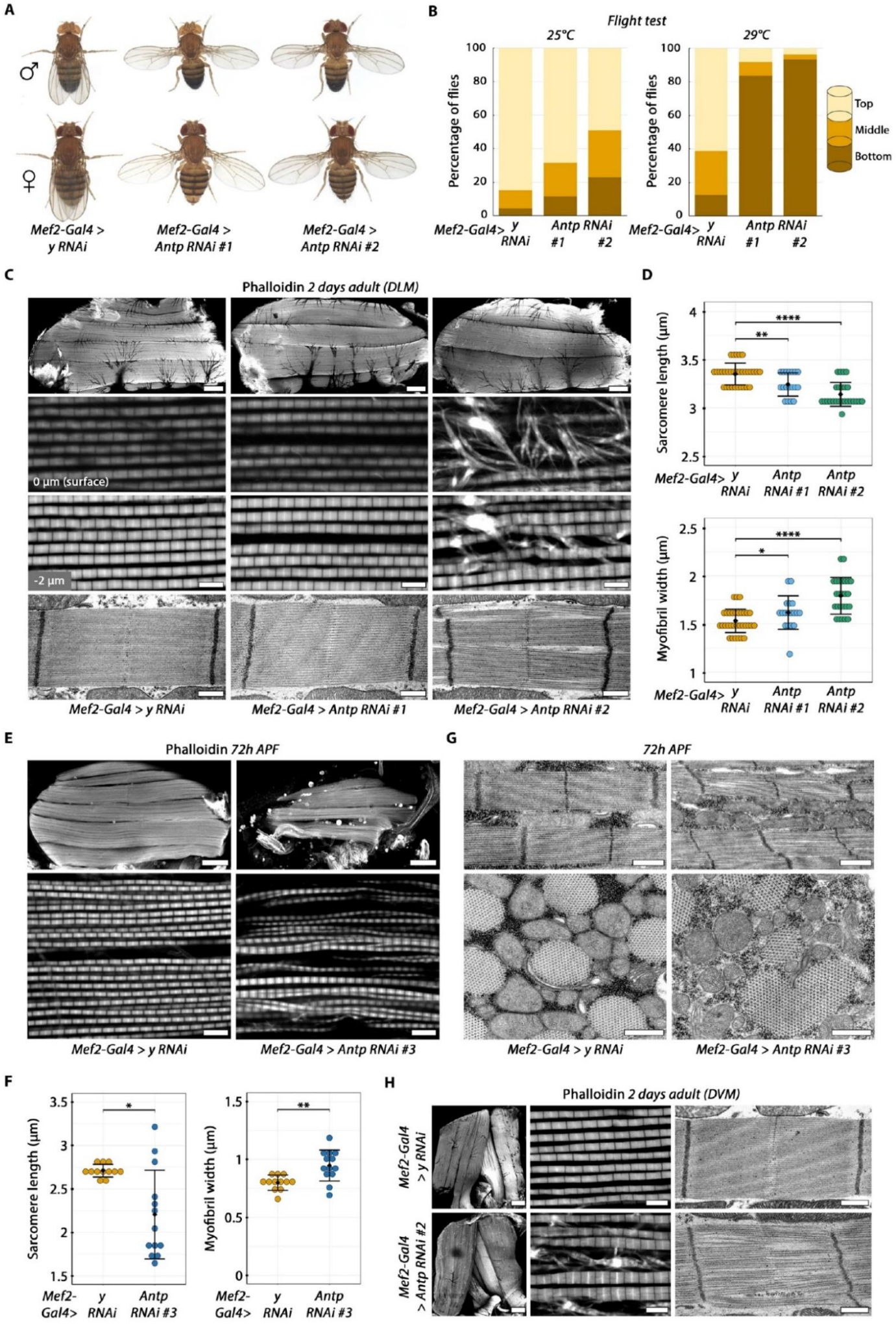
A
♂
♀
Mef2-Gal4 > y RNAi
Mef2-Gal4 > Antp RNAi #1
Mef2-Gal4 > Antp RNAi #2
B
Flight test
25°C
29°C
Percentage of flies
Top
Middle
Bottom
Mef2-Gal4> y RNAi
Antp RNAi #1
Antp RNAi #2
C
Phalloidin 2 days adult (DLM)
0 µm (surface)
-2 µm
Mef2-Gal4 > y RNAi
Mef2-Gal4 > Antp RNAi #1
Mef2-Gal4 > Antp RNAi #2
D
Sarcomere length (µm)
Myofibril width (µm)
E
Phalloidin 72h APF
Mef2-Gal4 > y RNAi
Mef2-Gal4 > Antp RNAi #3
G
72h APF
F
Sarcomere length (µm)
Myofibril width (µm)
Mef2-Gal4> y RNAi Antp RNAi #3
H
Phalloidin 2 days adult (DVM)
Mef2-Gal4 > y RNAi
Mef2-Gal4 > Antp RNAi #2

Fig. S4. *Antp* KD perturbs adult flight muscle myofibrillogenesis.

(A) Images of adult flies expressing *UAS-y RNAi* (as a control) or *UAS-Antp RNAi* (# depicts two different RNAi lines) driven by the *Mef2*-Gal4 driver, at 29°C. **(B)** Flight ability was scored as a percentage of male flies landing on each section of the column (top, middle or bottom section). The test was perfomed on flies kept at 25°C (n_{y_RNAi}=176, $n_{Antp_RNAi_\#1}$ =261 and $n_{Antp_RNAi_\#2}$ =216 flies) and at 29°C (n_{y_RNAi}=202, $n_{Antp_RNAi_\#1}$ =223 and $n_{Antp_RNAi_\#2}$ =202 flies). **(C)** Confocal sections of adult female DLM stained with phalloidin (Top), with zoomed views on sarcomeres and their surface (Middle). Scale bars are 100 µm for large and 5 µm for zoomed views. TEM micrographs of adult DLM sarcomeres are shown at the bottom. The scale bar is 500 nm. Genotypes are identical to (A). **(D)** Quantification of muscle parameters, sarcomere length (Top) and myofibril width (Bottom). Each point corresponds to a value obtained from one animal, mean and standard error are indicated (n_{y_RNAi}=32, $n_{Antp_RNAi_\#1}$ =18 and $n_{Antp_RNAi_\#2}$ =25 flies). Genotypes are identical to (A). **(E)** Confocal sections of pupal DLM at 72 h APF stained with phalloidin (Top), with zoomed view on sarcomeres (Bottom), at 25°C. Scale bars are 100 µm for large and 5 µm for zoomed views. Genotypes are *UAS-y RNAi* (as a control) and *UAS-Antp RNAi #3* driven by the *Mef2*-Gal4 driver. **(F)** As in (D) with (n_{y_RNAi}=12 and $n_{Antp_RNAi_\#3}$ =13 flies). Genotypes are identical to (E). **(G)** TEM micrographs of pupal sarcomeres at 72h APF, cut in longitudinal (Top) and cross-sections (Bottom). The scale bar is 500 nm for all images. Genotypes are identical to (E). **(H)** Confocal sections of adult female DVM stained with phalloidin (Left), with zoomed views on sarcomeres (Middle). Scale bars are 100 µm for large and 5 µm for zoomed views. TEM micrographs of adult DVM sarcomeres are shown on the right. The scale bar is 500 nm. Genotypes are *UAS-y RNAi* (as a control) and *UAS-Antp RNAi #2* driven by the *Mef2*-Gal4 driver.

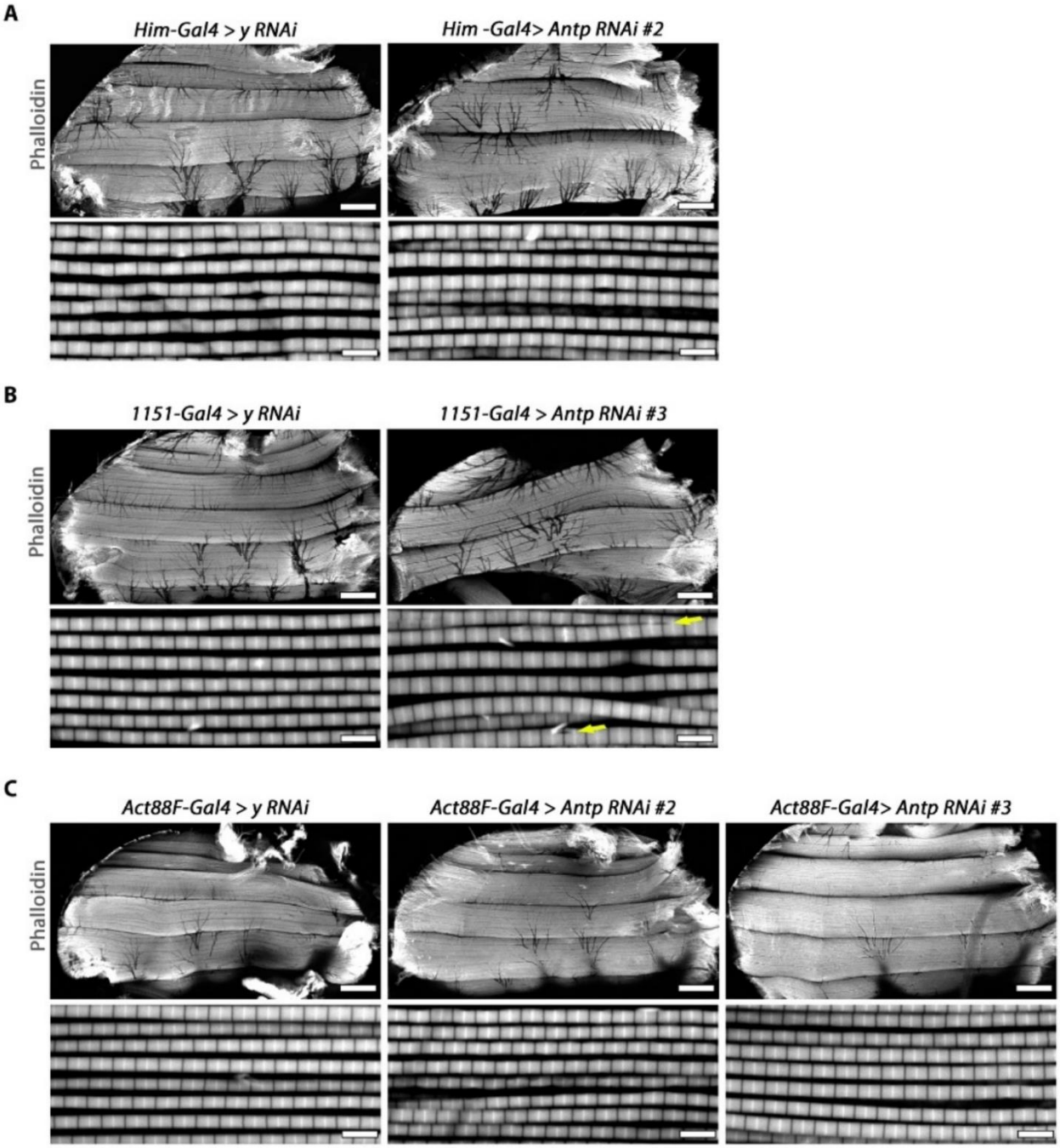
A
Him-Gal4 > y RNAi
Him -Gal4> Antp RNAi #2
Phalloidin
B
1151-Gal4 > y RNAi
1151-Gal4 > Antp RNAi #3
Phalloidin
C
Act88F-Gal4 > y RNAi
Act88F-Gal4 > Antp RNAi #2
Act88F-Gal4> Antp RNAi #3
Phalloidin

Fig. S5. *Antp* early pupal, but not late pupal downregulation perturbs adult flight myogenesis.

(A, B, C) Confocal sections of adult female DLM stained with phalloidin (Top), with zoomed views on sarcomeres (Bottom). Genotypes are (A) *UAS-y RNAi* (as a control), *UAS-Antp RNAi #2* driven by the *Him*-Gal4 driver showing defects in the number of DLM fibers upon Antp RNAi. (B) *UAS-y RNAi* (as a control), *UAS-Antp RNAi #3* driven by the *1151*-Gal4 driver, maintained at 29°C, showing splitting of myofibrils (arrow). (C) *UAS-y RNAi*, *UAS-Antp RNAi #2, UAS-Antp RNAi #3* driven by the *Act88F*-Gal4 driver results in no visible defects to DLM development. Scale bars are 100 μm for large and 5 μm for zoomed views.

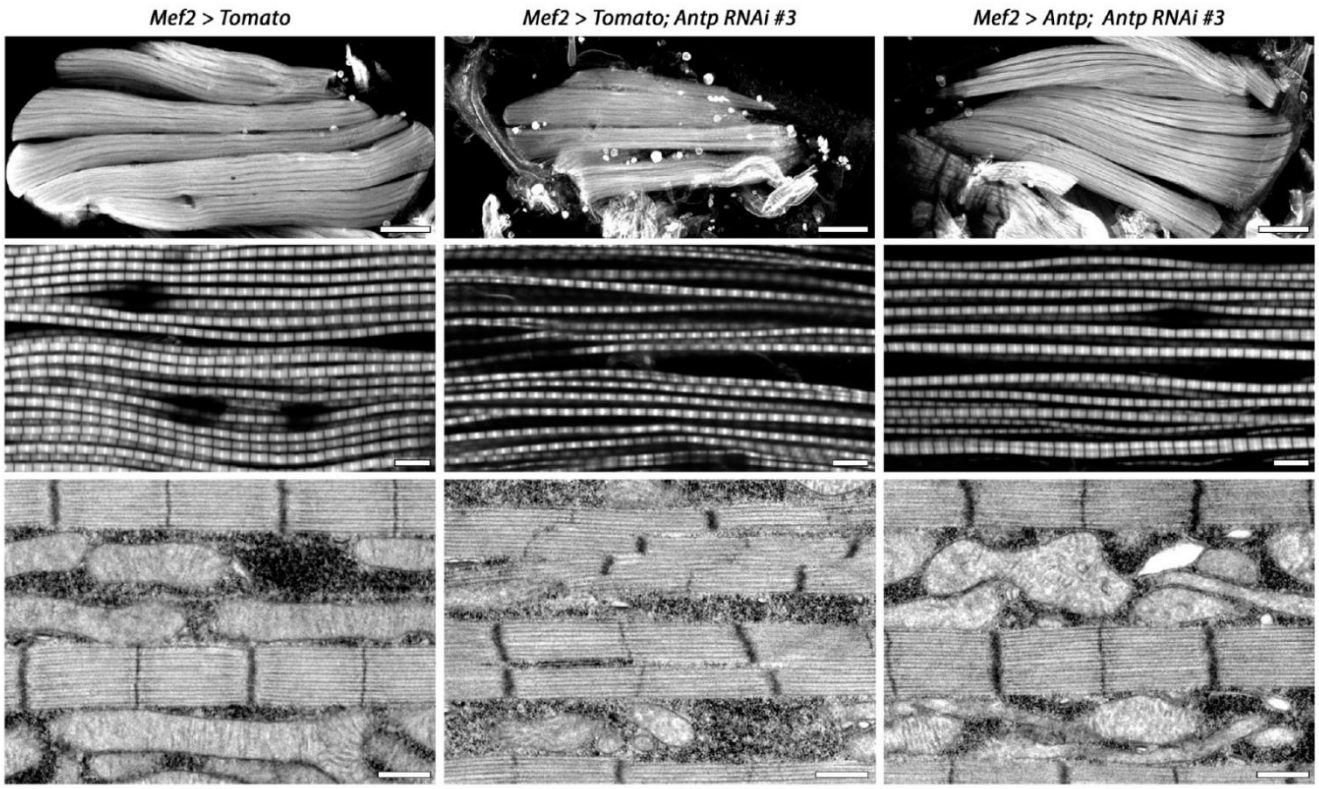
Mef2 > Tomato
Mef2 > Tomato; Antp RNAi #3
Mef2 > Antp; Antp RNAi #3

Fig. S6. Defaults in pupal flight muscle development in the *Antp* KD can be rescued with *Antp* overexpression.

Confocal sections of female pupal DLM at 72h APF stained with phalloidin (Top), with zoomed views on sarcomeres (Middle). Scale bars are 100 μm for large and 5 μm for zoomed views. TEM micrographs of 72h pupal sarcomeres are shown at the bottom. The scale bar is 500 nm. Genotypes are *UAS-Tomato* (Left), *UAS-Tomato; UAS-Antp RNAi #3* (Middle) and *UAS-Antp; UAS-Antp RNAi #3* (Right), driven by the *Mef2*-Gal4 driver.

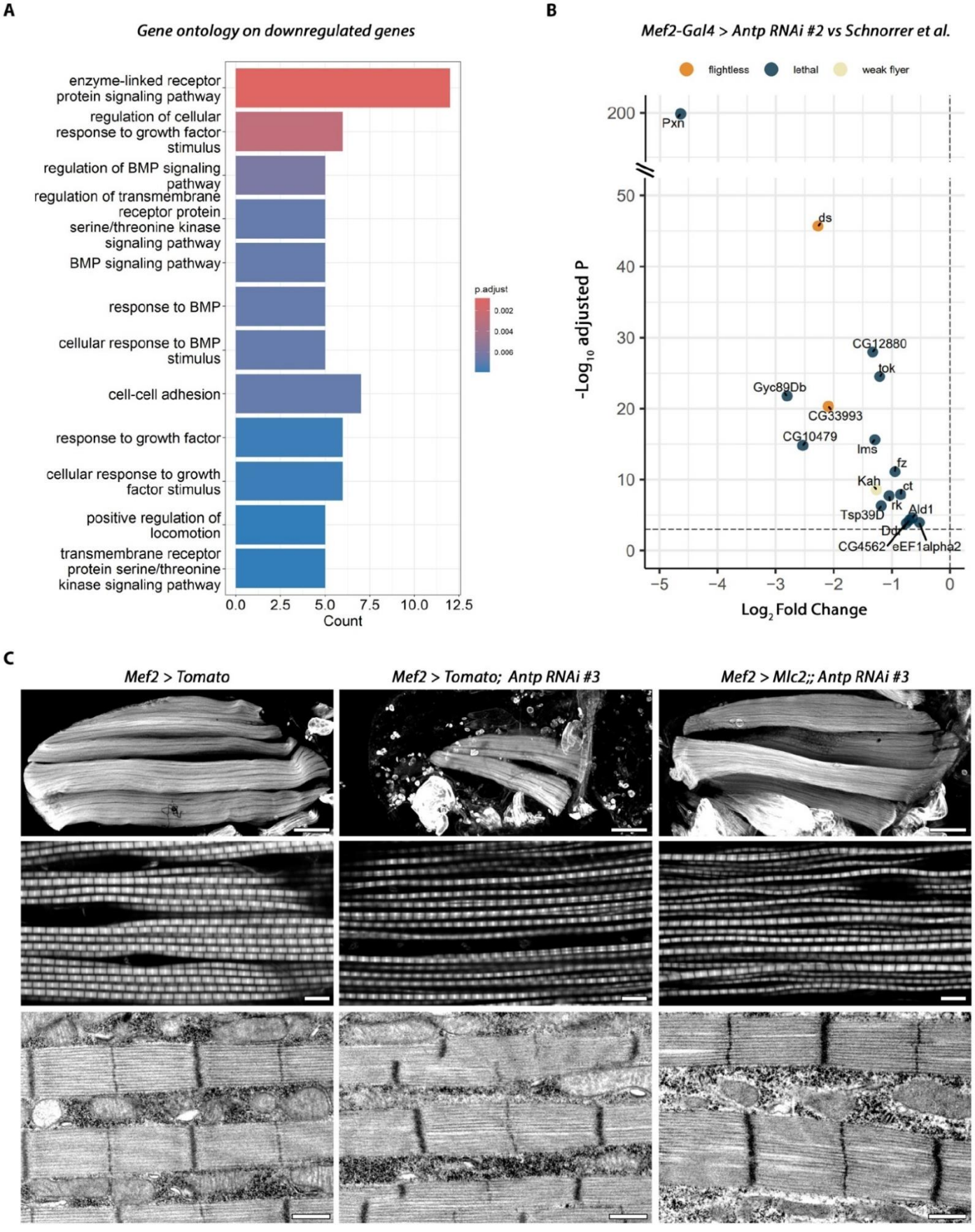
A
Gene ontology on downregulated genes
enzyme-linked receptor protein signaling pathway
regulation of cellular response to growth factor stimulus
regulation of BMP signaling pathway
regulation of transmembrane receptor protein serine/threonine kinase signaling pathway
BMP signaling pathway
response to BMP
cellular response to BMP stimulus
cell-cell adhesion
response to growth factor
cellular response to growth factor stimulus
positive regulation of locomotion
transmembrane receptor protein serine/threonine kinase signaling pathway
0.0 2.5 5.0 7.5 10.0 12.5
Count
p.adjust
0.002
0.004
0.006
B
Mef2-Gal4 > Antp RNAi #2 vs Schnorrer et al.
flightless
lethal
weak flyer
-Log10 adjusted P
Log2 Fold Change
Pxn
ds
CG12880
tok
Gyc89Db
CG33993
CG10479
lms
fz
Kah
ct
rk
Ald1
Tsp39D
Dd
CG4562
eEF1alpha2
C
Mef2 > Tomato
Mef2 > Tomato; Antp RNAi #3
Mef2 > Mlc2;; Antp RNAi #3

Fig. S7. Defaults in pupal flight muscle development in the *Antp* KD can be rescued with *Mlc2* overexpression.

(A) Gene ontology analysis using significantly downregulated genes upon *Antp* KD in larval myoblasts. **(B)** Volcano plot showing significantly downregulated genes upon *Antp* KD having a phenotype in the RNAi screen from *Schnorrer et al. 2010* (*40*). **(C)** Confocal sections of female pupal DLM at 72h APF stained with phalloidin (Top), with zoomed views on sarcomeres (Middle). Scale bars are 100 µm for large and 5 µm for zoomed views. TEM micrographs of 72h pupal sarcomeres are shown at the Bottom. The scale bar is 500 nm. Genotypes are *UAS-Tomato* (Left), *UAS-Tomato; UAS- Antp RNAi #3* (Middle) and *UAS-Mlc2;; UAS- Antp RNAi #3* (Right) driven by the *Mef2-Gal4* driver.

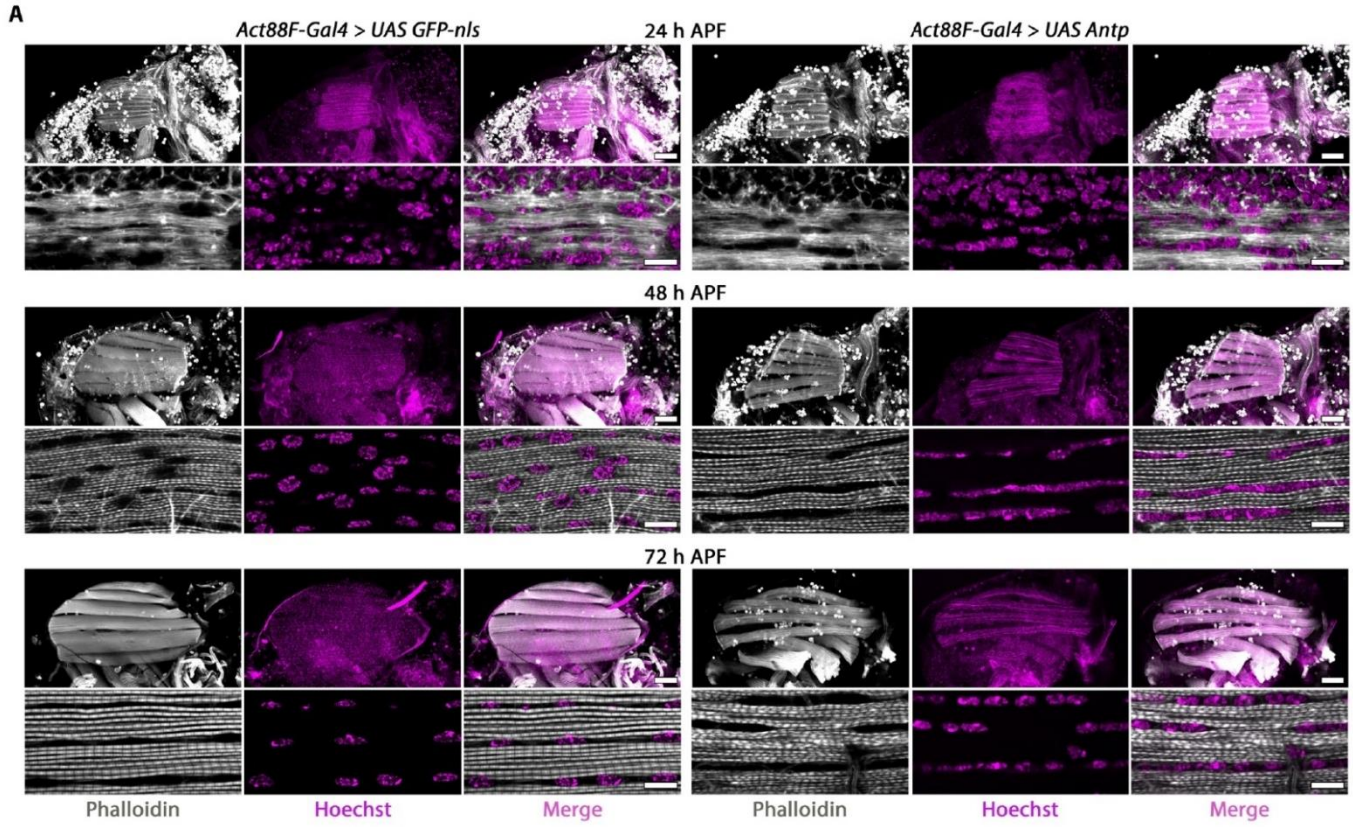
A
Act88F-Gal4 > UAS GFP-nls
24 h APF
Act88F-Gal4 > UAS Antp
48 h APF
72 h APF
Phalloidin
Hoechst
Merge
Phalloidin
Hoechst
Merge

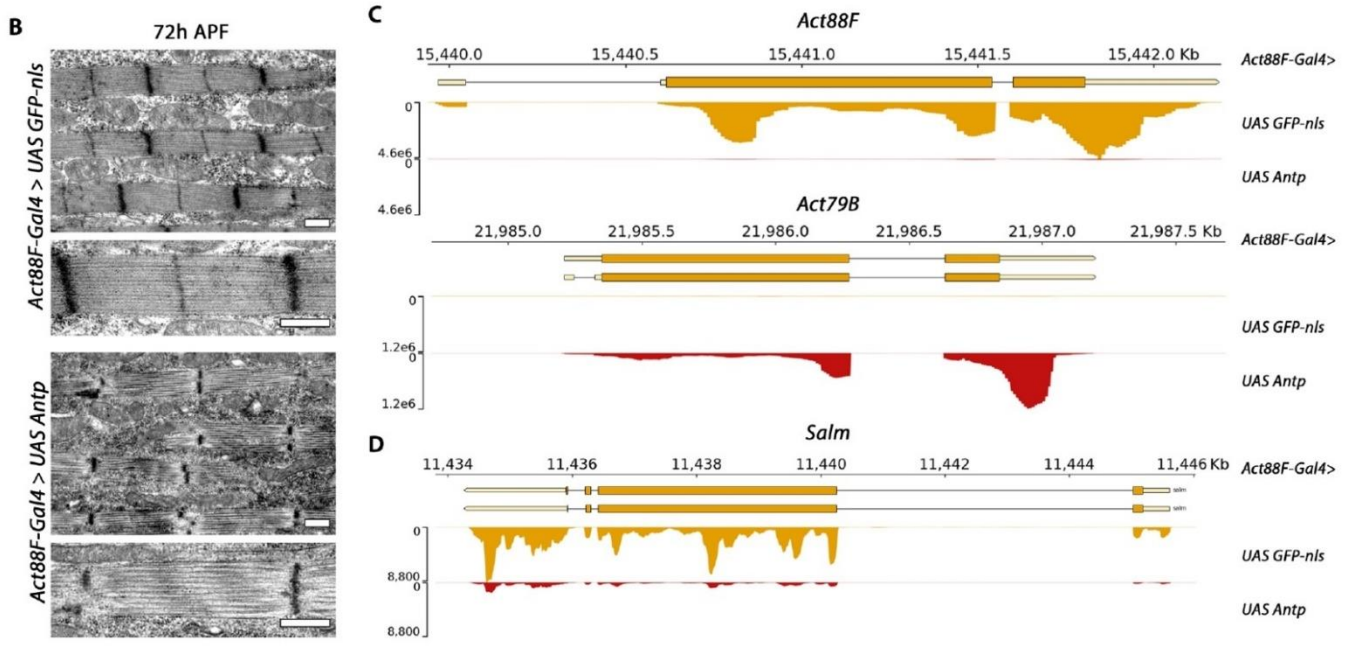
B
72h APF
Act88F-Gal4 > UAS GFP-nls
Act88F-Gal4 > UAS Antp
C
Act88F
15,440.0
15,440.5
15,441.0
15,441.5
15,442.0 Kb
Act88F-Gal4>
UAS GFP-nls
UAS Antp
Act79B
21,985.0
21,985.5
21,986.0
21,986.5
21,987.0
21,987.5 Kb
Act88F-Gal4>
UAS GFP-nls
UAS Antp
D
Salm
11,434
11,436
11,438
11,440
11,442
11,444
11,446 Kb
Act88F-Gal4>
UAS GFP-nls
UAS Antp

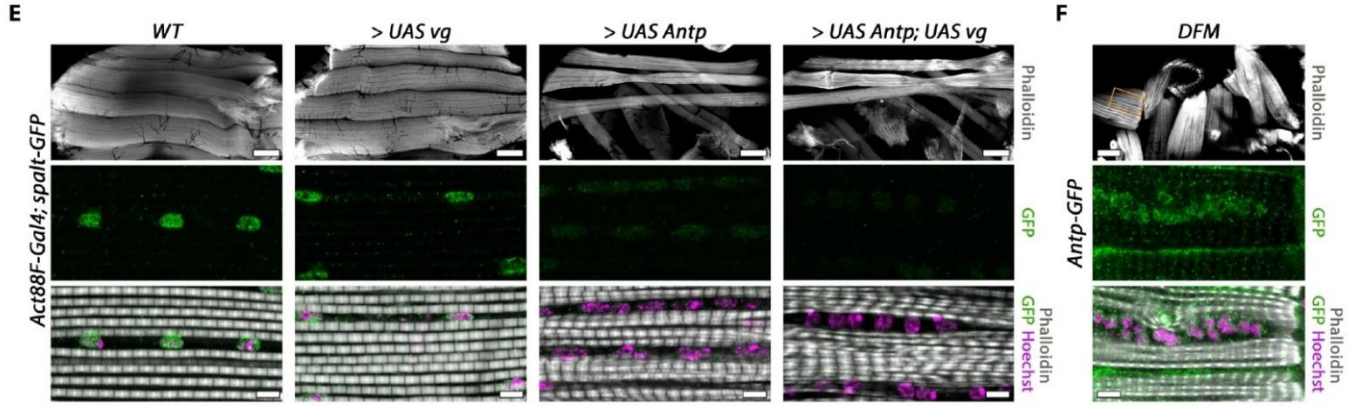
E
WT
> UAS vg
> UAS Antp
> UAS Antp; UAS vg
Act88F-Gal4; spalt-GFP
Phalloidin
GFP
Phalloidin
GFP Hoechst
F
DFM
Antp-GFP
Phalloidin
GFP
Phalloidin
GFP Hoechst

Fig. S8. *Antp* overexpression prevents fibrillar fibre fate.

(A) Confocal sections of pupal DLM at 24 h (Top), 48 h (Middle) and 72 h APF (Bottom), stained with phalloidin and Hoechst. For each timepoint zoomed views of sarcomeres are shown. Scale bars are 100 µm for large and 10 µm for zoomed views. Genotypes are *UAS-GFP-nls* (Left panel) and *UAS-Antp* (Right panel) driven by the *Act88F*-Gal4 driver. **(B)** TEM micrographs of 72h APF DLM, cut in longitudinal section, with a zoomed view on a sarcomere. The scale bar is 500 nm for all micrographs. Genotypes are identical to (A). **(C)** Genome browser images and normalised RNA-seq reads of *Act88F*-Gal4-driven *UAS-GFP* (gold tracks) or *UAS-Antp* (red tracks) for the fibrillar-specific *Act88F* gene (top) and tubular-specific *Act79B* gene (bottom) showing repression of *Act88F* and expression of *Act79B* upon Antp expression. **(D)** Genome browser image and normalised RNA-seq reads of *Act88F*-Gal4-driven *UAS-GFP* (gold tracks) or *UAS-Antp* (red tracks) of the *salm* locus, showing repression of *salm* when Antp is expressed. **(E)** Confocal sections of adult female DLM stained with anti-GFP (to visualise Salm), Phalloidin and Hoechst. Genotypes are wild-type (left), *UAS-Antp* (middle-left), *UAS-vg* (middle-right) and *UAS-Antp*; *UAS-vg* (Right), driven by the *Act88F*-Gal4 driver, combined with the *spalt::GFP* transgene. The scale bar for large IFM views (top) is 100 µm and for zooms on sarcomeres (bottom) 5 µm. **(F)** Confocal sections of female DFM stained with Phalloidin, anti-GFP (to visualise Antp) and Hoechst. The orange rectangle depicts the zoomed area on the DFM muscle 49. The scale bar is 50 µm for the large view (top) and 5 µm for the zoomed view (bottom). The genotype is homozygous *Antp-GFP*.

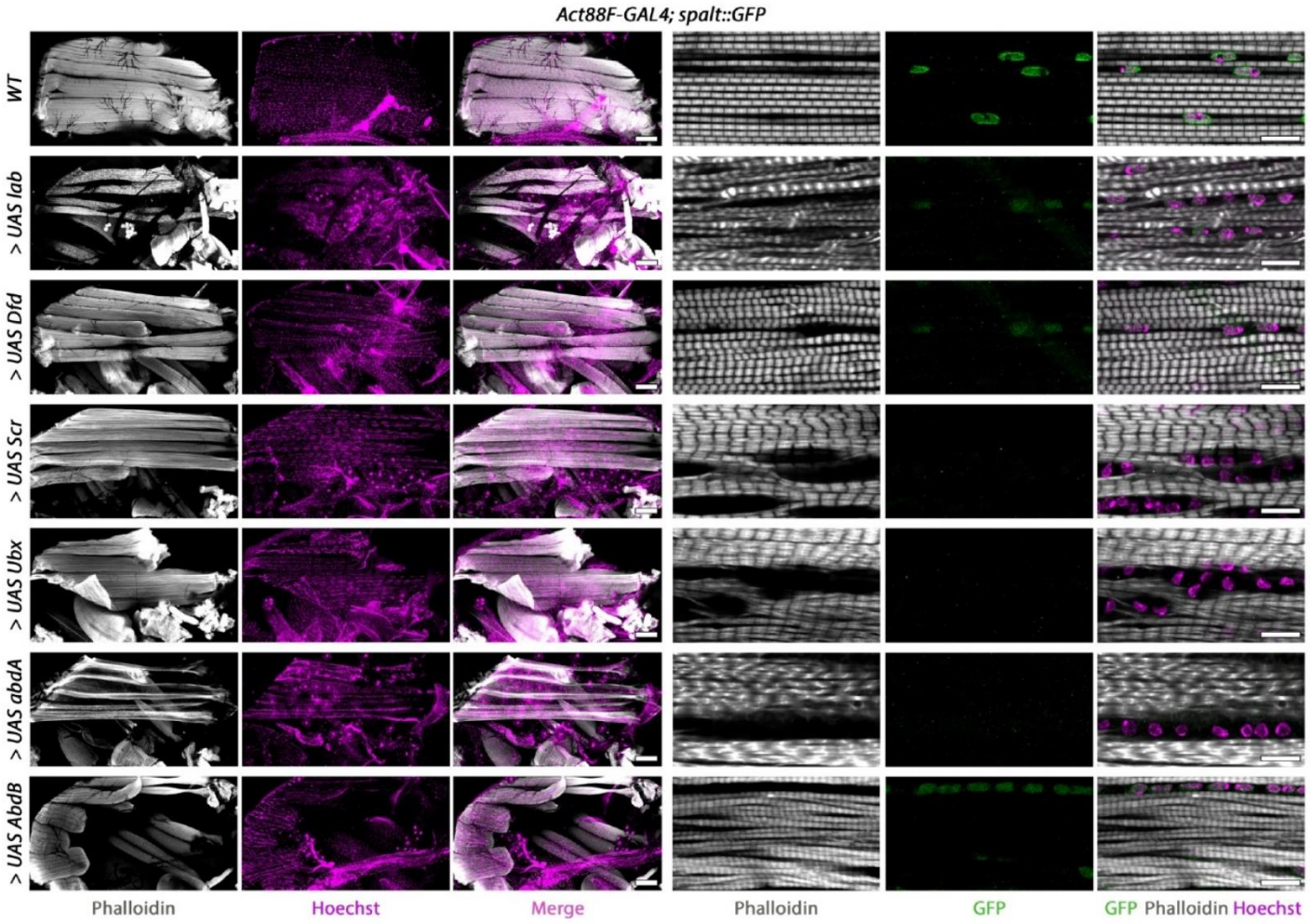
Act88F-GAL4; spalt::GFP
WT
> UAS lab
> UAS Dfd
> UAS Scr
> UAS Ubx
> UAS abdA
> UAS AbdB
Phalloidin
Hoechst
Merge
Phalloidin
GFP
GFP Phalloidin Hoechst

Fig. S9. Fibrillar fate and Spalt repression are shared *Hox* functions.

Confocal sections of adult female DLM stained with anti-GFP (to visualise Salm), Phalloidin and Hoechst. The scale bar is 100 µm for large views and 10 µm for zoomed views on sarcomeres. Genotypes are WT, *UAS-lab*, *UAS-Dfd*, *UAS-Scr*, *UAS-Ubx*, *UAS-abdA* and *UAS-AbdB* driven by the *Act88F*-Gal4 driver.

Movie S1. (separate file)

Spinning disc movie of developing flight muscles at 29°C, expressing *UAS-y RNAi* driven by the *Mef2*-Gal4 *driver,* with the *UAS-GFP-Gma* transgene added to visualise actin.

Movie S2. (separate file)

Spinning disc movie of developing flight muscles at 29°C, expressing *UAS- Antp RNAi #2* driven by the *Mef2*-Gal4 *driver,* with the *UAS-GFP-Gma* transgene added to visualise actin, corresponding to example 1.

Movie S3. (separate file)

Spinning disc movie of developing flight muscles at 29°C, expressing *UAS- Antp RNAi #2* driven by the *Mef2*-Gal4 *driver,* with the *UAS-GFP-Gma* transgene added to visualise actin, corresponding to example 2.

Data S1. (separate file)

Excel file containing differential gene expression analysis of RNA-sequencing following *Antp* RNAi #2 expression in myoblasts, driven by the *Mef2*-Gal4 driver.

Data S2. (separate file)

Excel file containing the comparison of differential gene expression analysis of RNA-sequencing following *Antp* RNAi #2 in myoblasts, driven by the *Mef2*-Gal4 driver, with the screen from *Schnorrer et al. 2010* (*40*).

Data S3. (separate file)

Excel file containing differential gene expression analysis of RNA-sequencing following Antp overexpression driven by the *Act88F*-GAL4 driver in 72 h APF pupa at 25°C.

Annexe

Article 3. Hox proteins in the Regulation of Muscle development (Review)

frontiers in Cell and Developmental Biology

REVIEW
published: 18 October 2021
doi: 10.3389/fcell.2021.731996

Hox Proteins in the Regulation of Muscle Development

*Gabriela Poliacikova, Corinne Maurel-Zaffran, Yacine Graba and Andrew J. Saurin**

Aix-Marseille University, CNRS, IBDM, UMR 7288, Marseille, France

Hox genes encode evolutionary conserved transcription factors that specify the anterior–posterior axis in all bilaterians. Being well known for their role in patterning ectoderm-derivatives, such as CNS and spinal cord, Hox protein function is also crucial in mesodermal patterning. While well described in the case of the vertebrate skeleton, much less is known about Hox functions in the development of different muscle types. In contrast to vertebrates however, studies in the fruit fly, *Drosophila melanogaster*, have provided precious insights into the requirement of Hox at multiple stages of the myogenic process. Here, we provide a comprehensive overview of Hox protein function in *Drosophila* and vertebrate muscle development, with a focus on the molecular mechanisms underlying target gene regulation in this process. Emphasizing a tight ectoderm/mesoderm cross talk for proper locomotion, we discuss shared principles between CNS and muscle lineage specification and the emerging role of Hox in neuromuscular circuit establishment.

Keywords: Hox, muscle, patterning, mesoderm, neuromuscular

OPEN ACCESS

Edited by:
Edwina McGlinn,
Monash University, Australia

Reviewed by:
Carlos Estella,
Centro de Biología Molecular Severo Ochoa (CSIC-UAM), Spain
Alain Vincent,
FR3743 Centre de Biologie Intégrative (CBI), France

***Correspondence:**
Andrew J. Saurin
andrew.saurin@univ-amu.fr

Specialty section:
This article was submitted to Morphogenesis and Patterning, a section of the journal Frontiers in Cell and Developmental Biology

Received: *28 June 2021*
Accepted: *28 September 2021*
Published: *18 October 2021*

Citation:
Poliacikova G, Maurel-Zaffran C, Graba Y and Saurin AJ (2021) Hox Proteins in the Regulation of Muscle Development. Front. Cell Dev. Biol. 9:731996. doi: 10.3389/fcell.2021.731996

INTRODUCTION

Homeotic or *Hox* genes are highly conserved homeodomain transcription factors that play a fundamental role in bilaterian animal body patterning (Pearson et al., 2005). Several characteristics are at the core of Hox gene function. First, Hox genes are differentially expressed along the anterior–posterior axis of the embryo allocating distinct morphological identities to each body part. Second, manipulation of their expression often results in spectacular homeotic transformations, where the morphology of one given body part is transformed into that of another. Third, Hox genes are grouped in clusters: one split cluster in *Drosophila*, the *Antennapedia* complex, ANT-C, harboring the Hox genes *lab*, *pb*, *Dfd*, *Scr*, *Antp* and the *Bithorax* complex, BX-C, harboring the Hox genes *Ubx*, *abd-A*, *Abd-B*; and at least four clusters in vertebrates (*HoxA-HoxD*) with each cluster harboring 1–13 Hox genes. Genomic clustering of Hox genes in such a way is essential for their correct spatio-temporal expression, which is controlled by important regulatory elements located within and around these clusters. Fourth, they all bind to a very similar set of "AT"-rich DNA-binding sites, achieving functional specificity by cooperating with transcriptional cofactors, the best characterized being PBC proteins (Extradenticle/Exd in *Drosophila*) and MEIS proteins (Homothorax/Hth in *Drosophila*), also encoding for homeodomain transcription factors. However, a large number of Hox-PBC/Meis independent functions have been reported and reciprocally, PBC/Meis proteins can function without binding to Hox (Mallo and Alonso, 2013; Rezsohazy et al., 2015).

Besides their canonical role in providing spatial coordinates that pattern the developing embryo, Hox genes play "non-homeotic" roles where they are involved in the regulation of virtually all basic cellular processes including cell death, cell proliferation, migration and differentiation, as well as in the development of whole structures/organs (Hombría and Lovegrove, 2003; Sánchez-Herrero, 2013). Yet relatively little is known into how much Hox proteins play a role in specification and development of vertebrate muscles, undoubtedly in part due to the large muscle diversification that exists in vertebrates, the large number of Hox genes present (more than 30), and a significant functional redundancy between paralogous group members. In *Drosophila melanogaster* however, there is now abundant evidence for Hox involvement in the patterning of several mesodermal derivatives, including somatic, cardiac and visceral muscles. It is now widely accepted that *Drosophila* myogenesis recapitulates, even though at different scales, all major muscle developmental events that are also at work in vertebrates, such as progenitor specification, myoblast migration and fusion, muscle attachment to tendons cells and assembly of contractile sarcomeres. Furthermore, a part of gene regulatory networks crucial for correct myogenesis such as *twist*, *mef2*, *lbx/ladybird* and the fusion machinery are well conserved (Schnorrer and Dickson, 2004; Taylor, 2006). Here, we focus specifically on Hox function in muscle precursor specification and in patterning of mesodermal derivatives, highlighting Hox target genes and their regulatory mechanisms, when available. We separate the topic in three sections, somatic/skeletal, cardiac and visceral muscles and in each section, we review available data from first *Drosophila* and then from vertebrates. In the somatic/skeletal section we further discuss an emerging role of Hox in the establishment of proper muscle-motoneuron connections. We distinguish Hox specific and non-specific, so-called generic functions, the first referring to functions performed by a single Hox that cannot be assumed by any other and the latter to functions that can be performed by several Hox genes (reviewed in Saurin et al., 2018).

SOMATIC/SKELETAL MUSCULATURE

Basics on Somatic/Skeletal Muscle Development

The somatic muscle development in *Drosophila* as well as the functional conservation with vertebrate muscles have been extensively reviewed (Taylor, 2006; Dobi et al., 2015; Schulman et al., 2015; Gunage et al., 2017; Poovathumkadavil and Jagla, 2020). Briefly, the *Drosophila* life cycle comprises two mobile stages, the larval stage where the crawling movements enable larval feeding and the adult stage where flies can fly, jump and walk. Distinct sets of muscles, produced by two rounds of myogenesis are used during each stage, with larval muscles being produced during embryogenesis and the adult muscles during metamorphosis. Interestingly, both groups develop from mesoderm-derived somatic muscle progenitors marked by high *twist* expression, even though at different developmental timepoints (Baylies and Bate, 1996). Embryonic muscle progenitors are singled out from so-called equivalence groups or promuscular clusters in each hemisegment by lateral inhibition via Notch signaling at stages 11–12 (Carmena et al., 2002). The remaining cells of the cluster become fusion-competent myoblasts, providing mass to the growing muscle by fusing with it. After specification, muscle progenitors undergo a symmetrical division producing two muscle founder cells (FCs), or an asymmetrical division producing either one FC and one adult muscle progenitor (AMP) or one FC and one pericardial progenitor (Ruiz Gómez and Bate, 1997; Carmena et al., 1998). FCs seed individual embryonic muscles and express a unique combination of identity transcription factors (iTFs), controlling all muscle characteristics, including muscle size, position, innervation and attachment. During embryonic stages 12–15 fusion competent myoblasts fuse with FCs assuring muscle growth. Until larval hatching, muscles are properly oriented, attached to tendons and innervated.

On the other hand, AMPs/myoblasts that retain high *twist* expression do not differentiate directly after their specification but are set aside in a quiescent state and associated with imaginal disks and nerves. During larval stages, myoblasts proliferate extensively until the beginning of metamorphosis where they migrate, fuse and differentiate at an appropriate body position to constitute the adult body musculature. For the development of the most prominent adult muscles, the indirect flight muscles (IFMs) composed of dorsal longitudinal muscles (DLM) and dorsal ventral muscles (DVM), two different strategies are employed: The DLMs that span the thorax antero-posteriorly develop by the fusion of myoblasts with three larval scaffolds that escape the histolysis process during first hours of pupal development; the DVMs, spanning the thorax dorso-ventrally, develop by *de novo* myoblast fusion without any scaffold, like in the case of the larval musculature (Fernandes et al., 1991). The larval and adult myogenic process are thus intimately linked since muscle progenitors giving rise to both larval and adult muscles are specified during embryogenesis (even though they do not differentiate at the same time), the fusion process seems to involve the same molecular players and certain larval muscles are reused for the development of a group of adult muscles, like the DLM flight muscles (**Figure 1A**).

In vertebrates, like in *Drosophila*, muscles develop from mesoderm-derived muscle progenitors (reviewed in Endo, 2015; Musumeci et al., 2015; Chal and Pourquié, 2017). Briefly, skeletal muscles develop from the paraxial mesoderm, bilaterally flanking the neural tube. The paraxial mesoderm in the trunk region transiently and progressively subdivides into somites, which are themselves compartmentalized into the dorsal epithelial dermomyotome (giving rise to muscles, dermis, and brown fat) and ventral mesenchymal sclerotome (giving rise to the axial skeleton, cartilage, and tendons). A layer of muscle precursors/myocytes called myotome forms beneath the dermomyotome at E8 in the mouse and E2.5 in the chick. Muscle precursors after their differentiation give rise to the body wall muscles and some undergo long-range migration toward future limb buds where they proliferate and differentiate into limb muscles. In the cranial region, paraxial mesoderm forms the cranial mesoderm that will give rise to the muscles,

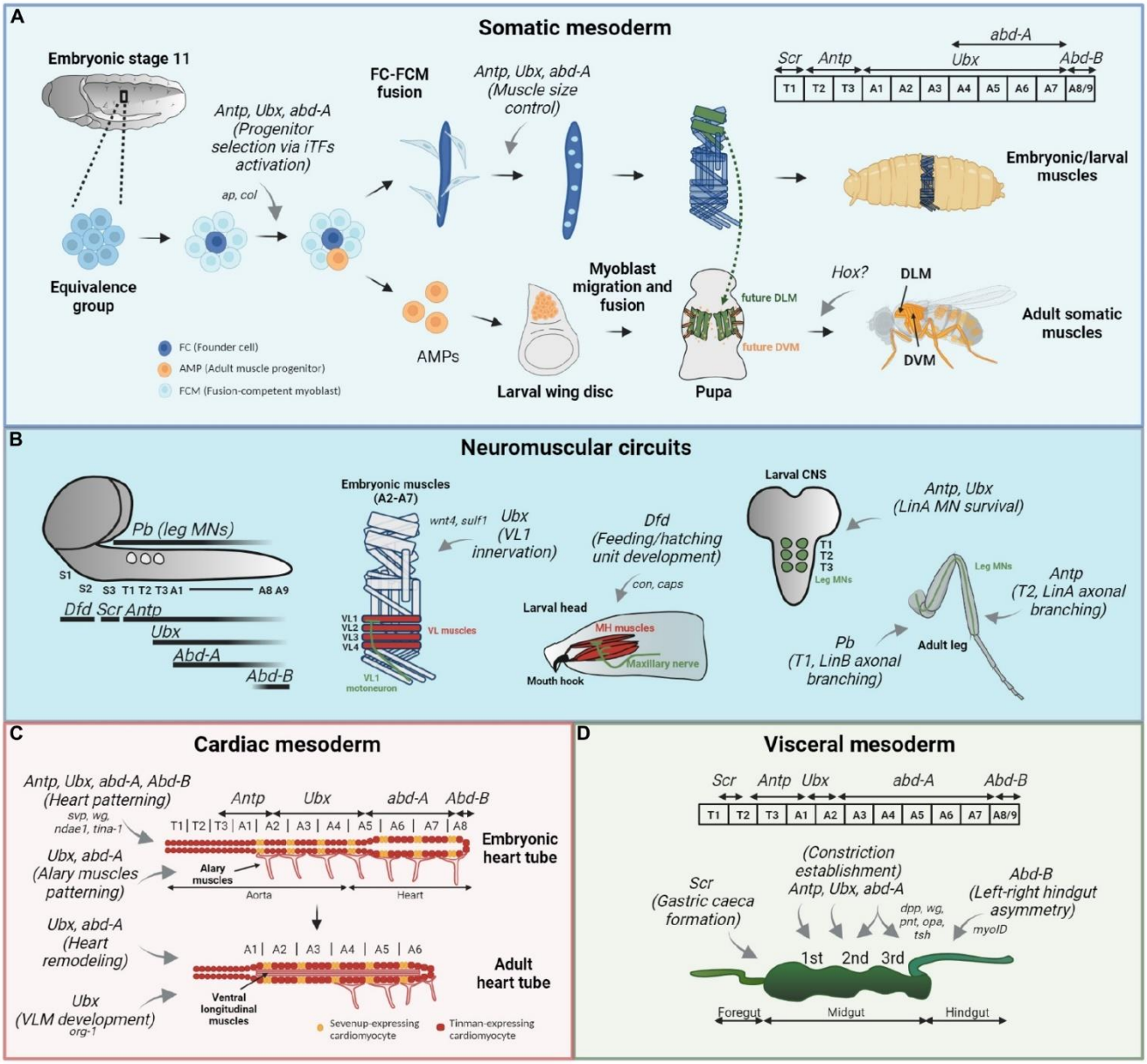

FIGURE 1 | Hox functions in *Drosophila* muscle patterning. Hox functions in the somatic **(A)** mesodermal patterning, neuromuscular circuit establishment **(B)** and cardiac **(C)** and visceral **(D)** mesodermal patterning are depicted by gray arrows, and their target genes are specified, if available. Their expression patterns are showed for each mesodermal derivative. **(A)** In the somatic muscle development, Antp, Ubx, and AbdA regulate progenitor selection from different equivalence groups (by binding to a muscle specific *cis*-regulatory region of *ap* and *col*, in LT and DA3 muscles, respectively) and later control muscle size by specifying the number of FCM (light blue cells) that will fuse with the FC (dark blue cell). The role for Hox in adult musculature, derived from AMPs (orange cells) is not clearly established. **(B)** Hox expression pattern in the larval CNS is depicted on the left, with Pb expression in leg MNs (circles). In this context, Ubx establishes proper connection between embryonic VL1 muscle and VL1-MN, by regulating *wnt4* and *sulf1* expression in the VL2 muscle. Dfd is responsible for the feeding and hatching motor unit development and maintenance in the larva, a process involving target genes *con* and *caps*. Antp and Ubx play a role in LinA lineage MN survival during larval development, and Antp further regulates correct morphology of this neurons in the adult T2 leg. Finally, Pb controls branching of some LinB MNs in T1 adult leg. **(C)** The heart tube is composed of *Svp*-expressing (orange cells) and *Tin*-expressing (red cells) cardioblasts and surrounding pericardial cells (not represented). Antp, Ubx, and AbdA are all involved in the patterning of embryonic heart tube, by controlling the expression of *svp* in the segment-specific manner. Furthermore, AbdA with Svp regulate *wg* expression in cardioblasts expressing Svp. AbdB on the other hand is a suppressor of cardiogenesis. Ubx and AbdA pattern alary muscles present in the abdominal segments. For proper heart remodeling, Ubx repression and AbdA function modulation are required. Finally, Ubx is involved in adult ventral longitudinal muscle (VLM) development. **(D)** In the embryonic visceral mesoderm, Antp establishes the first, Ubx and AbdA the second and AbdA the third midgut constriction. A complex genetic network involving *dpp*, *wg*, *pnt*, *opa*, and *tsh* is involved in the middle constriction development. Scr is involved in the formation of gastric caeca in the anterior midgut (caeca are not represented) and AbdB is responsible for the correct left-right embryonic hindgut asymmetric morphology via *myoID* regulation.

connective tissue and skeleton of the face and skull. The myogenic process can be subdivided into primary/embryonic myogenesis (E10.5–E12.5 in mice and E3–E7 in the chick) and secondary/fetal myogenesis (E14.5–E17.5 in mice and E8+ in the chick). In vertebrates, individual muscles are not seeded by a single founder myoblast like in *Drosophila*, but by scaffolds of primary fibers composed of several fused muscle precursors. Subsequently, additional fibers are added along them to assure the muscle growth.

Hox Control of *Drosophila* Embryonic/Larval Somatic Musculature

In the embryonic somatic mesoderm, *Hox* gene expression has a spatially restricted pattern, where *Sex combs reduced* (*Scr*) is expressed in the first thoracic segment, T1, *Antennapedia* (*Antp*) in T2 and T3, *Ultrabithorax* (*Ubx*) in abdominal segments A1–A7, *abdominal-A* (*abd-A*) in A4–A8 and *Abdominal-B* (*AbdB*) in A8–A9 (Michelson, 1994; Enriquez et al., 2010; **Figure 1A**). Their implication in the subdivision of somatic mesoderm began with the description of mutant alleles of *AbdB* (Lawrence and Johnston, 1984) and *Ubx* (Hooper, 1986) shown to transform larval muscles into more anterior ones. Conversely, the overexpression of Ubx or AbdA in the embryonic mesoderm led to the abdominal transformation of thoracic muscle precursors (Greig and Akam, 1993; Michelson, 1994). Collectively, these studies demonstrated a clear role for Hox genes in muscle patterning and argued toward a cell-autonomous role of Hox in the somatic mesoderm, meaning that Hox genes would confer a specific identity to the muscle precursors and account for segment-specific differences in the muscle pattern. Further evidence for cell-autonomous Hox function came from a pioneering study showing that Antp directly regulates the expression of the *apterous* muscle identity gene in the somatic mesoderm, specifying a subset of lateral transverse muscles (LT1–4) (**Figure 1A**). Importantly, it was shown that this regulation occurs via an *apterous* muscle-specific enhancer, providing a molecular mechanism by which a Hox protein can directly regulate its muscle target gene expression and contribute to the establishment of segment-specific muscle patterns via progenitor selection (Capovilla et al., 2001). Whether Ubx/AbdA specify abdominal LT1–4 muscles and/or regulate *apterous* expression was not addressed.

Building on the same principle, it was found that Antp, Ubx, and AbdA regulate progenitor selection via distinct *cis*-regulatory modules in a segment-specific manner (**Figure 1A**). Focusing on the dorsal acute DA3 muscle lineage, specified by the combinatorial activity of *nautilus* (*nau*, *Drosophila* ortholog of mammalian *MyoD*) and *collier* (*col*, ortholog of mammalian early B-cell factors, EBFs) it was shown that the progenitor specification via Hox-mediated regulation of muscle iTFs is superimposed on the A-P and D-V positional information. Furthermore, the precise timing of Hox activity was traced to the progenitor stage, where first, Hox activity controls the number of progenitors that express *col* and *nau* in a segment-specific manner and then Hox proteins interplay with iTFs to allocate a correct number of nuclei assigned to the DA3 muscle (Enriquez and Vincent, 2010; Enriquez et al., 2010; **Figure 1A**). Interestingly, this study highlighted a Hox generic function, where Antp, Ubx, and AbdA can all provide DA3 progenitor selection (reviewed in Saurin et al., 2018). This generic function is then followed by a Hox specific function, where each Hox determines the final size of the muscle in a segment-specific manner. These studies provided an important insight into the function of Hox genes in myogenesis, showing that Hox inputs were crucial in the process of progenitor selection, which gives rise to "founder" cells, seeding the formation of syncytial muscle fibers.

It was recently shown that Ubx is involved in the muscle differentiation process by directly repressing the master mesodermal regulator *twist* (*twi*) (Domsch et al., 2021). Here, a number of interesting points can be highlighted: (1) Ubx mesodermal downregulation interferes with abdominal embryonic muscle development because of failure to repress *twi*; (2) *twi* repression is mediated by direct Ubx binding to the *twi* promoter region, competing with binding of the transcription factors Tinman (Tin) and Muscle enhancer factor 2 (Mef2), providing another promoter-based molecular evidence about the Hox muscle patterning mechanism; (3) even though Ubx binding displaces Tin on the *twi* promoter, Tin must be bound to the promoter for Ubx to be recruited, once again demonstrating a tight link between Hox and tissue-specific transcription factors for the correct patterning establishment.

Collectively, these studies provide precious insight into the way muscle progenitors are patterned. Hox proteins activate and collaborate with some of the muscle iTFs in a segment-specific fashion and by doing so they are responsible for the specification of different muscle types.

Is Patterning of the T2 Mesoderm Hox Independent?

As the understanding of muscle development evolved, an important role in muscle patterning was attributed to the ectoderm. A large number of studies argued toward a Hox non-autonomous role in myogenesis, giving importance to Hox-controlled signals coming from the overlying epidermis and nervous systems (Roy and Raghavan, 1997; Roy et al., 1997; Rivlin et al., 2001; Dutta et al., 2010). For a long time, the patterning of mesoderm in T2 was considered as being non-autonomous, because of the lack of any Hox gene expression in this segment. In complement to this observation, it was shown that overexpression of Antp (highly expressed in T2 and T3 epidermis and nervous system) in the ectoderm of *Antp* mutant embryos completely rescued the disorganized T2 muscle pattern provoked by Antp loss-of-function (Roy et al., 1997). This was taken as evidence for a non-autonomous role of Antp in T2 muscle pattern establishment. However, Antp was later described as being expressed in the T2 mesoderm, although at a much weaker level than in the T3 mesoderm and to autonomously specify a subset of muscles in the T2 (Capovilla et al., 2001). Thus, the default in T2 muscle patterning in *Antp* mutant embryos is either pointing toward an autonomous role of Antp in the mesoderm or toward a combination of autonomous activity and inductive cues coming from the T2 ectoderm. It was also shown that Antp mesodermal overexpression did not modify T3 muscle

pattern, but was sufficient to transform the T2 into a T3 muscle pattern, which was interpreted as another evidence for the lack of Antp T2 expression (Roy et al., 1997). Knowing that Antp expression in the T2 mesoderm is weaker compared to that of T3, higher levels of Antp in T2 may convert its muscle pattern into a more posterior one, without excluding the presence of Antp in T2 mesoderm.

Hox Control of *Drosophila* Adult Musculature

As mentioned earlier, *Drosophila* adult musculature develops from pools of myoblasts associated with imaginal tissues and nerves. The most prominent adult muscles, thoracic flight muscles arise from myoblasts associated with the wing imaginal disks. Knowing that T2 mesoderm was mistakenly considered as a Hox-free region because of lack of *Antp* expression, it is possible that T2 wing disk-associated myoblasts also express Antp. In support of this, it was reported that Antp is transcribed from two distinct promoters, termed P1 and P2, with transcripts from P1 being localized to the anterior part of the wing disk epithelium and P2 transcripts in the presumptive notum region containing myoblasts (Jorgensen and Garber, 1987). Recently, antibody stainings have confirmed the presence of Antp protein in the myoblast-containing region of the wing disk (Paul et al., 2021). If indeed the expression of Antp is confirmed by appropriate markers in adult muscle precursors [such as Mef2, Holes in muscles (Him), or Twi], then it is highly possible that Antp is directly involved in T2 adult muscle development, including muscles used for flight and leg muscles.

Early myoblast transplantation experiments showed that T2 myoblasts, associated with the wing imaginal disks, can contribute to a vast population of adult muscles (Lawrence and Brower, 1982). Since T2 wing-associated myoblasts were considered as a Hox-free region (see above), it was proposed that they do not require any positional Hox input for their migration and fusion. Supporting this view, mesodermal overexpression of Ubx does not perturb thoracic myoblast migration pattern, demonstrating that the myoblast migration process is likely independent of Hox positional input. These myoblasts however fail to give rise to a proper adult flight muscle, because of their inability to activate Act88F, a fibrillar muscle differentiation marker, that is repressed due to Ubx overexpression (Roy and Raghavan, 1997).

Concerning myoblast fusion, the importance of Hox cues has not yet been clearly established. It is important to note that myoblasts transplanted from the second or the third thoracic segment, associated with wing and haltere imaginal disks, respectively, can both fuse to and contribute to abdominal muscles (Roy and Raghavan, 1997). It is thus possible that Antp could be involved in the thoracic myoblast fusion process, a hypothesis that has never been directly addressed because of a lack of appropriate tools. Rivlin et al. (2001) demonstrated using allelic combinations of Ubx mutations, leading to different levels of ectodermal transformation, that the transformed T3 segment could contain IFM, normally present solely in T2 (Rivlin et al., 2001). This placed ectodermal inductive cues in the central position of adult IFM patterning. However, this observation has not been reproduced (Egger et al., 1990; Fernandes et al., 1994; Dutta et al., 2010), leaving the role for Hox proteins in adult muscle development not elucidated. We note that no Hox regulatory networks were identified for the development of adult abdominal and leg muscles, leaving the role of Hox in adult muscle development largely undetermined.

It is noteworthy that the well-characterized Hox PBC cofactors, Exd and Hth are involved in the adult muscle development, controlling the fate decision between fibrillar flight and tubular leg muscles, but appear to do so in a Hox-independent fashion (Bryantsev et al., 2012). Knowing that for the proper somatic musculature patterning, Hox proteins use other muscle-specific transcription factors as cofactors, it is thus likely that Hox control of somatic muscle development is independent of their canonical cofactors and reciprocally, Exd/Hth function is independent of Hox proteins in this context.

Hox Control of Vertebrate Skeletal Musculature

In vertebrates, Hox involvement in skeletal, myotome-derived musculature patterning remains controversial. In the limb musculoskeletal system, Hox genes have an essential role in skeletal and connective tissue patterning, but limb muscle precursors seem to depend completely on environmental cues for their proper development (reviewed in Pineault and Wellik, 2014). Early grafting experiments in the chick/quail embryos demonstrated that muscle precursors do not possess intrinsic patterning information and their development is influenced by the surrounding mesenchyme (Chevallier et al., 1977; Christ et al., 1977). This view has been later challenged by a study suggesting that the axial identity of the somite is important for the generation of non-limb skeletal muscles, arguing toward an autonomous role for Hox in the body wall muscle patterning (Nowicki and Burke, 2000; Alvares et al., 2003). Furthermore, microarray analyses on purified skeletal muscle myoblasts showed that the Hox code is present along the cranio-caudal axis, specifically in embryonic, but not fetal myoblasts, indicating that myoblasts carry some intrinsic positional information (Biressi et al., 2007).

Direct evidence for Hox role in skeletal muscle patterning came from the mouse forelimb zeugopod, where Hoxa11 and Hoxd11 are expressed in the muscle connective tissue and tendons, but not in differentiated muscle cells (Swinehart et al., 2013). In Hoxa11/d11 double mutant mice, several muscles and tendons of the forelimb zeugopod are absent or improperly patterned, and importantly, this is a direct consequence of loss of Hox function and not a secondary effect due to defects in the skeletal patterning. In addition to extending the well-established role of Hox in the patterning of the axial skeleton to muscles and tendons, this study also reinforces the initial view that muscle precursors are patterned by their environment, at least at the level of the limb. However, it is still unknown whether the Hox positional information is conveyed by the muscle mesenchyme

or is encoded in muscle precursors themselves, which could be dependent on the somite axial level.

Recently, much attention has been given to the role of Hox proteins in adult muscle stem cells (MuSCs), also known as satellite cells, able to regenerate adult muscles upon injury (Machado et al., 2017; Evano et al., 2020; Yoshioka et al., 2021). It is now accepted that depending on the anatomical position of the muscle, satellite cells display heterogeneity in their proliferative and regenerative properties (Ono et al., 2010). Searching for underlying molecular determinants, Hox-A and Hox-C clusters were found to have different methylation profiles and thus be differentially expressed in adult muscles and their satellite cells derived from somites, compared to the ones derived from the cranial mesoderm (Evano et al., 2020; Yoshioka et al., 2021). Knowing that the cranial-derived, Hox-free, satellite cells display higher regenerative capacity than the limb, Hox-expressing satellite cells, an appealing possibility is that Hox could be involved in this process (Evano et al., 2020). Indeed, it has been demonstrated that during the aging process, *Hoxa9* is up-regulated in the limb satellite cells, leading to their cell cycle entry default and senescence (Schwörer et al., 2016). It does so by regulating the targets of several developmental pathways, including those of the Wnt, TGFβ, and JAK/STAT pathways. Interestingly, *Hoxa9* deletion in satellite cells from aged adult mice was sufficient to improve their regenerative capacity, suggesting that Hox expression in these cells would have a negative effect on muscle regeneration. A conditional depletion of *Hoxa10* leads to a repair default of some somite, but not cranio-derived muscles, explained by a genomic instability and consequent proliferation arrest of adult satellite cells (Yoshioka et al., 2021). Different Hox would thus assume opposed functions in satellite cell proliferation and could account for different capacities of distinct muscle groups to regenerate, a hypothesis that needs to be investigated further. In *Drosophila*, a muscle satellite cell population has been identified in adult thoracic flight muscles (Chaturvedi et al., 2017), but it remains unknown whether Hox proteins are involved in their transcriptional regulation like in vertebrates.

Hox Control of *Drosophila* Neuromuscular Circuits

Hox involvement in central nervous system development is clearly established and is out of the scope of this review (Rogulja-Ortmann and Technau, 2008; Estacio-Gómez and Díaz-Benjumea, 2014; Meng and Heckscher, 2021). It is nevertheless noteworthy here that several parallels can be drawn between neuronal and somatic muscle lineage specification by Hox. In both tissues Hox act at the very early steps of progenitor specification. Like in the larval DA3 muscle where Hox allocate a correct number of progenitors and further control muscle size in a segment-specific manner, in the neuroectoderm their expression is required to specify NB1-1 derived thoracic and abdominal lineage comprising a different number of neurons (Prokop and Technau, 1994; Prokop et al., 1998; Enriquez et al., 2010). Hox can convey the proper tissue pattern via the regulation of specific TFs, shared across distinct tissues. For example, Antp regulates the expression of *collier* (*col*) in both muscle and neural clusters to generate muscle/neuronal diversity (Enriquez et al., 2010; Karlsson et al., 2010). Yet the transcriptional control mechanisms at play would appear different, since the *cis*-regulatory element used by Antp in the muscle lineage is distinct from the CNS regulatory sequence, which has to date not been identified. One important difference though, is that in the CNS, the Hox cofactors Exd and Hth are directly involved in the control of *col* expression. Like in the somatic and cardiac mesoderm, AbdB is able to suppress neuronal fate in the most posterior abdominal segments (Lovato et al., 2002; Ponzielli et al., 2002; Birkholz et al., 2013).

Crosstalk between neuronal and muscle lineages, more specifically between motor neurons (MNs) and somatic/skeletal muscles are at the basis of voluntary movements, crucial for locomotion, feeding, mating and interactions with the environment. For their establishment, MNs need to be correctly specified and differentiated and project their axons toward specific muscle groups. Neuromuscular circuitry defaults are associated with numerous neuromuscular diseases, thus the understanding of their proper development has a direct clinical significance (reviewed in Tripodi and Arber, 2012; Li et al., 2018).

In the CNS, Hox expression is shifted posteriorly compared to their mesodermal expression. Dfd is expressed in two subesophageal segments (S1 and S2), Scr is expressed in S3, Antp is expressed in the ventral cord in T1 to A9, Ubx from T3 to A9, Abd-A from A1 to A9 and Abd-B from A7 to A9. Pb is expressed in the thoracic leg motoneurons (Baek, 2011; **Figure 1B**). Hox involvement in neuromuscular circuitry establishment was first proposed in the context of larval crawling movements, following the observation that Ubx and AbdA are necessary for their generation, providing a genetic explanation for locally specialized locomotor circuit establishment (Dixit et al., 2008). This study suggested that Ubx and AbdA not only specify larval abdominal muscles required for these peristaltic movements, but also the neuronal circuitry allowing for the properly synchronized movements. Moreover, the single removal of either Ubx or AbdA did not compromise the peristaltic movement, demonstrating a genetic redundancy in Hox function since Ubx and AbdA can substitute for each other in this context. Ubx and Antp have been shown to be required for motoneuron segmental diversity in the embryo (lineages NB7-3 and NB2-4t), by regulating cell-death and cell-survival, respectively, in an antagonistic manner (Rogulja-Ortmann et al., 2008). Several Ubx and Antp putative binding sites were identified in the pro-apoptotic *reaper* (*rpr*) gene enhancer, suggesting that their competitive binding could account for their opposed regulatory mode of motoneuron survival.

An example of a molecular mechanism behind the role of Ubx/AbdA in locomotor circuit establishment has been elucidated in embryonic abdominal ventrolateral (VL) muscles. Ubx is expressed in both muscle cells and MNs and is required for the correct establishment of contacts between them (**Figure 1B**). In the VL2 muscle, it controls the activation of Wnt4 signaling as it does in the visceral mesoderm (Graba et al., 1995), and the expression of Sulf1, a sulfatase implicated in Wnt and BMP gradient establishment at neuromuscular junctions. In the VL1

MN, Ubx interacts with the components of the Wnt4 pathway. Signaling molecules regulated by Ubx in VL2 upon their secretion serve for the proper VL1 MN axonal extension toward the more dorsal VL1 muscle. Interestingly, it was suggested that Ubx, TCF, and Armadillo (Arm) can form a Wnt4-induced transcriptional complex (Hessinger et al., 2017). The requirement of Hox in both muscles and MNs was also demonstrated in larval hatching and feeding motor units, with the central Hox, *Dfd* (Friedrich et al., 2016). Here, Dfd assures correct innervation of muscles required for mouth hook movements by the maxillary nerve (**Figure 1B**). This demonstrates that Hox could provide a regulatory code for the correct muscle-motoneuron recognition in different *Drosophila* neuromuscular circuits. In line with this hypothesis, taking advantage of available ChIP-seq data, several potential Dfd target genes with functions in muscles, nerves and synaptic recognition were identified, such as *Connectin* (*Con*) and *capricious* (*caps*) (Friedrich et al., 2016).

Concerning adult muscle innervation, the role of Hox is well established in the case of leg muscles, where the second leg pair is required for flight take-off, and T1 and T3 legs are required for grooming the head and the abdomen, respectively (Baek et al., 2013; Enriquez et al., 2015). Focusing on a major subpopulation of leg MNs, arising from the LinA (also called Lin15B) lineage, it was shown that during the third larval stage, Antp is expressed in the newborn LinA MNs in all three thoracic segments, whereas Ubx was localized only in T3 subpopulation. During mid-pupal stage, the expression of Hox changes, with Antp expression being confined to all LinA MNs solely in T2 and Ubx solely in T3 and this segment-specific expression pattern is maintained until the adult stage. Hox cofactors Exd and Hth are ubiquitously present from the larval until the adult stage. In this context, Antp and Ubx with their cofactors are required for LinA MN survival, and Antp with Hth are further required for the correct axonal and dendritic morphology and axonal branching (**Figure 1B**). We note that Hox proteins do not specify leg motoneurons *per se*, but assure instead motoneuron survival and offer a unique code for their correct branching to distinct leg parts. Interestingly, this highlighted the importance of Antp protein levels, serving as a timing mechanism for correct proximal (early born) vs. distal (late-born) axon targeting (Baek et al., 2013). Antp protein levels seem to play an instructive role as well in T2 vs. T3 somatic muscle pattern establishment (as mentioned above), suggesting that several Hox functions could be dose-dependent.

While looking for a genetic explanation for distinct morphological characteristics of individual motoneurons, an important role was attributed to anterior Hox *proboscipedia* (*pb*). Concentrating on the LinB (Lin24) lineage of leg MNs, it was demonstrated that Pb, expressed in three of seven neurons composing this population, is required for their proper dendritic morphology and axonal patterning (**Figure 1B**). Clonal removal of *pb* in T2 LinB MNs affected the linearity of path/stability during high speed walking (Enriquez et al., 2015).

A role for Hox in adult muscle innervation was also shown with Ubx whose misexpression in T2 MNs compromised adult IFM development (Dutta et al., 2010). Collectively, muscle development and homeostasis require both Hox autonomous and non-autonomous function, in the *Drosophila* mesoderm and neuroectoderm, respectively.

Hox Control of Vertebrate Neuromuscular Circuits

In vertebrates, abundant evidence argues toward an important Hox function in motor circuit establishment (reviewed in Jung and Dasen, 2015). For the correct locomotor circuitry establishment, a large variety of different MN subtypes need to form precise connections with target muscles. A well-studied group of MNs, spinal MNs display different columnar, divisional and pool identities allowing them to contact more than 50 different limb muscles. Concentrating on chick brachial lateral motor columnar (LMC) neurons, it was shown that Hox3, 4, 5, 7, and 8 proteins divide LMC into subdomains along the rostrocaudal axis. Importantly, changing MN transcriptional identity by manipulation of Hox protein levels resulted in corresponding changes in muscle connectivity. It has been proposed that in this context, Hox proteins confer different pool identities by regulating downstream transcription factors in MNs, such as Nkx6 (NK6 Homeobox 1) (Dasen et al., 2003, 2005). Hox6 proteins do not have a role in the initial LMC specification but are required for further LMC pool identity establishment and proper limb innervation (Lacombe et al., 2013). In the search for the link between neuronal identity specification by Hox and muscle innervation in chick and mice, the transcription factor FoxP1 (Forkhead box protein P1) was identified as a Hox accessory factor, allowing to fine-tune Hox output (Dasen et al., 2008). The molecular mechanism behind this process also involves cell surface receptor encoding genes *Ret proto-oncogene* (*Ret*) and *Glial cell line-derived neurotrophic factor receptor alpha* (*Gfrα*). In this context, Hox proteins in collaboration with their cofactor Meis1 were shown to regulate the spatial pattern and expression levels of these genes in LMC neurons, required for proper MN differentiation and connectivity (Catela et al., 2016). Interestingly, digit-innervating MNs in chick and mice also employ a Hox code for their specification, that is however different from the one used in more proximal limb muscles. In this context, joint expression of Hoxc8 and Hoxc9 are required for correct digit innervation (Mendelsohn et al., 2017).

Hox proteins not only control LMC neuromuscular circuitry at the limb level, but also at the thoracic level, where MNs innervating hypaxial muscles are specified by Hoxc9, acting as a repressor of a limb-innervating MN fate (Jung et al., 2010). Non-limb innervating MNs at the cervical spinal cord level within the phrenic motor column (PMC) also require Hox for their correct development. Interestingly, mice lacking *Hox5* genes (*Hoxa5* and *Hoxc5*) in these neurons die of respiratory failure as a consequence of altered diaphragm innervation (Philippidou et al., 2012; Philippidou and Dasen, 2013). Furthermore, spinocerebellar tract neurons (SCTNs) that relay sensory/proprioceptive information to the CNS from muscles and tendons also use Hox-dependent transcriptional program for their diversification. Discrete populations of SCTNs along rostro-caudal axis display a combinatorial expression of several Hox genes (from *Hox4* to *Hox10*) and their genetic

manipulation leads to defaults in muscle-cerebellum connectivity (Baek et al., 2019). Collectively, both spinal MNs and sensory SCTNs use Hox-code for their proper specification, suggesting a general role for Hox proteins in the proper muscle-neuron connectivity establishment.

CARDIAC MUSCLE

Hox Control of *Drosophila* Cardiac and Alary Muscles

Drosophila cardiac musculature develops during embryogenesis from lateral mesodermal cells that migrate toward the dorsal midline during dorsal closure and form a tube named the cardiac tube, also known as the dorsal vessel (reviewed in Monier et al., 2007; Bataillé et al., 2015; Rotstein and Paululat, 2016). The cardiac tube is subdivided into two parts, with the anterior narrow portion (T1–A4) named aorta and the posterior larger one (A5–A8) named heart, with the hemolymph flowing from the posterior to anterior, assuring its distribution throughout the organism (**Figure 1C**). Aorta can be further subdivided into anterior (T1–T3) and posterior (A1–A4) parts. In the anterior/thoracic aorta, each segment contains four pairs of cardiomyoblasts (CMs) that express the homeodomain-containing transcription factor Tinman (*tin*) (Nkx2.5 in vertebrates). The posterior/abdominal part is constituted of six pairs of CMs, with two anterior ones expressing the orphan nuclear receptor Seven-up (*svp*) (ortholog of Nuclear Receptor Subfamily 2 members) and the four posterior CM pairs expressing *tin* (except A8 that contains only two *tin*-expressing CM pairs). *Svp*-expressing cardioblasts in the heart further differentiate into ostiae, inflow valves that allow for the hemolymph pumping, accounting for the partially open circulatory system in *Drosophila* (Molina and Cripps, 2001). The metamerically repeated expression of *svp*, *tin* and other genes suggested the cell-identity specification in a segment-specific fashion. During metamorphosis, the heart part of the cardiac tube is histolyzed, and the adult heart develops from the larval posterior aorta myocytes that undergo a transdifferentiation without cell proliferation (Monier et al., 2005).

Hox genes have a rather complex expression pattern in the dorsal vessel. The anterior aorta is considered as a Hox-free region. The posterior aorta expresses *Antp* (in part of the T3, in A1 and weakly in A2 CM) and *Ubx* (from A2 to A5 CM) and the heart expresses *abd-A* (from the fifth pair of A5 CM to the second pair in A8) and *AbdB* (in the two posterior CM pairs in A8) in both cardioblasts and at least some pericardial cells (Lo et al., 2002; Lovato et al., 2002; Ponzielli et al., 2002; Zmojdzian et al., 2018; **Figure 1C**). Hox were shown to be responsible for dorsal vessel patterning in a cell-autonomous fashion (reviewed in Monier et al., 2007). Independent studies demonstrated that Ubx and AbdA are responsible for heart cardioblast specification (**Figure 1C**). In *abd-A* null embryos the heart is transformed into the aorta and conversely, its mesodermal overexpression is sufficient to specify aorta as heart cardioblasts instead (Lo et al., 2002; Ponzielli et al., 2002). In *Ubx* or *Ubx/abd-A* double mutants, the anterior part of the aorta is affected (Ponzielli et al., 2002). Antp does not specify cardiac lineage *per se* but generates CM diversity by controlling *svp* expression in the A1 segment (Perrin et al., 2004). Interestingly, *AbdB* mesodermal overexpression suppresses cardiac fate while its loss-of-function leads to supernumerary cardioblasts but also somatic nuclei (Lovato et al., 2002; Ponzielli et al., 2002). The combined mutations of *Scr*, *Antp*, *Ubx*, *abd-A*, and *AbdB* transformed the whole dorsal vessel into the aorta, further showing that the aorta fate is a ground state of the cardiac tube (Perrin et al., 2004).

Even though Hox proteins clearly regulate the cell lineage choice between the anterior aorta and posterior aorta/heart only a few of their target genes involved in this process have so far been identified. Antp, Ubx, and AbdA control *svp* expression in their respective segments in the embryonic heart, a function that can be once again considered as generic (Perrin et al., 2004; Ryan et al., 2005). *Svp* itself was shown to be regulated by Hedgehog (Hh) signaling coming from the ectoderm. Interestingly, it was suggested that cardioblasts can respond to Hh signals only in Hox-expressing cells, explaining why the anterior aorta (a Hox-free region) does not express *svp* even though it receives Hh (Ryan et al., 2005). To explain heart-patterning control by Hox, it was suggested that Hox could regulate symmetric/asymmetric division of progenitors giving rise to *tin* and *svp*-expressing cardioblasts and pericardiac cells, although this hypothesis remains to be tested. AbdA regulates the expression of *Troponin C-akin-1* (*Tina-1*), a heart-specific marker, of unspecified function (Lovato et al., 2002). Some target genes were identified at later stages, where Hox further pattern the individual cardiomyoblasts. AbdA in collaboration with Svp was suggested to activate *Wg* expression in heart cardioblasts expressing *svp*. In the Tin-expressing cardioblasts, AbdA activates expression of a Na^+-driven anion exchanger (*ndae1*), involved in ionic homeostasis (Perrin et al., 2004). No gene level mechanisms explaining the Hox cardiac target gene regulation have however been identified, leaving the possibility of the existence of tissue-specific *cis*-regulatory modules used by Hox, as is the case of the somatic musculature.

Interestingly, ecdysone-dependent repression of Ubx in A1-A4 *tin*-expressing myocytes is required during the mid-pupal stage for adult heart formation (**Figure 1C**). Adult heart develops during metamorphosis by a remodeling of the larval posterior aorta. If Ubx expression is maintained during pupal stages in posterior aorta *tin*-expressing cells, they adopt A5 characteristics, resulting in the adult remodeling alteration (Monier et al., 2005). This argues in favor of a hypothesis stipulating that in the process of organogenesis, Hox input is necessary for the activation of downstream signaling networks but once these are activated, Hox presence is no longer needed and can be even detrimental for the rest of the development (Hombría and Lovegrove, 2003). The modification of AbdA is also required for heart metamorphosis, but occurring at the functional instead of expression level, yet also in an ecdysone-dependent manner (**Figure 1C**). Instead of conferring heart fate to the CMs like AbdA does during embryogenesis, here it regulates the reprogramming of A5 segment that becomes the terminal chamber in the adult. It is interesting to note that the switch in AbdA function occurs also at the transcriptional level, where early during development

AbdA regulates positively *Ih* (a voltage-gated ion channel) expression but represses it in the pupa (Monier et al., 2005). We highlight that Hth is expressed only in the anterior aorta which does not express any Hox (Perrin et al., 2004), and thus Hox function in the *Drosophila* cardiac tube, like in the somatic muscle development (Bryantsev et al., 2012) is independent of Exd/Hth cofactors.

Besides cardiac muscle, Hox also control the patterning of seven pairs of alary muscles (AMs), specialized skeletal muscle connecting the cardiac tube at the level of Svp-expressing pericardial cells, with the lateral exoskeleton (LaBeau et al., 2009; Bataillé et al., 2015; **Figure 1C**). AMs were recently shown to maintain the dorsal vessel at the tracheal trunk position (Bataillé et al., 2020). During metamorphosis, four AM pairs remain, originating from larval posterior AMs (Lehmacher et al., 2012). Interestingly, three anterior AM pairs undergo a process of dedifferentiation and give rise to adult ventral longitudinal muscles (VLMs) of unknown function (Molina and Cripps, 2001; Schaub et al., 2015). Two Hox genes are expressed in AMs at the embryonic stage, *Ubx* in the three most anterior pairs and *abd-A* in the four posterior AM pairs. Consistent with the Ubx expression pattern, in *Ubx* mutant embryos, 2–3 anterior AM pairs do not form. The absence of AbdA does not compromise posterior AM formation, probably because Ubx and AbdA functions are redundant in this context. Conversely, Ubx or AbdA overexpression leads to supernumerary AM (LaBeau et al., 2009). Furthermore, modulation of Hox expression is required for correct AM transdifferentiation, since overexpression of AbdA in anterior AMs, leading to Ubx suppression, prevents VLM formation (**Figure 1C**). Like in the case of cardiac tube remodeling, ecdysone signaling is also required for AM transdifferentiation (Schaub et al., 2015). However, it is not known whether in this case ecdysone pathway modulates Hox activity like during adult heart development. Concerning Hox target genes, *optomor-blind-related-gene-1* (*org-1*, ortholog of vertebrate T-box Transcription factor Tbx1) was proposed as being directly or indirectly regulated by Ubx during adult VLM formation (Schaub et al., 2015). Knowing that *org-1* is also required for embryonic AM development, it is possible that Ubx (and also AbdA) could regulate *org-1* also during this stage (Boukhatmi et al., 2014).

Hox Control of Vertebrate Cardiac Muscle

Many similarities can be found between *Drosophila* and vertebrate cardiac myogenesis even though at a first glance they seem very distinct. Both are developed from mesodermal precursors that converge toward the midline to give rise to a linear, contractile tube, that is further looped and developed into a multi-chambered organ in vertebrates (Zaffran and Frasch, 2002; Zaffran and Kelly, 2012; Lescroart and Zaffran, 2018). In birds and mammalians, cardiogenic precursors/first heart field progenitors (FHF) converging at the anterior midline express Mesp1 (Mesoderm Posterior bHLH Transcription Factor 1) and form a so-called "cardiac crescent." The cardiac crescent develops into a transient heart tube with an inner endocardial and outer myocardial layer that will mainly contribute to the left ventricle. The heart tube elongates by the addition of second heart field (SHF) progenitors, located in the pharyngeal mesoderm (itself formed by cells of both splanchnic and paraxial mesoderm). SHF segregates along the AP axis into posterior SHF, contributing to the atrial myocardium at the venous pole and anterior SHF (also called AHF) that contribute to the outflow tract (OFT) (connecting the ventricles to the future aorta) and the right ventricle at the arterial pole. The heart is finally shaped by rightward looping and myocardium expansion leading to the formation of four integrated cardiac chambers, two ventricles and two atria. A specialized population of neural crest cells (NCC) contribute to the development of large arteries and outflow septum. A large number of inductive signaling molecules have been linked with vertebrate cardiac development, such as NK homeodomain proteins (e.g., Nkx2.5, *Drosophila tinman* ortholog), GATA (*Drosophila pannier* ortholog) and T-box families.

In contrast to skeletal muscles, a role for Hox in vertebrate cardiac muscle development is very well established (reviewed in Lescroart and Zaffran, 2018). It was recently shown that anterior Hox genes (*Hoxa1*, *Hoxa2*, *Hoxb1*, and *Hoxb2*) are expressed in a subpopulation of Mesp1-expressing cardiovascular progenitors that seem to be the last to emerge from the primitive streak. Interestingly, progenitors that do not express Hox seem to be unipotent in contrast with Hox-expressing progenitors that are bipotent, contributing either to cardiomyocytes and smooth muscles or cardiomyocytes and endothelial cells (Lescroart et al., 2014, 2018). Hox genes (*Hoxa1*, *Hoxa3*, and *Hoxb1*) are also expressed in SHF progenitors and their expression patterns subdivide this cell population in distinct domains: *Hoxa1* and *Hoxb1* are expressed in AHF with different anterior limits and *Hoxa3* is expressed in posterior SHF. While these progenitors contribute to both poles of the heart, *Hoxb1*-expressing progenitors are found only in the proximal OFT and atria and cells expressing *Hoxa1* and *Hoxa3* only in the distal OFT and some regions of the atria. SHF cells are thus pre-patterned before their addition to the developing heart (Bertrand et al., 2011). The same Hox genes are differentially expressed along the rostro-caudal axis in cardiac NCCs (Bertrand et al., 2011; Lescroart and Zaffran, 2018).

Concerning the role of Hox in cardiac development, it has been suggested (although not directly demonstrated) that *Hoxb1* could play a role in cardiac progenitor migration from the primitive streak (Lescroart and Zaffran, 2018). Mice mutant for *Hoxa1* develop heart patterning defects, such as OFT malformations, that have been also observed in human patients, giving a direct role to *Hoxa1* in OFT patterning (Makki and Capecchi, 2012). Additionally, mice lacking *Hoxb1* display OFT and ventricular septum (wall separating the two ventricles) defects. In this case, *Hoxb1* mutation led on the one hand to the upregulation of *fgf8* levels and abnormal SHF proliferation and on the other hand the upregulation of the SHF differentiation markers, α-actinin and MF20 and thus premature SHF differentiation. Furthermore, in compound *Hoxa1*, *Hoxb1* mutant mice, the OFT and ventral septum deficits were exacerbated, suggesting a genetic interaction

between them (Roux et al., 2015). Interestingly, not only *Hoxb1* loss of function but also its overexpression leads to cardiac malformations (Zaffran et al., 2018). Extending this concept further, transcriptional profiling has shown that *Hoxb1* activates the posterior program of the SHF and inhibits the premature differentiation of progenitors by directly repressing *Natriuretic peptide precursor A* (*Nppa*) and *B* (*Nppb*) expression (Stefanovic et al., 2020).

Anterior Hox genes also play a role in cardiac NCC (Chisaka and Capecchi, 1991; Roux et al., 2017). *Hoxa3*-mutant mice display defects in carotid arteries as well as defaults in size and shape of heart compartments (Chisaka and Capecchi, 1991). *Hoxa1* and *Hoxb1* are required for cardiac NCC migration and their mutation leads to subsequent large artery patterning and outflow septum defects (Roux et al., 2017). Interestingly, an *in vitro* study using mouse embryonic stem cells has demonstrated a role for *Hoxa10* in the timing of cardiac cell differentiation, suggesting an unexpected role for posterior Hox in vertebrate cardiac development (Behrens et al., 2013). In contrast to *Drosophila* heart development, Hox PBC/MEIS cofactors were found to be associated with Hox function in vertebrates (Lescroart and Zaffran, 2018).

VISCERAL MUSCLE

Hox Control of *Drosophila* Visceral Musculature

The *Drosophila* gut is formed by the assembly of cells originating from all three germ layers; ectodermal, endodermal and mesodermal cells. The mesodermal visceral muscles are located in the external midgut layer surrounding the endoderm and are responsible for peristaltic movements. Five Hox genes (*Scr*, *Antp*, *Ubx*, *abd-A*, and *AbdB*) are expressed in the midgut visceral mesoderm and all except *Scr* and *AbdB* pattern the unsegmented gut together with ectodermal cues. Their expression in this tissue is parasegmental (*Scr* and *AbdB* excepted), and non-overlapping (a parasegment is a metameric unit composed of a posterior part of one segment and an anterior part of the adjacent segment). *Scr* mostly overlaps with PS4, *Antp* is expressed in PS5 and 6, *Ubx* in PS7, *abd-A* in PS8-12 and *AbdB* in the end of the midgut (**Figure 1D**). Curiously, there is a one-to-two cell gap between *Scr* and *Antp* expression domains. In the gut inner endoderm only *labial* (*lab*) expression can be detected (Diederich et al., 1989). Antp, Ubx, and AbdA are responsible for three midgut constrictions establishment, subdividing the midgut into four distinct chambers and seemingly helping to the proper gut elongation (**Figure 1D**). In homozygous *Antp* mutant embryos, the first constriction doesn't form (Tremml and Bienz, 1989; Reuter and Scott, 1990). The establishment of the second constriction is dependent on both Ubx and AbdA. The third constriction is fully specified by AbdA (Tremml and Bienz, 1989). Scr is not involved in midgut subdivision, but in *Scr* mutant conditions, four protrusions located in the anterior midgut called gastric caeca do not form (Reuter and Scott, 1990). Finally, AbdB is required for the gut left-right asymmetry establishment by controlling the activity of a gene encoding for the type ID unconventional myosin (*myosinID*), a function presumed to be independent of Hox patterning function (Coutelis et al., 2013; **Figure 1D**).

Concerning Hox target genes in the visceral mesoderm, it was first predicted that Hox could regulate cytoskeleton or genes able to drive mesodermal cell contraction around the underlying endoderm, explaining the constriction establishment (Reuter and Scott, 1990). One such gene was identified, *beta3-tubulin*, encoding a cytoskeleton-associated protein whose expression is regulated by Ubx (Hinz et al., 1992). Importantly, Ubx is required for *decapentaplegic* (*dpp*) expression in the visceral mesoderm and together with AbdA controls *wingless* (*wg*) expression (Immerglück et al., 1990). The *cis*-regulatory region in the *dpp* gene regulated directly by Ubx and AbdA has been successfully identified and constituted the first example of a Hox target gene enhancer (Capovilla et al., 1994). Later, the enhancer in *wg* gene bound by AbdA and Mad (Mothers against dpp, transcription factor and Dpp signaling target), driving its expression was also identified (Grienenberger et al., 2003). In this particular case, the sole AbdA binding without Dpp input does not allow *wg* activation, once again demonstrating that a cooperative binding between Hox and transcription factors is required to convey a proper cell fate. All the following visceral mesoderm target genes identified are activated by Wg or Dpp and are thus indirect targets: In the anterior midgut mesoderm, Antp regulates *teashirt* (*tsh*) expression and Ubx, AbdA, Wg, and Dpp regulate its expression in the central part (Mathies et al., 1994). Through Wg and Dpp signaling, Ubx and AbdA activate *pointed* (*pnt*) and *odd-paired* (*opa*) in the specific posterior midgut mesodermal regions (Bilder et al., 1998).

Hox Control of Vertebrate Visceral Musculature

In vertebrates as in *Drosophila*, the gut develops both from endoderm and mesoderm. More precisely, it develops from the splanchnic mesoderm, itself derived from the lateral plate mesoderm. The splanchnic mesoderm and the endoderm involute to form a primitive gut tube. The tube develops further into foregut, midgut comprising the small intestine, cecum and anterior portion of the large intestine and hindgut comprising the remainder of the large intestine and rectum. Hox genes are collinearly expressed along the lateral plate mesodermal component of the gut but also in the endoderm and the expression of many persists in the adult (Beck et al., 2000; Beck, 2002). The detailed, complex Hox expression patterns in different organs of the gut mesoderm has been extensively summarized previously (Beck et al., 2000; Choi et al., 2006).

Few Hox functions have been identified in the mouse gut, notably because of the co-expression in the same gut regions of two or more Hox from different paralogous groups, leading to high functional redundancy. Despite this, it has been shown that *Hoxd13* and *Hoxd12* are required for the generation of the anal sphincter (Kondo et al., 1996). When all *Hoxd* genes are deleted (except *Hoxd1* and *Hoxd3*) the ileocecal sphincter (separating small and large intestine) doesn't form and the ileocecal smooth-musculature is disorganized (Zákány and Duboule, 1999). Hox

genes are thus clearly required to pattern the unsubdivided gut mesoderm both in *Drosophila* and vertebrates. Similarly, deletion of the anterior part of the *HoxD* locus (from *Hoxd1* to *Hoxd10*) provokes agenesis of the caecum (at the junction of the ileum and large intestine). Interestingly, it has been demonstrated that it is not the combined deletion of these genes but instead the resulting strong ectopic *Hoxd12* expression that accounts for this phenotype (Zacchetti et al., 2007). Trying to find a common framework for the role of the different *HoxD* genes, it has been recently reported that *Hoxd3* deletion alone results in gut growth deficit, giving an essential role in the gut development to this Hox gene (Zakany et al., 2017).

A role has also been attributed to Hox genes from other paralogous groups, such as *Hoxc4*, whose deletion results in esophageal musculature disorganization and obstruction of the organ (Boulet and Capecchi, 1996). Mice carrying a *Hoxa4* transgene, resulting in its strong overexpression in the gut, develop a congenital megacolon phenotype characterized by a largely distended colon (Wolgemuth et al., 1989). Deletion of *Hoxa5* leads to stomach morphogenesis defaults, presumably by controlling the epithelio-mesenchymal signaling. Indeed, in the *Hoxa5*-deficient mice stomach epithelium, the expression pattern of *Ihh*, *Shh*, and *Fgf10* changed and the expression levels of *Ptc* and *Gli* increased (Aubin et al., 2002). Misexpression of *Hoxc8* under the control of *Hoxa4* regulatory elements, resulting in a shift in the anterior boundary of its expression, results in several hamartomatous lesions, where gastric epithelium was found embedded within the stomach musculature (Pollock et al., 1992).

CONCLUDING REMARKS

Hox genes are involved in the patterning of all muscle types in *Drosophila* and vertebrates. While how they achieve this is not completely resolved, plethora studies in different model organisms have gone a long way to determine their role in the numerous muscle types. One emerging concept would appear that Hox act at numerous stages of muscle development, where at early stages, Hox appear to play a specifying role by providing spatial cues along the anterior–posterior axis, and at later stages controlling basic cellular functions such as proliferation, cell survival, death etc. This follows the role Hox play in patterning of the ectoderm and so it is perhaps without surprise that Hox contribute similarly in muscle development through mesoderm patterning.

As in patterning of the ectoderm, in muscle development there is often requirement for the cooperation between Hox and other tissue-specific transcription factors, which are themselves Hox target genes together with signaling molecules. Examples about Hox functional conservation can be found mainly in vertebrate cardiac muscle, but conservation also exists in skeletal and gut muscles, further suggesting a universal role for Hox in mesodermal patterning. While how this achieved is not fully understood, knowledge gained in how Hox generate diversity in the CNS should help understand their role in generating different muscle types, which together allow for the development of more complex organisms.

Even though a large number of Hox-dependent functions across different mesodermal derivatives are now known, there is however only sparse evidence about the underlying molecular mechanisms. To fully understand how Hox orchestrate muscle development, it is essential to define the network of genes they regulate, in addition to the tissue-specific transcription factors such as the identity TFs in muscle and temporal TFs in the CNS. The discovery of novel *cis*-regulatory regions of Hox target genes was historically a difficult and laborious process, but now with the vast advances in genome-wide approaches, both spatially and temporally, at the level of whole tissue or single cell, it is soon possible to better define Hox regulatory regions and target genes. Such a genome-wide spatio-temporal approach will thus allow us to fully grasp the complex and intricate networks defining how Hox proteins regulate muscle development.

AUTHOR CONTRIBUTIONS

GP designed and drew illustrations, and wrote the manuscript with inputs from CM-Z, YG, and AS. All authors contributed to the article and approved the submitted version.

ACKNOWLEDGMENTS

The authors would like to thank the Fondation ARC (grant PJA 20181208014) and AFM-Téléthon (grant 23721) for financial support of their research.

REFERENCES

Alvares, L. E., Schubert, F. R., Thorpe, C., Mootoosamy, R. C., Cheng, L., Parkyn, G., et al. (2003). Intrinsic, Hox-dependent cues determine the fate of skeletal muscle precursors. *Dev. Cell* 5, 379–390. doi: 10.1016/S1534-5807(03)00263-6

Aubin, J., Déry, U., Lemieux, M., Chailler, P., and Jeannotte, L. (2002). Stomach regional specification requires Hoxa5-driven mesenchymal-epithelial signaling. *Development* 129, 4075–4087. doi: 10.1242/dev.129.17.4075

Baek, M. (2011). *Development of Leg Motor Neurons in Drosophila Melanogaster*. Ph.D. thesis. New York, NY: Columbia University. doi: 10.7916/D84J0N30

Baek, M., Enriquez, J., and Mann, R. S. (2013). Dual role for Hox genes and Hox co-factors in conferring leg motoneuron survival and identity in *Drosophila*. *Development* 140, 2027–2038. doi: 10.1242/dev.090902

Baek, M., Menon, V., Jessell, T. M., Hantman, A. W., and Dasen, J. S. (2019). Molecular logic of spinocerebellar tract neuron diversity and connectivity. *Cell Rep.* 27, 2620–2635.e4. doi: 10.1016/j.celrep.2019.04.113

Bataillé, L., Colombié, N., Pelletier, A., Paululat, A., Lebreton, G., Carrier, Y., et al. (2020). Alary muscles and thoracic alary-related muscles are atypical striated muscles involved in maintaining the position of internal organs. *Development* 147:dev185645. doi: 10.1242/dev.185645

Bataillé, L., Frendo, J.-L., and Vincent, A. (2015). Hox control of *Drosophila* larval anatomy; The Alary and Thoracic Alary-Related Muscles. *Mech. Dev.* 138(Pt 2), 170–176. doi: 10.1016/j.mod.2015.07.005

Baylies, M. K., and Bate, M. (1996). twist: a myogenic switch in *Drosophila*. *Science* 272, 1481–1484. doi: 10.1126/science.272.5267.1481

Beck, F. (2002). Homeobox genes in gut development. *Gut* 51, 450–454. doi: 10.1136/gut.51.3.450

Beck, F., Tata, F., and Chawengsaksophak, K. (2000). Homeobox genes and gut development. *BioEssays* 22, 431–441. doi: 10.1002/(SICI)1521-1878(200005)22:5<431::AID-BIES5>3.0.CO;2-X

Behrens, A. N., Iacovino, M., Lohr, J. L., Ren, Y., Zierold, C., Harvey, R. P., et al. (2013). Nkx2-5 mediates differential cardiac differentiation through interaction with Hoxa10. *Stem Cells Dev.* 22, 2211–2220. doi: 10.1089/scd.2012.0611

Bertrand, N., Roux, M., Ryckebüsch, L., Niederreither, K., Dollé, P., Moon, A., et al. (2011). Hox genes define distinct progenitor sub-domains within the second heart field. *Dev. Biol.* 353, 266–274. doi: 10.1016/j.ydbio.2011.02.029

Bilder, D., Graba, Y., and Scott, M. P. (1998). Wnt and TGFbeta signals subdivide the AbdA Hox domain during Drosophila mesoderm patterning. *Development* 125, 1781–1790. doi: 10.1242/dev.125.9.1781

Biressi, S., Tagliafico, E., Lamorte, G., Monteverde, S., Tenedini, E., Roncaglia, E., et al. (2007). Intrinsic phenotypic diversity of embryonic and fetal myoblasts is revealed by genome-wide gene expression analysis on purified cells. *Dev. Biol.* 304, 633–651. doi: 10.1016/j.ydbio.2007.01.016

Birkholz, O., Vef, O., Rogulja-Ortmann, A., Berger, C., and Technau, G. M. (2013). Abdominal-B and caudal inhibit the formation of specific neuroblasts in the *Drosophila* tail region. *Development* 140, 3552–3564. doi: 10.1242/dev.096099

Boukhatmi, H., Schaub, C., Bataillé, L., Reim, I., Frendo, J.-L., Frasch, M., et al. (2014). An Org-1–Tup transcriptional cascade reveals different types of alary muscles connecting internal organs in *Drosophila*. *Development* 141, 3761–3771. doi: 10.1242/dev.111005

Boulet, A. M., and Capecchi, M. R. (1996). Targeted disruption of hoxc-4 causes esophageal defects and vertebral transformations. *Dev. Biol.* 177, 232–249. doi: 10.1006/dbio.1996.0159

Bryantsev, A. L., Duong, S., Brunetti, T. M., Chechenova, M. B., Lovato, T. L., Nelson, C., et al. (2012). Extradenticle and homothorax control adult muscle fiber identity in *Drosophila*. *Dev. Cell* 23, 664–673. doi: 10.1016/j.devcel.2012.08.004

Capovilla, M., Brandt, M., and Botas, J. (1994). Direct regulation of decapentaplegic by *Ultrabithorax* and its role in Drosophila midgut morphogenesis. *Cell* 76, 461–475. doi: 10.1016/0092-8674(94)90111-2

Capovilla, M., Kambris, Z., and Botas, J. (2001). Direct regulation of the muscle-identity gene apterous by a Hox protein in the somatic mesoderm. *Development* 128, 1221–1230. doi: 10.1242/dev.128.8.1221

Carmena, A., Buff, E., Halfon, M. S., Gisselbrecht, S., Jiménez, F., Baylies, M. K., et al. (2002). Reciprocal regulatory interactions between the Notch and Ras signaling pathways in the *Drosophila* embryonic mesoderm. *Dev. Biol.* 244, 226–242. doi: 10.1006/dbio.2002.0606

Carmena, A., Gisselbrecht, S., Harrison, J., Jiménez, F., and Michelson, A. M. (1998). Combinatorial signaling codes for the progressive determination of cell fates in the *Drosophila* embryonic mesoderm. *Genes Dev.* 12, 3910–3922. doi: 10.1101/gad.12.24.3910

Catela, C., Shin, M. M., Lee, D. H., Liu, J.-P., and Dasen, J. S. (2016). Hox proteins coordinate motor neuron differentiation and connectivity programs through Ret/Gfrα genes. *Cell Rep.* 14, 1901–1915. doi: 10.1016/j.celrep.2016.01.067

Chal, J., and Pourquié, O. (2017). Making muscle: skeletal myogenesis in vivo and in vitro. *Development* 144, 2104–2122. doi: 10.1242/dev.151035

Chaturvedi, D., Reichert, H., Gunage, R. D., and VijayRaghavan, K. (2017). Identification and functional characterization of muscle satellite cells in *Drosophila*. *ELife* 6:e30107. doi: 10.7554/eLife.30107.021

Chevallier, A., Kieny, M., and Mauger, A. (1977). Limb-somite relationship: origin of the limb musculature. *Development* 41, 245–258. doi: 10.1242/dev.41.1.245

Chisaka, O., and Capecchi, M. R. (1991). Regionally restricted developmental defects resulting from targeted disruption of the mouse homeobox gene hox-1.5. *Nature* 350, 473–479. doi: 10.1038/350473a0

Choi, M. Y., Romer, A. I., Hu, M., Lepourcelet, M., Mechoor, A., Yesilaltay, A., et al. (2006). A dynamic expression survey identifies transcription factors relevant in mouse digestive tract development. *Development* 133, 4119–4129. doi: 10.1242/dev.02537

Christ, B., Jacob, H. J., and Jacob, M. (1977). Experimental analysis of the origin of the wing musculature in avian embryos. *Anat. Embryol.* 150, 171–186. doi: 10.1007/BF00316649

Coutelis, J.-B., Géminard, C., Spéder, P., Suzanne, M., Petzoldt, A. G., and Noselli, S. (2013). Drosophila left/right asymmetry establishment is controlled by the Hox gene abdominal-B. *Dev. Cell* 24, 89–97. doi: 10.1016/j.devcel.2012.11.013

Dasen, J. S., De Camilli, A., Wang, B., Tucker, P. W., and Jessell, T. M. (2008). Hox repertoires for motor neuron diversity and connectivity gated by a single accessory factor, *FoxP1*. *Cell* 134, 304–316. doi: 10.1016/j.cell.2008.06.019

Dasen, J. S., Liu, J.-P., and Jessell, T. M. (2003). Motor neuron columnar fate imposed by sequential phases of Hox-c activity. *Nature* 425, 926–933. doi: 10.1038/nature02051

Dasen, J. S., Tice, B. C., Brenner-Morton, S., and Jessell, T. M. (2005). A Hox regulatory network establishes motor neuron pool identity and target-muscle connectivity. *Cell* 123, 477–491. doi: 10.1016/j.cell.2005.09.009

Diederich, R. J., Merrill, V. K., Pultz, M. A., and Kaufman, T. C. (1989). Isolation, structure, and expression of labial, a homeotic gene of the Antennapedia Complex involved in *Drosophila* head development. *Genes Dev.* 3, 399–414. doi: 10.1101/gad.3.3.399

Dixit, R., Vijayraghavan, K., and Bate, M. (2008). Hox genes and the regulation of movement in *Drosophila*. *Dev. Neurobiol.* 68, 309–316. doi: 10.1002/dneu.20589

Dobi, K. C., Schulman, V. K., and Baylies, M. K. (2015). Specification of the somatic musculature in *Drosophila*: Specification of the somatic musculature in *Drosophila*. *Wiley Interdiscip. Rev. Dev. Biol.* 4, 357–375. doi: 10.1002/wdev.182

Domsch, K., Schröder, J., Janeschik, M., Schaub, C., and Lohmann, I. (2021). The Hox transcription factor Ubx ensures somatic myogenesis by suppressing the mesodermal master regulator twist. *Cell Rep.* 34:108577. doi: 10.1016/j.celrep.2020.108577

Dutta, D., Umashankar, M., LewisEdward, B., Rodrigues, V., and VijayRaghavan, K. (2010). Hox genes regulate muscle founder cell pattern autonomously and regulate morphogenesis through motor neurons. *J. Neurogenet.* 24, 95–108. doi: 10.3109/01677063.2010.494317

Egger, M. D., Harris, S., Peng, B., Schneiderman, A. M., and Wyman, R. J. (1990). Morphometric analysis of thoracic muscles in wildtype and in bithorax *Drosophila*. *Anat. Rec.* 226, 373–382. doi: 10.1002/ar.1092260315

Endo, T. (2015). Molecular mechanisms of skeletal muscle development, regeneration, and osteogenic conversion. *Bone* 80, 2–13. doi: 10.1016/j.bone.2015.02.028

Enriquez, J., and Vincent, A. (2010). Segmental variations in the patterns of somatic muscles: what roles for Hox? *Fly* 4, 249–252. doi: 10.4161/fly.4.3.12281

Enriquez, J., Boukhatmi, H., Dubois, L., Philippakis, A. A., Bulyk, M. L., Michelson, A. M., et al. (2010). Multi-step control of muscle diversity by Hox proteins in the *Drosophila* embryo. *Development* 137, 457–466. doi: 10.1242/dev.045286

Enriquez, J., Venkatasubramanian, L., Baek, M., Peterson, M., Aghayeva, U., and Mann, R. S. (2015). Specification of individual adult motor neuron morphologies by combinatorial transcription factor codes. *Neuron* 86, 955–970. doi: 10.1016/j.neuron.2015.04.011

Estacio-Gómez, A., and Díaz-Benjumea, F. J. (2014). Roles of Hox genes in the patterning of the central nervous system of *Drosophila*. *Fly* 8, 26–32. doi: 10.4161/fly.27424

Evano, B., Gill, D., Hernando-Herraez, I., Comai, G., Stubbs, T. M., Commere, P.-H., et al. (2020). Transcriptome and epigenome diversity and plasticity of muscle stem cells following transplantation. *PLoS Genet.* 16:e1009022. doi: 10.1371/journal.pgen.1009022

Fernandes, J., Bate, M., and Vijayraghavan, K. (1991). Development of the indirect flight muscles of *Drosophila*. *Development* 113, 67–77. doi: 10.1242/dev.113.1.67

Fernandes, J., Celniker, S. E., Lewis, E. B., and VijayRaghavan, K. (1994). Muscle development in the four-winged *Drosophila* and the role of the *Ultrabithorax* gene. *Curr. Biol.* 4, 957–964. doi: 10.1016/S0960-9822(00)00219-0

Friedrich, J., Sorge, S., Bujupi, F., Eichenlaub, M. P., Schulz, N. G., Wittbrodt, J., et al. (2016). Hox function is required for the development and maintenance of the *Drosophila* feeding motor unit. *Cell Rep.* 14, 850–860. doi: 10.1016/j.celrep.2015.12.077

Graba, Y., Gieseler, K., Aragnol, D., Laurenti, P., Mariol, M. C., Berenger, H., et al. (1995). DWnt-4, a novel *Drosophila* Wnt gene acts downstream of homeotic complex genes in the visceral mesoderm. *Development* 121, 209–218. doi: 10.1242/dev.121.1.209

Greig, S., and Akam, M. (1993). Homeotic genes autonomously specify one aspect of pattern in the *Drosophilla* mesoderm. *Nature* 362, 630–632. doi: 10.1038/362630a0

Grienenberger, A., Merabet, S., Manak, J., Iltis, I., Fabre, A., Bérenger, H., et al. (2003). Tgfβ signaling acts on a Hox response element to confer specificity and diversity to Hox protein function. *Development* 130, 5445–5455. doi: 10.1242/dev.00760

Gunage, R. D., Dhanyasi, N., Reichert, H., and VijayRaghavan, K. (2017). Drosophila adult muscle development and regeneration. *Semin. Cell Dev. Biol.* 72, 56–66. doi: 10.1016/j.semcdb.2017.11.017

Hessinger, C., Technau, G. M., and Rogulja-Ortmann, A. (2017). The *Drosophila* Hox gene *Ultrabithorax* acts in both muscles and motoneurons to orchestrate formation of specific neuromuscular connections. *Development* 144, 139–150. doi: 10.1242/dev.143875

Hinz, U., Wolk, A., and Renkawitz-Pohl, R. (1992). Ultrabithorax is a regulator of beta 3 tubulin expression in the Drosophila visceral mesoderm. *Development* 116, 543–554. doi: 10.1242/dev.116.3.543

Hombría, J. C.-G., and Lovegrove, B. (2003). Beyond homeosis—HOX function in morphogenesis and organogenesis. *Differentiation* 71, 461–476. doi: 10.1046/j.1432-0436.2003.7108004.x

Hooper, J. E. (1986). Homeotic gene function in the muscles of *Drosophila* larvae. *EMBO J.* 5, 2321–2329. doi: 10.1002/j.1460-2075.1986.tb04500.x

Immerglück, K., Lawrence, P. A., and Bienz, M. (1990). Induction across germ layers in *Drosophila* mediated by a genetic cascade. *Cell* 62, 261–268. doi: 10.1016/0092-8674(90)90364-K

Jorgensen, E. M., and Garber, R. L. (1987). Function and misfunction of the two promoters of the *Drosophila Antennapedia* gene. *Genes Dev.* 1, 544–555. doi: 10.1101/gad.1.6.544

Jung, H., and Dasen, J. S. (2015). Evolution of patterning systems and circuit elements for locomotion. *Dev. Cell* 32, 408–422. doi: 10.1016/j.devcel.2015.01.008

Jung, H., Lacombe, J., Mazzoni, E. O., Liem, K. F., Grinstein, J., Mahony, S., et al. (2010). Global control of motor neuron topography mediated by the repressive actions of a single hox gene. *Neuron* 67, 781–796. doi: 10.1016/j.neuron.2010.08.008

Karlsson, D., Baumgardt, M., and Thor, S. (2010). Segment-specific neuronal subtype specification by the integration of anteroposterior and temporal cues. *PLoS Biol.* 8:e1000368. doi: 10.1371/journal.pbio.1000368

Kondo, T., Dolle, P., Zakany, J., and Duboule, D. (1996). Function of posterior HoxD genes in the morphogenesis of the anal sphincter. *Development* 122, 2651–2659. doi: 10.1242/dev.122.9.2651

LaBeau, E. M., Trujillo, D. L., and Cripps, R. M. (2009). Bithorax complex genes control alary muscle patterning along the cardiac tube of *Drosophila*. *Mech. Dev.* 126, 478–486. doi: 10.1016/j.mod.2009.01.001

Lacombe, J., Hanley, O., Jung, H., Philippidou, P., Surmeli, G., Grinstein, J., et al. (2013). Genetic and functional modularity of Hox activities in the specification of limb-innervating motor neurons. *PLoS Genet.* 9:e1003184. doi: 10.1371/journal.pgen.1003184

Lawrence, P. A., and Brower, D. L. (1982). Myoblasts from *Drosophila* wing disks can contribute to developing muscles throughout the fly. *Nature* 295, 55–57. doi: 10.1038/295055a0

Lawrence, P. A., and Johnston, P. (1984). The genetic specification of pattern in a *Drosophila* muscle. *Cell* 36, 775–782. doi: 10.1016/0092-8674(84)90357-X

Lehmacher, C., Abeln, B., and Paululat, A. (2012). The ultrastructure of *Drosophila* heart cells. *Arthropod Struct. Dev.* 41, 459–474. doi: 10.1016/j.asd.2012.02.002

Lescroart, F., and Zaffran, S. (2018). Hox and Tale transcription factors in heart development and disease. *Int. J. Dev. Biol.* 62, 837–846. doi: 10.1387/ijdb.180192sz

Lescroart, F., Chabab, S., Lin, X., Rulands, S., Paulissen, C., Rodolosse, A., et al. (2014). Early lineage restriction in temporally distinct populations of Mesp1 progenitors during mammalian heart development. *Nat. Cell Biol.* 16, 829–840. doi: 10.1038/ncb3024

Lescroart, F., Wang, X., Lin, X., Swedlund, B., Gargouri, S., Sànchez-Dànes, A., et al. (2018). Defining the earliest step of cardiovascular lineage segregation by single-cell RNA-seq. *Science* 359, 1177–1181. doi: 10.1126/science.aao4174

Li, L., Xiong, W.-C., and Mei, L. (2018). Neuromuscular junction formation, aging, and disorders. *Annu. Rev. Physiol.* 80, 159–188. doi: 10.1146/annurev-physiol-022516-034255

Lo, P. C. H., Skeath, J. B., Gajewski, K., Schulz, R. A., and Frasch, M. (2002). Homeotic genes autonomously specify the anteroposterior subdivision of the *Drosophila* dorsal vessel into aorta and heart. *Dev. Biol.* 251, 307–319. doi: 10.1006/dbio.2002.0839

Lovato, T. L., Nguyen, T. P., Molina, M. R., and Cripps, R. M. (2002). The Hox gene abdominal-a specifies heart cell fate in the *Drosophila* dorsal vessel. *Development* 129, 5019–5027. doi: 10.1242/dev.129.21.5019

Machado, L., Esteves de Lima, J., Fabre, O., Proux, C., Legendre, R., Szegedi, A., et al. (2017). In situ fixation redefines quiescence and early activation of skeletal muscle stem cells. *Cell Rep.* 21, 1982–1993. doi: 10.1016/j.celrep.2017.10.080

Makki, N., and Capecchi, M. R. (2012). Cardiovascular defects in a mouse model of HOXA1 syndrome. *Hum. Mol. Genet.* 21, 26–31. doi: 10.1093/hmg/ddr434

Mallo, M., and Alonso, C. R. (2013). The regulation of Hox gene expression during animal development. *Development* 140, 3951–3963. doi: 10.1242/dev.068346

Mathies, L. D., Kerridge, S., and Scott, M. P. (1994). Role of the teashirt gene in *Drosophila* midgut morphogenesis: secreted proteins mediate the action of homeotic genes. *Development* 120, 2799–2809. doi: 10.1242/dev.120.10.2799

Mendelsohn, A. I., Dasen, J. S., and Jessell, T. M. (2017). Divergent Hox coding and evasion of retinoid signaling specifies motor neurons innervating digit muscles. *Neuron* 93, 792–805.e4. doi: 10.1016/j.neuron.2017.01.017

Meng, J. L., and Heckscher, E. S. (2021). Development of motor circuits: from neuronal stem cells and neuronal diversity to motor circuit assembly. *Curr. Top. Dev. Biol.* 142, 409–442. doi: 10.1016/bs.ctdb.2020.11.010

Michelson, A. M. (1994). Muscle pattern diversification in *Drosophila* is determined by the autonomous function of homeotic genes in the embryonic mesoderm. *Development* 120, 755–768. doi: 10.1242/dev.120.4.755

Molina, M. R., and Cripps, R. M. (2001). Ostia, the inflow tracts of the *Drosophila* heart, develop from a genetically distinct subset of cardial cells. *Mech. Dev.* 109, 51–59. doi: 10.1016/S0925-4773(01)00509-3

Monier, B., Astier, M., Sémériva, M., and Perrin, L. (2005). Steroid-dependent modification of Hox function drives myocyte reprogramming in the *Drosophila* heart. *Development* 132, 5283–5293. doi: 10.1242/dev.02091

Monier, B., Tevy, F., Perrin, L., Capovilla, M., and Semeriva, M. (2007). Downstream of homeotic genes: in the heart of Hox function. *Fly* 1, 59–67. doi: 10.4161/fly.3993

Musumeci, G., Castrogiovanni, P., Coleman, R., Szychlinska, M. A., Salvatorelli, L., Parenti, R., et al. (2015). Somitogenesis: from somite to skeletal muscle. *Acta Histochem.* 117, 313–328. doi: 10.1016/j.acthis.2015.02.011

Nowicki, J. L., and Burke, A. C. (2000). Hox genes and morphological identity: axial versus lateral patterning in the vertebrate mesoderm. *Development* 127, 4265–4275. doi: 10.1242/dev.127.19.4265

Ono, Y., Boldrin, L., Knopp, P., Morgan, J. E., and Zammit, P. S. (2010). Muscle satellite cells are a functionally heterogeneous population in both somite-derived and branchiomeric muscles. *Dev. Biol.* 337, 29–41. doi: 10.1016/j.ydbio.2009.10.005

Paul, R., Giraud, G., Domsch, K., Duffraisse, M., Marmigère, F., Khan, S., et al. (2021). Hox dosage contributes to flight appendage morphology in *Drosophila*. *Nat. Commun.* 12:2892. doi: 10.1038/s41467-021-23293-8

Pearson, J. C., Lemons, D., and McGinnis, W. (2005). Modulating Hox gene functions during animal body patterning. *Nat. Rev. Genet.* 6, 893–904. doi: 10.1038/nrg1726

Perrin, L., Monier, B., Ponzielli, R., Astier, M., and Semeriva, M. (2004). Drosophila cardiac tube organogenesis requires multiple phases of Hox activity. *Dev. Biol.* 272, 419–431. doi: 10.1016/j.ydbio.2004.04.036

Philippidou, P., and Dasen, J. S. (2013). Hox genes: choreographers in neural development, architects of circuit organization. *Neuron* 80, 12–34. doi: 10.1016/j.neuron.2013.09.020

Philippidou, P., Walsh, C. M., Aubin, J., Jeannotte, L., and Dasen, J. S. (2012). Sustained Hox5 gene activity is required for respiratory motor neuron development. *Nat. Neurosci.* 15, 1636–1644. doi: 10.1038/nn.3242

Pineault, K. M., and Wellik, D. M. (2014). Hox genes and limb musculoskeletal development. *Curr. Osteoporos. Rep.* 12, 420–427. doi: 10.1007/s11914-014-0241-0

Pollock, R. A., Jay, G., and Bieberich, C. J. (1992). Altering the boundaries of Hox3.1 expression: evidence for antipodal gene regulation. *Cell* 71, 911–923.

Ponzielli, R., Astier, M., Chartier, A., Gallet, A., Thérond, P., and Sémériva, M. (2002). Heart tube patterning in *Drosophila* requires integration of axial and segmental information provided by the bithorax complex genes and hedgehog signaling. *Development* 129, 4509–4521.

Poovathumkadavil, P., and Jagla, K. (2020). Genetic control of muscle diversification and homeostasis: insights from *Drosophila*. *Cells* 9:1543.

Prokop, A., and Technau, G. (1994). Early tagma-specific commitment of *Drosophila* CNS progenitor NB1-1. *Development* 120, 2567–2578.

Prokop, A., Bray, S., Harrison, E., and Technau, G. M. (1998). Homeotic regulation of segment-specific differences in neuroblast numbers and proliferation in the *Drosophila* central nervous system. *Mech. Dev.* 74, 99–110.

Reuter, R., and Scott, M. P. (1990). Expression and function of the homoeotic genes Antennapedia and sex combs reduced in the embryonic midgut of *Drosophila*. *Development* 109, 289–303.

Rezsohazy, R., Saurin, A. J., Maurel-Zaffran, C., and Graba, Y. (2015). Cellular and molecular insights into Hox protein action. *Development* 142, 1212–1227.

Rivlin, P. K., Gong, A., Schneiderman, A. M., and Booker, R. (2001). The role of Ultrabithorax in the patterning of adult thoracic muscles in *Drosophila* melanogaster. *Dev. Genes Evol.* 211, 55–66. doi: 10.1007/s004270000126

Rogulja-Ortmann, A., and Technau, G. M. (2008). Multiple roles for Hox genes in segment-specific shaping of CNS lineages. *Fly* 2, 316–319. doi: 10.4161/fly.7464

Rogulja-Ortmann, A., Renner, S., and Technau, G. M. (2008). Antagonistic roles for Ultrabithorax and Antennapedia in regulating segment-specific apoptosis of differentiated motoneurons in the *Drosophila* embryonic central nervous system. *Development* 135, 3435–3445. doi: 10.1242/dev.023986

Rotstein, B., and Paululat, A. (2016). On the morphology of the *Drosophila* Heart. *J. Cardiovasc. Dev. Dis.* 3:15. doi: 10.3390/jcdd3020015

Roux, M., Laforest, B., Capecchi, M., Bertrand, N., and Zaffran, S. (2015). Hoxb1 regulates proliferation and differentiation of second heart field progenitors in pharyngeal mesoderm and genetically interacts with Hoxa1 during cardiac outflow tract development. *Dev. Biol.* 406, 247–258. doi: 10.1016/j.ydbio.2015.08.015

Roux, M., Laforest, B., Eudes, N., Bertrand, N., Stefanovic, S., and Zaffran, S. (2017). Hoxa1 and Hoxb1 are required for pharyngeal arch artery development. *Mech. Dev.* 143, 1–8. doi: 10.1016/j.mod.2016.11.006

Roy, S., and Raghavan, K. V. (1997). Homeotic genes and the regulation of myoblast migration, fusion, and fibre-specific gene expression during adult myogenesis in *Drosophila*. *Development* 124, 3333–3341. doi: 10.1242/dev.124.17.3333

Roy, S., Shashidhara, L. S., and VijayRaghavan, K. (1997). Muscles in the *Drosophila* second thoracic segment are patterned independently of autonomous homeotic gene function. *Curr. Biol.* 7, 222–227. doi: 10.1016/S0960-9822(06)00117-5

Ruiz Gómez, M., and Bate, M. (1997). Segregation of myogenic lineages in *Drosophila* requires numb. *Development* 124, 4857–4866. doi: 10.1242/dev.124.23.4857

Ryan, K., Dk, H., and Rm, C. (2005). Homeotic selector genes control the patterning of seven-up expressing cells in the *Drosophila* dorsal vessel. *Mech. Dev.* 122, 1023–1033. doi: 10.1016/j.mod.2005.04.007

Sánchez-Herrero, E. (2013). Hox targets and cellular functions. *Scientifica* 2013:738257. doi: 10.1155/2013/738257

Saurin, A. J., Delfini, M. C., Maurel-Zaffran, C., and Graba, Y. (2018). The generic facet of Hox protein function. *Trends Genet.* 34, 941–953. doi: 10.1016/j.tig.2018.08.006

Schaub, C., März, J., Reim, I., and Frasch, M. (2015). Org-1-dependent lineage reprogramming generates the ventral longitudinal musculature of the *Drosophila* heart. *Curr. Biol.* 25, 488–494. doi: 10.1016/j.cub.2014.12.029

Schnorrer, F., and Dickson, B. J. (2004). Muscle building: mechanisms of myotube guidance and attachment site selection. *Dev. Cell* 7, 9–20. doi: 10.1016/j.devcel.2004.06.010

Schulman, V. K., Dobi, K. C., and Baylies, M. K. (2015). Morphogenesis of the somatic musculature in *Drosophila melanogaster*: morphogenesis of the *Drosophila* musculature. *Wiley Interdiscip. Rev. Dev. Biol.* 4, 313–334. doi: 10.1002/wdev.180

Schwörer, S., Becker, F., Feller, C., Baig, A. H., Köber, U., Henze, H., et al. (2016). Epigenetic stress responses induce muscle stem-cell ageing by Hoxa9 developmental signals. *Nature* 540, 428–432. doi: 10.1038/nature20603

Stefanovic, S., Laforest, B., Desvignes, J.-P., Lescroart, F., Argiro, L., Maurel-Zaffran, C., et al. (2020). Hox-dependent coordination of mouse cardiac progenitor cell patterning and differentiation. *ELife* 9:e55124. doi: 10.7554/eLife.55124.sa2

Swinehart, I. T., Schlientz, A. J., Quintanilla, C. A., Mortlock, D. P., and Wellik, D. M. (2013). Hox11 genes are required for regional patterning and integration of muscle, tendon and bone. *Development* 140, 4574–4582. doi: 10.1242/dev.096693

Taylor, M. V. (2006). "Comparison of muscle development in *Drosophila* and vertebrates," in *Muscle Development in Drosophila*, ed. H. Sink (New York, NY: Springer New York), 169–203. doi: 10.1007/0-387-32963-3_14

Tremml, G., and Bienz, M. (1989). Homeotic gene expression in the visceral mesoderm of *Drosophila* embryos. *EMBO J.* 8, 2677–2685. doi: 10.1002/j.1460-2075.1989.tb08408.x

Tripodi, M., and Arber, S. (2012). Regulation of motor circuit assembly by spatial and temporal mechanisms. *Curr. Opin. Neurobiol.* 22, 615–623. doi: 0.1016/j.conb.2012.02.011

Wolgemuth, D. J., Behringer, R. R., Mostoller, M. P., Brinster, R. L., and Palmiter, R. D. (1989). Transgenic mice overexpressing the mouse homoeobox-containing gene Hox-1.4 exhibit abnormal gut development. *Nature* 337, 464–467. doi: 10.1038/337464a0

Yoshioka, K., Nagahisa, H., Miura, F., Araki, H., Kamei, Y., Kitajima, Y., et al. (2021). Hoxa10 mediates positional memory to govern stem cell function in adult skeletal muscle. *Sci. Adv.* 7:eabd7924. doi: 10.1126/sciadv.abd7924

Zacchetti, G., Duboule, D., and Zakany, J. (2007). Hox gene function in vertebrate gut morphogenesis: the case of the caecum. *Development* 134, 3967–3973. doi: 10.1242/dev.010991

Zaffran, S., and Frasch, M. (2002). Early signals in cardiac development. *Circ. Res.* 91, 457–469. doi: 10.1161/01.RES.0000034152.74523.A8

Zaffran, S., and Kelly, R. G. (2012). New developments in the second heart field. *Differ. Res. Biol. Divers.* 84, 17–24. doi: 10.1016/j.diff.2012.03.003

Zaffran, S., Odelin, G., Stefanovic, S., Lescroart, F., and Etchevers, H. C. (2018). Ectopic expression of Hoxb1 induces cardiac and craniofacial malformations. *Genesis* 56:e23221. doi: 10.1002/dvg.23221

Zákány, J., and Duboule, D. (1999). Hox genes and the making of sphincters. *Nature* 401, 761–762. doi: 10.1038/44511

Zakany, J., Darbellay, F., Mascrez, B., Necsulea, A., and Duboule, D. (2017). Control of growth and gut maturation by HoxD genes and the associated lncRNA Haglr. *Proc. Natl. Acad. Sci. U.S.A.* 114, E9290–E9299. doi: 10.1073/pnas.1712511114

Zmojdzian, M., de Joussineau, S., Da Ponte, J. P., and Jagla, K. (2018). Distinct subsets of Eve-positive pericardial cells stabilise cardiac outflow and contribute to Hox gene-triggered heart morphogenesis in *Drosophila*. *Development* 145:dev158717. doi: 10.1242/dev.158717

Conflict of Interest: The authors declare that the research was conducted in the absence of any commercial or financial relationships that could be construed as a potential conflict of interest.

Publisher's Note: All claims expressed in this article are solely those of the authors and do not necessarily represent those of their affiliated organizations, or those of the publisher, the editors and the reviewers. Any product that may be evaluated in this article, or claim that may be made by its manufacturer, is not guaranteed or endorsed by the publisher.

Copyright © 2021 Poliacikova, Maurel-Zaffran, Graba and Saurin. This is an open-access article distributed under the terms of the Creative Commons Attribution License (CC BY). The use, distribution or reproduction in other forums is permitted, provided the original author(s) and the copyright owner(s) are credited and that the original publication in this journal is cited, in accordance with accepted academic practice. No use, distribution or reproduction is permitted which does not comply with these terms.

Bibliography

Abbott, M. K. and Kaufman, T. C. (1986). The Relationship between the Functional Complexity and the Molecular Organization of the ANTENNAPEDIA Locus of DROSOPHILA MELANOGASTER. *Genetics*, 114(3), 919–942.

Abel, T., Michelson, A. M. and Maniatis, T. (1993). A Drosophila GATA family member that binds to Adh regulatory sequences is expressed in the developing fat body. *Dev. Camb. Engl.*, 119(3), 623–633. https://doi.org/10.1242/dev.119.3.623

Altamirano-Torres, C., Salinas-Hernández, J. E., Cárdenas-Chávez, D. L., Rodríguez-Padilla, C. and Reséndez-Pérez, D. (2018). Transcription factor TFIIEβ interacts with two exposed positions in helix 2 of the Antennapedia homeodomain to control homeotic function in Drosophila. *PloS One*, 13(10), e0205905. https://doi.org/10.1371/journal.pone.0205905

Anant, S., Roy, S. and VijayRaghavan, K. (1998). Twist and Notch negatively regulate adult muscle differentiation in Drosophila. *Development*, 125(8), 1361–1369. https://doi.org/10.1242/dev.125.8.1361

Aradhya, R., Zmojdzian, M., Da Ponte, J. P. and Jagla, K. (2015). Muscle niche-driven Insulin-Notch-Myc cascade reactivates dormant Adult Muscle Precursors in Drosophila. *eLife*, 4, e08497. https://doi.org/10.7554/eLife.08497

Arredondo, J. J., Ferreres, R. M., Maroto, M., Cripps, R. M., Marco, R., Bernstein, S. I. and Cervera, M. (2001). Control of Drosophila paramyosin/miniparamyosin gene expression. Differential regulatory mechanisms for muscle-specific transcription. *J. Biol. Chem.*, 276(11), 8278–8287. https://doi.org/10.1074/jbc.M009302200

Artero, R. D., Castanon, I. and Baylies, M. K. (2001). The immunoglobulin-like protein Hibris functions as a dose-dependent regulator of myoblast fusion and is differentially controlled by Ras and Notch signaling. *Development*, 128(21), 4251–4264. https://doi.org/10.1242/dev.128.21.4251

Atreya, K. B. and Fernandes, J. J. (2008). Founder cells regulate fiber number but not fiber formation during adult myogenesis in Drosophila. *Dev. Biol.*, 321(1), 123–140. https://doi.org/10.1016/j.ydbio.2008.06.023

Avellaneda, J., Rodier, C., Daian, F., Brouilly, N., Rival, T., Luis, N. M. and Schnorrer, F. (2021). Myofibril and mitochondria morphogenesis are coordinated by a mechanical feedback mechanism in muscle. *Nat. Commun.*, 12(1), Article 1. https://doi.org/10.1038/s41467-021-22058-7

Azevedo, M. and Baylies, M. K. (2020). Getting into Position: Nuclear Movement in Muscle Cells. *Trends Cell Biol.*, 30(4), 303–316. https://doi.org/10.1016/j.tcb.2020.01.002

Azpiazu, N. and Frasch, M. (1993). tinman and bagpipe: two homeo box genes that determine cell fates in the dorsal mesoderm of Drosophila. *Genes Dev.*, 7(7B), 1325–1340. https://doi.org/10.1101/gad.7.7b.1325

Azpiazu, N., Lawrence, P. A., Vincent, J. P. and Frasch, M. (1996). Segmentation and specification of the Drosophila mesoderm. *Genes Dev.*, 10(24), 3183–3194. https://doi.org/10.1101/gad.10.24.3183

Baek, M., Enriquez, J. and Mann, R. S. (2013). Dual role for Hox genes and Hox co-factors in conferring leg motoneuron survival and identity in Drosophila. *Development*, 140(9), 2027–2038. https://doi.org/10.1242/dev.090902

Baëza, M., Viala, S., Heim, M., Dard, A., Hudry, B., Duffraisse, M., Rogulja-Ortmann, A., Brun, C. and Merabet, S. (2015). Inhibitory activities of short linear motifs underlie Hox interactome specificity in vivo. *eLife*, 4, e06034. https://doi.org/10.7554/eLife.06034

Bag, I., Chen, S., Rosin, L. F., Chen, Y., Liu, C.-Y., Yu, G.-Y. and Lei, E. P. (2021). M1BP cooperates with CP190 to activate transcription at TAD borders and promote chromatin insulator activity. *Nat. Commun.*, 12(1), 4170. https://doi.org/10.1038/s41467-021-24407-y

Baker, P. W., Tanaka, K. K. K., Klitgord, N. and Cripps, R. M. (2005). Adult myogenesis in Drosophila melanogaster can proceed independently of myocyte enhancer factor-2. *Genetics*, 170(4), 1747–1759. https://doi.org/10.1534/genetics.105.041749

Baker and Schubiger, G. (1996). Autonomous and nonautonomous Notch functions for embryonic muscle and epidermis development in Drosophila. *Development*, 122(2), 617–626. https://doi.org/10.1242/dev.122.2.617

Baltzer, C., Tiefenböck, S. K., Marti, M. and Frei, C. (2009). Nutrition Controls Mitochondrial Biogenesis in the Drosophila Adipose Tissue through Delg and Cyclin D/Cdk4. *PLoS ONE*, 4(9), e6935. https://doi.org/10.1371/journal.pone.0006935

Banreti, A., Hudry, B., Sass, M., Saurin, A. J. and Graba, Y. (2014). Hox proteins mediate developmental and environmental control of autophagy. *Dev. Cell*, 28(1), 56–69. https://doi.org/10.1016/j.devcel.2013.11.024

Barthez, M. (2019). *Functional characterisation of Drosophila M1BP*. Thesis. Retrieved from https://theses.fr/2019AIXM0298

Barthez, M., Poplineau, M., Elrefaey, M., Caruso, N., Graba, Y. and Saurin, A. J. (2020). Human ZKSCAN3 and Drosophila M1BP are functionally homologous transcription factors in autophagy regulation. *Sci. Rep.*, 10(1), 9653. https://doi.org/10.1038/s41598-020-66377-z

Bataillé, L., Boukhatmi, H., Frendo, J.-L. and Vincent, A. (2017). Dynamics of transcriptional (re)-programming of syncytial nuclei in developing muscles. *BMC Biol.*, 15(1), 48. https://doi.org/10.1186/s12915-017-0386-2

Bataillé, L., Delon, I., Da Ponte, J. P., Brown, N. H. and Jagla, K. (2010). Downstream of identity genes: muscle-type-specific regulation of the fusion process. *Dev. Cell*, 19(2), 317–328. https://doi.org/10.1016/j.devcel.2010.07.008

Bate, M. (1990). The embryonic development of larval muscles in Drosophila. *Development*, 110(3), 791–804.

Bate, M., Rushton, E. and Currie, D. A. (1991). Cells with persistent twist expression are the embryonic precursors of adult muscles in Drosophila. *Development*, 113(1), 79–89. https://doi.org/10.1242/dev.113.1.79

Bate, M., Rushton, E. and Frasch, M. (1993). A dual requirement for neurogenic genes in Drosophila myogenesis. *Dev. Camb. Engl. Suppl.*, 149–161.

Bateson, W., Pierpont, F. H. and Clay, C. J. (1894). *Materials for the study of variation treated with especial regard to discontinuity in the origin of species* (pp. 1–624). London: Macmillan and co. https://doi.org/10.5962/bhl.title.1348

Baumann, D. G. and Gilmour, D. S. (2017). A sequence-specific core promoter-binding transcription factor recruits TRF2 to coordinately transcribe ribosomal protein genes. *Nucleic Acids Res.*, 45(18), 10481–10491. https://doi.org/10.1093/nar/gkx676

Baylies, M. K. and Bate, M. (1996). twist: a myogenic switch in Drosophila. *Science*, 272(5267), 1481–1484. https://doi.org/10.1126/science.272.5267.1481

Baylies, M. K., Martinez Arias, A. and Bate, M. (1995). wingless is required for the formation of a subset of muscle founder cells during Drosophila embryogenesis. *Development*, 121(11), 3829–3837. https://doi.org/10.1242/dev.121.11.3829

Beckett, K. and Baylies, M. K. (2007). 3D analysis of founder cell and fusion competent myoblast arrangements outlines a new model of myoblast fusion. *Dev. Biol.*, 309(1), 113–125. https://doi.org/10.1016/j.ydbio.2007.06.024

Beiman, M., Shilo, B. Z. and Volk, T. (1996). Heartless, a Drosophila FGF receptor homolog, is essential for cell migration and establishment of several mesodermal lineages. *Genes Dev.*, 10(23), 2993–3002. https://doi.org/10.1101/gad.10.23.2993

Bender, W., Akam, M., Karch, F., Beachy, P. A., Peifer, M., Spierer, P., Lewis, E. B. and Hogness, D. S. (1983). Molecular Genetics of the Bithorax Complex in Drosophila melanogaster. *Science*, 221(4605), 23–29. https://doi.org/10.1126/science.221.4605.23

Benevolenskaya, E. V. and Frolov, M. V. (2015). Emerging Links between E2F Control and Mitochondrial Function. *Cancer Res.*, 75(4), 619–623. https://doi.org/10.1158/0008-5472.CAN-14-2173

Berger, S., Schäfer, G., Kesper, D. A., Holz, A., Eriksson, T., Palmer, R. H., Beck, L., Klämbt, C., Renkawitz-Pohl, R. and Onel, S.-F. (2008). WASP and SCAR have distinct roles in activating the Arp2/3 complex during myoblast fusion. *J. Cell Sci.*, 121(Pt 8), 1303–1313. https://doi.org/10.1242/jcs.022269

Bermingham, J. R., Martinez-Arias, A., Petitt, M. G. and Scott, M. P. (1990). Different patterns of transcription from the two Antennapedia promoters during Drosophila embryogenesis. *Dev. Camb. Engl.*, 109(3), 553–566. https://doi.org/10.1242/dev.109.3.553

Bermingham, J. R. and Scott, M. P. (1988). Developmentally regulated alternative splicing of transcripts from the Drosophila homeotic gene Antennapedia can produce four different proteins. *EMBO J.*, 7(10), 3211–3222.

Bernard, F., Dutriaux, A., Silber, J. and Lalouette, A. (2006). Notch pathway repression by vestigial is required to promote indirect flight muscle differentiation in Drosophila melanogaster. *Dev. Biol.*, 295(1), 164–177. https://doi.org/10.1016/j.ydbio.2006.03.022

Bernard, F., Krejci, A., Housden, B., Adryan, B. and Bray, S. J. (2010). Specificity of Notch pathway activation: Twist controls the transcriptional output in adult muscle progenitors. *Development*, 137(16), 2633–2642. https://doi.org/10.1242/dev.053181

Bernard, F., Lalouette, A., Gullaud, M., Jeantet, A. Y., Cossard, R., Zider, A., Ferveur, J. F. and Silber, J. (2003). Control of apterous by vestigial drives indirect flight muscle development in drosophila. *Dev. Biol.*, 260(2), 391–403. https://doi.org/10.1016/S0012-1606(03)00255-0

Berrisford, J. M. and Sazanov, L. A. (2009). Structural Basis for the Mechanism of Respiratory Complex I. *J. Biol. Chem.*, 284(43), 29773–29783. https://doi.org/10.1074/jbc.M109.032144

Bezawork-Geleta, A., Rohlena, J., Dong, L., Pacak, K. and Neuzil, J. (2017). Mitochondrial Complex II: At the Crossroads. *Trends Biochem. Sci.*, 42(4), 312–325. https://doi.org/10.1016/j.tibs.2017.01.003

Blanchet, E., Annicotte, J.-S., Lagarrigue, S., Aguilar, V., Clapé, C., Chavey, C., Fritz, V., Casas, F., Apparailly, F., Auwerx, J., et al. (2011). E2F transcription factor-1 regulates oxidative metabolism. *Nat. Cell Biol.*, 13(9), 1146–1152. https://doi.org/10.1038/ncb2309

Bleck, C. K. E., Kim, Y., Willingham, T. B. and Glancy, B. (2018). Subcellular connectomic analyses of energy networks in striated muscle. *Nat. Commun.*, 9(1), 5111. https://doi.org/10.1038/s41467-018-07676-y

Blum, T. B., Hahn, A., Meier, T., Davies, K. M. and Kühlbrandt, W. (2019). Dimers of mitochondrial ATP synthase induce membrane curvature and self-assemble into rows. *Proc. Natl. Acad. Sci.*, 116(10), 4250–4255. https://doi.org/10.1073/pnas.1816556116

Bodmer, R. (1993). The gene tinman is required for specification of the heart and visceral muscles in Drosophila. *Dev. Camb. Engl.*, 118(3), 719–729.

Borkowski, O. M., Brown, N. H. and Bate, M. (1995). Anterior-posterior subdivision and the diversification of the mesoderm in Drosophila. *Dev. Camb. Engl.*, 121(12), 4183–4193. https://doi.org/10.1242/dev.121.12.4183

Bottje, W. G. (2019). Oxidative metabolism and efficiency: the delicate balancing act of mitochondria. *Poult. Sci.*, 98(10), 4223–4230. https://doi.org/10.3382/ps/pey405

Boube, M., Hudry, B., Immarigeon, C., Carrier, Y., Bernat-Fabre, S., Merabet, S., Graba, Y., Bourbon, H.-M. and Cribbs, D. L. (2014). Drosophila melanogaster Hox Transcription Factors Access the RNA Polymerase II Machinery through Direct Homeodomain Binding to a Conserved Motif of Mediator Subunit Med19. *PLOS Genet.*, 10(5), e1004303. https://doi.org/10.1371/journal.pgen.1004303

Boukhatmi, H., Frendo, J. L., Enriquez, J., Crozatier, M., Dubois, L. and Vincent, A. (2012). Tup/Islet1 integrates time and position to specify muscle identity in Drosophila. *Development*, 139(19), 3572–3582. https://doi.org/10.1242/dev.083410

Boulay, J. L., Dennefeld, C. and Alberga, A. (1987). The Drosophila developmental gene snail encodes a protein with nucleic acid binding fingers. *Nature*, 330(6146), 395–398. https://doi.org/10.1038/330395a0

Bour, B. A., Chakravarti, M., West, J. M. and Abmayr, S. M. (2000). Drosophila SNS, a member of the immunoglobulin superfamily that is essential for myoblast fusion. *Genes Dev.*, 14(12), 1498–1511.

Bour, O'Brien, M. A., Lockwood, W. L., Goldstein, E. S., Bodmer, R., Taghert, T., Abmayr, S. M. and Nguyen, H. T. (1995). Drosophila MEF2, a transcription factor that is essential for myogenesis. *Genes Dev.*, 9(6). https://doi.org/10.1101/gad.9.6.730

Bourgouin, C., Lundgren, S. E. and Thomas, J. B. (1992). apterous is a drosophila LIM domain gene required for the development of a subset of embryonic muscles. *Neuron*, 9(3), 549–561. https://doi.org/10.1016/0896-6273(92)90192-G

Bragoszewski, P., Gornicka, A., Sztolsztener, M. E. and Chacinska, A. (2013). The ubiquitin-proteasome system regulates mitochondrial intermembrane space proteins. *Mol. Cell. Biol.*, 33(11), 2136–2148. https://doi.org/10.1128/MCB.01579-12

Bragoszewski, P., Turek, M. and Chacinska, A. (2017). Control of mitochondrial biogenesis and function by the ubiquitin–proteasome system. *Open Biol.*, 7(4), 170007. https://doi.org/10.1098/rsob.170007

Brennan, C. M., Vaites, L. P., Wells, J. N., Santaguida, S., Paulo, J. A., Storchova, Z., Harper, J. W., Marsh, J. A. and Amon, A. (2019). Protein aggregation mediates stoichiometry of protein complexes in aneuploid cells. *Genes Dev.*, 33(15–16), 1031–1047. https://doi.org/10.1101/gad.327494.119

Brennan, K., Baylies, M. and Arias, A. M. (1999). Repression by Notch is required before Wingless signalling during muscle progenitor cell development in Drosophila. *Curr. Biol. CB*, 9(13), 707–710. https://doi.org/10.1016/s0960-9822(99)80313-3

Bridges, C. B., Morgan, T. H. and Washington, C. I. of. (1923). *The third-chromosome group of mutant characters of Drosophila melanogaster* (pp. 1–280). Washington: Carnegie Institution of Washington. https://doi.org/10.5962/bhl.title.24013

Brischigliaro, M., Cabrera-Orefice, A., Sturlese, M., Elurbe, D. M., Frigo, E., Fernandez-Vizarra, E., Moro, S., Huynen, M. A., Arnold, S., Viscomi, C., et al. (2022). CG7630 is the Drosophila melanogaster homolog of the cytochrome c oxidase subunit COX7B. *EMBO Rep.*, 23(8), e54825. https://doi.org/10.15252/embr.202254825

Broadie, K. S. and Bate, M. (1991). The development of adult muscles in Drosophila: ablation of identified muscle precursor cells. *Development*, 113(1), 103–118. https://doi.org/10.1242/dev.113.1.103

Brown, J. L., Mucci, D., Whiteley, M., Dirksen, M. L. and Kassis, J. A. (1998). The Drosophila Polycomb group gene pleiohomeotic encodes a DNA binding protein with homology to the transcription factor YY1. *Mol. Cell*, 1(7), 1057–1064. https://doi.org/10.1016/s1097-2765(00)80106-9

Brunetti, T. M., Fremin, B. J. and Cripps, R. M. (2015). Identification of singles bar as a direct transcriptional target of Drosophila Myocyte enhancer factor-2 and a regulator of adult myoblast fusion. *Dev. Biol.*, 401(2), 299–309. https://doi.org/10.1016/j.ydbio.2015.02.026

Bruni, F., Polosa, P. L., Gadaleta, M. N., Cantatore, P. and Roberti, M. (2010). Nuclear Respiratory Factor 2 Induces the Expression of Many but Not All Human Proteins Acting in Mitochondrial DNA Transcription and Replication 2. *J. Biol. Chem.*, 285(6), 3939–3948. https://doi.org/10.1074/jbc.M109.044305

Bryantsev, A. L., Baker, P. W., Lovato, T. L., Jaramillo, M. S. and Cripps, R. M. (2012). Differential requirements for Myocyte Enhancer Factor-2 during adult myogenesis in Drosophila. *Dev. Biol.*, 361(2), 191–207. https://doi.org/10.1016/j.ydbio.2011.09.031

Bryantsev, A. L., Duong, S., Brunetti, T. M., Chechenova, M. B., Lovato, T. L., Nelson, C., Shaw, E., Uhl, J. D., Gebelein, B. and Cripps, R. M. (2012). Extradenticle and Homothorax Control Adult Muscle Fiber Identity in Drosophila. *Dev. Cell*, 23(3), 664–673. https://doi.org/10.1016/j.devcel.2012.08.004

Buff, Carmena, A., Gisselbrecht, S., Jiménez, F. and Michelson, A. M. (1998a). Signalling by the Drosophila epidermal growth factor receptor is required for the specification and diversification of embryonic muscle progenitors. *Development*, 125(11), 2075–2086. https://doi.org/10.1242/dev.125.11.2075

Buff, E., Carmena, A., Gisselbrecht, S., Jiménez, F. and Michelson, A. M. (1998b). Signalling by the Drosophila epidermal growth factor receptor is required for the specification and diversification of embryonic muscle progenitors. *Dev. Camb. Engl.*, 125(11), 2075–2086. https://doi.org/10.1242/dev.125.11.2075

Caine, C., Kasherov, P., Silber, J. and Lalouette, A. (2014). Mef2 interacts with the Notch pathway during adult muscle development in Drosophila melanogaster. *PloS One*, 9(9), e108149. https://doi.org/10.1371/journal.pone.0108149

Campos-Ortega, J. A. (1993). Mechanisms of early neurogenesis in Drosophila melanogaster. *J. Neurobiol.*, 24(10), 1305–1327. https://doi.org/10.1002/neu.480241005

Capovilla, M., Kambris, Z. and Botas, J. (2001). Direct regulation of the muscle-identity gene apterous by a Hox protein in the somatic mesoderm. *Dev. Camb. Engl.*, 128(8), 1221–1230.

Carmena, Bate, M. and Jiménez, F. (1995). Lethal of scute, a proneural gene, participates in the specification of muscle progenitors during Drosophila embryogenesis. *Genes Dev.*, 9(19), 2373–2383. https://doi.org/10.1101/gad.9.19.2373

Carmena, Buff, E., Halfon, M. S., Gisselbrecht, S., Jiménez, F., Baylies, M. K. and Michelson, A. M. (2002). Reciprocal regulatory interactions between the Notch and Ras signaling pathways in the Drosophila embryonic mesoderm. *Dev. Biol.*, 244(2), 226–242. https://doi.org/10.1006/dbio.2002.0606

Carmena, Gisselbrecht, S., Harrison, J., Jiménez, F. and Michelson, A. M. (1998). Combinatorial signaling codes for the progressive determination of cell fates in the

Drosophila embryonic mesoderm. *Genes Dev.*, 12(24), 3910–3922. https://doi.org/10.1101/gad.12.24.3910

Carmena, Murugasu-Oei, B., Menon, D., Jiménez, F. and Chia, W. (1998). inscuteable and numb mediate asymmetric muscle progenitor cell divisions during Drosophila myogenesis. *Genes Dev.*, 12(3), 304–315.

Carrasco-Rando, M., Tutor, A. S., Prieto-Sánchez, S., González-Pérez, E., Barrios, N., Letizia, A., Martín, P., Campuzano, S. and Ruiz-Gómez, M. (2011). Drosophila araucan and caupolican integrate intrinsic and signalling inputs for the acquisition by muscle progenitors of the lateral transverse fate. *PLoS Genet.*, 7(7), e1002186. https://doi.org/10.1371/journal.pgen.1002186

Carroll, J., Fearnley, I. M., Skehel, J. M., Shannon, R. J., Hirst, J. and Walker, J. E. (2006). Bovine complex I is a complex of 45 different subunits. *J. Biol. Chem.*, 281(43), 32724–32727. https://doi.org/10.1074/jbc.M607135200

Carroll, S. B., Laymon, R. A., McCutcheon, M. A., Riley, P. D. and Scott, M. P. (1986). The localization and regulation of Antennapedia protein expression in Drosophila embryos. *Cell*, 47(1), 113–122. https://doi.org/10.1016/0092-8674(86)90372-7

Chau, C. M., Evans, M. J. and Scarpulla, R. C. (1992). Nuclear respiratory factor 1 activation sites in genes encoding the gamma-subunit of ATP synthase, eukaryotic initiation factor 2 alpha, and tyrosine aminotransferase. Specific interaction of purified NRF-1 with multiple target genes. *J. Biol. Chem.*, 267(10), 6999–7006. https://doi.org/10.1016/S0021-9258(19)50527-0

Chen, Liang, S., Zhao, Y. and Han, Z. (2012). miR-92b regulates Mef2 levels through a negative-feedback circuit during Drosophila muscle development. *Dev. Camb. Engl.*, 139(19), 3543–3552. https://doi.org/10.1242/dev.082719

Chen and Olson, E. N. (2001). Antisocial, an Intracellular Adaptor Protein, Is Required for Myoblast Fusion in Drosophila. *Dev. Cell*, 1(5), 705–715. https://doi.org/10.1016/S1534-5807(01)00084-3

Chen, Pryce, B. A., Tzeng, J. A., Gonzalez, G. A. and Olson, E. N. (2003). Control of myoblast fusion by a guanine nucleotide exchange factor, loner, and its effector ARF6. *Cell*, 114(6), 751–762. https://doi.org/10.1016/s0092-8674(03)00720-7

Chomyn, A., Cleeter, M. W., Ragan, C. I., Riley, M., Doolittle, R. F. and Attardi, G. (1986). URF6, last unidentified reading frame of human mtDNA, codes for an NADH dehydrogenase subunit. *Science*, 234(4776), 614–618. https://doi.org/10.1126/science.3764430

Chomyn, A., Mariottini, P., Cleeter, M. W., Ragan, C. I., Matsuno-Yagi, A., Hatefi, Y., Doolittle, R. F. and Attardi, G. (1985). Six unidentified reading frames of human mitochondrial DNA encode components of the respiratory-chain NADH dehydrogenase. *Nature*, 314(6012), 592–597. https://doi.org/10.1038/314592a0

Choo, S. W., White, R. and Russell, S. (2011). Genome-Wide Analysis of the Binding of the Hox Protein Ultrabithorax and the Hox Cofactor Homothorax in Drosophila. *PLOS ONE*, 6(4), e14778. https://doi.org/10.1371/journal.pone.0014778

Church, R. B. and Robertson, F. W. (1966). A biochemical study of the growth of Drosophila melanogaster. *J. Exp. Zool.*, 162(3), 337–351. https://doi.org/10.1002/jez.1401620309

Ciglar, L., Girardot, C., Wilczyński, B., Braun, M. and Furlong, E. E. M. (2014). Coordinated repression and activation of two transcriptional programs stabilizes cell fate during myogenesis. *Dev. Camb. Engl.*, 141(13), 2633–2643. https://doi.org/10.1242/dev.101956

Ciryam, P., Kundra, R., Morimoto, R. I., Dobson, C. M. and Vendruscolo, M. (2015). Supersaturation is a major driving force for protein aggregation in neurodegenerative diseases. *Trends Pharmacol. Sci.*, 36(2), 72–77. https://doi.org/10.1016/j.tips.2014.12.004

Clark, I. B. N., Boyd, J., Hamilton, G., Finnegan, D. J. and Jarman, A. P. (2006). *D-six4* plays a key role in patterning cell identities deriving from the *Drosophila* mesoderm. *Dev. Biol.*, 294(1), 220–231. https://doi.org/10.1016/j.ydbio.2006.02.044

Cogliati, S., Enriquez, J. A. and Scorrano, L. (2016). Mitochondrial Cristae: Where Beauty Meets Functionality. *Trends Biochem. Sci.*, 41(3), 261–273. https://doi.org/10.1016/j.tibs.2016.01.001

Cogliati, S., Lorenzi, I., Rigoni, G., Caicci, F. and Soriano, M. E. (2018). Regulation of Mitochondrial Electron Transport Chain Assembly. *J. Mol. Biol.*, 430(24), 4849–4873. https://doi.org/10.1016/j.jmb.2018.09.016

Corbin, V., Michelson, A. M., Abmayr, S. M., Neel, V., Alcamo, E., Maniatis, T. and Young, M. W. (1991). A role for the Drosophila neurogenic genes in mesoderm differentiation. *Cell*, 67(2), 311–323. https://doi.org/10.1016/0092-8674(91)90183-Y

Cripps, Black, B. L., Zhao, B., Lien, C.-L., Schulz, R. A. and Olson, E. N. (1998). The myogenic regulatory gene Mef2 is a direct target for transcriptional activation by Twist during Drosophila myogenesis. *Genes Dev.*, 12(3), 422–434.

Cripps, Lovato, T. L. and Olson, E. N. (2004). Positive autoregulation of the Myocyte enhancer factor-2 myogenic control gene during somatic muscle development in Drosophila. *Dev. Biol.*, 267(2), 536–547. https://doi.org/10.1016/j.ydbio.2003.12.004

Cripps and Olson, E. N. (1998). Twist is required for muscle template splitting during adult Drosophila myogenesis. *Dev. Biol.*, 203(1), 106–115. https://doi.org/10.1006/dbio.1998.9040

Crisp, S., Evers, J. F., Fiala, A. and Bate, M. (2008). The development of motor coordination in Drosophila embryos. *Dev. Camb. Engl.*, 135(22), 3707–3717. https://doi.org/10.1242/dev.026773

Crozatier, M. and Vincent, A. (1999). Requirement for the Drosophila COE transcription factor Collier in formation of an embryonic muscle: transcriptional response to Notch signalling. *Development*, 126(7), 1495–1504. https://doi.org/10.1242/dev.126.7.1495

Cunha, P. M. F., Sandmann, T., Gustafson, E. H., Ciglar, L., Eichenlaub, M. P. and Furlong, E. E. M. (2010). Combinatorial binding leads to diverse regulatory responses: Lmd is a tissue-specific modulator of Mef2 activity. *PLoS Genet.*, 6(7), e1001014. https://doi.org/10.1371/journal.pgen.1001014

Cunningham, J. T., Rodgers, J. T., Arlow, D. H., Vazquez, F., Mootha, V. K. and Puigserver, P. (2007). mTOR controls mitochondrial oxidative function through a YY1-PGC-1alpha transcriptional complex. *Nature*, 450(7170), 736–740. https://doi.org/10.1038/nature06322

Currie, D. A. and Bate, M. (1991). The development of adult abdominal muscles in Drosophila: myoblasts express twist and are associated with nerves. *Development*, 113(1), 91–102. https://doi.org/10.1242/dev.113.1.91

Dairaghi, D. J., Shadel, G. S. and Clayton, D. A. (1995). Addition of a 29 residue carboxyl-terminal tail converts a simple HMG box-containing protein into a transcriptional activator. *J. Mol. Biol.*, 249(1), 11–28. https://doi.org/10.1006/jmbi.1995.9889

de Joussineau, C., Bataillé, L., Jagla, T. and Jagla, K. (2012). Diversification of Muscle Types in Drosophila. In *Current Topics in Developmental Biology* (Vol. 98, pp. 277–301). Elsevier. https://doi.org/10.1016/B978-0-12-386499-4.00011-2

De Kumar, B. and Darland, D. C. (2021). The Hox protein conundrum: The "specifics" of DNA binding for Hox proteins and their partners. *Dev. Biol.*, 477, 284–292. https://doi.org/10.1016/j.ydbio.2021.06.002

Demontis, F. and Perrimon, N. (2009). Integration of Insulin receptor/Foxo signaling and dMyc activity during muscle growth regulates body size in Drosophila. *Dev. Camb. Engl.*, 136(6), 983–993. https://doi.org/10.1242/dev.027466

Denell, R. E. (1972). The nature of reversion of a dominant gene of Drosophila melanogaster. *Mutat. Res.*, 15(2), 221–223. https://doi.org/10.1016/0027-5107(72)90036-x

Denell, R. E. (1973). Homoeosis in Drosophila. I. Complementation Studies with Revertants of Nasobemia. *Genetics*, 75(2), 279–297.

Denell, R. E., Hummels, K. R., Wakimoto, B. T. and Kaufman, T. C. (1981). Developmental studies of lethality associated with the antennapedia gene complex in Drosophila melanogaster. *Dev. Biol.*, 81(1), 43–50. https://doi.org/10.1016/0012-1606(81)90346-8

Deng, H., Bell, J. B. and Simmonds, A. J. (2010). Vestigial Is Required during Late-Stage Muscle Differentiation in Drosophila melanogaster Embryos. *Mol. Biol. Cell*, 21(19), 3304–3316. https://doi.org/10.1091/mbc.E10-04-0364

Deshwal, S., Fiedler, K. U. and Langer, T. (2020). Mitochondrial Proteases: Multifaceted Regulators of Mitochondrial Plasticity. *Annu. Rev. Biochem.*, 89, 501–528. https://doi.org/10.1146/annurev-biochem-062917-012739

DeSimone, S., Coelho, C., Roy, S., VijayRaghavan, K. and White, K. (1996). ERECT WING, the Drosophila member of a family of DNA binding proteins is required in imaginal myoblasts for flight muscle development. *Dev. Camb. Engl.*, 122(1), 31–39. https://doi.org/10.1242/dev.122.1.31

Desplan, C., Theis, J. and O'Farrell, P. H. (1985). The Drosophila developmental gene, engrailed, encodes a sequence-specific DNA binding activity. *Nature*, 318(6047), 630–635. https://doi.org/10.1038/318630a0

Desplan, C., Theis, J. and O'Farrell, P. H. (1988). The Sequence Specificity of Homeodomain-DNA Interaction. *Cell*, 54(7), 1081–1090.

Dhanyasi, N., Segal, D., Shimoni, E., Shinder, V., Shilo, B.-Z., VijayRaghavan, K. and Schejter, E. D. (2015). Surface apposition and multiple cell contacts promote myoblast fusion in Drosophila flight muscles. *J. Cell Biol.*, 211(1), 191–203. https://doi.org/10.1083/jcb.201503005

Dickerson, B. H., de Souza, A. M., Huda, A. and Dickinson, M. H. (2019). Flies Regulate Wing Motion via Active Control of a Dual-Function Gyroscope. *Curr. Biol. CB*, 29(20), 3517-3524.e3. https://doi.org/10.1016/j.cub.2019.08.065

Dietzl, G., Chen, D., Schnorrer, F., Su, K.-C., Barinova, Y., Fellner, M., Gasser, B., Kinsey, K., Oppel, S., Scheiblauer, S., et al. (2007). A genome-wide transgenic RNAi library for conditional gene inactivation in Drosophila. *Nature*, 448(7150), 151–156. https://doi.org/10.1038/nature05954

Dikic, I. and Elazar, Z. (2018). Mechanism and medical implications of mammalian autophagy. *Nat. Rev. Mol. Cell Biol.*, 19(6), 349–364. https://doi.org/10.1038/s41580-018-0003-4

Diop, S. B., Bertaux, K., Vasanthi, D., Sarkeshik, A., Goirand, B., Aragnol, D., Tolwinski, N. S., Cole, M. D., Pradel, J., Yates, J. R., et al. (2008). Reptin and Pontin function antagonistically with PcG and TrxG complexes to mediate Hox gene control. *EMBO Rep.*, 9(3), 260–266. https://doi.org/10.1038/embor.2008.8

Doberstein, S. K., Fetter, R. D., Mehta, A. Y. and Goodman, C. S. (1997). Genetic Analysis of Myoblast Fusion: blown fuse Is Required for Progression Beyond the Prefusion Complex. *J. Cell Biol.*, 136(6), 1249–1261.

Dobi, K. C., Halfon, M. S. and Baylies, M. K. (2014). Whole-Genome Analysis of Muscle Founder Cells Implicates the Chromatin Regulator Sin3A in Muscle Identity. *Cell Rep.*, 8(3), 858–870. https://doi.org/10.1016/j.celrep.2014.07.005

Dobi, K. C., Schulman, V. K. and Baylies, M. K. (2015). Specification of the somatic musculature in *Drosophila*: Specification of the somatic musculature in *Drosophila*. *Wiley Interdiscip. Rev. Dev. Biol.*, 4(4), 357–375. https://doi.org/10.1002/wdev.182

Dohrmann, C., Azpiazu, N. and Frasch, M. (1990). A new Drosophila homeo box gene is expressed in mesodermal precursor cells of distinct muscles during embryogenesis. *Genes Dev.*, 4(12a), 2098–2111. https://doi.org/10.1101/gad.4.12a.2098

Donati, S., Sander, T. and Link, H. (2018). Crosstalk between transcription and metabolism: how much enzyme is enough for a cell? *WIREs Syst. Biol. Med.*, 10(1), e1396. https://doi.org/10.1002/wsbm.1396

Duan, Kim, J. H., Shilagardi, K., Schiffhauer, E., Lee, D. M., Son, S., Li, S., Thomas, C., Luo, T., Fletcher, D. A., et al. (2018). Spectrin is a mechanoresponsive protein shaping

fusogenic synapse architecture during myoblast fusion. *Nat. Cell Biol.*, 20(6), 688–698. https://doi.org/10.1038/s41556-018-0106-3

Duan, Skeath, J. B. and Nguyen, H. T. (2001). Drosophila Lame duck, a novel member of the Gli superfamily, acts as a key regulator of myogenesis by controlling fusion-competent myoblast development. *Development*, 128(22), 4489–4500. https://doi.org/10.1242/dev.128.22.4489

Duan, Zhang, C., Chen, J., Sink, H., Frei, E. and Noll, M. (2007). A key role of Pox meso in somatic myogenesis of Drosophila. *Dev. Camb. Engl.*, 134(22), 3985–3997. https://doi.org/10.1242/dev.008821

Dubois, L., Frendo, J.-L., Chanut-Delalande, H., Crozatier, M. and Vincent, A. (2016). Genetic dissection of the Transcription Factor code controlling serial specification of muscle identities in Drosophila. *eLife*, 5, e14979. https://doi.org/10.7554/eLife.14979

Duboule, D. and Dollé, P. (1989). The structural and functional organization of the murine HOX gene family resembles that of Drosophila homeotic genes. *EMBO J.*, 8(5), 1497–1505. https://doi.org/10.1002/j.1460-2075.1989.tb03534.x

Dutta. (2004). Founder myoblasts and fibre number during adult myogenesis in Drosophila. *Development*, 131(15), 3761–3772. https://doi.org/10.1242/dev.01249

Dutta, Shaw, S., Maqbool, T., Pandya, H. and VijayRaghavan, K. (2005). Drosophila Heartless Acts with Heartbroken/Dof in Muscle Founder Differentiation. *PLoS Biol.*, 3(10), e337. https://doi.org/10.1371/journal.pbio.0030337

Dutta, Umashankar, M., Lewis, Edward. B., Rodrigues, V. and VijayRaghavan, K. (2010). Hox Genes Regulate Muscle Founder Cell Pattern Autonomously and Regulate Morphogenesis Through Motor Neurons. *J. Neurogenet.*, 24(3), 95–108. https://doi.org/10.3109/01677063.2010.494317

Elgar, S. J., Han, J. and Taylor, M. V. (2008). mef2 activity levels differentially affect gene expression during Drosophila muscle development. *Proc. Natl. Acad. Sci. U. S. A.*, 105(3), 918–923. https://doi.org/10.1073/pnas.0711255105

Engström, Y., Schneuwly, S. and Gehring, W. J. (1992). Spatial and temporal expression of an Antennapedia/lac Z gene construct integrated into the endogenous Antennapedia gene of Drosophila melanogaster. *Rouxs Arch. Dev. Biol. Off. Organ EDBO*, 201(2), 65–80. https://doi.org/10.1007/BF00420417

Enriquez, J., Boukhatmi, H., Dubois, L., Philippakis, A. A., Bulyk, M. L., Michelson, A. M., Crozatier, M. and Vincent, A. (2010). Multi-step control of muscle diversity by Hox proteins in the Drosophila embryo. *Development*, 137(3), 457–466. https://doi.org/10.1242/dev.045286

Enriquez, J. and Vincent, A. (2010). Segmental variations in the patterns of somatic muscles: What roles for Hox? *Fly (Austin)*, 4(3), 249–252. https://doi.org/10.4161/fly.4.3.12281

Evans, M. J. and Scarpulla, R. C. (1989). Interaction of Nuclear Factors with Multiple Sites in the Somatic Cytochrome *c* Promoter. *J. Biol. Chem.*, 264(24), 14361–14368. https://doi.org/10.1016/S0021-9258(18)71686-4

Evans, M. J. and Scarpulla, R. C. (1990). NRF-1: a trans-activator of nuclear-encoded respiratory genes in animal cells. *Genes Dev.*, 4(6), 1023–1034. https://doi.org/10.1101/gad.4.6.1023

Everetts, N. J., Worley, M. I., Yasutomi, R., Yosef, N. and Hariharan, I. K. (2021). Single-cell transcriptomics of the Drosophila wing disc reveals instructive epithelium-to-myoblast interactions. *eLife*, 10, e61276. https://doi.org/10.7554/eLife.61276

Falk, E. (1964). *New mutants: Report of E. FALK. Drosophila Inform. Ser. 39: 60.*

Fang, C., Xin, Y., Sun, T., Monteiro, A., Ye, Z., Dai, F., Lu, C. and Tong, X. (2022). The Hox gene Antennapedia is essential for wing development in insects. *Dev. Camb. Engl.*, 149(2), dev199841. https://doi.org/10.1242/dev.199841

Farrell, E. R., Fernandes, J. and Keshishian, H. (1996). Muscle Organizers inDrosophila:The Role of Persistent Larval Fibers in Adult Flight Muscle Development. *Dev. Biol.*, 176(2), 220–229. https://doi.org/10.1006/dbio.1996.0129

Fazio, I. K., Bolger, T. A. and Gill, G. (2001). Conserved Regions of the Drosophila Erect Wing Protein Contribute Both Positively and Negatively to Transcriptional Activity *. *J. Biol. Chem.*, 276(22), 18710–18716. https://doi.org/10.1074/jbc.M100080200

Fernandes, Bate, M. and Vijayraghavan, K. (1991). Development of the indirect flight muscles of Drosophila. *Development*, 113(1), 67–77.

Fernandes, J. J. and Keshishian, H. (1998). Nerve-muscle interactions during flight muscle development in Drosophila. *Dev. Camb. Engl.*, 125(9), 1769–1779. https://doi.org/10.1242/dev.125.9.1769

Fernandes, J. J. and Keshishian, H. (2005). Motoneurons regulate myoblast proliferation and patterning in Drosophila. *Dev. Biol.*, 277(2), 493–505. https://doi.org/10.1016/j.ydbio.2004.09.038

Fernandes, J. and VijayRaghavan, K. (1993). The development of indirect flight muscle innervation in Drosophila melanogaster. *Development*, 118(1), 215–227.

Fernandes and Keshishian, H. (1996). Patterning the dorsal longitudinal flight muscles (DLM) of Drosophila: insights from the ablation of larval scaffolds. *Development*, 122(12), 3755–3763. https://doi.org/10.1242/dev.122.12.3755

Fiedorczuk, K., Letts, J. A., Degliesposti, G., Kaszuba, K., Skehel, M. and Sazanov, L. A. (2016). Atomic structure of the entire mammalian mitochondrial complex I. *Nature*, 538(7625), 406–410. https://doi.org/10.1038/nature19794

Figeac, N., Jagla, T., Aradhya, R., Da Ponte, J. P. and Jagla, K. (2010). Drosophila adult muscle precursors form a network of interconnected cells and are specified by the rhomboid-triggered EGF pathway. *Development*, 137(12), 1965–1973. https://doi.org/10.1242/dev.049080

Finley, D. (2009). Recognition and processing of ubiquitin-protein conjugates by the proteasome. *Annu. Rev. Biochem.*, 78, 477–513. https://doi.org/10.1146/annurev.biochem.78.081507.101607

Formosa, L. E., Dibley, M. G., Stroud, D. A. and Ryan, M. T. (2018). Building a complex complex: Assembly of mitochondrial respiratory chain complex I. *Semin. Cell Dev. Biol.*, 76, 154–162. https://doi.org/10.1016/j.semcdb.2017.08.011

Frasch, M. (1995). Induction of visceral and cardiac mesoderm by ectodermal Dpp in the early Drosophila embryo. *Nature*, 374(6521), 464–467. https://doi.org/10.1038/374464a0

Frasch, M. (1999). Controls in patterning and diversification of somatic muscles during *Drosophila* embryogenesis. *Curr. Opin. Genet. Dev.*, 9(5), 522–529. https://doi.org/10.1016/S0959-437X(99)00014-3

Frise, E., Knoblich, J. A., Younger-Shepherd, S., Jan, L. Y. and Jan, Y. N. (1996). The Drosophila Numb protein inhibits signaling of the Notch receptor during cell-cell interaction in sensory organ lineage. *Proc. Natl. Acad. Sci. U. S. A.*, 93(21), 11925–11932.

Fuerstenberg, S. and Giniger, E. (1998). Multiple Roles forNotchinDrosophilaMyogenesis. *Dev. Biol.*, 201(1), 66–77. https://doi.org/10.1006/dbio.1998.8944

Fujioka, M., Wessells, R. J., Han, Z., Liu, J., Fitzgerald, K., Yusibova, G. L., Zamora, M., Ruiz-Lozano, P., Bodmer, R. and Jaynes, J. B. (2005). Embryonic even skipped-dependent muscle and heart cell fates are required for normal adult activity, heart function, and lifespan. *Circ. Res.*, 97(11), 1108–1114. https://doi.org/10.1161/01.RES.0000191546.08532.B2

Fyrberg, E. A., Mahaffey, J. W., Bond, B. J. and Davidson, N. (1983). Transcripts of the six Drosophila actin genes accumulate in a stage- and tissue-specific manner. *Cell*, 33(1), 115–123. https://doi.org/10.1016/0092-8674(83)90340-9

Galant, R., Walsh, C. M. and Carroll, S. B. (2002). Hox repression of a target gene: extradenticle-independent, additive action through multiple monomer binding sites. *Dev. Camb. Engl.*, 129(13), 3115–3126. https://doi.org/10.1242/dev.129.13.3115

Gao, X., Wen, X., Esser, L., Quinn, B., Yu, L., Yu, C.-A. and Xia, D. (2003). Structural basis for the quinone reduction in the bc1 complex: a comparative analysis of crystal structures of mitochondrial cytochrome bc1 with bound substrate and inhibitors at the Qi site. *Biochemistry*, 42(30), 9067–9080. https://doi.org/10.1021/bi0341814

Garber, R. L., Kuroiwa, A. and Gehring, W. J. (1983). Genomic and cDNA clones of the homeotic locus Antennapedia in Drosophila. *EMBO J.*, 2(11), 2027–2036.

Garcia, C. J., Khajeh, J., Coulanges, E., Chen, E. I. and Owusu-Ansah, E. (2017). Regulation of Mitochondrial Complex I Biogenesis in Drosophila Flight Muscles. *Cell Rep.*, 20(1), 264–278. https://doi.org/10.1016/j.celrep.2017.06.015

Gehring, W. (1966). *Bildung eines vollstaendigen Mittelbeins mit Sternopleura in der Antennenregion bei der Mutante Nasobemia (Ns) von Drosophila melanogaster. Arch Klaus Stift Vererb Forsch 41:44–54.*

Gerdes, F., Tatsuta, T. and Langer, T. (2012). Mitochondrial AAA proteases--towards a molecular understanding of membrane-bound proteolytic machines. *Biochim. Biophys. Acta*, 1823(1), 49–55. https://doi.org/10.1016/j.bbamcr.2011.09.015

Ghazi, A., Anant, S. and Raghavan, K. V. (2000). Apterous mediates development of direct flight muscles autonomously and indirect flight muscles through epidermal cues. *Development*, 127(24), 5309–5318.

Gildor, B., Schejter, E. D. and Shilo, B.-Z. (2012). Bidirectional Notch activation represses fusion competence in swarming adult Drosophila myoblasts. *Development*, 139(21), 4040–4050. https://doi.org/10.1242/dev.077495

Gisselbrecht, S., Skeath, J. B., Doe, C. Q. and Michelson, A. M. (1996). heartless encodes a fibroblast growth factor receptor (DFR1/DFGF-R2) involved in the directional migration of early mesodermal cells in the Drosophila embryo. *Genes Dev.*, 10(23), 3003–3017. https://doi.org/10.1101/gad.10.23.3003

Glicksman, M. A. and Brower, D. L. (1988). Expression of the Sex combs reduced protein in Drosophila larvae. *Dev. Biol.*, 127(1), 113–118. https://doi.org/10.1016/0012-1606(88)90193-5

Gnaiger, E. (2023). Complex II ambiguities—FADH2 in the electron transfer system. *J. Biol. Chem.*, 300(1), 105470. https://doi.org/10.1016/j.jbc.2023.105470

Graham, A., Papalopulu, N. and Krumlauf, R. (1989). The murine and Drosophila homeobox gene complexes have common features of organization and expression. *Cell*, 57(3), 367–378. https://doi.org/10.1016/0092-8674(89)90912-4

Gramates, L. S., Agapite, J., Attrill, H., Calvi, B. R., Crosby, M. A., Dos Santos, G., Goodman, J. L., Goutte-Gattat, D., Jenkins, V. K., Kaufman, T., et al. (2022). FlyBase: a guided tour of highlighted features. *Genetics*, 220(4), iyac035. https://doi.org/10.1093/genetics/iyac035

Green, D. E. and Tzagoloff, A. (1966). The mitochondrial electron transfer chain. *Arch. Biochem. Biophys.*, 116(1), 293–304. https://doi.org/10.1016/0003-9861(66)90036-1

Greene, A. W., Grenier, K., Aguileta, M. A., Muise, S., Farazifard, R., Haque, M. E., McBride, H. M., Park, D. S. and Fon, E. A. (2012). Mitochondrial processing peptidase regulates PINK1 processing, import and Parkin recruitment. *EMBO Rep.*, 13(4), 378–385. https://doi.org/10.1038/embor.2012.14

Greig, S. and Akam, M. (1993). Homeotic genes autonomously specify one aspect of pattern in the Drosophlla mesoderm. *Nature*, 362(6421), Article 6421. https://doi.org/10.1038/362630a0

Grosshans, J. and Wieschaus, E. (2000). A genetic link between morphogenesis and cell division during formation of the ventral furrow in Drosophila. *Cell*, 101(5), 523–531. https://doi.org/10.1016/s0092-8674(00)80862-4

Gu, J., Wu, M., Guo, R., Yan, K., Lei, J., Gao, N. and Yang, M. (2016). The architecture of the mammalian respirasome. *Nature*, 537(7622), 639–643. https://doi.org/10.1038/nature19359

Guan, S., Zhao, L. and Peng, R. (2022). Mitochondrial Respiratory Chain Supercomplexes: From Structure to Function. *Int. J. Mol. Sci.*, 23(22), 13880. https://doi.org/10.3390/ijms232213880

Gunage, R. D., Reichert, H. and VijayRaghavan, K. (2014). Identification of a new stem cell population that generates Drosophila flight muscles. *eLife*, 3, e03126. https://doi.org/10.7554/eLife.03126

Hajirnis, N. and Mishra, R. K. (2021). Homeotic Genes: Clustering, Modularity, and Diversity. *Front. Cell Dev. Biol.*, 9, 718308. https://doi.org/10.3389/fcell.2021.718308

Halfon, M. S., Carmena, A., Gisselbrecht, S., Sackerson, C. M., Jiménez, F., Baylies, M. K. and Michelson, A. M. (2000). Ras Pathway Specificity Is Determined by the Integration of Multiple Signal-Activated and Tissue-Restricted Transcription Factors. *Cell*, 103(1), 63–74. https://doi.org/10.1016/S0092-8674(00)00105-7

Haralalka, S., Shelton, C., Cartwright, H. N., Katzfey, E., Janzen, E. and Abmayr, S. M. (2011). Asymmetric Mbc, active Rac1 and F-actin foci in the fusion-competent myoblasts during myoblast fusion in Drosophila. *Dev. Camb. Engl.*, 138(8), 1551–1562. https://doi.org/10.1242/dev.057653

Harbauer, A. B., Zahedi, R. P., Sickmann, A., Pfanner, N. and Meisinger, C. (2014). The protein import machinery of mitochondria-a regulatory hub in metabolism, stress, and disease. *Cell Metab.*, 19(3), 357–372. https://doi.org/10.1016/j.cmet.2014.01.010

Harrington, J. S., Ryter, S. W., Plataki, M., Price, D. R. and Choi, A. M. K. (2023). Mitochondria in health, disease, and aging. *Physiol. Rev.*, 103(4), 2349–2422. https://doi.org/10.1152/physrev.00058.2021

Hatori, R. and Kornberg, T. B. (2020). Hedgehog produced by the Drosophila wing imaginal disc induces distinct responses in three target tissues. *Development*, 147(22). https://doi.org/10.1242/dev.195974

Hay, B. A., Wassarman, D. A. and Rubin, G. M. (1995). Drosophila homologs of baculovirus inhibitor of apoptosis proteins function to block cell death. *Cell*, 83(7), 1253–1262. https://doi.org/10.1016/0092-8674(95)90150-7

Herranz, R. (2004). Expression patterns of the whole Troponin C gene repertoire during Drosophila development. *Gene Expr. Patterns*, 4(2), 183–190. https://doi.org/10.1016/j.modgep.2003.09.008

Herzig, S., Long, F., Jhala, U. S., Hedrick, S., Quinn, R., Bauer, A., Rudolph, D., Schutz, G., Yoon, C., Puigserver, P., et al. (2001). CREB regulates hepatic gluconeogenesis through the coactivator PGC-1. *Nature*, 413(6852), 179–183. https://doi.org/10.1038/35093131

Hessinger, C., Technau, G. M. and Rogulja-Ortmann, A. (2017). The *Drosophila* Hox gene *Ultrabithorax* acts in both muscles and motoneurons to orchestrate formation of

specific neuromuscular connections. *Development*, 144(1), 139–150. https://doi.org/10.1242/dev.143875

Heuer, B. (2021). Mitochondrial DNA: Unraveling the “other” genome. *J. Am. Assoc. Nurse Pract.*, 33(9), 673. https://doi.org/10.1097/JXX.0000000000000646

Hooper, J. E. (1986). Homeotic gene function in the muscles of Drosophila larvae. *EMBO J.*, 5(9), 2321–2329.

Houtkooper, R. H., Mouchiroud, L., Ryu, D., Moullan, N., Katsyuba, E., Knott, G., Williams, R. W. and Auwerx, J. (2013). Mitonuclear protein imbalance as a conserved longevity mechanism. *Nature*, 497(7450), 451–457. https://doi.org/10.1038/nature12188

Hueber, S. D., Rauch, J., Djordjevic, M. A., Gunter, H., Weiller, G. F. and Frickey, T. (2013). Analysis of central Hox protein types across bilaterian clades: On the diversification of central Hox proteins from an Antennapedia/Hox7-like protein. *Dev. Biol.*, 383(2), 175–185. https://doi.org/10.1016/j.ydbio.2013.09.009

Hueber, S. D., Weiller, G. F., Djordjevic, M. A. and Frickey, T. (2010). Improving Hox Protein Classification across the Major Model Organisms. *PLOS ONE*, 5(5), e10820. https://doi.org/10.1371/journal.pone.0010820

Hunte, C., Zickermann, V. and Brandt, U. (2010). Functional modules and structural basis of conformational coupling in mitochondrial complex I. *Science*, 329(5990), 448–451. https://doi.org/10.1126/science.1191046

Huxley and Hanson, J. (1954). Changes in the Cross-Striations of Muscle during Contraction and Stretch and their Structural Interpretation. *Nature*, 173(4412), 973–976. https://doi.org/10.1038/173973a0

Huxley and Niedergerke, R. (1954). Structural Changes in Muscle During Contraction: Interference Microscopy of Living Muscle Fibres. *Nature*, 173(4412), 971–973. https://doi.org/10.1038/173971a0

Ingham, P. W. and Martinez-Arias, A. (1986). The correct activation of Antennapedia and bithorax complex genes requires the fushi tarazu gene. *Nature*, 324(6097), Article 6097. https://doi.org/10.1038/324592a0

Ip, Y. T., Park, R. E., Kosman, D., Yazdanbakhsh, K. and Levine, M. (1992). dorsal-twist interactions establish snail expression in the presumptive mesoderm of the Drosophila embryo. *Genes Dev.*, 6(8), 1518–1530. https://doi.org/10.1101/gad.6.8.1518

Irish, V. F., Martinez-Arias, A. and Akam, M. (1989). Spatial regulation of the Antennapedia and Ultrabithorax homeotic genes during Drosophila early development. *EMBO J.*, 8(5), 1527–1537. https://doi.org/10.1002/j.1460-2075.1989.tb03537.x

Iverson, T. M. (2013). Catalytic mechanisms of complex II enzymes: A structural perspective. *Biochim. Biophys. Acta BBA - Bioenerg.*, 1827(5), 648–657. https://doi.org/10.1016/j.bbabio.2012.09.008

Jagla, T., Bellard, F., Lutz, Y., Dretzen, G., Bellard, M. and Jagla, K. (1998). ladybird determines cell fate decisions during diversification of Drosophila somatic

muscles. *Development*, 125(18), 3699–3708. https://doi.org/10.1242/dev.125.18.3699

Jagla, T., Bidet, Y., Da Ponte, J. P., Dastugue, B. and Jagla, K. (2002). Cross-repressive interactions of identity genes are essential for proper specification of cardiac and muscular fates in Drosophila. *Development*, 129(4), 1037–1047. https://doi.org/10.1242/dev.129.4.1037

Jiang, J., Kosman, D., Ip, Y. T. and Levine, M. (1991). The dorsal morphogen gradient regulates the mesoderm determinant twist in early Drosophila embryos. *Genes Dev.*, 5(10), 1881–1891. https://doi.org/10.1101/gad.5.10.1881

Jiménez-Mejía, G., Montalvo-Méndez, R., Hernández-Bautista, C., Altamirano-Torres, C., Vázquez, M., Zurita, M. and Reséndez-Pérez, D. (2022). Trimeric complexes of Antp-TBP with TFIIEβ or Exd modulate transcriptional activity. *Hereditas*, 159(1), 23. https://doi.org/10.1186/s41065-022-00239-8

Jin, P., Duan, R., Luo, F., Zhang, G., Hong, S. N. and Chen, E. H. (2011). Competition between Blown Fuse and WASP for WIP binding regulates the dynamics of WASP-dependent actin polymerization in vivo. *Dev. Cell*, 20(5), 623–638. https://doi.org/10.1016/j.devcel.2011.04.007

Jin, Suh, H.-W., Kim, S.-J. and Jo, E.-K. (2017). Mitochondrial Control of Innate Immunity and Inflammation. *Immune Netw.*, 17(2), 77. https://doi.org/10.4110/in.2017.17.2.77

Jonckheere, A. I., Smeitink, J. A. M. and Rodenburg, R. J. T. (2012). Mitochondrial ATP synthase: architecture, function and pathology. *J. Inherit. Metab. Dis.*, 35(2), 211–225. https://doi.org/10.1007/s10545-011-9382-9

Jones, A. J. Y., Blaza, J. N., Varghese, F. and Hirst, J. (2017). Respiratory Complex I in Bos taurus and Paracoccus denitrificans Pumps Four Protons across the Membrane for Every NADH Oxidized. *J. Biol. Chem.*, 292(12), 4987–4995. https://doi.org/10.1074/jbc.M116.771899

Jorgensen, E. M. and Garber, R. L. (1987). Function and misfunction of the two promoters of the Drosophila Antennapedia gene. *Genes Amp Dev.*, 1(6), 544–555. https://doi.org/10.1101/gad.1.6.544

Junion, G., Jagla, T., Duplant, S., Tapin, R., Da Ponte, J.-P. and Jagla, K. (2005). Mapping Dmef2-binding regulatory modules by using a ChIP-enriched in silico targets approach. *Proc. Natl. Acad. Sci. U. S. A.*, 102(51), 18479–18484. https://doi.org/10.1073/pnas.0507030102

Kadenbach, B. and Hüttemann, M. (2015). The subunit composition and function of mammalian cytochrome c oxidase. *Mitochondrion*, 24, 64–76. https://doi.org/10.1016/j.mito.2015.07.002

Kaipa, B. R., Shao, H., Schäfer, G., Trinkewitz, T., Groth, V., Liu, J., Beck, L., Bogdan, S., Abmayr, S. M. and Önel, S.-F. (2013). Dock mediates Scar- and WASp-dependent actin polymerization through interaction with cell adhesion molecules in founder cells and fusion-competent myoblasts. *J. Cell Sci.*, 126(1), 360–372. https://doi.org/10.1242/jcs.113860

Kane, L. A., Lazarou, M., Fogel, A. I., Li, Y., Yamano, K., Sarraf, S. A., Banerjee, S. and Youle, R. J. (2014). PINK1 phosphorylates ubiquitin to activate Parkin E3 ubiquitin ligase activity. *J. Cell Biol.*, 205(2), 143–153. https://doi.org/10.1083/jcb.201402104

Kanehisa, M. and Goto, S. (2000). KEGG: Kyoto Encyclopedia of Genes and Genomes. *Nucleic Acids Res.*, 28(1), 27–30.

Katti, P., Ajayi, P. T., Aponte, A., Bleck, C. K. E. and Glancy, B. (2022). Identification of evolutionarily conserved regulators of muscle mitochondrial network organization. *Nat. Commun.*, 13(1), 6622. https://doi.org/10.1038/s41467-022-34445-9

Kaufman, T. C. and Abbott, M. K. (1984). Homoeotic Genes and the Specification of Segmental Identity in the Embryo and Adult Thorax of Drosophila Melanogaster. In G. M. Malacinski and W. H. Klein (Eds.), *Molecular Aspects of Early Development* (pp. 189–218). Boston, MA: Springer US. https://doi.org/10.1007/978-1-4684-4628-9_9

Kaufman, T. C., Lewis, R. and Wakimoto, B. (1980). Cytogenetic Analysis of Chromosome 3 in DROSOPHILA MELANOGASTER: The Homoeotic Gene Complex in Polytene Chromosome Interval 84a-B. *Genetics*, 94(1), 115–133. https://doi.org/10.1093/genetics/94.1.115

Kaufman, T. C., Seeger, M. A. and Olsen, G. (1990). Molecular and genetic organization of the antennapedia gene complex of Drosophila melanogaster. *Adv. Genet.*, 27, 309–362. https://doi.org/10.1016/s0065-2660(08)60029-2

Keller, C. A., Erickson, M. S. and Abmayr, S. M. (1997). Misexpression of nautilus induces myogenesis in cardioblasts and alters the pattern of somatic muscle fibers. *Dev. Biol.*, 181(2), 197–212. https://doi.org/10.1006/dbio.1996.8434

Kelly, D. P. and Scarpulla, R. C. (2004). Transcriptional regulatory circuits controlling mitochondrial biogenesis and function. *Genes Dev.*, 18(4), 357–368. https://doi.org/10.1101/gad.1177604

Kesper, D. A., Stute, C., Buttgereit, D., Kreisköther, N., Vishnu, S., Fischbach, K.-F. and Renkawitz-Pohl, R. (2007). Myoblast fusion in Drosophila melanogaster is mediated through a fusion-restricted myogenic-adhesive structure (FuRMAS). *Dev. Dyn.*, 236(2), 404–415. https://doi.org/10.1002/dvdy.21035

Killackey, S. A., Philpott, D. J. and Girardin, S. E. (2020). Mitophagy pathways in health and disease. *J. Cell Biol.*, 219(11), e202004029. https://doi.org/10.1083/jcb.202004029

Kim, Ren, Y., Ng, W. P., Li, S., Son, S., Kee, Y.-S., Zhang, S., Zhang, G., Fletcher, D. A., Robinson, D. N., et al. (2015). Mechanical tension drives cell membrane fusion. *Dev. Cell*, 32(5), 561–573. https://doi.org/10.1016/j.devcel.2015.01.005

Kim, Shilagardi, K., Zhang, S., Hong, S. N., Sens, K. L., Bo, J., Gonzalez, G. A. and Chen, E. H. (2007). A Critical Function for the Actin Cytoskeleton in Targeted Exocytosis of Prefusion Vesicles during Myoblast Fusion. *Dev. Cell*, 12(4), 571–586. https://doi.org/10.1016/j.devcel.2007.02.019

Kim, Y., Parry, H. A., Willingham, T. B., Alspaugh, G., Lindberg, E., Combs, C. A., Knutson, J. R., Bleck, C. K. E. and Glancy, B. (2024). Reorganization of mitochondria-organelle interactions during postnatal development in skeletal muscle. *J. Physiol.*, 602(5), 891–912. https://doi.org/10.1113/JP285014

Kim, Y., Yang, D. S., Katti, P. and Glancy, B. (2019). Protein composition of the muscle mitochondrial reticulum during postnatal development. *J. Physiol.*, 597(10), 2707–2727. https://doi.org/10.1113/JP277579

Knirr, S., Azpiazu, N. and Frasch, M. (1999). The role of the NK-homeobox gene slouch (S59) in somatic muscle patterning. *Dev. Camb. Engl.*, 126(20), 4525–4535. https://doi.org/10.1242/dev.126.20.4525

Kolley, F., Sidor, C., Dehapiot, B., Schnorrer, F. and Friedrich, B. M. (2024). Mechanisms of Sarcomere Assembly in Muscle Cells Inferred from Sequential Ordering of Myofibril Components. *PRX Life*, 2(1), 013002. https://doi.org/10.1103/PRXLife.2.013002

Kosman, D., Ip, Y. T., Levine, M. and Arora, K. (1991). Establishment of the Mesoderm-Neuroectoderm Boundary in the Drosophila Embryo. *Science*, 254(5028), 118–122. https://doi.org/10.1126/science.1925551

Koyano, F., Okatsu, K., Kosako, H., Tamura, Y., Go, E., Kimura, M., Kimura, Y., Tsuchiya, H., Yoshihara, H., Hirokawa, T., et al. (2014). Ubiquitin is phosphorylated by PINK1 to activate parkin. *Nature*, 510(7503), 162–166. https://doi.org/10.1038/nature13392

Kozopas, K. M. and Nusse, R. (2002). Direct flight muscles in Drosophila develop from cells with characteristics of founders and depend on DWnt-2 for their correct patterning. *Dev. Biol.*, 243(2), 312–325. https://doi.org/10.1006/dbio.2002.0572

Kribelbauer, J. F., Loker, R. E., Feng, S., Rastogi, C., Abe, N., Rube, H. T., Bussemaker, H. J. and Mann, R. S. (2020). Context-Dependent Gene Regulation by Homeodomain Transcription Factor Complexes Revealed by Shape-Readout Deficient Proteins. *Mol. Cell*, 78(1), 152-167.e11. https://doi.org/10.1016/j.molcel.2020.01.027

Kumar, R. P., Dobi, K. C., Baylies, M. K. and Abmayr, S. M. (2015). Muscle Cell Fate Choice Requires the T-Box Transcription Factor Midline in Drosophila. *Genetics*, 199(3), 777–791. https://doi.org/10.1534/genetics.115.174300

Kurata, S., Go, M. J., Artavanis-Tsakonas, S. and Gehring, W. J. (2000). Notch signaling and the determination of appendage identity. *Proc. Natl. Acad. Sci. U. S. A.*, 97(5), 2117–2122.

Landgraf, M., Bossing, T., Technau, G. M. and Bate, M. (1997). The origin, location, and projections of the embryonic abdominal motorneurons of Drosophila. *J. Neurosci. Off. J. Soc. Neurosci.*, 17(24), 9642–9655. https://doi.org/10.1523/JNEUROSCI.17-24-09642.1997

Laughon, A., Boulet, A. M., Bermingham, J. R., Laymon, R. A. and Scott, M. P. (1986). Structure of transcripts from the homeotic Antennapedia gene of Drosophila melanogaster: two promoters control the major protein-coding region. *Mol. Cell. Biol.*, 6(12), 4676–4689.

Laughon, A. and Scott, M. P. (1984). Sequence of a Drosophila segmentation gene: protein structure homology with DNA-binding proteins. *Nature*, 310(5972), 25–31. https://doi.org/10.1038/310025a0

Laurichesse, Q. and Soler, C. (2020). Muscle development : a view from adult myogenesis in Drosophila. *Semin. Cell Dev. Biol.*, 104, 39–50. https://doi.org/10.1016/j.semcdb.2020.02.009

Lavergne, G., Soler, C., Zmojdzian, M. and Jagla, K. (2017). Characterization of Drosophila Muscle Stem Cell-Like Adult Muscle Precursors. *Methods Mol. Biol. Clifton NJ*, 1556, 103–116. https://doi.org/10.1007/978-1-4939-6771-1_5

Lavergne, G., Zmojdzian, M., Da Ponte, J. P., Junion, G. and Jagla, K. (2020). Drosophila adult muscle precursor cells contribute to motor axon pathfinding and proper innervation of embryonic muscles. *Dev. Camb. Engl.*, 147(4), dev183004. https://doi.org/10.1242/dev.183004

Lavie, J., De Belvalet, H., Sonon, S., Ion, A. M., Dumon, E., Melser, S., Lacombe, D., Dupuy, J.-W., Lalou, C. and Bénard, G. (2018). Ubiquitin-Dependent Degradation of Mitochondrial Proteins Regulates Energy Metabolism. *Cell Rep.*, 23(10), 2852–2863. https://doi.org/10.1016/j.celrep.2018.05.013

Lawrence, Bodmer, R. and Vincent, J.-P. (1995). Segmental patterning of heart precursors in *Drosophila*. *Development*, 121(12), 4303–4308. https://doi.org/10.1242/dev.121.12.4303

Lawrence, P. A. (1982). Cell lineage of the thoracic muscles of drosophila. *Cell*, 29(2), 493–503. https://doi.org/10.1016/0092-8674(82)90166-0

Lawrence, P. A. and Johnston, P. (1984). The genetic specification of pattern in a Drosophila muscle. *Cell*, 36(3), 775–782. https://doi.org/10.1016/0092-8674(84)90357-x

Lazarou, M., Sliter, D. A., Kane, L. A., Sarraf, S. A., Wang, C., Burman, J. L., Sideris, D. P., Fogel, A. I. and Youle, R. J. (2015). The ubiquitin kinase PINK1 recruits autophagy receptors to induce mitophagy. *Nature*, 524(7565), 309–314. https://doi.org/10.1038/nature14893

Le Calvez, J. (1948). An Aristapedia mutation, dominant heterozygote, homozygous lethal, in Drosophila melanogaster. *Comptes Rendus Hebd. Seances Acad. Sci.*, 226(1), 123.

Lee and Chen, E. H. (2019). Drosophila Myoblast Fusion: Invasion and Resistance for the Ultimate Union. *Annu. Rev. Genet.*, 53, 67–91. https://doi.org/10.1146/annurev-genet-120116-024603

Lee and Frasch, M. (2000). Wingless effects mesoderm patterning and ectoderm segmentation events via induction of its downstream target sloppy paired. *Development*, 127(24), 5497–5508. https://doi.org/10.1242/dev.127.24.5497

Lee, J. J., Sanchez-Martinez, A., Zarate, A. M., Benincá, C., Mayor, U., Clague, M. J. and Whitworth, A. J. (2018). Basal mitophagy is widespread in Drosophila but minimally affected by loss of Pink1 or parkin. *J. Cell Biol.*, 217(5), 1613–1622. https://doi.org/10.1083/jcb.201801044

Lefebvre-Legendre, L., Salin, B., Schaëffer, J., Brèthes, D., Dautant, A., Ackerman, S. H. and Rago, J.-P. di. (2005). Failure to Assemble the α3 β3 Subcomplex of the ATP Synthase Leads to Accumulation of the α and β Subunits within Inclusion Bodies and the Loss of Mitochondrial Cristae in Saccharomyces cerevisiae. *J. Biol. Chem.*, 280(18), 18386–18392. https://doi.org/10.1074/jbc.M410789200

Lemasters, J. J. (2005). Selective mitochondrial autophagy, or mitophagy, as a targeted defense against oxidative stress, mitochondrial dysfunction, and aging. *Rejuvenation Res.*, 8(1), 3–5. https://doi.org/10.1089/rej.2005.8.3

Lemke, S. B. and Schnorrer, F. (2017). Mechanical forces during muscle development. *Mech. Dev.*, 144, 92–101. https://doi.org/10.1016/j.mod.2016.11.003

Lemke, S. B. and Schnorrer, F. (2018). In Vivo Imaging of Muscle-tendon Morphogenesis in Drosophila Pupae. *J. Vis. Exp.*, *132*, 57312. https://doi.org/10.3791/57312

Leonhard, K., Stiegler, A., Neupert, W. and Langer, T. (1999). Chaperone-like activity of the AAA domain of the yeast Yme1 AAA protease. *Nature*, 398(6725), 348–351. https://doi.org/10.1038/18704

Leptin, M. and Grunewald, B. (1990). Cell shape changes during gastrulation in Drosophila. *Development*, 110(1), 73–84. https://doi.org/10.1242/dev.110.1.73

Letts, J. A., Fiedorczuk, K. and Sazanov, L. A. (2016). The architecture of respiratory supercomplexes. *Nature*, 537(7622), 644–648. https://doi.org/10.1038/nature19774

Levine, M., Hafen, E., Garber, R. L. and Gehring, W. J. (1983). Spatial distribution of Antennapedia transcripts during Drosophila development. *EMBO J.*, 2(11), 2037–2046.

Levine, M., Rubin, G. M. and Tjian, R. (1984). Human DNA sequences homologous to a protein coding region conserved between homeotic genes of Drosophila. *Cell*, 38(3), 667–673. https://doi.org/10.1016/0092-8674(84)90261-7

Lewis, E. B. (1956). *The phenomenon of position effect. Advan. Genetics 3: 73-115.*

Lewis, E. B. (1963). Genes and Developmental Pathways. *Am. Zool.*, 3(1), 33–56.

Lewis, E. B. (1978). A gene complex controlling segmentation in Drosophila. *Nature*, 276(5688), Article 5688. https://doi.org/10.1038/276565a0

Lewis, R. A., Kaufman, T. C., Denell, R. E. and Tallerico, P. (1980). Genetic Analysis of the Antennapedia Gene Complex (Ant-C) and Adjacent Chromosomal Regions of DROSOPHILA MELANOGASTER. I. Polytene Chromosome Segments 84b-D. *Genetics*, 95(2), 367–381. https://doi.org/10.1093/genetics/95.2.367

Lewis, R. A., Wakimoto, B. T., Denell, R. E. and Kaufman, T. C. (1980). Genetic Analysis of the Antennapedia Gene Complex (Ant-C) and Adjacent Chromosomal Regions of DROSOPHILA MELANOGASTER. II. Polytene Chromosome Segments 84A-84B1,2. *Genetics*, 95(2), 383–397. https://doi.org/10.1093/genetics/95.2.383

Leyfer, D. and Fetterman, J. L. (2023). Beyond MitoCarta—expanding the list of candidate proteins involved in mitochondrial functions using a biological network approach.

NAR Genomics Bioinforma., 5(4), lqad107. https://doi.org/10.1093/nargab/lqad107

Li, B., Wang, J., Liao, J., Wu, M., Yuan, X., Fang, H., Shen, L. and Jiang, M. (2022). YY1 promotes pancreatic cancer cell proliferation by enhancing mitochondrial respiration. *Cancer Cell Int.*, 22. https://doi.org/10.1186/s12935-022-02712-w

Li and Gilmour. (2013). Distinct mechanisms of transcriptional pausing orchestrated by GAGA factor and M1BP, a novel transcription factor. *EMBO J.*, 32(13), 1829–1841. https://doi.org/10.1038/emboj.2013.111

Li, H., Janssens, J., De Waegeneer, M., Kolluru, S. S., Davie, K., Gardeux, V., Saelens, W., David, F. P. A., Brbić, M., Spanier, K., et al. (2022). Fly Cell Atlas: A single-nucleus transcriptomic atlas of the adult fruit fly. *Science*, 375(6584), eabk2432. https://doi.org/10.1126/science.abk2432

Li, J. and Gilmour, D. S. (2013). Distinct mechanisms of transcriptional pausing orchestrated by GAGA factor and M1BP, a novel transcription factor. *EMBO J.*, 32(13), 1829–1841. https://doi.org/10.1038/emboj.2013.111

Lilly, B., Zhao, B., Ranganayakulu, G., Paterson, B. M., Schulz, R. A. and Olson, E. N. (1995). Requirement of MADS Domain Transcription Factor D-MEF2 for Muscle Formation in Drosophila. *Science*, 267(5198), 688–693. https://doi.org/10.1126/science.7839146

Lin, M. H., Nguyen, H. T., Dybala, C. and Storti, R. V. (1996). Myocyte-specific enhancer factor 2 acts cooperatively with a muscle activator region to regulate Drosophila tropomyosin gene muscle expression. *Proc. Natl. Acad. Sci. U. S. A.*, 93(10), 4623–4628.

Linda, S., Lund, I., Torbergsen, T., Aasly, J., Mellgren, S. I., Borud, O. and Monstad, P. (1992). Mitochondrial Diseases and Myopathies: A Series of Muscle Biopsy Specimens with Ultrastructural Changes in the Mitochondria. *Ultrastruct. Pathol.*, 16(3), 263–275. https://doi.org/10.3109/01913129209061355

Lindsey, D. L. and Grell, E. H. (1968). *Genetic Variations of Drosophila melanogaster. Carnegie Inst. Wash. Publ. No. 627*.

Liotta, D., Han, J., Elgar, S., Garvey, C., Han, Z. and Taylor, M. V. (2007). The Him gene reveals a balance of inputs controlling muscle differentiation in Drosophila. *Curr. Biol. CB*, 17(16), 1409–1413. https://doi.org/10.1016/j.cub.2007.07.039

Lis, J. (1998). Promoter-associated pausing in promoter architecture and postinitiation transcriptional regulation. *Cold Spring Harb. Symp. Quant. Biol.*, 63, 347–356. https://doi.org/10.1101/sqb.1998.63.347

Liu, L., Feng, D., Chen, G., Chen, M., Zheng, Q., Song, P., Ma, Q., Zhu, C., Wang, R., Qi, W., et al. (2012). Mitochondrial outer-membrane protein FUNDC1 mediates hypoxia-induced mitophagy in mammalian cells. *Nat. Cell Biol.*, 14(2), 177–185. https://doi.org/10.1038/ncb2422

Livneh, I., Cohen-Kaplan, V., Cohen-Rosenzweig, C., Avni, N. and Ciechanover, A. (2016). The life cycle of the 26S proteasome: from birth, through regulation and function, and onto its death. *Cell Res.*, 26(8), 869–885. https://doi.org/10.1038/cr.2016.86

Lovato, T. L., Benjamin, A. R. and Cripps, R. M. (2005). Transcription of Myocyte enhancer factor-2 in adult Drosophila myoblasts is induced by the steroid hormone ecdysone. *Dev. Biol.*, 288(2), 612–621. https://doi.org/10.1016/j.ydbio.2005.09.007

Malicki, J., Schughart, K. and McGinnis, W. (1990). Mouse *Hox-2.2* specifies thoracic segmental identity in Drosophila embryos and larvae. *Cell*, 63(5), 961–967. https://doi.org/10.1016/0092-8674(90)90499-5

Mallo, M. and Alonso, C. R. (2013). The regulation of Hox gene expression during animal development. *Development*, 140(19), 3951–3963. https://doi.org/10.1242/dev.068346

Mandal, L., Martinez-Agosto, J. A., Evans, C. J., Hartenstein, V. and Banerjee, U. (2007). A Hedgehog- and Antennapedia-dependent niche maintains Drosophila haematopoietic precursors. *Nature*, 446(7133), 320–324. https://doi.org/10.1038/nature05585

Mann, R. S. and Chan, S.-K. (1996). Extra specificity from *extradenticle*: the partnership between HOX and PBX/EXD homeodomain proteins. *Trends Genet.*, 12(7), 258–262. https://doi.org/10.1016/0168-9525(96)10026-3

Maqbool, T., Soler, C., Jagla, T., Daczewska, M., Lodha, N., Palliyil, S., VijayRaghavan, K. and Jagla, K. (2006). Shaping Leg Muscles in Drosophila: Role of ladybird, a Conserved Regulator of Appendicular Myogenesis. *PLOS ONE*, 1(1), e122. https://doi.org/10.1371/journal.pone.0000122

Maréchal, A., Xu, J.-Y., Genko, N., Hartley, A. M., Haraux, F., Meunier, B. and Rich, P. R. (2020). A common coupling mechanism for A-type heme-copper oxidases from bacteria to mitochondria. *Proc. Natl. Acad. Sci.*, 117(17), 9349–9355. https://doi.org/10.1073/pnas.2001572117

Margineantu, D. H., Emerson, C. B., Diaz, D. and Hockenbery, D. M. (2007). Hsp90 Inhibition Decreases Mitochondrial Protein Turnover. *PLOS ONE*, 2(10), e1066. https://doi.org/10.1371/journal.pone.0001066

Marinozzi, V., Derenzini, M., Nardi, F. and Gallo, P. (1977). Mitochondrial inclusions in human cancer of the gastrointestinal tract. *Cancer Res.*, 37(5), 1556–1563.

Mark, M., Rijli, F. M. and Chambon, P. (1997). Homeobox Genes in Embryogenesis and Pathogenesis. *Pediatr. Res.*, 42(4), 421–429. https://doi.org/10.1203/00006450-199710000-00001

Martinez-Arias, A. (1986). The Antennapedia gene is required and expressed in parasegments 4 and 5 of the Drosophila embryo. *EMBO J.*, 5(1), 135–141. https://doi.org/10.1002/j.1460-2075.1986.tb04187.x

Massarwa, R., Carmon, S., Shilo, B.-Z. and Schejter, E. D. (2007). WIP/WASp-based actin-polymerization machinery is essential for myoblast fusion in Drosophila. *Dev. Cell*, 12(4), 557–569. https://doi.org/10.1016/j.devcel.2007.01.016

Matsushima, Y., Goto, Y. and Kaguni, L. S. (2010). Mitochondrial Lon protease regulates mitochondrial DNA copy number and transcription by selective degradation of

mitochondrial transcription factor A (TFAM). *Proc. Natl. Acad. Sci. U. S. A.*, 107(43), 18410–18415. https://doi.org/10.1073/pnas.1008924107

Matsushima, Y., Hirofuji, Y., Aihara, M., Yue, S., Uchiumi, T., Kaguni, L. S. and Kang, D. (2017). Drosophila protease ClpXP specifically degrades DmLRPPRC1 controlling mitochondrial mRNA and translation. *Sci. Rep.*, 7(1), 8315. https://doi.org/10.1038/s41598-017-08088-6

McGinnis, W., Hart, C. P., Gehring, W. J. and Ruddle, F. H. (1984). Molecular cloning and chromosome mapping of a mouse DNA sequence homologous to homeotic genes of Drosophila. *Cell*, 38(3), 675–680. https://doi.org/10.1016/0092-8674(84)90262-9

McGinnis, W., Levine, M. S., Hafen, E., Kuroiwa, A. and Gehring, W. J. (1984). A conserved DNA sequence in homoeotic genes of the Drosophila Antennapedia and bithorax complexes. *Nature*, 308(5958), Article 5958. https://doi.org/10.1038/308428a0

McWilliams, T. G., Prescott, A. R., Montava-Garriga, L., Ball, G., Singh, F., Barini, E., Muqit, M. M. K., Brooks, S. P. and Ganley, I. G. (2018). Basal Mitophagy Occurs Independently of PINK1 in Mouse Tissues of High Metabolic Demand. *Cell Metab.*, 27(2), 439-449.e5. https://doi.org/10.1016/j.cmet.2017.12.008

Menon, Carrillo, R. A. and Zinn, K. (2013). Development and plasticity of the Drosophila larval neuromuscular junction. *Wiley Interdiscip. Rev. Dev. Biol.*, 2(5), 647–670. https://doi.org/10.1002/wdev.108

Menon and Chia, W. (2001). Drosophila Rolling pebbles: A Multidomain Protein Required for Myoblast Fusion that Recruits D-Titin in Response to the Myoblast Attractant Dumbfounded. *Dev. Cell*, 1(5), 691–703. https://doi.org/10.1016/S1534-5807(01)00075-2

Menon, Osman, Z., Chenchill, K. and Chia, W. (2005). A positive feedback loop between Dumbfounded and Rolling pebbles leads to myotube enlargement in Drosophila. *J. Cell Biol.*, 169(6), 909–920. https://doi.org/10.1083/jcb.200501126

Merabet, S. and Mann, R. S. (2016). To Be Specific or Not: The Critical Relationship Between Hox And TALE Proteins. *Trends Genet. TIG*, 32(6), 334–347. https://doi.org/10.1016/j.tig.2016.03.004

Michelson, A. M. (1994). Muscle pattern diversification in Drosophila is determined by the autonomous function of homeotic genes in the embryonic mesoderm. *Development*, 120(4), 755–768.

Michelson, A. M., Abmayr, S. M., Bate, M., Arias, A. M. and Maniatis, T. (1990). Expression of a MyoD family member prefigures muscle pattern in Drosophila embryos. *Genes Dev.*, 4(12a), 2086–2097. https://doi.org/10.1101/gad.4.12a.2086

Michelson, A. M., Gisselbrecht, S., Zhou, Y., Baek, K. H. and Buff, E. M. (1998). Dual functions of the heartless fibroblast growth factor receptor in development of the Drosophila embryonic mesoderm. *Dev. Genet.*, 22(3), 212–229. https://doi.org/10.1002/(SICI)1520-6408(1998)22:3<212::AID-DVG4>3.0.CO;2-9

Mishra, P., Varuzhanyan, G., Pham, A. H. and Chan, D. C. (2015). Mitochondrial Dynamics Is a Distinguishing Feature of Skeletal Muscle Fiber Types and Regulates Organellar Compartmentalization. *Cell Metab.*, 22(6), 1033–1044. https://doi.org/10.1016/j.cmet.2015.09.027

Mitchell, P. (1961). Coupling of Phosphorylation to Electron and Hydrogen Transfer by a Chemi-Osmotic type of Mechanism. *Nature*, 191(4784), 144–148. https://doi.org/10.1038/191144a0

Mnatsakanyan, N., Llaguno, M. C., Yang, Y., Yan, Y., Weber, J., Sigworth, F. J. and Jonas, E. A. (2019). A mitochondrial megachannel resides in monomeric F1FO ATP synthase. *Nat. Commun.*, 10(1), 5823. https://doi.org/10.1038/s41467-019-13766-2

Morriss, G. R., Bryantsev, A. L., Chechenova, M., LaBeau, E. M., Lovato, T. L., Ryan, K. M. and Cripps, R. M. (2012). Analysis of skeletal muscle development in Drosophila. *Methods Mol. Biol. Clifton NJ*, 798, 127–152. https://doi.org/10.1007/978-1-61779-343-1_8

Moucaud, B., Prince, E., Jagla, K. and Soler, C. (2023). Developmental origin of tendon diversity in Drosophila melanogaster. *Front. Physiol.*, 14, 1176148. https://doi.org/10.3389/fphys.2023.1176148

Mukherjee, P., Gildor, B., Shilo, B.-Z., VijayRaghavan, K. and Schejter, E. D. (2011). The actin nucleator WASp is required for myoblast fusion during adult Drosophila myogenesis. *Development*, 138(11), 2347–2357. https://doi.org/10.1242/dev.055012

Müller, D., Jagla, T., Bodart, L. M., Jährling, N., Dodt, H.-U., Jagla, K. and Frasch, M. (2010). Regulation and Functions of the lms Homeobox Gene during Development of Embryonic Lateral Transverse Muscles and Direct Flight Muscles in Drosophila. *PLoS ONE*, 5(12), e14323. https://doi.org/10.1371/journal.pone.0014323

Muñoz-Carvajal, F. and Sanhueza, M. (2020). The Mitochondrial Unfolded Protein Response: A Hinge Between Healthy and Pathological Aging. *Front. Aging Neurosci.*, 12. Retrieved from https://www.frontiersin.org/article/10.3389/fnagi.2020.581849

Murre, C., McCaw, P. S. and Baltimore, D. (1989). A new DNA binding and dimerization motif in immunoglobulin enhancer binding, daughterless, MyoD, and myc proteins. *Cell*, 56(5), 777–783. https://doi.org/10.1016/0092-8674(89)90682-X

Nabel-Rosen, H., Toledano-Katchalski, H., Volohonsky, G. and Volk, T. (2005). Cell divisions in the drosophila embryonic mesoderm are repressed via posttranscriptional regulation of string/cdc25 by HOW. *Curr. Biol. CB*, 15(4), 295–302. https://doi.org/10.1016/j.cub.2005.01.045

Narendra, D. P., Jin, S. M., Tanaka, A., Suen, D.-F., Gautier, C. A., Shen, J., Cookson, M. R. and Youle, R. J. (2010). PINK1 Is Selectively Stabilized on Impaired Mitochondria to Activate Parkin. *PLOS Biol.*, 8(1), e1000298. https://doi.org/10.1371/journal.pbio.1000298

Nargund, A. M., Pellegrino, M. W., Fiorese, C. J., Baker, B. M. and Haynes, C. M. (2012). Mitochondrial import efficiency of ATFS-1 regulates mitochondrial UPR activation. *Science*, 337(6094), 587–590. https://doi.org/10.1126/science.1223560

Ndi, M., Marin-Buera, L., Salvatori, R., Singh, A. P. and Ott, M. (2018). Biogenesis of the bc1 Complex of the Mitochondrial Respiratory Chain. *J. Mol. Biol.*, 430(21), 3892–3905. https://doi.org/10.1016/j.jmb.2018.04.036

Nguyen, P.-K. and Cheng, L. Y. (2022). Non-autonomous regulation of neurogenesis by extrinsic cues: a Drosophila perspective. *Oxf. Open Neurosci.*, 1, kvac004. https://doi.org/10.1093/oons/kvac004

Nguyen, T., Wang, J. and Schulz, R. A. (2002). Mutations within the conserved MADS box of the D-MEF2 muscle differentiation factor result in a loss of DNA binding ability and lethality in Drosophila. *Differentiation*, 70(8), 438–446. https://doi.org/10.1046/j.1432-0436.2002.700806.x

Nose. (2012). Generation of neuromuscular specificity in Drosophila: novel mechanisms revealed by new technologies. *Front. Mol. Neurosci.*, 5. https://doi.org/10.3389/fnmol.2012.00062

Nose, Isshiki, T. and Takeichi, M. (1998). Regional specification of muscle progenitors in Drosophila: the role of the msh homeobox gene. *Development*, 125(2), 215–223. https://doi.org/10.1242/dev.125.2.215

Nüsslein-Volhard, C. (1979). Maternal effect mutations that alter the spatial coordinates of the embryo of Drosophila melanogaster. In *Determinants of Spatial Organization* (pp. 185–211). New York: Academic Press Inc.

Nüsslein-Volhard, C., Wieschaus, E. and Kluding, H. (1984). Mutations affecting the pattern of the larval cuticle inDrosophila melanogaster : I. Zygotic loci on the second chromosome. *Wilhelm Rouxs Arch. Dev. Biol.*, 193(5), 267–282. https://doi.org/10.1007/BF00848156

Ogata, T. and Yamasaki, Y. (1985). Scanning electron-microscopic studies on the three-dimensional structure of mitochondria in the mammalian red, white and intermediate muscle fibers. *Cell Tissue Res.*, 241(2), 251–256. https://doi.org/10.1007/BF00217168

Ohler, U., Liao, G., Niemann, H. and Rubin, G. M. (2002). Computational analysis of core promoters in the Drosophila genome. *Genome Biol.*, 3(12), research0087.1. https://doi.org/10.1186/gb-2002-3-12-research0087

Ongwijitwat, S., Liang, H. L., Graboyes, E. M. and Wong-Riley, M. T. T. (2006). Nuclear respiratory factor 2 senses changing cellular energy demands and its silencing down-regulates cytochrome oxidase and other target gene mRNAs. *Gene*, 374, 39–49. https://doi.org/10.1016/j.gene.2006.01.009

Orfanos, Z. and Sparrow, J. C. (2013). Myosin isoform switching during assembly of the *Drosophila* flight muscle thick filament lattice. *J. Cell Sci.*, 126(1), 139–148. https://doi.org/10.1242/jcs.110361

Orrenius, S., Zhivotovsky, B. and Nicotera, P. (2003). Regulation of cell death: the calcium–apoptosis link. *Nat. Rev. Mol. Cell Biol.*, 4(7), 552–565. https://doi.org/10.1038/nrm1150

Ortiz-Lombardia, M., Foos, N., Maurel-Zaffran, C., Saurin, A. J. and Graba, Y. (2017). Hox functional diversity: Novel insights from flexible motif folding and plastic protein interaction. *BioEssays*, 39(4), 1600246. https://doi.org/10.1002/bies.201600246

Pai, C.-Y., Kuo, T.-S., Jaw, T. J., Kurant, E., Chen, C.-T., Bessarab, D. A., Salzberg, A. and Sun, Y. H. (1998). The Homothorax homeoprotein activates the nuclear localization of another homeoprotein, Extradenticle, and suppresses eye development in Drosophila. *Genes Dev.*, 12(3), 435–446.

Palade, G. E. (1952). The fine structure of mitochondria. *Anat. Rec.*, 114(3), 427–451. https://doi.org/10.1002/ar.1091140304

Papadopoulos, D. K., Resendez-Perez, D., Cardenas-Chavez, D. L., Villanueva-Segura, K., Canales-del-Castillo, R., Felix, D. A., Funfschilling, R. and Gehring, W. J. (2011). Functional synthetic Antennapedia genes and the dual roles of YPWM motif and linker size in transcriptional activation and repression. *Proc. Natl. Acad. Sci.*, 108(29), 11959–11964. https://doi.org/10.1073/pnas.1108686108

Papadopoulos, D. K., Skouloudaki, K., Engström, Y., Terenius, L., Rigler, R., Zechner, C., Vukojević, V. and Tomancak, P. (2019). Control of Hox transcription factor concentration and cell-to-cell variability by an auto-regulatory switch. *Development*, 146(12), dev168179. https://doi.org/10.1242/dev.168179

Pardo, L., Valor, L. M., Eraso-Pichot, A., Barco, A., Golbano, A., Hardingham, G. E., Masgrau, R. and Galea, E. (2017). CREB Regulates Distinct Adaptive Transcriptional Programs in Astrocytes and Neurons. *Sci. Rep.*, 7(1), 6390. https://doi.org/10.1038/s41598-017-06231-x

Pareek, G., Thomas, R. E., Vincow, E. S., Morris, D. R. and Pallanck, L. J. (2018). Lon protease inactivation in Drosophila causes unfolded protein stress and inhibition of mitochondrial translation. *Cell Death Discov.*, 4(1), 1–14. https://doi.org/10.1038/s41420-018-0110-1

Patel, A., Wu, Y., Han, X., Su, Y., Maugel, T., Shroff, H. and Roy, S. (2022). Cytonemes coordinate asymmetric signaling and organization in the Drosophila muscle progenitor niche. *Nat. Commun.*, 13(1), 1185. https://doi.org/10.1038/s41467-022-28587-z

Paul, R., Giraud, G., Domsch, K., Duffraisse, M., Marmigère, F., Khan, S., Vanderperre, S., Lohmann, I., Stoks, R., Shashidhara, L. S., et al. (2021). Hox dosage contributes to flight appendage morphology in Drosophila. *Nat. Commun.*, 12(1), Article 1. https://doi.org/10.1038/s41467-021-23293-8

Peifer, M. and Wieschaus, E. (1990). Mutations in the Drosophila gene extradenticle affect the way specific homeo domain proteins regulate segmental identity. *Genes Dev.*, 4(7), 1209–1223. https://doi.org/10.1101/gad.4.7.1209

Perkins, L. A., Holderbaum, L., Tao, R., Hu, Y., Sopko, R., McCall, K., Yang-Zhou, D., Flockhart, I., Binari, R., Shim, H.-S., et al. (2015). The Transgenic RNAi Project at Harvard

Medical School: Resources and Validation. *Genetics*, 201(3), 843–852. https://doi.org/10.1534/genetics.115.180208

Pezeron, G., Millen, K., Boukhatmi, H. and Bray, S. (2014). Notch directly regulates the cell morphogenesis genes Reck, talin and trio in adult muscle progenitors. *J. Cell Sci.*, 127(21), 4634–4644. https://doi.org/10.1242/jcs.151787

Pierron, D., Wildman, D. E., Hüttemann, M., Markondapatnaikuni, G. C., Aras, S. and Grossman, L. I. (2012). Cytochrome c oxidase: evolution of control via nuclear subunit addition. *Biochim. Biophys. Acta*, 1817(4), 590–597. https://doi.org/10.1016/j.bbabio.2011.07.007

Pines, M., Das, R., Ellis, S. J., Morin, A., Czerniecki, S., Yuan, L., Klose, M., Coombs, D. and Tanentzapf, G. (2012). Mechanical force regulates integrin turnover in Drosophila in vivo. *Nat. Cell Biol.*, 14(9), 935–943. https://doi.org/10.1038/ncb2555

Pinke, G., Zhou, L. and Sazanov, L. A. (2020). Cryo-EM structure of the entire mammalian F-type ATP synthase. *Nat. Struct. Mol. Biol.*, 27(11), 1077–1085. https://doi.org/10.1038/s41594-020-0503-8

Pirozzi, N. M., Kuipers, J. and Giepmans, B. N. G. (2021). Sample preparation for energy dispersive X-ray imaging of biological tissues. *Methods Cell Biol.*, 162, 89–114. https://doi.org/10.1016/bs.mcb.2020.10.023

Ploumi, C., Daskalaki, I. and Tavernarakis, N. (2017). Mitochondrial biogenesis and clearance: a balancing act. *FEBS J.*, 284(2), 183–195. https://doi.org/10.1111/febs.13820

Poliacikova, G., Barthez, M., Rival, T., Aouane, A., Luis, N. M., Richard, F., Daian, F., Brouilly, N., Schnorrer, F., Maurel-Zaffran, C., et al. (2023). M1BP is an essential transcriptional activator of oxidative metabolism during Drosophila development. *Nat. Commun.*, 14(1), Article 1. https://doi.org/10.1038/s41467-023-38986-5

Poliacikova, G., Maurel-Zaffran, C., Graba, Y. and Saurin, A. J. (2021). Hox Proteins in the Regulation of Muscle Development. *Front. Cell Dev. Biol.*, 9, 2940. https://doi.org/10.3389/fcell.2021.731996

Poovathumkadavil, P. and Jagla, K. (2020). Genetic Control of Muscle Diversification and Homeostasis: Insights from Drosophila. *Cells*, 9(6). https://doi.org/10.3390/cells9061543

Porcelli, D., Fischer, B., Russell, S. and White, R. (2019). Chromatin accessibility plays a key role in selective targeting of Hox proteins. *Genome Biol.*, 20(1), 115. https://doi.org/10.1186/s13059-019-1721-4

Postigo, A. A., Ward, E., Skeath, J. B. and Dean, D. C. (1999). zfh-1, the Drosophila homologue of ZEB, is a transcriptional repressor that regulates somatic myogenesis. *Mol. Cell. Biol.*, 19(10), 7255–7263. https://doi.org/10.1128/MCB.19.10.7255

Poulson, D. F. (1950). Histogenesis, organogenesis and differentiation in the embryo of Drosophila melanogaster Meigen. In *In Biology of Drosophila (ed. M. Demerec)* (Wiley, pp. 168–274). New York.

Poveda-Huertes, D., Mulica, P. and Vögtle, F. N. (2017). The versatility of the mitochondrial presequence processing machinery: cleavage, quality control and turnover. *Cell Tissue Res.*, 367(1), 73–81. https://doi.org/10.1007/s00441-016-2492-9

Priesnitz, C. and Becker, T. (2018). Pathways to balance mitochondrial translation and protein import. *Genes Dev.*, 32(19–20). https://doi.org/10.1101/gad.316547.118

Prince, F., Katsuyama, T., Oshima, Y., Plaza, S., Resendez-Perez, D., Berry, M., Kurata, S. and Gehring, W. J. (2008). The YPWM motif links Antennapedia to the basal transcriptional machinery. *Development*, 135(9), 1669–1679. https://doi.org/10.1242/dev.018028

Protasoni, M., Pérez-Pérez, R., Lobo-Jarne, T., Harbour, M. E., Ding, S., Peñas, A., Diaz, F., Moraes, C. T., Fearnley, I. M., Zeviani, M., et al. (2020). Respiratory supercomplexes act as a platform for complex III-mediated maturation of human mitochondrial complexes I and IV. *EMBO J.*, 39(3), e102817. https://doi.org/10.15252/embj.2019102817

Qian, Y. Q., Billeter, M., Otting, G., Müller, M., Gehring, W. J. and Wüthrich, K. (1989). The structure of the Antennapedia homeodomain determined by NMR spectroscopy in solution: Comparison with prokaryotic repressors. *Cell*, 59(3), 573–580. https://doi.org/10.1016/0092-8674(89)90040-8

Qiu, F., Brendel, S., Cunha, P. M. F., Astola, N., Song, B., Furlong, E. E. M., Leonard, K. R. and Bullard, B. (2005). Myofilin, a protein in the thick filaments of insect muscle. *J. Cell Sci.*, 118(Pt 7), 1527–1536. https://doi.org/10.1242/jcs.02281

Quiles, J. M. and Gustafsson, Å. B. (2020). Mitochondrial Quality Control and Cellular Proteostasis: Two Sides of the Same Coin. *Front. Physiol.*, 11, 515. https://doi.org/10.3389/fphys.2020.00515

Quinsay, M. N., Thomas, R. L., Lee, Y. and Gustafsson, Å. B. (2010). Bnip3-mediated mitochondrial autophagy is independent of the mitochondrial permeability transition pore. *Autophagy*, 6(7), 855–862. https://doi.org/10.4161/auto.6.7.13005

Rai, M., Katti, P. and Nongthomba, U. (2014). Drosophila Erect wing (Ewg) controls mitochondrial fusion during muscle growth and maintenance by regulation of the Opa1-like gene. *J. Cell Sci.*, 127(1), 191–203. https://doi.org/10.1242/jcs.135525

Raj, A., Chimata, A. V. and Singh, A. (2020). Motif 1 Binding Protein suppresses wingless to promote eye fate in Drosophila. *Sci. Rep.*, 10(1), 17221. https://doi.org/10.1038/s41598-020-73891-7

Ramachandran, B., Yu, G. and Gulick, T. (2008). Nuclear Respiratory Factor 1 Controls Myocyte Enhancer Factor 2A Transcription to Provide a Mechanism for Coordinate Expression of Respiratory Chain Subunits *. *J. Biol. Chem.*, 283(18), 11935–11946. https://doi.org/10.1074/jbc.M707389200

Ranganayakulu, Schulz, R. A. and Olson, E. N. (1996). Wingless Signaling InducesnautilusExpression in the Ventral Mesoderm of theDrosophilaEmbryo. *Dev. Biol.*, 176(1), 143–148. https://doi.org/10.1006/dbio.1996.9987

Ranganayakulu, Zhao, B., Dokidis, A., Molkentin, J. D., Olson, E. N. and Schulz, R. A. (1995). A series of mutations in the D-MEF2 transcription factor reveal multiple functions in larval and adult myogenesis in Drosophila. *Dev. Biol.*, 171(1), 169–181. https://doi.org/10.1006/dbio.1995.1269

Rasheed, M. and Gabor, T. (2018). Succinate Dehydrogenase Complex: An Updated Review. *Arch. Pathol. Lab. Med.*, 142(12). https://doi.org/10.5858/arpa.2017-0285-RS

Rath, S., Sharma, R., Gupta, R., Ast, T., Chan, C., Durham, T. J., Goodman, R. P., Grabarek, Z., Haas, M. E., Hung, W. H. W., et al. (2020). MitoCarta3.0: an updated mitochondrial proteome now with sub-organelle localization and pathway annotations. *Nucleic Acids Res.*, 49(D1), D1541–D1547. https://doi.org/10.1093/nar/gkaa1011

Rau, A., Buttgereit, D., Holz, A., Fetter, R., Doberstein, S. K., Paululat, A., Staudt, N., Skeath, J., Michelson, A. M. and Renkawitz-Pohl, R. (2001). rolling pebbles (rols) is required in Drosophila muscle precursors for recruitment of myoblasts for fusion. *Development*, 128(24), 5061–5073. https://doi.org/10.1242/dev.128.24.5061

Rawat, S., Anusha, V., Jha, M., Sreedurgalakshmi, K. and Raychaudhuri, S. (2019). Aggregation of Respiratory Complex Subunits Marks the Onset of Proteotoxicity in Proteasome Inhibited Cells. *J. Mol. Biol.*, 431(5), 996–1015. https://doi.org/10.1016/j.jmb.2019.01.022

Reed, H. C., Hoare, T., Thomsen, S., Weaver, T. A., White, R. A. H., Akam, M. and Alonso, C. R. (2010). Alternative Splicing Modulates Ubx Protein Function in Drosophila melanogaster. *Genetics*, 184(3), 745–758. https://doi.org/10.1534/genetics.109.112086

Regulski, M., Harding, K., Kostriken, R., Karch, F., Levine, M. and McGinnis, W. (1985). Homeo box genes of the Antennapedia and bithorax complexes of Drosophila. *Cell*, 43(1), 71–80. https://doi.org/10.1016/0092-8674(85)90013-3

Rembold, M., Ciglar, L., Yáñez-Cuna, J. O., Zinzen, R. P., Girardot, C., Jain, A., Welte, M. A., Stark, A., Leptin, M. and Furlong, E. E. M. (2014). A conserved role for Snail as a potentiator of active transcription. *Genes Dev.*, 28(2), 167–181. https://doi.org/10.1101/gad.230953.113

Reuter, R. and Scott, M. P. (1990). Expression and function of the homoeotic genes Antennapedia and Sex combs reduced in the embryonic midgut of Drosophila. *Development*, 109(2), 289–303.

Rezsohazy, R., Saurin, A. J., Maurel-Zaffran, C. and Graba, Y. (2015). Cellular and molecular insights into Hox protein action. *Development*, 142(7), 1212–1227. https://doi.org/10.1242/dev.109785

Rhooms, S.-K., Murari, A., Goparaju, N. S. V., Vilanueva, M. and Owusu-Ansah, E. (2020). Insights from Drosophila on mitochondrial complex I. *Cell. Mol. Life Sci.*, 77(4), 607–618. https://doi.org/10.1007/s00018-019-03293-0

Richardson, B. E., Beckett, K., Nowak, S. J. and Baylies, M. K. (2007). SCAR/WAVE and Arp2/3 are crucial for cytoskeletal remodeling at the site of myoblast fusion. *Dev. Camb. Engl.*, 134(24), 4357–4367. https://doi.org/10.1242/dev.010678

Riechmann, V., Irion, U., Wilson, R., Grosskortenhaus, R. and Leptin, M. (1997). Control of cell fates and segmentation in the Drosophila mesoderm. *Development*, 124(15), 2915–2922. https://doi.org/10.1242/dev.124.15.2915

Riley, G. R., Jorgensen, E. M., Baker, R. K. and Garber, R. L. (1991). Positive and negative control of the Antennapedia promoter P2. *Dev. Camb. Engl. Suppl.*, 1, 177–185.

Rivlin, P. K., Schneiderman, A. M. and Booker, R. (2000). Imaginal Pioneers Prefigure the Formation of Adult Thoracic Muscles in *Drosophila melanogaster*. *Dev. Biol.*, 222(2), 450–459. https://doi.org/10.1006/dbio.2000.9676

Rosales-Vega, M., Reséndez-Pérez, D. and Vázquez, M. (2024). Antennapedia: The complexity of a master developmental transcription factor. *genesis*, 62(1), e23561. https://doi.org/10.1002/dvg.23561

Roth, S., Stein, D. and Nüsslein-Volhard, C. (1989). A gradient of nuclear localization of the dorsal protein determines dorsoventral pattern in the Drosophila embryo. *Cell*, 59(6), 1189–1202. https://doi.org/10.1016/0092-8674(89)90774-5

Roy, S. and Raghavan, K. V. (1997). Homeotic genes and the regulation of myoblast migration, fusion, and fibre-specific gene expression during adult myogenesis in Drosophila. *Development*, 124(17), 3333–3341.

Roy, S., Shashidhara, L. S. and VijayRaghavan, K. (1997). Muscles in the Drosophila second thoracic segment are patterned independently of autonomous homeotic gene function. *Curr. Biol.*, 7(4), 222–227. https://doi.org/10.1016/S0960-9822(06)00117-5

Roy, S. and VijayRaghavan, K. (1998). Patterning Muscles Using Organizers: Larval Muscle Templates and Adult Myoblasts Actively Interact to Pattern the Dorsal Longitudinal Flight Muscles of Drosophila. *J. Cell Biol.*, 141(5), 1135–1145. https://doi.org/10.1083/jcb.141.5.1135

Ruiz Gómez, M. and Bate, M. (1997). Segregation of myogenic lineages in Drosophila requires numb. *Dev. Camb. Engl.*, 124(23), 4857–4866. https://doi.org/10.1242/dev.124.23.4857

Ruiz-Gómez, Coutts, N., Price, A., Taylor, M. V. and Bate, M. (2000). Drosophila dumbfounded: a myoblast attractant essential for fusion. *Cell*, 102(2), 189–198. https://doi.org/10.1016/s0092-8674(00)00024-6

Ruiz-Gómez, Romani, S., Hartmann, C., Jäckle, H. and Bate, M. (1997). Specific muscle identities are regulated by Krüppel during Drosophila embryogenesis. *Development*, 124(17), 3407–3414. https://doi.org/10.1242/dev.124.17.3407

Rusconi, J. C. and Corbin, V. (1998). Evidence for a novel Notch pathway required for muscle precursor selection in Drosophila. *Mech. Dev.*, 79(1–2), 39–50. https://doi.org/10.1016/s0925-4773(98)00170-1

Rushlow, C. A., Han, K., Manley, J. L. and Levine, M. (1989). The graded distribution of the dorsal morphogen is initiated by selective nuclear transport in Drosophila. *Cell*, 59(6), 1165–1177. https://doi.org/10.1016/0092-8674(89)90772-1

Rushton, E., Drysdale, R., Abmayr, S. M., Michelson, A. M. and Bate, M. (1995). Mutations in a novel gene, myoblast city, provide evidence in support of the founder cell hypothesis for Drosophila muscle development. *Development*, 121(7), 1979–1988. https://doi.org/10.1242/dev.121.7.1979

Rutledge, B. J., Zhang, K., Bier, E., Jan, Y. N. and Perrimon, N. (1992). The Drosophila spitz gene encodes a putative EGF-like growth factor involved in dorsal-ventral axis formation and neurogenesis. *Genes Dev.*, 6(8), 1503–1517. https://doi.org/10.1101/gad.6.8.1503

Ryoo, H. D., Marty, T., Casares, F., Affolter, M. and Mann, R. S. (1999). Regulation of Hox target genes by a DNA bound Homothorax/Hox/Extradenticle complex. *Dev. Camb. Engl.*, 126(22), 5137–5148. https://doi.org/10.1242/dev.126.22.5137

Sánchez-Herrero, E. (2013). Hox Targets and Cellular Functions. *Scientifica*, 2013, 1–26. https://doi.org/10.1155/2013/738257

Sandmann, T., Girardot, C., Brehme, M., Tongprasit, W., Stolc, V. and Furlong, E. E. M. (2007). A core transcriptional network for early mesoderm development in Drosophila melanogaster. *Genes Dev.*, 21(4), 436–449. https://doi.org/10.1101/gad.1509007

Sandmann, T., Jensen, L. J., Jakobsen, J. S., Karzynski, M. M., Eichenlaub, M. P., Bork, P. and Furlong, E. E. M. (2006). A Temporal Map of Transcription Factor Activity: Mef2 Directly Regulates Target Genes at All Stages of Muscle Development. *Dev. Cell*, 10(6), 797–807. https://doi.org/10.1016/j.devcel.2006.04.009

Sarkissian, T., Arya, R., Gyonjyan, S., Taylor, B. and White, K. (2016). Cell death regulates muscle fiber number. *Dev. Biol.*, 415(1), 87–97. https://doi.org/10.1016/j.ydbio.2016.04.018

Satoh, J.-I., Kawana, N. and Yamamoto, Y. (2013). Pathway Analysis of ChIP-Seq-Based NRF1 Target Genes Suggests a Logical Hypothesis of their Involvement in the Pathogenesis of Neurodegenerative Diseases. *Gene Regul. Syst. Biol.*, 7, 139–152. https://doi.org/10.4137/GRSB.S13204

Sauerwald, J., Backer, W., Matzat, T., Schnorrer, F. and Luschnig, S. (2019). Matrix metalloproteinase 1 modulates invasive behavior of tracheal branches during entry into Drosophila flight muscles. *eLife*, 8, e48857. https://doi.org/10.7554/eLife.48857

Saurin, A. J., Delfini, M. C., Maurel-Zaffran, C. and Graba, Y. (2018). The Generic Facet of Hox Protein Function. *Trends Genet.*, 34(12), 941–953. https://doi.org/10.1016/j.tig.2018.08.006

Scarpulla, R. C. (2008). Transcriptional paradigms in mammalian mitochondrial biogenesis and function. *Physiol. Rev.*, 88(2), 611–638. https://doi.org/10.1152/physrev.00025.2007

Scarpulla, R. C., Vega, R. B. and Kelly, D. P. (2012). Transcriptional integration of mitochondrial biogenesis. *Trends Endocrinol. Metab. TEM*, 23(9), 459–466. https://doi.org/10.1016/j.tem.2012.06.006

Schäfer, G., Weber, S., Holz, A., Bogdan, S., Schumacher, S., Müller, A., Renkawitz-Pohl, R. and Onel, S.-F. (2007). The Wiskott-Aldrich syndrome protein (WASP) is essential for myoblast fusion in Drosophila. *Dev. Biol.*, 304(2), 664–674. https://doi.org/10.1016/j.ydbio.2007.01.015

Schägger, H., Link, T. A., Engel, W. D. and von Jagow, G. (1986). Isolation of the eleven protein subunits of the bc1 complex from beef heart. *Methods Enzymol.*, 126, 224–237. https://doi.org/10.1016/s0076-6879(86)26024-3

Schägger, H. and Pfeiffer, K. (2000). Supercomplexes in the respiratory chains of yeast and mammalian mitochondria. *EMBO J.*, 19(8), 1777–1783. https://doi.org/10.1093/emboj/19.8.1777

Schaub, C., Nagaso, H., Jin, H. and Frasch, M. (2012). Org-1, the Drosophila ortholog of Tbx1, is a direct activator of known identity genes during muscle specification. *Development*, 139(5), 1001–1012. https://doi.org/10.1242/dev.073890

Schneuwly, S., Klemenz, R. and Gehring, W. J. (1987). Redesigning the body plan of Drosophila by ectopic expression of the homoeotic gene Antennapedia. *Nature*, 325(6107), 816–818. https://doi.org/10.1038/325816a0

Schneuwly, S., Kuroiwa, A., Baumgartner, P. and Gehring, W. J. (1986). Structural organization and sequence of the homeotic gene Antennapedia of Drosophila melanogaster. *EMBO J.*, 5(4), 733–739.

Scholtes, C. and Giguère, V. (2022). Transcriptional control of energy metabolism by nuclear receptors. *Nat. Rev. Mol. Cell Biol.* https://doi.org/10.1038/s41580-022-00486-7

Schönbauer, C., Distler, J., Jährling, N., Radolf, M., Dodt, H.-U., Frasch, M. and Schnorrer, F. (2011). Spalt mediates an evolutionarily conserved switch to fibrillar muscle fate in insects. *Nature*, 479(7373), Article 7373. https://doi.org/10.1038/nature10559

Schröter, R. H., Lier, S., Holz, A., Bogdan, S., Klämbt, C., Beck, L. and Renkawitz-Pohl, R. (2004). kette and blown fuse interact genetically during the second fusion step of myogenesis in Drosophila. *Development*, 131(18), 4501–4509. https://doi.org/10.1242/dev.01309

Schulman, V. K., Dobi, K. C. and Baylies, M. K. (2015). Morphogenesis of the somatic musculature in *Drosophila melanogaster*: Morphogenesis of the *Drosophila* musculature. *Wiley Interdiscip. Rev. Dev. Biol.*, 4(4), 313–334. https://doi.org/10.1002/wdev.180

Schweitzer, R., Zelzer, E. and Volk, T. (2010). Connecting muscles to tendons: tendons and musculoskeletal development in flies and vertebrates. *Dev. Camb. Engl.*, 137(17), 2807–2817. https://doi.org/10.1242/dev.047498

Scott, M. P. and Weiner, A. J. (1984). Structural relationships among genes that control development: sequence homology between the Antennapedia, Ultrabithorax, and fushi tarazu loci of Drosophila. *Proc. Natl. Acad. Sci. U. S. A.*, 81(13), 4115–4119.

Scott, M. P., Weiner, A. J., Hazelrigg, T. I., Polisky, B. A., Pirrotta, V., Scalenghe, F. and Kaufman, T. C. (1983). The molecular organization of the Antennapedia locus of

drosophila. *Cell*, 35(3), 763–776. https://doi.org/10.1016/0092-8674(83)90109-5

Seelan, R. S. and Grossman, L. I. (1997). Structural organization and promoter analysis of the bovine cytochrome c oxidase subunit VIIc gene. A functional role for YY1. *J. Biol. Chem.*, 272(15), 10175–10181. https://doi.org/10.1074/jbc.272.15.10175

Segal, D., Dhanyasi, N., Schejter, E. D. and Shilo, B.-Z. (2016). Adhesion and Fusion of Muscle Cells Are Promoted by Filopodia. *Dev. Cell*, 38(3), 291–304. https://doi.org/10.1016/j.devcel.2016.07.010

Sens, K. L., Zhang, S., Jin, P., Duan, R., Zhang, G., Luo, F., Parachini, L. and Chen, E. H. (2010). An invasive podosome-like structure promotes fusion pore formation during myoblast fusion. *J. Cell Biol.*, 191(5), 1013–1027. https://doi.org/10.1083/jcb.201006006

Shah, A. J., Sahgal, V., Muschler, G., Subramani, V. and Singh, H. (1982). Morphogenesis of the mitochondrial alterations in muscle diseases. *J. Neurol. Sci.*, 55(1), 25–37. https://doi.org/10.1016/0022-510X(82)90167-8

Shao, D., Liu, Y., Liu, X., Zhu, L., Cui, Y., Cui, A., Qiao, A., Kong, X., Liu, Y., Chen, Q., et al. (2010). PGC-1 beta-regulated mitochondrial biogenesis and function in myotubes is mediated by NRF-1 and ERR alpha. *Mitochondrion*, 10(5), 516–527. https://doi.org/10.1016/j.mito.2010.05.012

Shelton, C., Kocherlakota, K. S., Zhuang, S. and Abmayr, S. M. (2009). The immunoglobulin superfamily member Hbs functions redundantly with Sns in interactions between founder and fusion-competent myoblasts. *Development*, 136(7), 1159–1168. https://doi.org/10.1242/dev.026302

Shepherd, J. C. W., McGinnis, W., Carrasco, A. E., De Robertis, E. M. and Gehring, W. J. (1984). Fly and frog homoeo domains show homologies with yeast mating type regulatory proteins. *Nature*, 310(5972), Article 5972. https://doi.org/10.1038/310070a0

Shiba-Fukushima, K., Inoshita, T., Hattori, N. and Imai, Y. (2014). PINK1-Mediated Phosphorylation of Parkin Boosts Parkin Activity in Drosophila. *PLoS Genet.*, 10(6), e1004391. https://doi.org/10.1371/journal.pgen.1004391

Shimada, S., Shinzawa-Itoh, K., Baba, J., Aoe, S., Shimada, A., Yamashita, E., Kang, J., Tateno, M., Yoshikawa, S. and Tsukihara, T. (2017). Complex structure of cytochrome c-cytochrome c oxidase reveals a novel protein-protein interaction mode. *EMBO J.*, 36(3), 291–300. https://doi.org/10.15252/embj.201695021

Signes, A. and Fernandez-Vizarra, E. (2018). Assembly of mammalian oxidative phosphorylation complexes I-V and supercomplexes. *Essays Biochem.*, 62(3), 255–270. https://doi.org/10.1042/EBC20170098

Simpson. (1983). Maternal-Zygotic Gene Interactions during Formation of the Dorsoventral Pattern in Drosophila Embryos. *Genetics*, 105(3), 615–632. https://doi.org/10.1093/genetics/105.3.615

Simpson, J. H. (2016). Rationally subdividing the fly nervous system with versatile expression reagents. *J. Neurogenet.*, 30(3–4), 185–194. https://doi.org/10.1080/01677063.2016.1248761

Smith, D. S. (1961). THE STRUCTURE OF INSECT FIBRILLAR FLIGHT MUSCLE : A Study Made with Special Reference to the Membrane Systems of the Fiber. *J. Biophys. Biochem. Cytol.*, 10(4), 123–158. https://doi.org/10.1083/jcb.10.4.123

Soler, C., Han, J. and Taylor, M. V. (2012). The conserved transcription factor Mef2 has multiple roles in adult Drosophila musculature formation. *Development*, 139(7), 1270–1275. https://doi.org/10.1242/dev.077875

Soler, Daczewska, M., Da Ponte, J. P., Dastugue, B. and Jagla, K. (2004). Coordinated development of muscles and tendons of the *Drosophila* leg. *Development*, 131(24), 6041–6051. https://doi.org/10.1242/dev.01527

Son, S.-H., Son, Y.-E., Cho, H.-J., Chen, W., Lee, M.-K., Kim, L.-H., Han, D.-M. and Park, H.-S. (2020). Homeobox proteins are essential for fungal differentiation and secondary metabolism in Aspergillus nidulans. *Sci. Rep.*, 10(1), 6094. https://doi.org/10.1038/s41598-020-63300-4

Sousa, J. S., D'Imprima, E. and Vonck, J. (2018). Mitochondrial Respiratory Chain Complexes. *Subcell. Biochem.*, 87, 167–227. https://doi.org/10.1007/978-981-10-7757-9_7

Spana, E. P. and Doe, C. Q. (1996). Numb Antagonizes Notch Signaling to Specify Sibling Neuron Cell Fates. *Neuron*, 17(1), 21–26. https://doi.org/10.1016/S0896-6273(00)80277-9

Spikes, T. E., Montgomery, M. G. and Walker, J. E. (2020). Structure of the dimeric ATP synthase from bovine mitochondria. *Proc. Natl. Acad. Sci. U. S. A.*, 117(38), 23519–23526. https://doi.org/10.1073/pnas.2013998117

Spletter, M. L., Barz, C., Yeroslaviz, A., Schönbauer, C., Ferreira, I. R. S., Sarov, M., Gerlach, D., Stark, A., Habermann, B. H. and Schnorrer, F. (2015). The RNA-binding protein Arrest (Bruno) regulates alternative splicing to enable myofibril maturation in Drosophila flight muscle. *EMBO Rep.*, 16(2), 178–191. https://doi.org/10.15252/embr.201439791

Spletter, M. L., Barz, C., Yeroslaviz, A., Zhang, X., Lemke, S. B., Bonnard, A., Brunner, E., Cardone, G., Basler, K., Habermann, B. H., et al. (2018). A transcriptomics resource reveals a transcriptional transition during ordered sarcomere morphogenesis in flight muscle. *eLife*, 7, e34058. https://doi.org/10.7554/eLife.34058

Staehling-Hampton, K., Hoffmann, F. M., Baylies, M. K., Rushtont, E. and Bate, M. (1994). dpp induces mesodermal gene expression in Drosophila. *Nature*, 372(6508), 783–786. https://doi.org/10.1038/372783a0

Stathopoulos, A., Drenth, M. V., Erives, A., Markstein, M. and Levine, M. (2002). Whole-Genome Analysis of Dorsal-Ventral Patterning in the Drosophila Embryo. *Cell*, 111(5), 687–701. https://doi.org/10.1016/S0092-8674(02)01087-5

Stathopoulos, A., Tam, B., Ronshaugen, M., Frasch, M. and Levine, M. (2004). pyramus and thisbe: FGF genes that pattern the mesoderm of Drosophila embryos. *Genes Dev.*, 18(6), 687–699. https://doi.org/10.1101/gad.1166404

Steward, R. (1989). Relocalization of the dorsal protein from the cytoplasm to the nucleus correlates with its function. *Cell*, 59(6), 1179–1188. https://doi.org/10.1016/0092-8674(89)90773-3

Stroeher, V. L., Gaiser, J. C. and Garber, R. L. (1988). Alternative RNA splicing that is spatially regulated: generation of transcripts from the Antennapedia gene of Drosophila melanogaster with different protein-coding regions. *Mol. Cell. Biol.*, 8(10), 4143–4154. https://doi.org/10.1128/mcb.8.10.4143-4154.1988

Stroeher, V. L., Jorgensen, E. M. and Garber, R. L. (1986). Multiple transcripts from the Antennapedia gene of Drosophila melanogaster. *Mol. Cell. Biol.*, 6(12), 4667–4675. https://doi.org/10.1128/mcb.6.12.4667-4675.1986

Stroud, D. A., Surgenor, E. E., Formosa, L. E., Reljic, B., Frazier, A. E., Dibley, M. G., Osellame, L. D., Stait, T., Beilharz, T. H., Thorburn, D. R., et al. (2016). Accessory subunits are integral for assembly and function of human mitochondrial complex I. *Nature*, 538(7623), 123–126. https://doi.org/10.1038/nature19754

Struhl, G. (1981). A homoeotic mutation transforming leg to antenna in Drosophila. *Nature*, 292(5824), Article 5824. https://doi.org/10.1038/292635a0

Strünkelnberg, M., Bonengel, B., Moda, L. M., Hertenstein, A., de Couet, H. G., Ramos, R. G. P. and Fischbach, K.-F. (2001). rst and its paralogue kirre act redundantly during embryonic muscle development in Drosophila. *Development*, 128(21), 4229–4239. https://doi.org/10.1242/dev.128.21.4229

Strünkelnberg, M., de Couet, H. G., Hertenstein, A. and Fischbach, K.-F. (2003). Interspecies comparison of a gene pair with partially redundant function: the rst and kirre genes in D. virilis and D. melanogaster. *J. Mol. Evol.*, 56(2), 187–197. https://doi.org/10.1007/s00239-002-2393-2

Sudarsan, V., Anant, S., Guptan, P., VijayRaghavan, K. and Skaer, H. (2001). Myoblast Diversification and Ectodermal Signaling in Drosophila. *Dev. Cell*, 1(6), 829–839. https://doi.org/10.1016/S1534-5807(01)00089-2

Sun, F., Huo, X., Zhai, Y., Wang, A., Xu, J., Su, D., Bartlam, M. and Rao, Z. (2005). Crystal structure of mitochondrial respiratory membrane protein complex II. *Cell*, 121(7), 1043–1057. https://doi.org/10.1016/j.cell.2005.05.025

Sung, M.-K., Reitsma, J. M., Sweredoski, M. J., Hess, S. and Deshaies, R. J. (2016). Ribosomal proteins produced in excess are degraded by the ubiquitin–proteasome system. *Mol. Biol. Cell*, 27(17), 2642–2652. https://doi.org/10.1091/mbc.E16-05-0290

Sykiotis, G. P. and Bohmann, D. (2008). Keap1/Nrf2 signaling regulates oxidative stress tolerance and lifespan in Drosophila. *Dev. Cell*, 14(1), 76–85. https://doi.org/10.1016/j.devcel.2007.12.002

Talbot, J. and Maves, L. (2016). Skeletal muscle fiber type: using insights from muscle developmental biology to dissect targets for susceptibility and resistance to

muscle disease. *Wiley Interdiscip. Rev. Dev. Biol.*, 5(4), 518–534. https://doi.org/10.1002/wdev.230

Tan, P., Feng, Z., Zhang, L., Hou, T. and Li, Y. (2015). The mechanism of proton translocation in respiratory complex I from molecular dynamics. *J. Recept. Signal Transduct. Res.*, 35(2), 170–179. https://doi.org/10.3109/10799893.2014.942464

Tapanes-Castillo, A. and Baylies, M. K. (2004). Notch signaling patterns Drosophila mesodermal segments by regulating the bHLH transcription factor twist. *Development*, 131(10), 2359–2372. https://doi.org/10.1242/dev.01113

Teixeira, P. F. and Glaser, E. (2013). Processing peptidases in mitochondria and chloroplasts. *Biochim. Biophys. Acta*, 1833(2), 360–370. https://doi.org/10.1016/j.bbamcr.2012.03.012

Thisse, B., Stoetzel, C., Gorostiza-Thisse, C. and Perrin-Schmitt, F. (1988). Sequence of the twist gene and nuclear localization of its protein in endomesodermal cells of early Drosophila embryos. *EMBO J.*, 7(7), 2175–2183. https://doi.org/10.1002/j.1460-2075.1988.tb03056.x

Tiefenböck, S. K., Baltzer, C., Egli, N. A. and Frei, C. (2010). The Drosophila PGC-1 homologue Spargel coordinates mitochondrial activity to insulin signalling. *EMBO J.*, 29(1), 171–183. https://doi.org/10.1038/emboj.2009.330

Timón-Gómez, A., Nývltová, E., Abriata, L. A., Vila, A. J., Hosler, J. and Barrientos, A. (2018). Mitochondrial cytochrome c oxidase biogenesis: Recent developments. *Semin. Cell Dev. Biol.*, 76, 163–178. https://doi.org/10.1016/j.semcdb.2017.08.055

Tixier, V., Bataillé, L., Etard, C., Jagla, T., Weger, M., Daponte, J. P., Strähle, U., Dickmeis, T. and Jagla, K. (2013). Glycolysis supports embryonic muscle growth by promoting myoblast fusion. *Proc. Natl. Acad. Sci. U. S. A.*, 110(47), 18982–18987. https://doi.org/10.1073/pnas.1301262110

Tripoli, G., D'Elia, D., Barsanti, P. and Caggese, C. (2005). Comparison of the oxidative phosphorylation (OXPHOS) nuclear genes in the genomes of Drosophila melanogaster, Drosophila pseudoobscura and Anopheles gambiae. *Genome Biol.*, 6(2), R11. https://doi.org/10.1186/gb-2005-6-2-r11

Trumpower, B. L. (1990). The protonmotive Q cycle. Energy transduction by coupling of proton translocation to electron transfer by the cytochrome bc1 complex. *J. Biol. Chem.*, 265(20), 11409–11412.

Trumpower, B. L. (2002). A concerted, alternating sites mechanism of ubiquinol oxidation by the dimeric cytochrome bc(1) complex. *Biochim. Biophys. Acta*, 1555(1–3), 166–173. https://doi.org/10.1016/s0005-2728(02)00273-6

Tsukihara, T., Aoyama, H., Yamashita, E., Tomizaki, T., Yamaguchi, H., Shinzawa-Itoh, K., Nakashima, R., Yaono, R. and Yoshikawa, S. (1996). The whole structure of the 13-subunit oxidized cytochrome c oxidase at 2.8 A. *Science*, 272(5265), 1136–1144. https://doi.org/10.1126/science.272.5265.1136

Vakifahmetoglu-Norberg, H., Ouchida, A. T. and Norberg, E. (2017). The role of mitochondria in metabolism and cell death. *Biochem. Biophys. Res. Commun.*, 482(3), 426–431. https://doi.org/10.1016/j.bbrc.2016.11.088

van Dijk, M. A. and Murre, C. (1994). extradenticle raises the DNA binding specificity of homeotic selector gene products. *Cell*, 78(4), 617–624. https://doi.org/10.1016/0092-8674(94)90526-6

Van Melderen, L. and Aertsen, A. (2009). Regulation and quality control by Lon-dependent proteolysis. *Res. Microbiol.*, 160(9), 645–651. https://doi.org/10.1016/j.resmic.2009.08.021

van Waveren, C. and Moraes, C. T. (2008). Transcriptional co-expression and co-regulation of genes coding for components of the oxidative phosphorylation system. *BMC Genomics*, 9(1), 18. https://doi.org/10.1186/1471-2164-9-18

Vazquez, M., Moore, L. and Kennison, J. A. (1999). The trithorax group gene osa encodes an ARID-domain protein that genetically interacts with the brahma chromatin-remodeling factor to regulate transcription. *Development*, 126(4), 733–742. https://doi.org/10.1242/dev.126.4.733

Vega, R. B., Huss, J. M. and Kelly, D. P. (2000). The Coactivator PGC-1 Cooperates with Peroxisome Proliferator-Activated Receptor α in Transcriptional Control of Nuclear Genes Encoding Mitochondrial Fatty Acid Oxidation Enzymes. *Mol. Cell. Biol.*, 20(5), 1868–1876.

Vercauteren, K., Gleyzer, N. and Scarpulla, R. C. (2008). PGC-1-related Coactivator Complexes with HCF-1 and NRF-2β in Mediating NRF-2(GABP)-dependent Respiratory Gene Expression *. *J. Biol. Chem.*, 283(18), 12102–12111. https://doi.org/10.1074/jbc.M710150200

Vercellino, I. and Sazanov, L. A. (2022). The assembly, regulation and function of the mitochondrial respiratory chain. *Nat. Rev. Mol. Cell Biol.*, 23(2), 141–161. https://doi.org/10.1038/s41580-021-00415-0

Vigoreaux, J. O., Saide, J. D., Valgeirsdottir, K. and Pardue, M. L. (1993). Flightin, a novel myofibrillar protein of Drosophila stretch-activated muscles. *J. Cell Biol.*, 121(3), 587–598. https://doi.org/10.1083/jcb.121.3.587

Villarreal-Puente, A., Altamirano-Torres, C., Jiménez-Mejía, G., Hernández-Bautista, C., Montalvo-Méndez, R., Vázquez, M., Zurita, M. and Reséndez-Pérez, D. (2024). Novel Antennapedia and Ultrabithorax trimeric complexes with TBP and Exd regulate transcription. *Hereditas*, 161, 25. https://doi.org/10.1186/s41065-024-00327-x

Vishal, K., Barajas Alonso, E., DeAguero, A. A., Waters, J. A., Chechenova, M. B. and Cripps, R. M. (2023). Phosphorylation of the Myogenic Factor Myocyte Enhancer Factor-2 Impacts Myogenesis In Vivo. *Mol. Cell. Biol.*, 1–13. https://doi.org/10.1080/10985549.2023.2198167

Vishal, K., Brooks, D. S., Bawa, S., Gameros, S., Stetsiv, M. and Geisbrecht, E. R. (2017). Adult Muscle Formation Requires *Drosophila* Moleskin for Proliferation of Wing Disc-Associated Muscle Precursors. *Genetics*, 206(1), 199–213. https://doi.org/10.1534/genetics.116.193813

Vishal, K., Lovato, T. L., Bragg, C., Chechenova, M. B. and Cripps, R. M. (2020). FGF signaling promotes myoblast proliferation through activation of wingless signaling. *Dev. Biol.*, 464(1), 1–10. https://doi.org/10.1016/j.ydbio.2020.05.009

Viswanatha, R., Li, Z., Hu, Y. and Perrimon, N. (2018). Pooled genome-wide CRISPR screening for basal and context-specific fitness gene essentiality in Drosophila cells. *eLife*, 7, e36333. https://doi.org/10.7554/eLife.36333

Vorbrüggen, G., Constien, R., Zilian, O., Wimmer, E. A., Dowe, G., Taubert, H., Noll, M. and Jäckle, H. (1997). Embryonic expression and characterization of a Ptx1 homolog in Drosophila. *Mech. Dev.*, 68(1–2), 139–147. https://doi.org/10.1016/s0925-4773(97)00139-1

Wagner-Bernholz, J. T., Wilson, C., Gibson, G., Schuh, R. and Gehring, W. J. (1991). Identification of target genes of the homeotic gene Antennapedia by enhancer detection. *Genes Dev.*, 5(12b), 2467–2480. https://doi.org/10.1101/gad.5.12b.2467

Wakimoto, B. T. and Kaufman, T. C. (1981). Analysis of larval segmentation in lethal genotypes associated with the antennapedia gene complex in Drosophila melanogaster. *Dev. Biol.*, 81(1), 51–64. https://doi.org/10.1016/0012-1606(81)90347-x

Wan, B. and Moreadith, R. W. (1995). Structural Characterization and Regulatory Element Analysis of the Heart Isoform of Cytochrome *c* Oxidase VIa (∗). *J. Biol. Chem.*, 270(44), 26433–26440. https://doi.org/10.1074/jbc.270.44.26433

Wang, S., Stoops, E., Cp, U., Markus, B., Reuveny, A., Ordan, E. and Volk, T. (2018). Mechanotransduction via the LINC complex regulates DNA replication in myonuclei. *J. Cell Biol.*, 217(6), 2005–2018. https://doi.org/10.1083/jcb.201708137

Wang, X. and Chen, X. J. (2015). A cytosolic network suppressing mitochondria-mediated proteostatic stress and cell death. *Nature*, 524(7566), 481–484. https://doi.org/10.1038/nature14859

Watson, S. A. and McStay, G. P. (2020). Functions of Cytochrome c Oxidase Assembly Factors. *Int. J. Mol. Sci.*, 21(19), 7254. https://doi.org/10.3390/ijms21197254

Weitkunat, M., Brasse, M., Bausch, A. R. and Schnorrer, F. (2017). Mechanical tension and spontaneous muscle twitching precede the formation of cross-striated muscle in vivo. *Dev. Camb. Engl.*, 144(7), 1261–1272. https://doi.org/10.1242/dev.140723

Weitkunat, M., Kaya-Çopur, A., Grill, S. W. and Schnorrer, F. (2014). Tension and force-resistant attachment are essential for myofibrillogenesis in Drosophila flight muscle. *Curr. Biol. CB*, 24(7), 705–716. https://doi.org/10.1016/j.cub.2014.02.032

Weitkunat, M. and Schnorrer, F. (2014). A guide to study Drosophila muscle biology. *Methods*, 68(1), 2–14. https://doi.org/10.1016/j.ymeth.2014.02.037

Whitworth, A. J., Lee, J. R., Ho, V. M.-W., Flick, R., Chowdhury, R. and McQuibban, G. A. (2008). Rhomboid-7 and HtrA2/Omi act in a common pathway with the Parkinson's disease factors Pink1 and Parkin. *Dis. Model. Mech.*, 1(2–3), 168–174; discussion 173. https://doi.org/10.1242/dmm.000109

Wikstrom, M. K. (1977). Proton pump coupled to cytochrome c oxidase in mitochondria. *Nature*, 266(5599), 271–273. https://doi.org/10.1038/266271a0

Williams, R. W. (1998). Plant homeobox genes: many functions stem from a common motif. *BioEssays News Rev. Mol. Cell. Dev. Biol.*, 20(4), 280–282. https://doi.org/10.1002/(SICI)1521-1878(199804)20:4<280::AID-BIES2>3.0.CO;2-U

Willingham, T. B., Zhang, Y., Andreoni, A., Knutson, J. R., Lee, D.-Y. and Glancy, B. (2019). MitoRACE: evaluating mitochondrial function in vivo and in single cells with subcellular resolution using multiphoton NADH autofluorescence. *J. Physiol.*, 597(22), 5411–5428. https://doi.org/10.1113/JP278611

Wirz, J., Fessler, L. I. and Gehring, W. J. (1986). Localization of the Antennapedia protein in Drosophila embryos and imaginal discs. *EMBO J.*, 5(12), 3327–3334.

Xia, D., Esser, L., Tang, W.-K., Zhou, F., Zhou, Y., Yu, L. and Yu, C.-A. (2013). Structural Analysis of Cytochrome bc1 Complexes: Implications to the Mechanism of Function. *Biochim. Biophys. Acta*, 1827(0), 1278–1294. https://doi.org/10.1016/j.bbabio.2012.11.008

Yang, Drumea, K., Mott, S., Wang, J. and Rosmarin, A. G. (2014). GABP transcription factor (nuclear respiratory factor 2) is required for mitochondrial biogenesis. *Mol. Cell. Biol.*, 34(17), 3194–3201. https://doi.org/10.1128/MCB.00492-12

Yang, X. H. and Trumpower, B. L. (1986). Purification of a three-subunit ubiquinol-cytochrome c oxidoreductase complex from Paracoccus denitrificans. *J. Biol. Chem.*, 261(26), 12282–12289. https://doi.org/10.1016/S0021-9258(18)67236-9

Yim, A., Koti, P., Bonnard, A., Marchiano, F., Dürrbaum, M., Garcia-Perez, C., Villaveces, J., Gamal, S., Cardone, G., Perocchi, F., et al. (2020). mitoXplorer, a visual data mining platform to systematically analyze and visualize mitochondrial expression dynamics and mutations. *Nucleic Acids Res.*, 48(2), 605–632. https://doi.org/10.1093/nar/gkz1128

Yin, J. C. P., Wallach, J. S., Wilder, E. L., Klingensmith, J., Dang, D., Perrimon, N., Zhou, H., Tully, T. and Quinn, W. G. (1995). A Drosophila CREB/CREM Homolog Encodes Multiple Isoforms, Including a Cyclic AMP-Dependent Protein Kinase-Responsive Transcriptional Activator and Antagonist. *Mol. Cell. Biol.*, 15(9), 5123–5130. https://doi.org/10.1128/MCB.15.9.5123

Zaid, A., Li, R., Luciakova, K., Barath, P., Nery, S. and Nelson, B. D. (1999). On the role of the general transcription factor Sp1 in the activation and repression of diverse mammalian oxidative phosphorylation genes. *J. Bioenerg. Biomembr.*, 31(2), 129–135. https://doi.org/10.1023/a:1005499727732

Zappia, M. P., de Castro, L., Ariss, M. M., Jefferson, H., Islam, A. B. and Frolov, M. V. (2020). A cell atlas of adult muscle precursors uncovers early events in fibre-type divergence in Drosophila. *EMBO Rep.*, e49555. https://doi.org/10.15252/embr.201949555

Zappia, M. P., Rogers, A., Islam, A. B. M. M. K. and Frolov, M. V. (2019). Rbf Activates the Myogenic Transcriptional Program to Promote Skeletal Muscle Differentiation. *Cell Rep.*, 26(3), 702-719.e6. https://doi.org/10.1016/j.celrep.2018.12.080

Zeitlinger, J., Zinzen, R. P., Stark, A., Kellis, M., Zhang, H., Young, R. A. and Levine, M. (2007). Whole-genome ChIP-chip analysis of Dorsal, Twist, and Snail suggests integration of diverse patterning processes in the Drosophila embryo. *Genes Dev.*, 21(4), 385–390. https://doi.org/10.1101/gad.1509607

Zhao, X., Xu, C., Ding, Y. and Yan, N. (2024). The multifaceted functions of NFE2L1 in metabolism and associated disorders. *Life Sci.*, 352, 122906. https://doi.org/10.1016/j.lfs.2024.122906

Zhu, J., Vinothkumar, K. R. and Hirst, J. (2016). Structure of mammalian respiratory complex I. *Nature*, 536(7616), 354–358. https://doi.org/10.1038/nature19095

Zouaz, A., Auradkar, A., Delfini, M. C., Macchi, M., Barthez, M., Ela Akoa, S., Bastianelli, L., Xie, G., Deng, W., Levine, S. S., et al. (2017). The Hox proteins Ubx and AbdA collaborate with the transcription pausing factor M1 BP to regulate gene transcription. *EMBO J.*, 36(19), 2887–2906. https://doi.org/10.15252/embj.201695751